การประเมินความเสียหายของโครงสร้างเชิงสถิติโดยใช้การประมาณค่าพารามิเตอร์
จากผลตอบสนองเชิงโหมด

นาย มนตรี จิตต์หมวด

STATISTICAL DAMAGE ASSESSMENT OF STRUCTURES
USING PARAMETER ESTIMATION FROM MODAL RESPONSE

Mr. Montree Jitmoud

Thesis Title   Statistical Damage Assessment of Structures using Parameter Estimation from Modal Response

By   Mr. Montree Jitmoud

Field of Study Civil Engineering

Thesis Advisor Thanyawat Pothisiri, Ph.D.

Accepted by the Faculty of Engineering, Chulalongkorn University in Partial Fulfillment of Requirements for the Master's Degree

..…………………………… Dean of Faculty of Engineering

(Professor Somsak Panyakeow, D.Eng.)

THESIS COMMITTEE

………………………………….. Chairman

(Professor Thaksin Thepchatri, Ph.D.)

…………………………………. Thesis Advisor

(Thanyawat Pothisiri, Ph.D.)

…………………………………. Member

(Assistant Professor Teerapong Senjuntichai, Ph.D.)

มนตรี   จิตต์หมวด : การประเมินความเสียหายของโครงสร้างเชิงสถิติโดยใช้การประมาณค่าพารามิเตอร์จากผลตอบสนองเชิงโหมด (STATISTICAL DAMAGE ASSESSMENT OF STRUCTURES USING PARAMETER ESTIMATION FROM MODAL RESPONSE) อาจารย์ที่ปรึกษา : อาจารย์ ดร.ธัญวัฒน์ โพธิศิริ, จำนวน 187 หน้า, ISBN : 974-17-4080-8

วิทยานิพนธ์ฉบับนี้ศึกษาวิธีการประเมินความเสียหายเชิงสถิติสำหรับโครงสร้างที่มีชิ้นส่วนซึ่งประกอบด้วยพารามิเตอร์ค่าเดียวหรือหลายค่า ค่าพารามิเตอร์ที่พิจารณาอาจประกอบด้วยค่าสติฟเนสพารามิเตอร์การยืดหดตัวในแนวแกน การเฉือน หรือการดัด วิธีการที่นำเสนอคำนึงถึงปัญหาเรื่องความคลาดเคลื่อนของผลตอบสนองของโครงสร้างที่ได้จากการวัด สำหรับชิ้นส่วนของโครงสร้างซึ่งประกอบด้วยพารามิเตอร์ค่าเดียว วิธีการเชิงสถิติที่เสนอมี 3 วิธี ได้แก่ (1) วิธีการจำลองแบบมอนติคาโล (2) วิธีการอิงความไหวตัวที่เหมาะสมที่สุด และ (3) วิธีการอิงความไหวตัว หลักการสำคัญของวิธีการเหล่านี้คือการเปรียบเทียบการกระจายตัวทางสถิติของค่าพารามิเตอร์ที่ประมาณระหว่างโครงสร้างที่เสียหายและโครงสร้างที่ไม่เสียหาย วิธีการหาปริพันธ์เชิงตัวเลขสามารถนำมาใช้ในการคำนวณความน่าจะเป็นของความเสียหายของชิ้นส่วนโครงสร้างแต่ละชิ้นในรูปฟังก์ชันของระดับความเสียหาย

จากการศึกษาพบว่า ประสิทธิภาพของวิธีการประเมินความเสียหายที่นำเสนอสำหรับชิ้นส่วนโครงสร้างซึ่งประกอบด้วยพารามิเตอร์ค่าเดียวขึ้นอยู่กับคุณภาพของค่าพารามิเตอร์ที่ประมาณได้ ในการศึกษานี้ ได้ประยุกต์ใช้วิธีเรกูลาร์ไรเซชันเพื่อลดระดับการขาดเสถียรภาพของคำตอบของปัญหาการประมาณค่าพารามิเตอร์เมื่อมีความคลาดเคลื่อนจากการวัด ระดับความสำเร็จในการประเมินความเสียหายของโครงสร้างถูกกำหนดโดยดัชนีบ่งชี้ความคลาดเคลื่อนเชิงสถิติ ซึ่งมีค่าเข้าใกล้ศูนย์เมื่อการประเมินสัมฤทธิ์ผล

สำหรับการตรวจสอบความเสียหายของชิ้นส่วนโครงสร้างซึ่งประกอบด้วยพารามิเตอร์หลายค่า ได้นำเสนอฟังก์ชันพื้นฐานเพื่อใช้ในการตัดสินว่าชิ้นส่วนโครงสร้างอยู่ใน "สภาวะปกติ" หรือ "สภาวะเสียหาย" ขีดจำกัดซึ่งใช้แบ่งระหว่างสภาวะทั้งสองเรียกว่า "สภาวะสุดขีด" ความน่าจะเป็นของ   ความเสียหายสามารถคำนวณในรูปของฟังก์ชันของระยะทางระหว่างเส้นสภาวะขีดสุดและจุดกำเนิดของปริภูมิตัวแปรลดรูป ซึ่งมีค่าเข้าใกล้หนึ่งเมื่อสามารถประเมินความเสียหายได้อย่างสัมฤทธิ์ผล

ภาควิชา _____วิศวกรรมโยธา_____ ลายมือชื่อนิสิต _____
สาขาวิชา _____วิศวกรรมโยธา_____ ลายมือชื่ออาจารย์ที่ปรึกษา _____
ปีการศึกษา _____2546_____

MONTREE JITMOUD : STATISTICAL DAMAGE ASSESSMENT OF STRUCTURES
USING PARAMETER ESTIMATION FROM MODAL RESPONSE. THESIS ADVISOR :
THANYAWAT POTHISIRI, Ph.D., 187 pp. ISBN : 974-17-4080-8.

This thesis investigates the statistical damage assessment method for structures with members consisting of one or more parameters. The parameters under consideration may comprise of the axial, shear or bending stiffness parameters. The proposed method takes into account the problem of noise contamination in the measured response of the structures. For the single-parameter structural members, three distinct statistical methods were introduced: (1) the Monte-Carlo simulation method; (2) the optimum sensitivity-based method; and (3) the sensitivity-based method. The underlying principle of these methods is to compare the statistical distribution of the estimated parameters for the damaged structure with the undamaged structure. A numerical integration scheme can then be used to compute the probability of damage for each structural member as a function of the level of damage.

It was found from the current study that the performance of the proposed damage assessment scheme for the single-parameter structural members depends considerably upon the quality of the estimated system parameters. In the present study, the regularization technique was adopted to reduce the degree of instabilities of solutions to the parameter estimation problem in the presence of the measurement noise. The level of success for the damage assessment is identified by the statistical identification error index that approaches zero when the assessment is considered effective.

To identify damage in the multi-parameter structural members, a baseline function was proposed to identify whether a structural member is in the "healthy state" or the "damaged state." The boundary separating these two states is referred to as the "limit state." The probability of damage can then be computed as a function of the distance of the limit-state line to the origin of the reduced-variate space which approaches the unit value when the damage can be assessed effectively.

Department	CIVIL ENGINEERING	Student's signature	
Field of study	CIVIL ENGINEERING	Advisor's signature	
Academic year	2003		

ACKNOWLEDGEMENTS

TABLE OF CONTENTS

TABLE OF CONTENTS (Cont.)

TABLE OF CONTENTS (Cont.)

LIST OF TABLES

LIST OF TABLES (Cont.)

LIST OF FIGURES

LIST OF FIGURES (Cont.)

LIST OF FIGURES (Cont.)

LIST OF FIGURES (Cont.)

LIST OF FIGURES (Cont.)

LIST OF FIGURES (Cont.)

LIST OF FIGURES (Cont.)

LIST OF FIGURES (Cont.)

LIST OF FIGURES (Cont.)

LIST OF FIGURES (Cont.)

CHAPTER 1

INTRODUCTION

1.1 Introduction

Structural parameter estimation from the measured modal response of a structure can be used as an effective means for assessing the structural damage (Doebling et al. 1996; Shin and Hjelmstad 1996). This method requires a modal test in which a structure is stimulated by being shaken under the resonance forces at the natural frequencies of the structure. The modal response of the structure (i.e., natural frequencies and mode shapes) is obtained from the signals of the displacement sensors, which are installed at certain locations on the structure.

The assessment of damage for structural systems using the measured modal response is difficult because of the error (or noise) in the measurements (Shin and Hjelmstad 1994; Law et al. 1998). Generally, if the measured data are noise-free the damage of a structural member can be evaluated directly from the difference between the current and the baseline parameter values. However, with the presence of the measurement noise, the parameter values of a structural member can differ from the baseline values even when the member is not damaged. Thus, it is important to account for the effect of measurement errors in the estimation of the member parameters.

The structural damage assessment method proposed in the current study compares the statistical distribution of the system parameters for the current and the baseline structures to account for the sensitivity of the system parameters to the noise. The statistical distribution of the parameters can be obtained from a Monte Carlo sample of the parameter estimates which is generated by repeating the parameter estimation algorithms many times using different sets of measured data. Each of the measurement data sets can be simulated by adding a random error to the noise-free measured data. Hence, the parameter estimates can be treated as random variables.

In the current study we apply the output error estimator (OEE) of Banan and Hjelmstad (1993) to estimate parameters for the structures under consideration and we use the measured data perturbation scheme of Shin and Hjelmstad (1997) to simulate the measured response of the structures. Furthermore, we adopt the sensitivity-based method and the optimum sensitivity-based method of Araki and Hjelmstad (2001) as alternatives to the Monte Carlo simulation method in the statistical parameter estimation process. In these methods, the parameter estimation problem is solved only once to find the solution from the mean of the measured response. Upon completion of the statistical parameter estimation algorithm, a numerical integration scheme is applied to the statistical distribution of the system parameters to compute the probability of damage. The computed probability indicates the likelihood of a member being damaged as a function of the level of damage. To reduce the degree of instabilities of solutions to the statistical parameter estimation problem, a regularization scheme of Pothisiri and Vatcharatanyakorn (2002) is adopted by adding a regularization function algebraically as a penalty term to the parameter estimation objective function for the output error estimator (OEE) of Banan and Hjelmstad (1993). The proposed method is referred to as the regularized output error estimator (ROEE).

There are many benefits and drawbacks to the statistical damage assessment algorithm using the above mentioned statistical parameter estimation methods—the Monte Carlo simulation method, the sensitivity-based method, and the optimum sensitivity-based method—in conjunction with the OEE and ROEE algorithms. Generally, the performance of a statistical damage assessment method can be identified by the accuracy of the method in assessing damage. For the current study, a statistical identification error (SIE) is proposed to examine the variation in the accuracy of the damage assessment algorithm from using different methods of statistical parameter estimation.

1.2 Literature Review of Parameter Estimation and Damage Assessment

The modal test of a structure—in which the entire structure is excited by a resonant forced vibration and the structural response is measured at certain locations—has shown promise as a tool in global damage detection (Doebling et al. 1996, Shin and Hjelmstad 1996). The measured response of a structural system (i.e., natural frequencies and mode shapes), obtained from a modal test, can be used to estimate the system parameters. The assessment of damage is carried out by monitoring changes in the values of parameters for the structural systems.

It has been shown that the least-squares minimization of the error function of the measured data from a static force test can be used to estimate the stiffness parameters of a reinforced concrete bridge structure (Sanayei and Scampoli 1991). In particular, the error function, which is nonlinear, is transformed to a linear function by using the first-order derivatives of the Taylor's series approximation. The linearized error function is in the form of a Euclidean norm of the difference between the measured stiffness parameters and the stiffness parameters from finite element models. The minimization problem is solved iteratively until the error function approaches zero.

The problem of structural parameter estimation from the measured response can be cast as the least-squares minimization of the equation errors or the mode output errors (Banan and Hjelmstad 1993). The minimization problem can be solved by using the recursive quadratic programming (RQP) scheme. In this method, the nonlinear objective function is approximated by a series of quadratic functions and the corresponding constraints are approximated with linear functions. A set of a priori parameter estimates is required to initiate the algorithm, and the parameter values in the next iterations are computed from the estimated step lengths and search directions of the previous iterations.

The estimation of the system parameters in the present study uses the measured modal response of the structure under consideration as input to the parameter estimation algorithm. These response measurements are unavoidably contaminated with measurement errors. The measurement error can make the estimated parameters for the current structure to be different from the baseline values even when there is no damage, leading to an incorrect assessment of damage for the structure (Shin and

Hjelmstad 1994 and Law et al. 1998). To account for the sensitivity of the parameter estimates to the measurement error, a statistical method in which the probability density function of the system parameters for the healthy and the damaged structural systems can be used to assess damage of the structural members (Papadopoulas and Garcia 1998).

Yeo et al. (2000) proposed a method for the statistical damage assessment of members of a structure by comparing between the probability density function of the healthy and damaged system parameters. A hypothesis test is used to identify whether to accept or to refuse the existence of damage in members of the structure.

Pothisiri and Hjelmstad (2003) proposed a statistical damage assessment scheme that compares the statistical distribution of the estimated parameters for members of the current and the baseline structures. In this method, the output error least-square estimator of Banan and Hjelmstad (1993) is used in conjunction with the measured data perturbation scheme of Shin and Hjelmstad (1997) to generate a Monte Carlo sample of parameter estimates from a set of noisy measurements. The generated set of parameter estimates is used to construct the statistical distribution of the system parameters that is used to assess damage.

The statistical distribution of the parameter estimates which is used as the key component to the statistical damage assessment methods may be obtained by using various algorithms. One such algorithm is to estimate the statistical indices of the parameter estimates and use them as the bases for constructing the required statistical distribution by assuming certain distribution functions. The statistical indices of the parameter estimates (i.e., the mean and the covariance matrix) can generally be obtained by using a statistical parameter estimation algorithm. For the current study we adopt the sensitivity-based method and the optimum sensitivity-based method proposed by Araki and Hjelmstad (2001) to perform statistical parameter estimation.

One of the key concerns in solving a parameter estimation problem is the instabilities of solutions arising from using spatially sparse and noise-polluted measurement data. To reduce the degree of instabilities of solutions to the parameter estimation problem investigated in the current study, we adopt the regularization scheme proposed by Pothisiri and Vatcharatanyakorn (2002). In this technique, a

regularization function is added to the initial objective function as a penalty term that eradicates the out-of-bound solutions. With the improvement in the accuracy of the estimated system parameters by using the regularization technique, the performance of a statistical damage assessment scheme is expected to also improve. The technique is applied to different methods of the statistical parameter estimation—the Monte Carlo simulation method, the sensitivity-based method, and the optimum sensitivity-based method.

1.3 Research Objectives

The main objective of this research is to develop an effective damage assessment algorithm for structural systems from noise-polluted modal response. The present study investigates a statistical damage assessment scheme in which the statistics of the structural parameters are obtained by using three different methods of statistical parameter estimation—the Monte Carlo simulation method, the sensitivity-based method, and the optimum sensitivity-based method. These methods are also used in conjunction with two optimization algorithms—the output error estimator (OEE) and the regularized output error estimator (ROEE)—to perform statistical parameter estimations. We characterize a structural system by using a parameterized finite-element model, and we infer damage from changes in the element parameters in the finite-element model of the structure. To account for the effect of the measurement noise on the parameter estimates, the measured data perturbation scheme of Shin and Hjelmstad (1994) is used to generate a set of noisy measurement data to be used in the statistical parameter estimation algorithms. The damage is assessed by comparing the statistical distribution of the member parameters for the damaged and the associated baseline structure.

The key objectives of this research can be summarized in the following list

1.3.1   To implement three different methods of statistical parameter estimation, i.e. the Monte Carlo simulation method, the optimum sensitivity-based method and the sensitivity-based method and compare their performance when used in conjunction with the current statistical damage assessment method.

1.3.2 To evaluate the effectiveness of using the regularization method in the structural parameter estimation algorithm to improve the accuracy of the statistical damage assessment scheme.

1.3.3 To improve the computation of the statistical distribution of the parameter estimates by using efficient methods of statistical parameter estimation (the sensitivity-based method and the optimum sensitivity-based method).

1.3.4 To develop a computer program that can assess damage of structural systems with various types of structural elements, e.g. trusses, frames, beams, etc.

1.3.5 To device an algorithm that is capable of assessing damage in structural members with multiple stiffness parameters.

1.4 Scope of Research

The aim of the current research is to investigate the performance improvement of the statistical damage assessment method proposed by Pothisiri and Hjelmstad (2003) by using different methods of statistical parameter estimation and the regularization technique. For a structure with members consisting of multiple stiffness parameters, the statistical damage assessment algorithm is applied by using the optimum sensitivity-based method and the regularization technique in the statistical parameter estimation. Numerical simulation studies are employed to examine the capabilities of the investigated algorithms in assessing damage of two model structures; a simply-supported bridge truss and a two-story braced frame. The numerical simulation procedure is selected over the real case study because our objective is to quantify the performance of the algorithm rather than to plainly illustrate its use. In the simulation process, the measured data are generated by adding proportional random errors to the analytical modal response of a finite-element model of the structure. This allows us to investigate different levels of noise in the measurements by simply varying the amplitude of the imposed random errors.

The assumptions adopted in the current study are listed as follows:

1.4.1 A refined finite element model of the structure is defined.

1.4.2 The baseline or undamaged properties of the structure are known.

1.4.3   The stiffness parameters, i.e. the axial stiffness (EA), the bending stiffness (EI) and the shear stiffness (GA) decrease from the baseline values as a result of damage while the mass density (ρ) remains constant.

1.4.4   For a structure with members consisting of a single stiffness parameter, damage is defined as a drop in a member stiffness parameter between two discrete time points. For a structure with members consisting of multiple stiffness parameters, damage is modeled by reducing different stiffness parameters of the structural members.

1.4.5   The structure is linear elastic.

1.4.6   For the measurement data only the mode shapes are subject to measurement noise whereas the natural frequencies are noise-free.

1.4.7   The mode shapes for all modes and degrees of freedom of the structure are used as the measurement data.

1.4.8   The measurement noise is represented by the uniform random variates.

The manuscript consists of six chapters. Chapter 1 is an introduction. A number of research works in the areas of statistical parameter estimation and damage assessment are briefly summarized in this chapter. Chapter 2 addresses the issue of the concept, principle and theory of the statistical parameter estimation and damage assessment. The three algorithms of statistical parameter estimation—i.e., the Monte Carlo simulation method, the sensitivity-based method and the optimum sensitivity-based method—using the output error estimator (OEE) of Banan and Hjelmstad (1993) and the regularized output error estimator (ROEE) proposed by Pothisiri and Vatcharatanyakorn (2002) are described. Based on the statistical distribution of the system parameters, a procedure for assessing the severity of damage proposed by Pothisiri and Hjelmstad (2001) is used to compare the results among the three methods of statistical parameter estimation that are used in conjunction with the OEE and ROEE algorithms. In Chapter 3, simulation studies are carried out for a two-dimensional, simply supported bridge truss. The simulated single component of damage and the two-damage cases are investigated for different levels of noise in the measurements. Through simulation studies, the performance of each of the investigated algorithms in assessing damage is illustrated. In Chapter 4, statistical

simulation studies are carried out for the same structure as in Chapter 3. A statistical identification error (SIE) is devised to quantify the levels of performance for each algorithm. One hundred different damage cases of the single-damaged-member cases, the two-damaged-member cases, and the three-damaged-member cases are investigated by examining the SIE values for different levels of noise in the measurements. The performance of each of the investigated algorithms in assessing damage is evaluated by using the plot of the SIE values and the probability of success in detecting damage with respect to different levels of noise in the measurements. In Chapter 5, the statistical damage assessment algorithm described in Chapter 2 is applied to a two-story braced frame with members consisting of multiple stiffness parameters. Again, the simulated cases of single component and multiple components of damage are investigated for different levels of measurement noise. The damage is modeled by reducing different stiffness parameters of the structural members. Chapter 6 summarizes principal findings obtained from the current study and discusses future research work.

CHAPTER 2

STRUCTURAL PARAMETER ESTIMATION AND DAMAGE ASSESSMENT

2.1 Introduction

Damage in civil engineering structures is inevitable in the face of many uncontrollable factors such as fault topographical features of the structural supports, hazardous surrounding climates, and severe imposed loading conditions. Damage to a structural system can generally be characterized by the reduction of the overall stiffness of the structure. The level of the overall structural stiffness reduction is indicated by the degree of damage to the structural components, i.e. members of the structural system. By using a straightforward parameterization scheme for the structural stiffness, damage can be defined as a reduction of the stiffness parameters of the structural members between two discrete time inferences. The schematic representation of damage is illustrated in Figure 2.1.
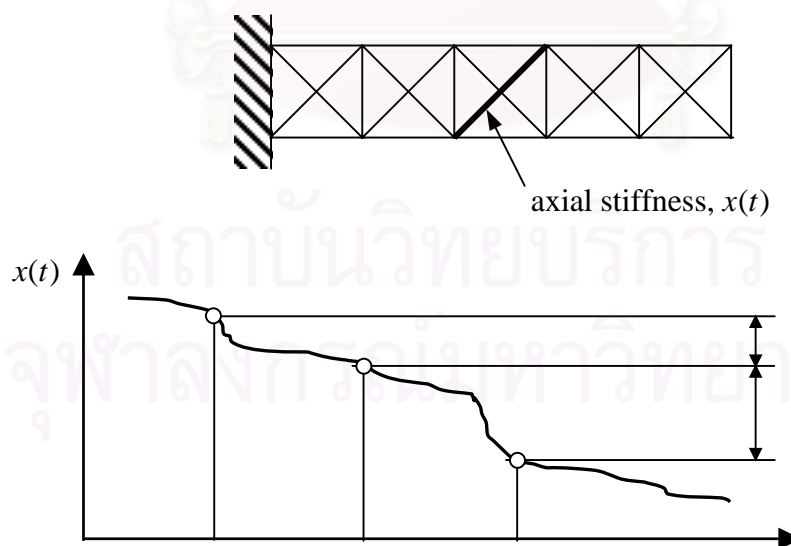
Figure 2.1 The definition of damage as a drop in element constitutive parameter value.

The structure in Figure 2.1 is a truss structure with each member consisting of a single stiffness parameter x (i.e., the axial stiffness). A drop in this parameter, therefore, directly indicates damage of the truss. However, the structures in general may be modeled with multiple stiffness parameters to characterize the distinct modes of deformation (i.e., axial, bending, and shear). For these general cases the same definition of damage still holds but the assessment is somewhat more complicated as will be discussed later.

For the current study we adopt the method of Pothisiri and Hjelmstad (2003) that compares the probability density distribution of the estimated system parameters for the baseline and the current structures to assess damage. A key step to the implementation of the damage assessment method is a statistical parameter estimation of the structure. We select three methods to carry out the estimation, i.e., the Monte Carlo simulation, the sensitivity-based method and the optimum sensitivity method. These methods are used in conjunction with the output error estimator (OEE) of Banan and Hjelmstad (1993) to estimate the system parameters from sparse and noisy data sets. Further, we adopt the regularized output error estimator (ROEE) of Pothisiri and Vatcharatanyakorn (2002) to reduce the degree of instabilities of solutions to the parameter estimation problem. The numerical study of the proposed algorithms by using an 11-degree-of-freedom truss model is presented in Chapter 3 and Chapter 4 to illustrate the implementation of the process and to investigate the performance of the algorithms.

2.2 System Parameter Estimation from Modal Response

The algorithm selected for the estimation of the system parameters in the current study is cast in the form of a constrained least-squares minimization problem (Banan and Hjelmstad 1993):

$$\underset{\mathbf{x}\in\Re^{N_p}}{\text{Minimize}} \quad J_E(\mathbf{x},\hat{\mathbf{\Phi}})=\frac{1}{2}\sum_{i=1}^{N_m}\delta_i\mathbf{e}_i(\mathbf{x},\hat{\mathbf{\Phi}}_i)\cdot\mathbf{e}_i(\mathbf{x},\hat{\mathbf{\Phi}}_i) \qquad (2.1)$$

$$\text{subject to} \quad \mathbf{c}_L^0 \leq \mathbf{x} \leq \mathbf{c}_U^0$$

in which

$\mathbf{x}$ is the system parameters;

$\hat{\boldsymbol{\Phi}}$ is the vector of measurements comprising N_m mode shapes which is defined as $\hat{\boldsymbol{\Phi}} \equiv \left\{ \hat{\boldsymbol{\Phi}}_1^T, \hat{\boldsymbol{\Phi}}_2^T, ..., \hat{\boldsymbol{\Phi}}_{N_m}^T \right\}^T$ where $\hat{\boldsymbol{\Phi}}_i$ is the measured mode shape for the ith vibration mode;

$\mathbf{e}_i(\mathbf{x}, \hat{\boldsymbol{\Phi}}_i)$ is the error function for the ith mode;

δ_i is the weight factor for the ith mode;

N_m is the number of modes with the measured data;

N_p is the number of stiffness parameters in the model;

$\mathbf{c}_L^0$ is the lower constraints of $\mathbf{x}$;

and $\mathbf{c}_U^0$ is the upper constraints of $\mathbf{x}$.

Pothisiri and Vatcharatanyakorn (2002) have shown that the Tikhonov regularization technique can be used to alleviate the problem of discontinuities of solutions to the above parameter estimation problem by adding a regularization function to the objective function $J_E(\mathbf{x}, \hat{\boldsymbol{\Phi}})$. The regularized output error estimator (ROEE) is expressed as

$$\underset{\mathbf{x} \in \mathfrak{R}^{N_p}}{\text{Minimize}} \quad J(\mathbf{x}, \hat{\boldsymbol{\Phi}}) = \frac{1}{2} \sum_{i=1}^{N_m} \delta_i \mathbf{e}_i(\mathbf{x}, \hat{\boldsymbol{\Phi}}_i) \cdot \mathbf{e}_i(\mathbf{x}, \hat{\boldsymbol{\Phi}}_i) + \frac{1}{2} \alpha^2 \left\| \mathbf{x} - \mathbf{x}_0 \right\|^2 \quad (2.2)$$

$$\text{subject to} \quad \mathbf{c}_L^0 \leq \mathbf{x} \leq \mathbf{c}_U^0$$

in which

α is the regularization factor;

and $\mathbf{x}_0$ is the *a priori* estimates of the system parameters which are normally taken as zero.

The derivation of the error function $\mathbf{e}_i(\mathbf{x}, \hat{\mathbf{\Phi}}_i)$ in equations (2.1) and (2.2) is based upon the generalized eigenvalue problem of the free undamped vibrational response for the ith vibration mode of a structure.

$$\mathbf{K}(\mathbf{x})\mathbf{\Phi}_i = \lambda_i \mathbf{M}\mathbf{\Phi}_i \tag{2.3}$$

in which

$\quad$ **K(x)** $\quad$ is the linear stiffness matrix of the structural model that is parameterized by the parameters **x** ;

$\quad$ λ_i $\quad$ is the eigenvalue (the square of the natural frequency) for the ith vibration mode;

$\quad$ $\mathbf{\Phi}_i$ $\quad$ is the the eigenvector (mode shape) for the ith vibration mode;

and $\quad$ **M** $\quad$ is the mass matrix which is composed of the material density properties and is assumed to be constant.

Following the work of Pothisiri and Hjelmstad (2001), the first N_m natural frequencies and natural modes are assumed to be obtained from a modal test. For each mode, it is assumed that the frequency is measured accurately and that the mode shape is sampled at certain discrete locations. These measurement locations correspond with the degrees of freedom of the finite element model of the structure. In particular, the set of degrees of freedom associated with the measurement locations of the test structure is defined as $\hat{\aleph}$ and the set of remaining degrees of freedom is defined as $\bar{\aleph}$. Moreover, the number of measured and unmeasured degrees of freedom are denoted, respectively, as $\hat{N}_d$ and $\bar{N}_d$. As such, the measured eigenvector and the structural system matrices can be partitioned based on these two sets. The ith eigenvector can be reordered and partitioned as

$$\tilde{\mathbf{\Phi}}_i \equiv \mathbf{P}\mathbf{\Phi}_i = \begin{bmatrix} \hat{\mathbf{\Phi}}_i \\ \hline \bar{\mathbf{\Phi}}_i \end{bmatrix} \tag{2.4}$$

in which

    $\mathbf{P}$ is a column permutation of the identity matrix;

    $\hat{\mathbf{\Phi}}_i$ is the submatrix of the eigenvector components for the ith vibration

                mode associated with the measured degrees of freedom;

and $\bar{\mathbf{\Phi}}_i$ is the submatrix of the eigenvector components for the ith vibration

                mode associated with the unmeasured degrees of freedom.

The structural matrices can be reordered as

$$\tilde{\mathbf{K}} \equiv \mathbf{PKP}^{\mathbf{T}}; \text{ and } \tilde{\mathbf{M}} \equiv \mathbf{PMP}^{\mathbf{T}}. \tag{2.5}$$

The reordered mass matrix can be partitioned as follows

$$\tilde{\mathbf{M}} = \begin{bmatrix} \tilde{\mathbf{M}}_{11} & \tilde{\mathbf{M}}_{12} \\ \tilde{\mathbf{M}}_{21} & \tilde{\mathbf{M}}_{22} \end{bmatrix} \tag{2.6}$$

in which

    $\tilde{\mathbf{M}}_{i1}$ is the portion of the mass matrix associated with the measured

                degrees of freedom of the structural model;

and $\tilde{\mathbf{M}}_{i2}$ is the portion of the mass matrix associated with the unmeasured

                degrees of freedom of the structural model.

The partitioned mass matrices are defined as

$$\bar{\mathbf{M}} \equiv \begin{bmatrix} \mathbf{0} & \tilde{\mathbf{M}}_{12} \\ \tilde{\mathbf{M}}_{21} & \tilde{\mathbf{M}}_{22} \end{bmatrix}; \text{ and } \hat{\mathbf{M}} \equiv \begin{bmatrix} \tilde{\mathbf{M}}_{11} \\ \mathbf{0} \end{bmatrix} \tag{2.7}$$

With a given definition of the matrix $\mathbf{B}_i(\mathbf{x}) \equiv \tilde{\mathbf{K}}(\mathbf{x}) - \lambda_i \bar{\mathbf{M}}$, a straightforward manipulation of equation (2.3) yields the equivalent expression

$$\mathbf{B}_i(\mathbf{x})\tilde{\mathbf{\Phi}}_i = \lambda_i\hat{\mathbf{M}}\hat{\mathbf{\Phi}}_i \qquad (2.8)$$

The right hand side of the above equation involves only the measured response $\hat{\mathbf{\Phi}}_i$ rather than a complete response vector. Also, it should be noted that $\mathbf{B}_i(\mathbf{x})$ is symmetric, which is different from the definition of Banan and Hjelmstad (1993). With these definitions, a measure of error for the output error estimator can be defined as

$$\mathbf{e}_i(\mathbf{x},\hat{\mathbf{\Phi}}_i) \equiv \hat{\mathbf{\Phi}}_i - \lambda_i\mathbf{Q}\mathbf{B}_i^{-1}(\mathbf{x})\hat{\mathbf{M}}\hat{\mathbf{\Phi}}_i \qquad (2.9)$$

in which

$\mathbf{Q}$ is the boolean matrix extracting the components of the response vector associated with measured degrees of freedom from the complete eigenvector by the relationship of $\hat{\mathbf{\Phi}}_i = \mathbf{Q}\mathbf{\Phi}_i$.

2.3 Statistical Parameter Estimation

The statistical parameter estimation techniques can be used to account for the sensitivity of the solution of a parameter estimation problem due to the uncertainty of the measured data. In these methods one can obtain, for the estimated system parameters $\mathbf{x}$, the mean $\bar{\mathbf{x}}$ and the covariance matrix $\mathbf{R}^{\mathbf{x}}$ from the mean $\bar{\mathbf{\Phi}}$ and the covariance matrix $\mathbf{R}^{\mathbf{\Phi}}$ of the measurements $\hat{\mathbf{\Phi}}$, respectively. The process of a statistical parameter estimation method is illustrated schematically in Figure 2.2.

$\bar{\mathbf{\Phi}}$ and $\mathbf{R}^{\mathbf{\Phi}}$ $\longrightarrow$ | Statistical Parameter Estimation | $\longrightarrow$ $\bar{\mathbf{x}}$ and $\mathbf{R}^{\mathbf{x}}$
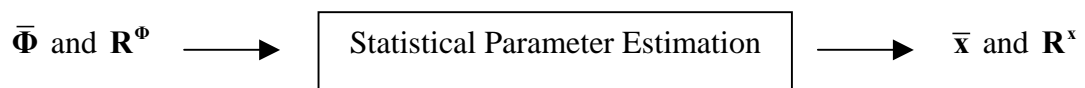
Figure 2.2 The process of statistical parameter estimation.

The problem of the system parameters estimation from the measured response is generally cast as a least-squares minimization problem. If the error function is a linear function of the system parameters, the least-squares minimization is a quadratic programming problem, and a closed-form expression of the estimates of the system parameters is possible. Furthermore, if the error function is linear with respect to not only the system parameters but also to the measured data, one can obtain closed-form expressions for $\bar{x}$ and $\mathbf{R}^x$, respectively, in terms of $\bar{\Phi}$ and $\mathbf{R}^\Phi$. On the other hand, if the error function is nonlinear, iterative procedures are generally required to solve the nonlinear optimization problem. Alternatively, we may use the methods providing a second-order or higher-order approximation of the statistical indices of the system parameters which allow us to assess the bias due to the nonlinearities in the error function. Many parameter estimation problems in the field of structural mechanics fall into this class of nonlinear optimization problems. We shall classify the statistical parameter estimation methods frequently used in the literature into the following three categories: the Monte Carlo simulation method, the sensitivity-based method, and the optimum sensitivity-based method.

In the current study, we use the output error estimator (OEE) proposed by Banan and Hjelmstad (1993) and the regularized output error estimator (ROEE) proposed by Pothisiri and Vatcharatanyakorn (2002) in conjunction with the selected statistical parameter estimation schemes for the performance investigation of the present damage assessment method. The derivations of these estimators are summarized as follows.

The output error estimator (OEE) proposed by Banan and Hjelmstad (1993) as previously shown in equation (2.1) can be rewritten by replacing the dot product of the error function with a norm quantity. The resulting expression is in the following form

$$\underset{\mathbf{x} \in \Re^{N_p}}{\text{Minimize}} \quad J_E(\mathbf{x}) = \frac{1}{2} \sum_{i=1}^{N_m} \delta_i \left\| \hat{\Phi}_i - \Phi_i^c(\mathbf{x}) \right\|^2 \qquad (2.10)$$

$$\text{subject to} \quad \mathbf{c}(\mathbf{x}) \leq \mathbf{0}$$

in which

$\hat{\Phi}_i$ is the measured mode shape for the ith mode;

and $\Phi_i^c(\mathbf{x})$ is the equivalent mode shape for the ith mode which is define as

$$\Phi_i^c(\mathbf{x}) = \lambda\mathbf{QB}_i^{-1}(\mathbf{x})\hat{\mathbf{M}}\hat{\Phi}_i .$$

For the current study we adopt the recursive quadratic programming (RQP) technique to solve the above nonlinear least-squares minimization problem. In this technique, the estimated system parameters in the $(k+1)$th iteration of the minimization process can be computed as

$$\mathbf{x}_{k+1} = \mathbf{x}_k + \beta_k\mathbf{d}_k \tag{2.11}$$

in which

β_k is the step length for the kth iteration of the minimization algorithm;

and $\mathbf{d}_k$ is the search direction for the kth iteration of the minimization algorithm.

By using the Taylor's series expansion of the objective function in equation (2.10) up to the second-order derivative with respect to the system parameters at the kth iteration $\mathbf{x}_k$, we obtain the following expression

$$J_E(\mathbf{x}_{k+1}) = J_E(\mathbf{x}_k + \mathbf{d}_k) \approx J_E(\mathbf{x}_k) + \nabla J_E(\mathbf{x}_k)^T\mathbf{d}_k + \frac{1}{2}\mathbf{d}_k^T\nabla^2 J_E(\mathbf{x}_k)\mathbf{d}_k \tag{2.12}$$

Similarly, we can use the first-order Taylor's series expansion to linearize the constraints

$$\mathbf{c}(\mathbf{x}_{k+1}) = \mathbf{c}(\mathbf{x}_k + \mathbf{d}_k) \approx \mathbf{c}(\mathbf{x}_k) + \nabla\mathbf{c}(\mathbf{x}_k)^T\mathbf{d}_k \tag{2.13}$$

The optimum search direction for the kth iteration of the minimization process $\mathbf{d}_k$ can be obtained from the quadratic subproblem

$$\underset{\mathbf{d}_k}{\text{Minimize}} \quad \frac{1}{2}\mathbf{d}_k^{\mathrm{T}}\nabla^2 J_E(\mathbf{x}_k)\mathbf{d}_k + \nabla J_E(\mathbf{x}_k)^{\mathrm{T}}\mathbf{d}_k \tag{2.14}$$

$$\text{subject to} \quad \mathbf{c}(\mathbf{x}_k) + \nabla\mathbf{c}(\mathbf{x}_k)^{\mathrm{T}}\mathbf{d}_k \leq \mathbf{0}$$

The gradient of the objective function with respect to the system parameters $\mathbf{x}_k$ is expressed as

$$\nabla J_E(\mathbf{x}) = \sum_{i=1}^{N_m} \delta_i \nabla \mathbf{e}_i(\mathbf{x})^{\mathrm{T}} \mathbf{e}_i(\mathbf{x}) = -\sum_{i=1}^{N_m} \delta_i \mathbf{S}_i^{\mathrm{T}} \mathbf{e}_i(\mathbf{x}) \tag{2.15}$$

in which

$\mathbf{S}_i$ is the sensitivity matrix of the parameter estimates for the ith measured mode which is given by $\mathbf{S}_i = \nabla \mathbf{e}_i(\mathbf{x})$.

The Gauss-Newton approximation method can be used to evaluate the Hessian matrix of the parameter estimates by neglecting the second-order derivative term of the error function. The resulting expression for the positive-definite Hessian matrix can be written as

$$\mathbf{H} = \sum_{i=1}^{N_m} \delta_i \nabla \mathbf{e}_i(\mathbf{x})^{\mathrm{T}} \nabla \mathbf{e}_i(\mathbf{x}) + \sum_{i=1}^{N_m} \delta_i \nabla^2 \mathbf{e}_i(\mathbf{x}) \mathbf{e}_i(\mathbf{x})$$

$$\approx \sum_{i=1}^{N_m} \delta_i \nabla \mathbf{e}_i(\mathbf{x})^{\mathrm{T}} \nabla \mathbf{e}_i(\mathbf{x}) \tag{2.16}$$

$$\approx \sum_{i=1}^{N_m} \delta_i \mathbf{S}_i^{\mathrm{T}} \mathbf{S}_i$$

Substituting $\nabla J_E(\mathbf{x})$ and $\mathbf{H}$ from equations (2.15) and (2.16), respectively, into equation (2.14) leads to

$$\underset{\mathbf{d}_k}{\text{Minimize}} \quad \frac{1}{2}\mathbf{d}_k^{\mathrm{T}}\mathbf{H}_k\mathbf{d}_k - \sum_{i=1}^{N_m} \delta_i \mathbf{d}_k^{\mathrm{T}} \mathbf{S}_i^{k^{\mathrm{T}}} \mathbf{e}_i^k \tag{2.17}$$

$$\text{subject to} \quad \mathbf{A}_k\mathbf{d}_k \leq \mathbf{b}_k$$

where
$$\mathbf{A}_k = \nabla \mathbf{c}(\mathbf{x}_k)^{\mathrm{T}};\ \mathbf{b}_k = -\mathbf{c}(\mathbf{x}_k);\ \text{and}\ \mathbf{e}_i^k = \mathbf{e}_i^k(\mathbf{x}_k) \tag{2.18}$$

and the subscript k denotes the kth iteration of the minimization procedures.

Equation (2.17) can be expressed in the form of a Lagrangian function as

$$\ell(\mathbf{d}_k, \boldsymbol{\Lambda}_k) = \frac{1}{2}\mathbf{d}_k^{\mathrm{T}}\mathbf{H}_k\mathbf{d}_k - \sum_{i=1}^{N_m} \delta_i \mathbf{d}_k^{\mathrm{T}} \mathbf{S}_i^{k^{\mathrm{T}}} \mathbf{e}_i^k + \boldsymbol{\Lambda}_k^{\mathrm{T}}(\mathbf{A}_k\mathbf{d}_k - \mathbf{b}_k) \tag{2.19}$$

in which

$\boldsymbol{\Lambda}_k$ is the vector of Lagrange multipliers for the kth iteration of the minimization process.

The first-order essential conditions for the optimum search direction $\mathbf{d}_k$ are

$$\nabla_{\mathbf{d}_k}\ell(\mathbf{d}_k, \boldsymbol{\Lambda}_k) = 0 \quad \rightarrow \quad \mathbf{H}_k\mathbf{d}_k - \sum_{i=1}^{N_m} \delta_i \mathbf{S}_i^{k^{\mathrm{T}}} \mathbf{e}_i^k + \mathbf{A}_k^{\mathrm{T}}\boldsymbol{\Lambda}_k = 0 \tag{2.20}$$

and
$$\nabla_{\boldsymbol{\Lambda}_k}\ell(\mathbf{d}_k, \boldsymbol{\Lambda}_k) = 0 \quad \rightarrow \quad \mathbf{A}_k\mathbf{d}_k - \mathbf{b}_k = 0 \tag{2.21}$$

Note that equation (2.21) is satisfied when the constraints are active at the kth iteration. In the matrix form, equations (2.20) and (2.21) can be rewritten as

$$\begin{bmatrix} \mathbf{H}_k & \mathbf{A}_k^{\mathrm{T}} \\ \mathbf{A}_k & \mathbf{0} \end{bmatrix}\begin{Bmatrix} \mathbf{d}_k \\ \boldsymbol{\Lambda}_k \end{Bmatrix} = \begin{Bmatrix} \sum_{i=1}^{N_m} \delta_i \mathbf{S}_i^{k^{\mathrm{T}}} \mathbf{e}_i^k \\ \mathbf{b}_k \end{Bmatrix} \tag{2.22}$$

Solving equation (2.22) leads to

$$\mathbf{\Lambda}_k = -\left[\mathbf{A}_k\mathbf{H}_k^{-1}\mathbf{A}_k^{\mathrm{T}}\right]^{-1}\left[\mathbf{b}_k - \mathbf{A}_k\mathbf{H}_k^{-1}\sum_{i=1}^{N_m}\delta_i\mathbf{S}_i^{k^{\mathrm{T}}}\mathbf{e}_i^k\right] \tag{2.23}$$

and
$$\mathbf{d}_k = \mathbf{H}_k^{-1}\left[\sum_{i=1}^{N_m}\delta_i\mathbf{S}_i^{k^{\mathrm{T}}}\mathbf{e}_i^k - \mathbf{A}_k^{\mathrm{T}}\mathbf{\Lambda}_k\right] \tag{2.24}$$

The regularized output error estimator (ROEE) proposed by Pothisiri and Vatcharatanyakorn (2002) as shown in equation (2.2) can also be rewritten as

$$\underset{\mathbf{x}\in\mathfrak{R}^{N_p}}{\text{Minimize}} \quad J(\mathbf{x}) = \frac{1}{2}\sum_{i=1}^{N_m}\delta_i\left\|\hat{\mathbf{\Phi}}_i - \mathbf{\Phi}_i^c(\mathbf{x})\right\|^2 + \frac{1}{2}\alpha^2\left\|\mathbf{x}-\mathbf{x}_0\right\|^2 \tag{2.25}$$

subject to $\quad \mathbf{c}(\mathbf{x})\leq\mathbf{0}$

Again, we can use the Taylor's series expansion to approximate the objective function in the above minimization problem at the $(k+1)$th iteration from its derivatives with respect to the estimated parameters at the kth iteration $\mathbf{x}_k$.

$$\begin{aligned}J(\mathbf{x}_{k+1}) &= J(\mathbf{x}_k + \mathbf{d}_k)\\ &\approx J(\mathbf{x}_k) + \nabla J_E(\mathbf{x}_k)^{\mathrm{T}}\mathbf{d}_k + \frac{1}{2}\mathbf{d}_k^{\mathrm{T}}\nabla^2 J_E(\mathbf{x}_k)\mathbf{d}_k + \alpha^2\left[\frac{1}{2}\mathbf{d}_k^{\mathrm{T}}\mathbf{d}_k + \mathbf{d}_k^{\mathrm{T}}(\mathbf{x}_k - \mathbf{x}_0)\right]\end{aligned} \tag{2.26}$$

To obtain the optimum search direction $\mathbf{d}_k$, we use the following quadratic subproblem

$$\underset{\mathbf{d}_k}{\text{Minimize}} \quad \frac{1}{2}\mathbf{d}_k^{\mathrm{T}}\nabla^2 J_E(\mathbf{x}_k)\mathbf{d}_k + \nabla J_E(\mathbf{x}_k)^{\mathrm{T}}\mathbf{d}_k + \alpha^2\left[\frac{1}{2}\mathbf{d}_k^{\mathrm{T}}\mathbf{d}_k + \mathbf{d}_k^{\mathrm{T}}(\mathbf{x}_k - \mathbf{x}_0)\right] \tag{2.27}$$

subject to $\quad \mathbf{c}(\mathbf{x}_k) + \nabla\mathbf{c}(\mathbf{x}_k)^{\mathrm{T}}\mathbf{d}_k \leq \mathbf{0}$

By substituting $\nabla J_E(\mathbf{x})$ and $\mathbf{H}$ from equations (2.15) and (2.16), respectively, into equation (2.27), we obtain the following expression

$$\text{Minimize}_{\mathbf{d}_k} \quad \frac{1}{2}\mathbf{d}_k^T\mathbf{H}_k\mathbf{d}_k - \sum_{i=1}^{N_m}\delta_i\mathbf{d}_k^T\mathbf{S}_i^{k^T}\mathbf{e}_i^k + \alpha^2\left[\frac{1}{2}\mathbf{d}_k^T\mathbf{d}_k - \mathbf{d}_k^T(\mathbf{x}_0 - \mathbf{x}_k)\right] \tag{2.28}$$

subject to $\quad \mathbf{A}_k\mathbf{d}_k \leq \mathbf{b}_k$

The Lagrangian function for the above minimization problem can be expressed as

$$\ell(\mathbf{d}_k, \mathbf{\Lambda}_k) = \frac{1}{2}\mathbf{d}_k^T\mathbf{H}_k\mathbf{d}_k - \sum_{i=1}^{N_m}\delta_i\mathbf{d}_k^T\mathbf{S}_i^{k^T}\mathbf{e}_i^k + \alpha^2\left[\frac{1}{2}\mathbf{d}_k^T\mathbf{d}_k - \mathbf{d}_k^T(\mathbf{x}_0 - \mathbf{x}_k)\right] + \mathbf{\Lambda}_k^T(\mathbf{A}_k\mathbf{d}_k - \mathbf{b}_k) \tag{2.29}$$

The first-order essential conditions for the optimum search direction $\mathbf{d}_k$ are

$$\nabla_{\mathbf{d}_k}\ell(\mathbf{d}_k, \mathbf{\Lambda}_k) = \mathbf{0} \quad \rightarrow \quad \mathbf{H}_k\mathbf{d}_k + \alpha^2\mathbf{d}_k - \sum_{i=1}^{N_m}\delta_i\mathbf{S}_i^{k^T}\mathbf{e}_i^k - \alpha^2(\mathbf{x}_0 - \mathbf{x}_k) + \mathbf{A}_k^T\mathbf{\Lambda}_k = \mathbf{0} \tag{2.30}$$

and the expression in equation (2.21).

Equations (2.30) and (2.21) can be written in the matrix form as

$$\begin{bmatrix} \mathbf{H}_k + \alpha^2\mathbf{I} & \mathbf{A}_k^T \\ \mathbf{A}_k & \mathbf{0} \end{bmatrix}\begin{Bmatrix} \mathbf{d}_k \\ \mathbf{\Lambda}_k \end{Bmatrix} = \begin{Bmatrix} \sum_{i=1}^{N_m}\delta_i\mathbf{S}_i^{k^T}\mathbf{e}_i^k + \alpha^2(\mathbf{x}_0 - \mathbf{x}_k) \\ \mathbf{b}_k \end{Bmatrix} \tag{2.31}$$

Solving equation (2.31) leads to

$$\mathbf{\Lambda}_k = -\left[\mathbf{A}_k\left(\mathbf{H}_k + \alpha^2\mathbf{I}\right)^{-1}\mathbf{A}_k^T\right]^{-1}\left[\mathbf{b}_k - \mathbf{A}_k\left(\mathbf{H}_k + \alpha^2\mathbf{I}\right)^{-1}\left(\sum_{i=1}^{N_m}\delta_i\mathbf{S}_i^{k^T}\mathbf{e}_i^k + \alpha^2(\mathbf{x}_0 - \mathbf{x}_k)\right)\right]$$

$$\tag{2.32}$$

$$\mathbf{d}_k = \left(\mathbf{H}_k + \alpha^2\mathbf{I}\right)^{-1}\left[\sum_{i=1}^{N_m}\delta_i\mathbf{S}_i^{k^T}\mathbf{e}_i^k + \alpha^2(\mathbf{x}_0 - \mathbf{x}_k) - \mathbf{A}_k^T\mathbf{\Lambda}_k\right] \tag{2.33}$$

The optimal regularization factor α is computed as (Pothisiri and Vatcharatanyakorn 2002)

$$\alpha = \sqrt{\sigma_{\max}^2} \qquad (2.34)$$

in which

$\sigma_{\max}$ is the maximum singular value of the sensitivity matrix
$$\mathbf{S} = \left\{ \mathbf{S}_1, \mathbf{S}_2, \ldots, \mathbf{S}_{N_m} \right\}.$$

2.3.1 Monte Carlo Simulation

In the Monte Carlo simulation method, synthetic measurements are created from a single measurement data set by using computer-generated random numbers. For the current study we adopt the data perturbation scheme proposed by Shin and Hjelmstad (1994) to generate the measurement data which is given by the following expression

$$\tilde{\phi}_{ij} = \hat{\phi}_{ij}(1 + \xi\eta_{ij}) \qquad (2.35)$$

in which

$\tilde{\phi}_{ij}$ is the simulated noisy mode shape at the jth degree of freedom of the ith vibration mode of the structural model;

$\hat{\Phi}_{ij}$ is the noise-free mode shape at the jth degree of freedom of the ith vibration mode of the structural model;

η_{ij} is a uniform random variate in the range [-1, 1];

and ξ is the percentage noise amplitude.

Let us generate N_t sets of $\tilde{\Phi}_t (t = 1, 2, 3 \ldots N_t)$. The specified statistical indices $\bar{\Phi}$ and $\mathbf{R}^{\Phi}$ can be obtained from the population of synthetic observations. Next, a set of parameter estimates $\mathbf{x}(\tilde{\Phi}_t)$ is obtained by repeating the nonlinear least-squares minimization for each artificial observation. Approximated estimates of $\bar{\mathbf{x}}$ and $\mathbf{R}^{\mathbf{x}}$

can be directly extracted from the set of estimated system parameters according to the standard definition of the mean and the covariance of a finite discrete data set.

$$\bar{\mathbf{x}} = \frac{1}{N_t}\sum_{t=1}^{N_t}\mathbf{x}_t; \quad \text{and} \quad \mathbf{R}^{\mathbf{x}} = \left\{\frac{1}{N_t}\sum_{t=1}^{N_t}\mathbf{x}_t \otimes \mathbf{x}_t\right\} - \frac{1}{N_t}\sum_{t=1}^{N_t}\mathbf{x}_t \otimes \frac{1}{N_t}\sum_{t=1}^{N_t}\mathbf{x}_t \quad (2.36)$$

in which

$\otimes$	denotes the tensor operator;
$\bar{\mathbf{x}}$	is the mean of the parameter estimates;
$\mathbf{R}^{\mathbf{x}}$	is the covariance matrix of the parameter estimates;
$\mathbf{x}_t$	is the tth sample of parameter estimates;
and N_t	is the size of the Monte Carlo population.

The statistical distribution of the parameter estimates can be obtained directly from the Monte Carlo sample by creating the probability density function (PDF) of each parameter as the frequency distribution for a discrete random variable. The basic concept behind the Monte Carlo simulation is simple and straightforward. The approximations improve as the number of synthetic measurements increases. The process of statistical parameter estimation with Monte Carlo simulation is illustrated schematically in Figure 2.3.

$$\bar{\mathbf{x}}, \ \mathbf{R}^{\mathbf{x}} \text{ and PDF}(X_i), \ i = 1, 2, ..., N_p$$
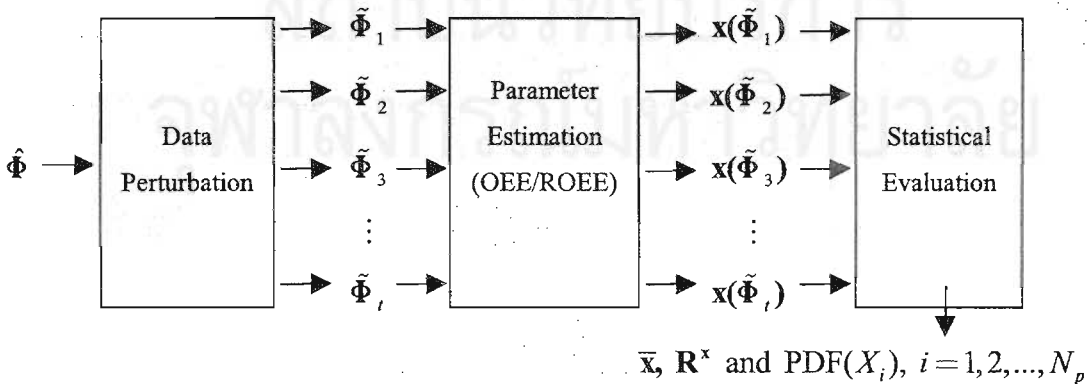
Figure 2.3 The process of statistical parameter estimation with the Monte Carlo simulation method.

2.3.2 The Sensitivity-Based Method

In the sensitivity-based method, nonlinear least-squares minimization is performed only once for the mean of the measured response $\bar{\Phi}$. At each iteration in the nonlinear minimization, the error function is linearized with respect to the system parameters, and the estimates of the system parameters are updated by solving the quadratic programming problem (QPP) resulting from this linearization. The error function is also linearized with respect to the measured response, from which we can obtain the statistical indices of the parameter estimates at each iteration. The process of statistical parameter estimation with the sensitivity-based method is illustrated schematically in Figure 2.4.

Both the sensitivity-based method and the Monte Carlo simulation method have their strengths and drawbacks. The sensitivity-based method is comparatively efficient because nonlinear optimization, which can be computationally intensive, is performed only once to find $\bar{x}$ and R^x. However, the statistical indices obtained from the sensitivity-based method may be unreliable when the error function is highly nonlinear because of the linear approximation of the error function. Moreover, the sensitivity-based method provides no information on the bias of $\bar{x}$ due to the nonlinearities in the error function. On the other hand, the Monte Carlo simulation is
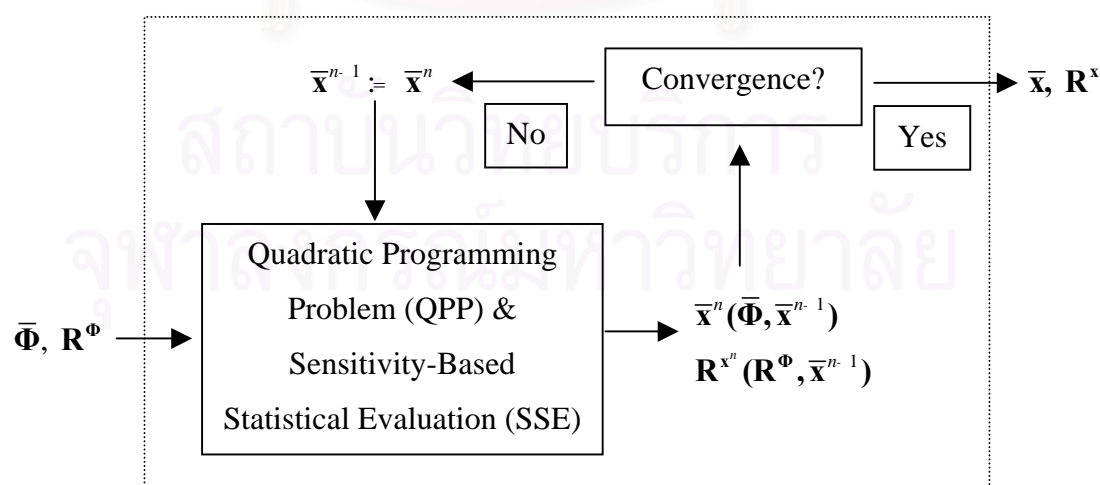
Figure 2.4 The process of statistical parameter estimation with the sensitivity-based method.

robust with respect to these nonlinearities and can provide information on the bias. The Monte Carlo simulation is, however, often computationally expensive because nonlinear optimization is repeated many times.

In the sensitivity-based method, we first derive the formulation necessary for the output error estimator defined in equation (2.1). Note that we omit the inequality constraints in this section to simplify the discussion although it is straightforward to incorporate them. As mentioned in the previous paragraph, nonlinear least-squares minimization is performed only once for the mean of the observations $\overline{\Phi}$. Let a superscript n (=1, 2, 3...) indicate that the variable is evaluated at the nth iteration in the nonlinear optimization process. Let us suppose that all variables are known at the $(n-1)$th iteration. The subproblem at the nth iteration is, then, to find $\Delta \mathbf{x}^n \equiv \mathbf{x}^n - \mathbf{x}^{n-1}$ that minimizes the objective function defined below. With the first-order Taylor's series expansion about $\mathbf{x}^{n-1}$, the linearized error function for the ith modal case can be defined as

$$\mathbf{e}_i^1(\Delta \mathbf{x}^n, \overline{\Phi}_i) \equiv \mathbf{e}_i(\mathbf{x}^{n-1}, \overline{\Phi}_i) + \nabla \mathbf{e}_i(\mathbf{x}^{n-1}, \overline{\Phi}_i)\Delta \mathbf{x}^n \qquad (2.37)$$

in which

$\overline{\Phi}_i$ is the mean of the measured mode shapes for the ith modal case;

and ∇ is the gradient with respect to the estimated system parameters $\mathbf{x}$.

For convenience in the following derivations, we use the differential operators defined in component form as

$$\nabla_k(\ ) \equiv \frac{\partial(\ )}{\partial x_k}, \quad \nabla_{kl}^2(\ ) \equiv \frac{\partial^2(\ )}{\partial x_k \partial x_l}, \quad \nabla_{klm}^3(\ ) \equiv \frac{\partial^3(\ )}{\partial x_k \partial x_l \partial x_m}, \qquad (2.38)$$

with all the subscripts k, l, m ranging from 1 to N_p.

With the linearized error function, we can define the objective function for the OEE algorithm as

$$J_1^E(\Delta\mathbf{x}^n,\bar{\boldsymbol{\Phi}}) \equiv \frac{1}{2}\sum_{i=1}^{N_m}\delta_i\mathbf{e}_i^1(\Delta\mathbf{x}^n,\bar{\boldsymbol{\Phi}}_i)\cdot\mathbf{e}_i^1(\Delta\mathbf{x}^n,\bar{\boldsymbol{\Phi}}_i) \tag{2.39}$$

in which

$$\mathbf{e}_i^1(\Delta\mathbf{x}^n,\bar{\boldsymbol{\Phi}}_i)\cdot\mathbf{e}_i^1(\Delta\mathbf{x}^n,\bar{\boldsymbol{\Phi}}_i) = \mathbf{e}_i(\mathbf{x}^{n-1},\bar{\boldsymbol{\Phi}}_i)\cdot\mathbf{e}_i(\mathbf{x}^{n-1},\bar{\boldsymbol{\Phi}}_i) + 2\mathbf{e}_i(\mathbf{x}^{n-1},\bar{\boldsymbol{\Phi}}_i)\cdot\nabla_k\mathbf{e}_i(\mathbf{x}^{n-1},\bar{\boldsymbol{\Phi}}_i)\Delta\mathbf{x}^n$$
$$+ \nabla_k\mathbf{e}_i(\mathbf{x}^{n-1},\bar{\boldsymbol{\Phi}}_i)\Delta\mathbf{x}^n\cdot\nabla_l\mathbf{e}_i(\mathbf{x}^{n-1},\bar{\boldsymbol{\Phi}}_i)\Delta\mathbf{x}^n$$

$$\tag{2.40}$$

For the ROEE algorithm defined in equation (2.2), equation (2.39) can be rewritten as

$$J_1(\Delta\mathbf{x}^n,\bar{\boldsymbol{\Phi}}) \equiv \frac{1}{2}\sum_{i=1}^{N_m}\delta_i\mathbf{e}_i^1(\Delta\mathbf{x}^n,\bar{\boldsymbol{\Phi}}_i)\cdot\mathbf{e}_i^1(\Delta\mathbf{x}^n,\bar{\boldsymbol{\Phi}}_i)$$
$$+ \frac{1}{2}\alpha^2\left[\left(\mathbf{x}^{n-1}+\Delta\mathbf{x}^n\right)-\mathbf{x}_0\right]\cdot\left[\left(\mathbf{x}^{n-1}+\Delta\mathbf{x}^n\right)-\mathbf{x}_0\right]$$

$$\tag{2.41}$$

The increment $\Delta\mathbf{x}^n$ is obtained, for the OEE method, by solving the simultaneous linear equation

$$\frac{\partial J_1^E(\Delta\mathbf{x}^n,\bar{\boldsymbol{\Phi}})}{\partial\Delta\mathbf{x}^n} = \sum_{i=1}^{N_m}\delta_i\left\{\mathbf{e}_i(\mathbf{x}^{n-1},\bar{\boldsymbol{\Phi}}_i)\cdot\nabla_k\mathbf{e}_i(\mathbf{x}^{n-1},\bar{\boldsymbol{\Phi}}_i)+\nabla_k\mathbf{e}_i(\mathbf{x}^{n-1},\bar{\boldsymbol{\Phi}}_i)\cdot\nabla_l\mathbf{e}_i(\mathbf{x}^{n-1},\bar{\boldsymbol{\Phi}}_i)\Delta\mathbf{x}^n\right\}$$
$$= \mathbf{H}_1^E(\mathbf{x}^{n-1},\bar{\boldsymbol{\Phi}})\Delta\mathbf{x}^n + \mathbf{C}_0^E(\mathbf{x}^{n-1},\bar{\boldsymbol{\Phi}})$$
$$= \mathbf{0}$$

$$\tag{2.42}$$

where

$$\left[\mathbf{H}_1^E\right]_{kl} \equiv \sum_{i=1}^{N_m}\delta_i\nabla_k\mathbf{e}_i(\mathbf{x}^{n-1},\bar{\boldsymbol{\Phi}}_i)\cdot\nabla_l\mathbf{e}_i(\mathbf{x}^{n-1},\bar{\boldsymbol{\Phi}}_i) \tag{2.43}$$

and

$$\left[\mathbf{C}_0^E\right]_k \equiv \sum_{i=1}^{N_m}\delta_i\mathbf{e}_i(\mathbf{x}^{n-1},\bar{\boldsymbol{\Phi}}_i)\cdot\nabla_k\mathbf{e}_i(\mathbf{x}^{n-1},\bar{\boldsymbol{\Phi}}_i) \tag{2.44}$$

For the ROEE method, we obtain $\Delta\mathbf{x}^n$ by solving the following equation

$$\frac{\partial J_1(\Delta\mathbf{x}^n,\overline{\mathbf{\Phi}})}{\partial\Delta\mathbf{x}^n} = \sum_{i=1}^{N_m}\delta_i\left\{\mathbf{e}_i(\mathbf{x}^{n-1},\overline{\mathbf{\Phi}}_i)\cdot\nabla_k\mathbf{e}_i(\mathbf{x}^{n-1},\overline{\mathbf{\Phi}}_i)+\nabla_k\mathbf{e}_i(\mathbf{x}^{n-1},\overline{\mathbf{\Phi}}_i)\cdot\nabla_l\mathbf{e}_i(\mathbf{x}^{n-1},\overline{\mathbf{\Phi}}_i)\Delta\mathbf{x}^n\right\}$$
$$+\alpha^2\left[\left(\mathbf{x}^{n-1}+\Delta\mathbf{x}^n\right)-\mathbf{x}_0\right]$$
$$= \mathbf{H}_1(\mathbf{x}^{n-1},\overline{\mathbf{\Phi}})\Delta\mathbf{x}^n+\mathbf{C}_0(\mathbf{x}^{n-1},\overline{\mathbf{\Phi}})$$
$$= \mathbf{0}$$

$$(2.45)$$

where

$$\left[\mathbf{H}_1\right]_{kl}\equiv\sum_{i=1}^{N_m}\delta_i\nabla_k\mathbf{e}_i(\mathbf{x}^{n-1},\overline{\mathbf{\Phi}}_i)\cdot\nabla_l\mathbf{e}_i(\mathbf{x}^{n-1},\overline{\mathbf{\Phi}}_i)+\alpha^2\mathbf{I} \qquad (2.46)$$

and

$$\left[\mathbf{C}_0\right]_k\equiv\sum_{i=1}^{N_m}\delta_i\mathbf{e}_i(\mathbf{x}^{n-1},\overline{\mathbf{\Phi}}_i)\cdot\nabla_k\mathbf{e}_i(\mathbf{x}^{n-1},\overline{\mathbf{\Phi}}_i)+\alpha^2\left(\mathbf{x}^{n-1}-\mathbf{x}_0\right) \qquad (2.47)$$

Observe that equations (2.43) and (2.46) correspond to the Gauss-Newton approximation of the Hessian of the objective function $J_E(\mathbf{x})$ and $J(\mathbf{x})$ of equations (2.1) and (2.2), respectively.

By using the sensitivity-based method, we linearize the error function $\mathbf{e}_i$ with respect not only to $\mathbf{x}$ but also to the measured modal responses $\hat{\mathbf{\Phi}}$. Let us define another linearized error function $\mathbf{e}_i^2$ as

$$\mathbf{e}_i^2(\Delta\mathbf{x}^n,\Delta\hat{\mathbf{\Phi}}_i)\equiv\mathbf{e}_i^1(\Delta\mathbf{x}^n,\overline{\mathbf{\Phi}}_i)+\sum_{\mu=1}^{\hat{N}_d N_m}\mathbf{e}_{i,\mu}(\mathbf{x}^{n-1},\overline{\mathbf{\Phi}}_i)\Delta\hat{\mathbf{\Phi}}_\mu \qquad (2.48)$$

in which

$$\Delta\hat{\mathbf{\Phi}}_i\equiv\hat{\mathbf{\Phi}}_i-\overline{\mathbf{\Phi}}_i \qquad (2.49)$$

and

$$\mathbf{e}_{i,\mu}(\mathbf{x}^{n-1},\overline{\mathbf{\Phi}}_i)=\frac{\partial\mathbf{e}_i(\mathbf{x}^{n-1},\overline{\mathbf{\Phi}}_i)}{\partial\hat{\mathbf{\Phi}}_\mu} \qquad (2.50)$$

Further, let us define a new objective function J_2 as

$$J_2(\Delta\mathbf{x}^n, \Delta\hat{\boldsymbol{\Phi}}) \equiv \frac{1}{2}\sum_{i=1}^{N_m}\delta_i\mathbf{e}_i^2(\Delta\mathbf{x}^n, \Delta\hat{\boldsymbol{\Phi}}_i)\cdot\mathbf{e}_i^2(\Delta\mathbf{x}^n, \Delta\hat{\boldsymbol{\Phi}}_i) \qquad (2.51)$$

in which, for the OEE method;

$$\begin{aligned}
\mathbf{e}_i^2(\Delta\mathbf{x}^n, \Delta\hat{\boldsymbol{\Phi}}_i)\cdot\mathbf{e}_i^2(\Delta\mathbf{x}^n, \Delta\hat{\boldsymbol{\Phi}}_i) &= \mathbf{e}_i(\mathbf{x}^{n-1}, \overline{\boldsymbol{\Phi}}_i)\cdot\mathbf{e}_i(\mathbf{x}^{n-1}, \overline{\boldsymbol{\Phi}}_i) + 2\mathbf{e}_i(\mathbf{x}^{n-1}, \overline{\boldsymbol{\Phi}}_i)\cdot\nabla_k\mathbf{e}_i(\mathbf{x}^{n-1}, \overline{\boldsymbol{\Phi}}_i)\Delta\mathbf{x}^n \\
&\quad + \nabla_k\mathbf{e}_i(\mathbf{x}^{n-1}, \overline{\boldsymbol{\Phi}}_i)\Delta\mathbf{x}^n \cdot \nabla_l\mathbf{e}_i(\mathbf{x}^{n-1}, \overline{\boldsymbol{\Phi}}_i)\Delta\mathbf{x}^n \\
&\quad + 2\mathbf{e}_i(\mathbf{x}^{n-1}, \overline{\boldsymbol{\Phi}}_i)\cdot\sum_{\mu=1}^{\hat{N}_d N_m}\mathbf{e}_{i,\mu}(\mathbf{x}^{n-1}, \overline{\boldsymbol{\Phi}}_i)\Delta\hat{\boldsymbol{\Phi}}_\mu \\
&\quad + 2\nabla_k\mathbf{e}_i(\mathbf{x}^{n-1}, \overline{\boldsymbol{\Phi}}_i)\Delta\mathbf{x}^n\cdot\sum_{\mu=1}^{\hat{N}_d N_m}\mathbf{e}_{i,\mu}(\mathbf{x}^{n-1}, \overline{\boldsymbol{\Phi}}_i)\Delta\hat{\boldsymbol{\Phi}}_\mu \\
&\quad + \sum_{\mu=1}^{\hat{N}_d N_m}\mathbf{e}_{i,\mu}(\mathbf{x}^{n-1}, \overline{\boldsymbol{\Phi}}_i)\Delta\hat{\boldsymbol{\Phi}}_\mu\cdot\sum_{\mu=1}^{\hat{N}_d N_m}\mathbf{e}_{i,\mu}(\mathbf{x}^{n-1}, \overline{\boldsymbol{\Phi}}_i)\Delta\hat{\boldsymbol{\Phi}}_\mu
\end{aligned}$$

$$(2.52)$$

We can now obtain $\Delta\mathbf{x}^n$ for the OEE method by solving

$$\begin{aligned}
\frac{\partial J_2(\Delta\mathbf{x}^n, \Delta\hat{\boldsymbol{\Phi}})}{\partial\Delta\mathbf{x}^n} &\equiv \sum_{i=1}^{N_m}\delta_i\Big[\mathbf{e}_i(\mathbf{x}^{n-1}, \overline{\boldsymbol{\Phi}}_i)\cdot\nabla_k\mathbf{e}_i(\mathbf{x}^{n-1}, \overline{\boldsymbol{\Phi}}_i) + \nabla_k\mathbf{e}_i(\mathbf{x}^{n-1}, \overline{\boldsymbol{\Phi}}_i)\cdot\nabla_l\mathbf{e}_i(\mathbf{x}^{n-1}, \overline{\boldsymbol{\Phi}}_i)\Delta\mathbf{x}^n \\
&\quad + \nabla_k\mathbf{e}_i(\mathbf{x}^{n-1}, \overline{\boldsymbol{\Phi}}_i)\cdot\mathbf{e}_{i,\mu}(\mathbf{x}^{n-1}, \overline{\boldsymbol{\Phi}}_i)\Delta\hat{\boldsymbol{\Phi}}_\mu\Big] \\
&= \mathbf{H}_1^E(\mathbf{x}^{n-1}, \overline{\boldsymbol{\Phi}})\Delta\mathbf{x}^n + \mathbf{C}_0^E(\mathbf{x}^{n-1}, \overline{\boldsymbol{\Phi}}) + \mathbf{H}_2(\mathbf{x}^{n-1}, \overline{\boldsymbol{\Phi}})\Delta\hat{\boldsymbol{\Phi}} \\
&= 0
\end{aligned}$$

$$(2.53)$$

in which $\left[\mathbf{H}_1^E\right]_{kl}$ and $\left[\mathbf{C}_0^E\right]_k$ are defined in equations (2.43) and (2.44), respectively. For the ROEE method, the above equation can be applied by replacing $\mathbf{H}_1^E$ and $\mathbf{C}_0^E$ with $\mathbf{H}_1$ and $\mathbf{C}_0$ in equations (2.46) and (2.47). The $k\mu$th element of $\mathbf{H}_2$ is defined as

$$[\mathbf{H}_2]_{k\mu} \equiv \sum_{i=1}^{N_m}\delta_i\nabla_k\mathbf{e}_i(\mathbf{x}^{n-1}, \overline{\boldsymbol{\Phi}}_i)\cdot\mathbf{e}_{i,\mu}(\mathbf{x}^{n-1}, \overline{\boldsymbol{\Phi}}_i) \qquad (2.54)$$

The solution $\Delta\mathbf{x}^n$ can be obtained by solving the following equation.

$$\Delta\mathbf{x}^n = -\mathbf{H}_1^+\mathbf{C}^0 - \mathbf{H}_1^+\mathbf{H}_2\Delta\hat{\boldsymbol{\Phi}} \qquad (2.55)$$

where $\mathbf{H}_1^+$ indicates a generalized inverse of $\mathbf{H}_1^E$ and $\mathbf{H}_1$, respectively, for the OEE and ROEE method.

Noticing that $E[\Delta\hat{\boldsymbol{\Phi}}] = \mathbf{0}$ and $E[\Delta\hat{\boldsymbol{\Phi}} \otimes \Delta\hat{\boldsymbol{\Phi}}] = \mathbf{R}^{\Phi}$, in which $\otimes$ indicates the tensor product, we obtain the statistical indices of $\mathbf{x}^n$ as

$$\bar{\mathbf{x}}^n \equiv E[\mathbf{x}^{n-1} + \Delta\mathbf{x}^n] = \bar{\mathbf{x}}^{n-1} - \mathbf{H}_1^+\mathbf{C}^0 \qquad (2.56)$$

$$\mathbf{R}^{\mathbf{x}^n} \equiv E[(\mathbf{x}^n - \bar{\mathbf{x}}^n) \otimes (\mathbf{x}^n - \bar{\mathbf{x}}^n)] = \mathbf{H}_1^+\mathbf{H}_2\mathbf{R}^{\Phi}\mathbf{H}_1^{+^T}\mathbf{H}_2^T \qquad (2.57)$$

When equations (2.56) and (2.57) converge ($\Delta\mathbf{x}^n \to \mathbf{0}$), we can obtain the mean $\bar{\mathbf{x}}$ and the covariance matrix $\mathbf{R}^{\mathbf{x}}$ of the estimated system parameters, respectively.

2.3.3 The Optimum Sensitivity-Based Method

Based on the concept of the optimum sensitivity-based method proposed by Araki and Hjelmstad (2001), we present a statistical parameter estimation method for our nonlinear least-squares estimators (OEE and ROEE). Unlike the sensitivity-based method, the present method provides a second-order approximation of the statistical indices of the system parameters and allows us to assess the bias due to the nonlinearities in the error function. Like the sensitivity-based method, the present method preserves computational efficiency compared with the Monte Carlo simulation method. The process of statistical parameter estimation with the optimum sensitivity-based method is illustrated schematically in Figure 2.5.
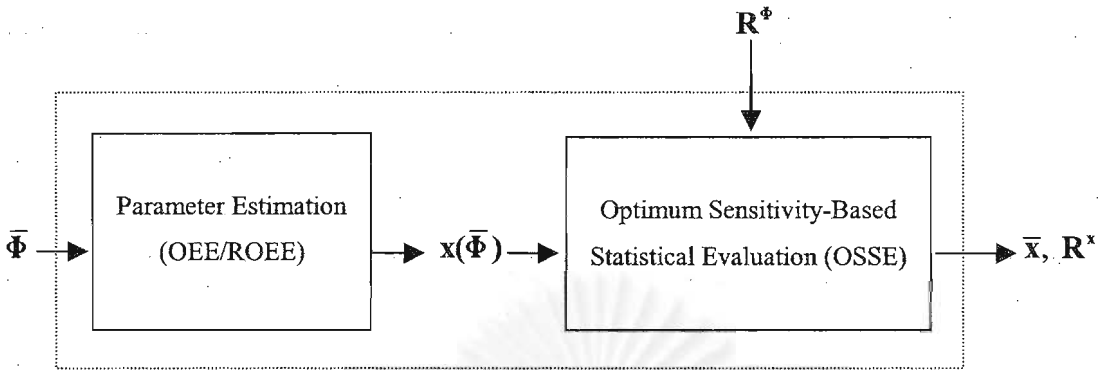
Figure 2.5 The process of statistical parameter estimation with
the optimum sensitivity-based method.

The parameter estimates can be found using a standard numerical technique for constrained nonlinear optimization. From the OEE algorithm in equation (2.1), we define the Lagrangian function as

$$\ell(\mathbf{x}, \mathbf{\Lambda}, \hat{\mathbf{\Phi}}) \equiv J_E(\mathbf{x}, \hat{\mathbf{\Phi}}) + \mathbf{\Lambda}_L \cdot (\mathbf{c}_L - \mathbf{x}_L) + \mathbf{\Lambda}_U \cdot (\mathbf{x}_U - \mathbf{c}_U) \qquad (2.58)$$

Here, $\mathbf{c}_L$ and $\mathbf{x}_L$ are the subsets of $\mathbf{c}_L^0$ and $\mathbf{x}$ in equation (2.1), respectively, associated with the active set of constraints for the lower bounds, and $\mathbf{\Lambda}_L$ is the vector of the Lagrangian multipliers corresponding to $\mathbf{x}_L$. The vectors $\mathbf{c}_U$, $\mathbf{x}_U$ and $\mathbf{\Lambda}_U$ are defined similarly for the active constraints of the upper bounds. The optimal solution $\mathbf{x}$ and $\mathbf{\Lambda}$ satisfy the Kuhn-Tucker conditions

$$\nabla\ell(\mathbf{x}) = \nabla J_E(\mathbf{x}) - \mathbf{Q}_L\mathbf{\Lambda}_L + \mathbf{Q}_U\mathbf{\Lambda}_U = \mathbf{0} \qquad (2.59)$$

$$\mathbf{x}_L = \mathbf{c}_L, \quad \mathbf{x}_U = \mathbf{c}_U, \quad \mathbf{\Lambda}_L \geq \mathbf{0}, \quad \mathbf{\Lambda}_U \geq \mathbf{0} \qquad (2.60)$$

where the boolean matrices $\mathbf{Q}_L$ and $\mathbf{Q}_U$ are defined as $\mathbf{Q}_L \equiv (\nabla\mathbf{x}_L)^T$ and $\mathbf{Q}_U \equiv (\nabla\mathbf{x}_U)^T$.

Suppose that we have the solution of the minimization problem (2.1). Then, noticing that all $\mathbf{x}$, $\boldsymbol{\Lambda}_L$ and $\boldsymbol{\Lambda}_U$ are functions of $\hat{\boldsymbol{\Phi}}$, we can obtain the optimum sensitivity by direct differentiation of the Kuhn-Tucker condition in equation (2.59). Let $\hat{\boldsymbol{\Phi}}_\mu$ denote the μth component of $\hat{\boldsymbol{\Phi}}$, and let the optimum sensitivity derivatives be indicated by

$$\mathbf{x}_{,\mu} \equiv \frac{\partial \mathbf{x}}{\partial \hat{\boldsymbol{\Phi}}_\mu}; \quad \text{and} \quad \mathbf{x}_{,\mu\nu} \equiv \frac{\partial^2 \mathbf{x}}{\partial \hat{\boldsymbol{\Phi}}_\mu \partial \hat{\boldsymbol{\Phi}}_\nu} \tag{2.61}$$

Differentiating equations (2.59) and (2.60) with respect to $\hat{\boldsymbol{\Phi}}_\mu$, we have

$$\nabla^2 J_E \mathbf{x}_{,\mu} - \mathbf{Q}_L \boldsymbol{\Lambda}_{L,\mu} + \mathbf{Q}_U \boldsymbol{\Lambda}_{U,\mu} + \mathbf{C}_\mu^1 = \mathbf{0} \tag{2.62}$$

$$\mathbf{x}_{L,\mu} = \mathbf{x}_{U,\mu} = \mathbf{0} \tag{2.63}$$

where the coefficient $\nabla^2 J_E$ and the known vector $\mathbf{C}_\mu^1$ are obtained in component as

$$\nabla_{kl}^2 J_E = \sum_{i=1}^{N_m} \delta_i \left(\mathbf{e}_i(\mathbf{x},\hat{\boldsymbol{\Phi}}_i) \cdot \nabla_{kl}^2 \mathbf{e}_i(\mathbf{x},\hat{\boldsymbol{\Phi}}_i) + \nabla_k \mathbf{e}_i(\mathbf{x},\hat{\boldsymbol{\Phi}}_i) \cdot \nabla_l \mathbf{e}_i(\mathbf{x},\hat{\boldsymbol{\Phi}}_i) \right) \tag{2.64}$$

$$\left[\mathbf{C}_\mu^1 \right]_k \equiv \nabla_k J_{E,\mu} = \sum_{i=1}^{N_m} \delta_i \left(\mathbf{e}_i(\mathbf{x},\hat{\boldsymbol{\Phi}}_i) \cdot \nabla_k \mathbf{e}_{i,\mu}(\mathbf{x},\hat{\boldsymbol{\Phi}}_i) + \nabla_k \mathbf{e}_i(\mathbf{x},\hat{\boldsymbol{\Phi}}_i) \cdot \mathbf{e}_{i,\mu}(\mathbf{x},\hat{\boldsymbol{\Phi}}_i) \right) \tag{2.65}$$

in which

$$\left. \begin{array}{ll} \nabla_k \mathbf{e}_i(\mathbf{x},\hat{\boldsymbol{\Phi}}_i) = -\lambda_i \mathbf{Q} \nabla_k \mathbf{B}_i^{-1}(\mathbf{x}) \hat{\mathbf{M}} \hat{\boldsymbol{\Phi}}_i, & \nabla_{kl}^2 \mathbf{e}_i(\mathbf{x},\hat{\boldsymbol{\Phi}}_i) = -\lambda_i \mathbf{Q} \nabla_{kl}^2 \mathbf{B}_i^{-1}(\mathbf{x}) \hat{\mathbf{M}} \hat{\boldsymbol{\Phi}}_i \\ \mathbf{e}_{i,\mu}(\mathbf{x},\hat{\boldsymbol{\Phi}}_i) = \hat{\boldsymbol{\Phi}}_{i,\mu} - \lambda_i \mathbf{Q} \mathbf{B}_i^{-1}(\mathbf{x}) \hat{\mathbf{M}} \hat{\boldsymbol{\Phi}}_{i,\mu}, & \nabla_k \mathbf{e}_{i,\mu}(\mathbf{x},\hat{\boldsymbol{\Phi}}_i) = -\lambda_i \mathbf{Q} \nabla_k \mathbf{B}_i^{-1}(\mathbf{x}) \hat{\mathbf{M}} \hat{\boldsymbol{\Phi}}_{i,\mu} \end{array} \right\} \tag{2.66}$$

where $\hat{\boldsymbol{\Phi}}_i$, λ_i, $\mathbf{Q}$, $\mathbf{B}_i^{-1}(\mathbf{x})$ and $\hat{\mathbf{M}}$ are defined in equations (2.8) and (2.9),

and
$$\left. \begin{aligned} \nabla_k \mathbf{B}_i^{-1}(\mathbf{x}) &= -\mathbf{B}_i^{-1}(\mathbf{x})\nabla_k\mathbf{B}_i(\mathbf{x})\mathbf{B}_i^{-1}(\mathbf{x}) \\ \nabla_{kl}^2\mathbf{B}_i^{-1}(\mathbf{x}) &= -\nabla_l\mathbf{B}_i^{-1}(\mathbf{x})\nabla_k\mathbf{B}_i(\mathbf{x})\mathbf{B}_i^{-1}(\mathbf{x}) - \mathbf{B}_i^{-1}(\mathbf{x})\nabla_k\mathbf{B}_i(\mathbf{x})\nabla_l\mathbf{B}_i^{-1}(\mathbf{x}) \end{aligned} \right\} \quad (2.67)$$

By solving equations (2.62) and (2.63) for each index μ, we can obtain the first-order optimum sensitivity derivatives $\mathbf{x}_{,\mu}$, $\mathbf{\Lambda}_{L,\mu}$ and $\mathbf{\Lambda}_{U,\mu}$. Note that $\nabla^2 J_E$ is the same for every μ and needs to be factored only once.

We can obtain higher-order derivatives by repeated differentiation of the Kuhn-Tucker conditions. For instance, differentiation of equations (2.62) and (2.63) with respect to $\hat{\Phi}_\nu$ yields the equations for the second-order optimum sensitivity derivatives $\mathbf{x}_{,\mu\nu}$, $\mathbf{\Lambda}_{L,\mu\nu}$ and $\mathbf{\Lambda}_{U,\mu\nu}$ as

$$\nabla^2 J_E \mathbf{x}_{,\mu\nu} - \mathbf{Q}_L\mathbf{\Lambda}_{L,\mu\nu} + \mathbf{Q}_U\mathbf{\Lambda}_{U,\mu\nu} + \mathbf{C}_{\mu\nu}^2 = 0 \quad (2.68)$$

$$\mathbf{x}_{L,\mu\nu} = \mathbf{x}_{U,\mu\nu} = 0 \quad (2.69)$$

where the known vector $\mathbf{C}_{\mu\nu}^2$ in equation (2.68) can be expressed as

$$\left[\mathbf{C}_{\mu\nu}^2\right]_k = \mathbf{x}_{,\mu}\cdot\left[\nabla^3 J_E\right]_k\mathbf{x}_{,\nu} + \left[\nabla^2 J_{E,\mu}\mathbf{x}_{,\nu}\right]_k + \left[\nabla^2 J_{E,\nu}\mathbf{x}_{,\mu}\right]_k + \nabla_k J_{E,\mu\nu} \quad (2.70)$$

where $\left[\nabla^3 J_E\right]_k$ is the kth second-order tensor of $\nabla^3 J_E$, and the derivatives of J_E are given by

$$\left[\nabla^3 J_E\right]_k = \nabla_{klm}^3 J_E = \sum_{i=1}^{N_m}\delta_i\Big(\mathbf{e}_i(\mathbf{x},\hat{\Phi}_i)\cdot\nabla_{klm}^3\mathbf{e}_i(\mathbf{x},\hat{\Phi}_i) + \nabla_k\mathbf{e}_i(\mathbf{x},\hat{\Phi}_i)\cdot\nabla_{lm}^2\mathbf{e}_i(\mathbf{x},\hat{\Phi}_i) \\ + \nabla_l\mathbf{e}_i(\mathbf{x},\hat{\Phi}_i)\cdot\nabla_{mk}^2\mathbf{e}_i(\mathbf{x},\hat{\Phi}_i) + \nabla_m\mathbf{e}_i(\mathbf{x},\hat{\Phi}_i)\cdot\nabla_{kl}^2\mathbf{e}_i(\mathbf{x},\hat{\Phi}_i)\Big) \quad (2.71)$$

$$\left[\nabla^2 J_{E,\mu}\right]_k = \nabla_{kl}^2 J_{E,\mu} = \sum_{i=1}^{N_m}\delta_i\Big(\mathbf{e}_i(\mathbf{x},\hat{\Phi}_i)\cdot\nabla_{kl}^2\mathbf{e}_{i,\mu}(\mathbf{x},\hat{\Phi}_i) + \nabla_k\mathbf{e}_i(\mathbf{x},\hat{\Phi}_i)\cdot\nabla_l\mathbf{e}_{i,\mu}(\mathbf{x},\hat{\Phi}_i) \\ + \nabla_l\mathbf{e}_i(\mathbf{x},\hat{\Phi}_i)\cdot\nabla_k\mathbf{e}_{i,\mu}(\mathbf{x},\hat{\Phi}_i) + \mathbf{e}_{i,\mu}(\mathbf{x},\hat{\Phi}_i)\cdot\nabla_{kl}^2\mathbf{e}_i(\mathbf{x},\hat{\Phi}_i)\Big) \quad (2.72)$$

$$\nabla_k J_{E,\mu\nu} = \sum_{i=1}^{N_m} \delta_i \Big(\mathbf{e}_i(\mathbf{x},\hat{\boldsymbol{\Phi}}_i) \cdot \nabla_k \mathbf{e}_{i,\mu\nu}(\mathbf{x},\hat{\boldsymbol{\Phi}}_i) + \nabla_k \mathbf{e}_i(\mathbf{x},\hat{\boldsymbol{\Phi}}_i) \cdot \mathbf{e}_{i,\mu\nu}(\mathbf{x},\hat{\boldsymbol{\Phi}}_i)$$
$$+ \mathbf{e}_{i,\mu}(\mathbf{x},\hat{\boldsymbol{\Phi}}_i) \cdot \nabla_k \mathbf{e}_{i,\nu}(\mathbf{x},\hat{\boldsymbol{\Phi}}_i) + \mathbf{e}_{i,\nu}(\mathbf{x},\hat{\boldsymbol{\Phi}}_i) \cdot \nabla_k \mathbf{e}_{i,\mu}(\mathbf{x},\hat{\boldsymbol{\Phi}}_i) \Big) \tag{2.73}$$

in which

$$\nabla^3_{klm} \mathbf{e}_i(\mathbf{x},\hat{\boldsymbol{\Phi}}_i) = -\lambda_i \mathbf{Q} \nabla^3_{klm} \mathbf{B}_i^{-1}(\mathbf{x})\hat{\mathbf{M}}\hat{\boldsymbol{\Phi}}_i, \quad \nabla^2_{kl} \mathbf{e}_{i,\mu}(\mathbf{x},\hat{\boldsymbol{\Phi}}_i) = -\lambda_i \mathbf{Q} \nabla^2_{kl} \mathbf{B}_i^{-1}(\mathbf{x})\hat{\mathbf{M}}\hat{\boldsymbol{\Phi}}_{i,\mu} \Bigg]$$
$$\mathbf{e}_{i,\mu\nu}(\mathbf{x},\hat{\boldsymbol{\Phi}}_i) = \nabla_k \mathbf{e}_{i,\mu\nu}(\mathbf{x},\hat{\boldsymbol{\Phi}}_i) = 0 \tag{2.74}$$

where

$$\nabla^3_{klm} \mathbf{B}_i^{-1}(\mathbf{x}) = -\nabla^2_{lm} \mathbf{B}_i^{-1}(\mathbf{x})\nabla_k \mathbf{B}_i(\mathbf{x})\mathbf{B}_i^{-1}(\mathbf{x}) - \nabla_l \mathbf{B}_i^{-1}(\mathbf{x})\nabla_k \mathbf{B}_i(\mathbf{x})\nabla_m \mathbf{B}_i^{-1}(\mathbf{x})$$
$$- \nabla_m \mathbf{B}_i^{-1}(\mathbf{x})\nabla_k \mathbf{B}_i(\mathbf{x})\nabla_l \mathbf{B}_i^{-1}(\mathbf{x}) - \mathbf{B}_i^{-1}(\mathbf{x})\nabla_k \mathbf{B}_i(\mathbf{x})\nabla^2_{lm} \mathbf{B}_i^{-1}(\mathbf{x}) \tag{2.75}$$

The optimum sensitivity derivation is similar for the regularized output error estimator (ROEE) in equation (2.2). The Lagrangian function is defined as

$$\ell(\mathbf{x},\boldsymbol{\Lambda},\hat{\boldsymbol{\Phi}}) \equiv J(\mathbf{x},\hat{\boldsymbol{\Phi}}) + \boldsymbol{\Lambda}_L \cdot (\mathbf{c}_L - \mathbf{x}_L) + \boldsymbol{\Lambda}_U \cdot (\mathbf{x}_U - \mathbf{c}_U) \tag{2.76}$$

Again, the optimal solution $\mathbf{x}$ and $\boldsymbol{\Lambda}$ satisfy the Kuhn-Tucker conditions

$$\nabla \ell(\mathbf{x}) = \nabla J(\mathbf{x}) - \mathbf{Q}_L \boldsymbol{\Lambda}_L + \mathbf{Q}_U \boldsymbol{\Lambda}_U = \mathbf{0} \tag{2.77}$$

and the expression in equation (2.60).

Differentiating equations (2.77) and (2.60) with respect to $\hat{\boldsymbol{\Phi}}_\mu$, we have

$$\nabla^2 J \mathbf{x}_{,\mu} - \mathbf{Q}_L \boldsymbol{\Lambda}_{L,\mu} + \mathbf{Q}_U \boldsymbol{\Lambda}_{U,\mu} + \mathbf{C}_\mu^1 = \mathbf{0} \tag{2.78}$$

and the expression in equation (2.63).

where the known vector $\mathbf{C}_\mu^1$ is obtained in component as shown in equation (2.65) and the coefficient $\nabla^2 J$ is obtained in component as

$$\nabla_{kl}^2 J = \sum_{i=1}^{N_m} \delta_i \left(\mathbf{e}_i(\mathbf{x}, \hat{\boldsymbol{\Phi}}_i) \cdot \nabla_{kl}^2 \mathbf{e}_i(\mathbf{x}, \hat{\boldsymbol{\Phi}}_i) + \nabla_k \mathbf{e}_i(\mathbf{x}, \hat{\boldsymbol{\Phi}}_i) \cdot \nabla_l \mathbf{e}_i(\mathbf{x}, \hat{\boldsymbol{\Phi}}_i) \right) + \alpha^2 \mathbf{I} \quad (2.79)$$

By solving equations (2.78) and (2.63) for each index μ, we can obtain the first-order optimum sensitivity derivatives $\mathbf{x}_{,\mu}$, $\boldsymbol{\Lambda}_{L,\mu}$ and $\boldsymbol{\Lambda}_{U,\mu}$. As for the previous case, $\nabla^2 J$ is the same for every μ and needs to be factored only once.

We can obtain higher-order derivatives by repeating the differentiation of the Kuhn-Tucker conditions. The differentiation of equations (2.78) and (2.63) with respect to $\hat{\Phi}_\nu$ yields the equations for the second-order optimum sensitivity derivatives $\mathbf{x}_{,\mu\nu}$, $\boldsymbol{\Lambda}_{L,\mu\nu}$ and $\boldsymbol{\Lambda}_{U,\mu\nu}$ as

$$\nabla^2 J \mathbf{x}_{,\mu\nu} - \mathbf{Q}_L \boldsymbol{\Lambda}_{L,\mu\nu} + \mathbf{Q}_U \boldsymbol{\Lambda}_{U,\mu\nu} + \mathbf{C}_{\mu\nu}^2 = \mathbf{0} \qquad (2.80)$$

and the expression in equation (2.69).

It should be noted that if the evaluation of higher-order derivatives requires more computational time than reoptimization, or the finite difference method, (this might occur, e.g., when the number of parameter estimates is very large), it may be better to use the finite difference method to obtain the optimum sensitivity derivatives.

Based on the perturbation method, one can derive the formula for the approximate statistical indices of system parameters. Suppose that we have the mean and the covariance matrix of measurements defined respectively as

$$\bar{\boldsymbol{\Phi}} \equiv E\left[\hat{\boldsymbol{\Phi}}\right] \qquad (2.81)$$

$$\mathbf{R}^\Phi \equiv E\left[\left(\hat{\boldsymbol{\Phi}} - \bar{\boldsymbol{\Phi}}\right) \otimes \left(\hat{\boldsymbol{\Phi}} - \bar{\boldsymbol{\Phi}}\right)\right] \qquad (2.82)$$

where $\otimes$ indicates the tensor product. And suppose that we have the optimum sensitivity derivatives up to the second-order. Our goal is to estimate the mean $\bar{x}$ and the covariance matrix $\mathbf{R}^x$ of system parameters. With a Taylor's series expansion, we can express the estimated system parameter vector as

$$\mathbf{x}(\hat{\Phi}) = \mathbf{x}(\overline{\Phi}) + \sum_{\mu=1}^{\hat{N}_d N_m} \mathbf{x}_{,\mu}(\overline{\Phi})\left(\hat{\Phi}_\mu - \overline{\Phi}_\mu\right) + \frac{1}{2}\sum_{\mu=1}^{\hat{N}_d N_m}\sum_{\nu=1}^{\hat{N}_d N_m} \mathbf{x}_{,\mu\nu}(\overline{\Phi})\left(\hat{\Phi}_\mu - \overline{\Phi}_\mu\right)\left(\hat{\Phi}_\nu - \overline{\Phi}_\nu\right) \quad (2.83)$$

Equation (2.83) is valid unless the active set of the constraint conditions changes. With these definitions, the statistical indices of system parameters are approximated as

$$\bar{x} \equiv E\left[\mathbf{x}(\hat{\Phi})\right] = \mathbf{x}(\overline{\Phi}) + \frac{1}{2}\sum_{\mu=1}^{\hat{N}_d N_m}\sum_{\nu=1}^{\hat{N}_d N_m} \mathbf{x}_{,\mu\nu}(\overline{\Phi})R_{\mu\nu}^{\Phi} \quad (2.84)$$

$$\mathbf{R}^x \equiv E\left[\mathbf{x}(\hat{\Phi}) \otimes \mathbf{x}(\hat{\Phi})\right] = \sum_{\mu=1}^{\hat{N}_d N_m}\sum_{\nu=1}^{\hat{N}_d N_m} \mathbf{x}_{,\mu}(\overline{\Phi}) \otimes \mathbf{x}_{,\nu}(\overline{\Phi})R_{\mu\nu}^{\Phi} \quad (2.85)$$

Let us consider the proportional error given by equation (2.35). Equations (2.84) and (2.85) lead to the following formula

$$\bar{x}(\alpha) = \mathbf{x}(\hat{\Phi}) + \frac{\alpha^2}{6}\sum_{\mu=1}^{\hat{N}_d N_m} \mathbf{x}_{,\mu\mu}(\hat{\Phi})\hat{\Phi}_\mu^2 \quad (2.86)$$

$$\mathbf{R}^x(\alpha) = \frac{\alpha^2}{3}\sum_{\mu=1}^{\hat{N}_d N_m}\sum_{\nu=1}^{\hat{N}_d N_m} \mathbf{x}_{,\mu}(\hat{\Phi}) \otimes \mathbf{x}_{,\nu}(\hat{\Phi})\hat{\Phi}_\mu\hat{\Phi}_\nu \quad (2.87)$$

2.4 Structural Damage Assessment

The statistical damage assessment algorithm investigated in the current study compares the statistical distribution of the parameter estimates between the baseline and the current structure to assess damage. If the measured data are noise-free, a

structural member can be viewed as damaged if its estimated parameter is different from the baseline value. This simple assessment is complicated by the presence of the measurement noise. The noise in the measurements can cause the estimated parameter for an element to be different from the baseline value even if there is no damage at all. It therefore seems reasonable to incorporate the sensitivity of the estimated parameter to noise in evaluating the severity of damage.

Various statistical parameter estimation methods can be used to obtain the sensitivity of the estimated system parameters to the measurement noise. For instance, in the Monte Carlo simulation method the statistical distribution of the system parameters can be directly extracted from the frequency distribution of the computed population of parameter estimates. Approximations to the mean and the covariance matrix of the system parameters, $\overline{x}$ and $\mathbf{R}^x$, can be obtained based on the standard definition of the mean and the covariance matrix of a finite discrete data set. The concept behind Monte Carlo simulation is fairly simple and straightforward. The statistical distribution improves as the size of the population of parameter estimates increases. The idea of using the frequency distribution of the parameter estimates to assess damage can be illustrated in Figure 2.6(a) where discrete random variables are used to represent the population of parameter estimates.

In the optimum sensitivity-based method and the sensitivity-based method, we construct the statistical distribution of the parameter estimates by assuming their probability density function (PDF) to be normal distribution with the mean $\overline{x}$ and the covariance matrix $\mathbf{R}^x$ of the parameter estimates from the statistical parameter estimation process. The normal probability density function is computed as

$$f_{X_m}(x_m) = \frac{1}{\sqrt{2\pi R^{x_m}}} e^{-\frac{1}{2R^{x_m}}(x_m - \overline{x}_m)^2} \tag{2.88}$$

in which

$\quad x_m \qquad$ is an estimated parameter for member m of the structure;

$\quad \overline{x}_m \qquad$ is the mean of an estimated parameter for member m;

and R^{x_m} is the covariance of an estimated parameter for member m.

The cumulative distribution function (CDF) of a member parameter x_m can be obtained by integrating equation (2.88) in the interval $(-\infty, x_m]$ as follows

$$F_{X_m}(x_m) = \int_{-\infty}^{x_m} f(t)dt = \frac{1}{\sqrt{2\pi R^{x_m}}} \int_{-\infty}^{x_m} e^{-\frac{1}{2R^{x_m}}(t-\bar{x}_m)^2} dt \qquad (2.89)$$

The schematic representation of the statistical assessment of damage by assuming a continuous distribution for the system parameters are shown in Figure 2.6(b).

2.4.1 Damage Assessment of Single-Parameter Structural Members

The single-parameter structural members are those parameterized with a single stiffness parameter that can change as a result of damage. As previously discussed, the mass density parameter of the member is assumed not to be affected by damage and is taken as constant.
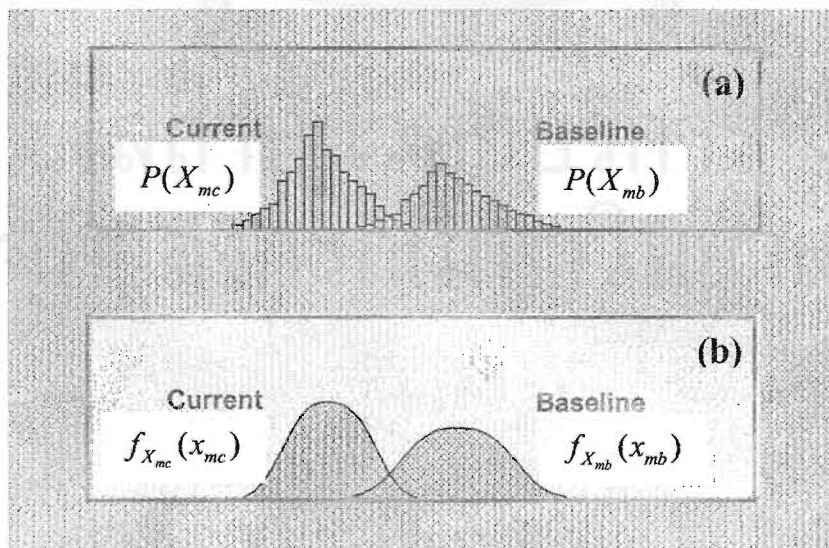
Figure 2.6 Statistical distribution of system parameters for baseline and current structures: (a) discrete random variables and (b) continuous random variables.

Following the work of Pothisiri and Hjelmstad (2001), let us assume that the statistical distribution of the parameter estimates of member m is known for both the baseline and the current structures. Further, let us denote a random variable X_{mc} as the parameter estimate for member m in the current structure and a random variable X_{mb} as the parameter estimate for the same member that corresponds to a parameter estimation problem of the associated baseline structure. Damage in member m of the current structure can be assessed by comparing the statistical distributions of the member parameters in the baseline and the current structure as shown in Figure 2.7 where the random variables X_{mc} and X_{mb} are assumed to be continuous. In the illustration, $f_{X_{mc}}$ and $F_{X_{mc}}$ denote the probability density function and the cumulative distribution function, respectively, of the random variable X_{mc}, and $f_{X_{mb}}$ denotes the probability density function of the random variable X_{mb}. Member m is regarded as damaged in the event that $X_{mc} < X_{mb}$. This event can be described in terms of probability $P(X_{mc} < X_{mb})$ to account for the uncertainty of the parameter estimates. The probability $P(X_{mc} < X_{mb})$ represents a realistic measure of the state of the structural system. Let us denote x_{mc} and $\hat{x}_{mb}$ as a current estimate and the a priori known baseline parameter value for member m, respectively. We define the level of damage as
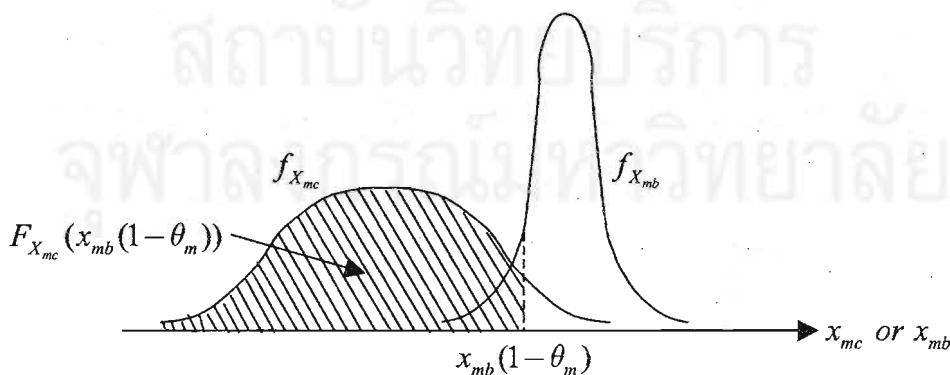
Figure 2.7 Assessment of damage based on statistical distribution of system parameters.

$$\theta_m = \frac{\hat{x}_{mb} - x_{mc}}{\hat{x}_{mb}} \tag{2.90}$$

With the above definition, the state of member m of the current structure can be described by the event that the actual level of damage lies beyond the prescribed level of damage (i.e., $X_{mc} < X_{mb}(1-\theta_m)$). Let us assume, for the moment, that X_{mc} and X_{mb} are discrete random variables. With a specified level of damage θ_m, the required probability can be formulated as follows:

$$P(X_{mc} < X_{mb}(1-\theta_m)) = \sum_{all\ x_{mb}} P(X_{mc} < X_{mb}(1-\theta_m) \mid X_{mb} = x_{mb})P(X_{mb} = x_{mb}) \tag{2.91}$$

It is reasonable to assume that the parameter estimates in the current and the baseline structure, X_{mc} and X_{mb}, are statistically independent; that is,

$$P(X_{mc} < X_{mb}(1-\theta_m) \mid X_{mb} = x_{mb}) = P(X_{mc} < x_{mb}(1-\theta_m)) \tag{2.92}$$

For continuous X_{mc} and X_{mb}, equation (2.92) becomes

$$P(X_{mc} < X_{mb}(1-\theta_m)) = \int_0^\infty F_{X_{mc}}(x_{mb}(1-\theta_m)) f_{X_{mb}}(x_{mb}) dx_{mb} \tag{2.93}$$

The quantity $F_{X_{mc}}(x_{mb}(1-\theta_m))$ on the right hand side of the above equation is illustrated by the shaded area under the curve $f_{X_{mc}}$ in Figure 2.7 in the range $(-\infty, x_{mb}(1-\theta_m)]$. The damage statements of single-parameter structural members will be illustrated later in the simulation study by the relation between $P(X_{mc} < X_{mb}(1-\theta_m))$ and θ_m.

2.4.2   Damage Assessment of Multi-Parameter Structural Members

For the structural members consisting of multiple stiffness parameters, the proposed statistical damage assessment algorithm must be modified to account for the presence of all structural parameters. These parameters may be an axial stiffness, a bending stiffness, and a shearing stiffness. In this case, damage should be modeled by reducing the different stiffness parameters of the structural members that correspond with the physics of the actual damage.

By using a similar concept to the reliability analysis (Ang and Tang, 1990), the status of the current structure and the baseline structure is computed as illustrated in Figure 2.8. The status of the structure can be written as a function of the structural member parameters. In the illustration, the shaded area denotes the event that the structure is not damaged. The calculation of the probability of the event that the structure is damaged, or not damaged, requires the knowledge of the distributions $f_{X_{mc}}(x_{mc})$ and $f_{X_{mb}}(x_{mb})$ for the current structure and the baseline structure, respectively, or the joint distribution $f_{X_{mc}, X_{mb}}(x_{mc}, x_{mb})$. In practice, this information is often unavailable or difficult to obtain for reasons of insufficient data. Furthermore, even when the required distributions can be specified, the exact evaluation of the probabilities, generally requiring the numerical integration, may be impractical. As a practical alternative, equivalent normal distributions may be resorted to in the approximation.
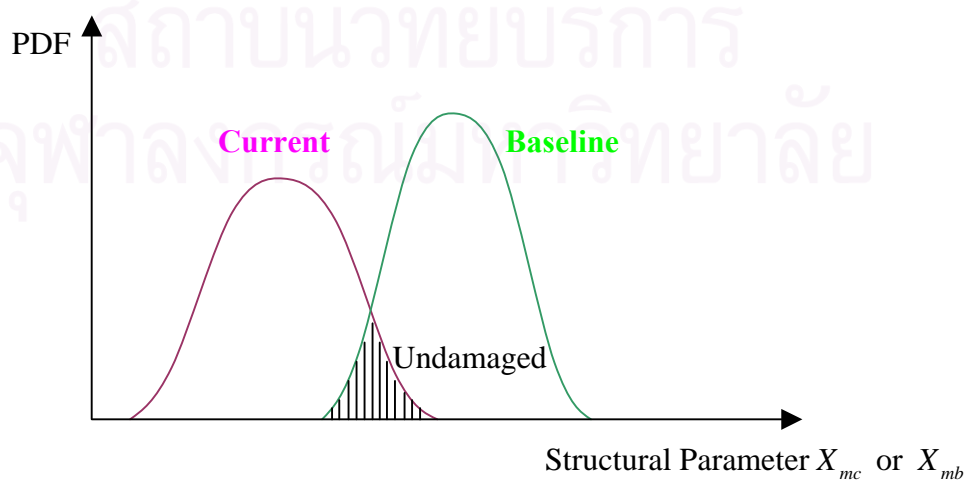
Figure 2.8 Identification of the damage statement

Not infrequently, the available information or data may be sufficient only to evaluate the first and second moments; namely, the mean values and variances of the respective random variables. Practical measures of the status of a structure, therefore, must be limited to functions of these first two moments. Under this condition, the implementation of damage assessment concepts must necessarily be limited to a formulation that is based on the first and second moments of the random variables—that is, restricted to the second-moment formulation (Cornell, 1969; Ang and Cornell, 1974). It may be emphasized that the second-moment approach is consistent also with the equivalent normal representation of non-normal distributions. With the second-moment approach, if the appropriate forms of the distributions are prescribed, the corresponding probability may be evaluated on the basis of equivalent normal distributions.

Let us consider a structural member m comprising multiple stiffness parameters $\mathbf{X}_m = \{X_m^1, X_m^2, \kappa, X_m^{N_p^m}\}$. The random variables representing the current and the baseline parameters are denoted as $\mathbf{X}_{mc}$ and $\mathbf{X}_{mb}$, respectively, and N_p^m denotes the number of different stiffness parameters for member m. We introduce a baseline margin of the member parameters—or the deviation from the baseline parameter values—of this structural member as

$$\mathbf{H}_m = \mathbf{X}_{mb} - \mathbf{X}_{mc} \qquad (2.94)$$

Based on this definition, the event that $\mathbf{H}_m < \mathbf{0}$ represents the "undamaged or healthy state" of member m. Likewise, the "damaged state" of member m is described by the event that $\mathbf{H}_m > \mathbf{0}$. The boundary separating these two states—the so-called "limit state"—is defined as the event when $\mathbf{H}_m = \mathbf{0}$.

For the current study we propose a linear function of the baseline margin for the member parameters in order to assess damage. The proposed function will hereafter be referred to as the "baseline function." Aside from its own usefulness, certain

aspects of the linear case would be the basis for an approximation to nonlinear baseline functions.

A linear baseline function for a structural member m can be written as

$$g\left(\mathbf{H}_m\right) = a_0^m + \sum_{i=1}^{N_p^m} a_i^m H_i^m \tag{2.95}$$

where a_0^m and a_i^m's are constants. The corresponding limit-state equation, therefore, is

$$a_0^m + \sum_{i=1}^{N_p^m} a_i^m H_i^m = 0 \tag{2.96}$$

To satisfy equation (2.94), the coefficient a_0^m must be zero. Thus, equation (2.96) can be rewritten as

$$\sum_{i=1}^{N_p^m} a_i^m H_i^m = 0 \tag{2.97}$$

In terms of the reduced variates, the limit-state equation becomes

$$\sum_{i=1}^{N_p^m} a_i^m \left[SD^{H_i^m} \tilde{H}_i^m + \bar{H}_i^m \right] = 0 \tag{2.98}$$

in which

$\tilde{H}_i^m$ is the reduced variate of the baseline margin H_i^m;

$\bar{H}_i^m$ is the mean of the baseline margin of parameter i for member m which is defined as $\bar{H}_i^m = \bar{X}_i^{mb} - \bar{X}_i^{mc}$ where $\bar{X}_i^{mb}$ and $\bar{X}_i^{mc}$ are the mean of the random variables representing the baseline and the current estimates of the ith parameter, respectively, for member m;

and $SD^{H_i^m}$ is the standard deviation of the baseline margin of parameter i for member m which is defined as $SD^{H_i^m} = \sqrt{\left(SD^{X_i^{mb}}\right)^2 + \left(SD^{X_i^{mc}}\right)^2}$ where $SD^{X_i^{mb}}$ and $SD^{X_i^{mc}}$ are the standard deviation of the random variables representing the baseline and the current estimates of the ith parameter, respectively, for member m.

Figure 2.9 illustrates an example of a baseline function composing of two reduced random variates $\tilde{H}_1^m$ and $\tilde{H}_2^m$ in which case equation (2.98) becomes

$$a_1^m\left[SD^{H_1^m}\tilde{H}_1^m + \bar{H}_1^m\right] + a_2^m\left[SD^{H_2^m}\tilde{H}_2^m + \bar{H}_2^m\right] = 0 \qquad (2.99)$$

which is a limit-state line in the two-dimensional $\tilde{H}_1^m$-$\tilde{H}_2^m$ coordinate space as shown in the figure.

The distance of the limit-state line in equation (2.99) to the origin of the reduced variates $\tilde{\mathbf{H}}_m$ can be computed as
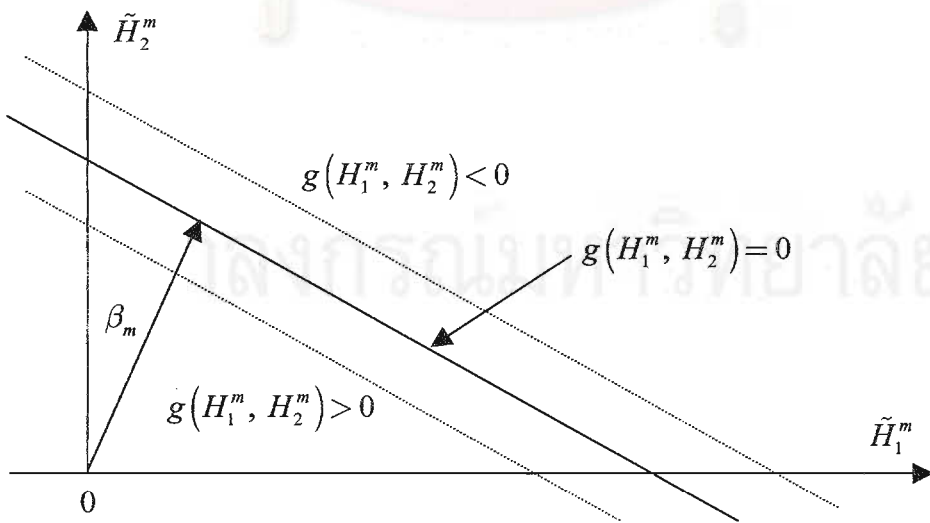
Figure 2.9 Healthy and damage states in coordinate of reduced variates.

$$\beta_m = \frac{\sum_{i=1}^{N_p^m} a_i^m \overline{H}_i^m}{\sqrt{\sum_{i=1}^{N_p^m} \left(a_i^m SD^{H_i^m}\right)^2}} \qquad (2.100)$$

For two uncorrelated normal variates, H_1^m and H_2^m, we can compute the probability of the damage state P_d^m directly as a function of the distance of the limit-state line to the origin of the reduced variates; that is, the distance β_m. This result can be generalized for N_p^m member parameters—if the random variables H_1^m, H_2^m, ..., $H_{N_p^m}^m$ are uncorrelated normal variables—in which case the probability of the damage state becomes

$$P_d^m = P\left(\sum_{i=1}^{N_p^m} a_i^m H_i^m > 0\right) = 1 - \Phi\left[\frac{-\sum_{i=1}^{N_p^m} a_i^m \overline{H}_i^m}{\sqrt{\sum_{i=1}^{N_p^m} \left(a_i^m SD^{H_i^m}\right)^2}}\right] = \Phi\left[\frac{\sum_{i=1}^{N_p^m} a_i^m \overline{H}_i^m}{\sqrt{\sum_{i=1}^{N_p^m} \left(a_i^m SD^{H_i^m}\right)^2}}\right] \qquad (2.101)$$

Comparing equations (2.100) and (2.101), we see that the argument inside the brackets of equation (2.101) is the distance β_m. Therefore, the probability P_d^m is again a function of the distance from the limit-state line $g(\mathbf{H}_m) = 0$ to the origin of the reduced variates. Therefore, in the general case of N_p^m uncorrelated normal variates, the probability of damage is

$$P_d^m = \Phi(\beta_m) \qquad (2.102)$$

where $\Phi(\beta_m)$ is the normal cumulative distribution function of the distance β_m which is defined as

$$\Phi\left(\beta_m\right) = \frac{1}{\sqrt{2\pi}} \int_{-\infty}^{\beta_m} e^{-\frac{1}{2}t^2} dt \qquad (2.103)$$

In the statistical damage assessment of a structure whose members consist of multiple parameters, the calculated probability of damage depends upon the coefficients a_i^m's, which represent many factors such as the type and the complexity of the structure, the location of the investigated structural members, etc. It can be observed from equation (2.95) that the weight factor a_i^m is obtained from a direct differentiation of $g\left(\mathbf{H}_m\right)$ with respect to the random variate H_i^m. Thus, the fluctuation of H_i^m from the actual value directly affects the approximation of $g\left(\mathbf{H}_m\right)$, and consequently the outcome of the damage assessment. One possible measure of the fluctuation in the value of H_i^m is the standard deviation of the corresponding baseline member parameter. In the current study, to investigate the effect of a_i^m's on the damage assessment results, two alternatives of a_i^m's are examined.

In the first scheme, we select a single value of a_i^m's for all parameters of member m as follows

$$a_i^m = \frac{1}{N_p^m} \qquad (2.104)$$

The value of a_i^m's in equation (2.104) represents the case in which all the parameters of member m affect the damage assessment with equal weight.

The selection of a_i^m's in the second scheme is based on the idea that the accuracy in assessing damage depends directly upon the accuracy of the outcome of the statistical parameter estimation. Generally, for the case of normal approximation the accuracy of the parameter estimates is determined by the value of the standard deviation. As such, we compute the weight factor for each member parameter taking into account its accuracy with respect to the baseline value as

$$a_i^m = \frac{1/SD^{X_i^{mb}}}{\sum_{i=1}^{N_p^m}\left(1/SD^{X_i^{mb}}\right)} \tag{2.105}$$

in which

$SD^{X_i^{mb}}$ is the standard deviation of the baseline parameter i for member m.

Note that the summation of the weight factors a_i^m's is equal to one in both of the proposed schemes.

2.5 Chapter Summary

The statistical damage assessment of a structure based on the statistical parameter estimation algorithm from the measured response is a complicated problem. The noise in the measurements poses a direct effect on the sensitivity of the parameter estimates. The statistical damage assessment algorithms that compare the probability density functions of the healthy and damaged system parameters have been proved effective for the identification of damage in the presence of the measurement noise. The performance of these methods, however, depends considerably upon the quality of the estimated system parameters. The present study adopts the regularization technique to reduce the degree of instabilities of solutions to the statistical parameter estimation problem by adding a regularization function to the initial objective function as a penalty term. The statistical parameter estimation methods investigated are the Monte Carlo simulation method, the optimum sensitivity method and the sensitivity-based method. The performance of the proposed damage assessment scheme is examined in Chapter 4.

CHAPTER 3

SIMULATION STUDY—A BRIDGE TRUSS

3.1 Introduction

In this chapter, we examine the efficacy of the statistical damage assessment method presented in Chapter 2 by using a truss structure as the model problem. We consider two distinct cases of damage: the single-damaged-member case and the two-damaged-member case. For each of these damage cases, we generate 10 different damage scenarios by randomly varying the location and the severity of damage. The performance of the algorithm is assessed in terms of the probability in which the actual level of damage for a structural member lies beyond the prescribed level of damage, $P\left(X_{mc} < X_{mb}(1-\theta_m) \right)$. This assessment is illustrated through the plot of the probability distribution $P\left(X_{mc} < X_{mb}(1-\theta_m) \right)$ for the range 0-100% of the level of damage for all members in the structure.

Due to the presence of noise in the measurements, the statistical parameter estimation methods are used to construct the statistical distribution of the parameter estimates for the statistical damage assessment. For the current study we examine three methods of statistical parameter estimation; i.e., the Monte Carlo simulation method, the sensitivity-based method and the optimum sensitivity-based method. We use these three methods in conjunction with the output error estimator (OEE) and the regularized output error estimator (ROEE) to investigate the performance of the present statistical damage assessment scheme from using different statistical evaluation schemes and estimators to approximate the distribution of the system parameters. This investigation is carried out by examining the plot of the probability distribution $P(X_{mc} < X_{mb}(1-\theta_m))$ for the member parameters with respect to different levels of damage. The effect of varying the levels of noise in the measurements on the performance of each algorithm is also investigated in the current study.

3.2 Description of the Example Structure

The structure we investigate herein is a simple-support truss structure with the geometry and topology shown in Figure 3.1. In this figure the numbers in circles represent the member identification numbers and the numbers in triangles represent the nodal identification numbers. The finite-element model of the truss structure consists of 11 elements with 11 degrees of freedom. The baseline properties of the truss members can be characterized by eleven stiffness parameters, each representing the axial stiffness for each member. The cross-sectional area, the stiffness, and the mass associated with each of the truss members are listed in Table 3.1. Note that in addition to the self weight of the structural members shown in the table, we assume that the dead load being imposed upon the structure is uniformly distributed along the length of all 11 members with a value of 0.017 kips-sec^2/ft/ft. Moreover, all members are assumed to have a Young's modulus of 4.176ด 10^6 kips/ft^2.

In the current study we assume that all of the 11 structural vibration modes are measured and all natural frequencies and mode shapes of the structure are available as our measurement information. In addition, the mode shapes are assumed to be measured at all 11 degrees of freedom of the structural model as shown in Figure 3.2. The free-vibration responses obtained from an eigenvalue analysis of the baseline structure are shown in Table 3.2, in which the ith mode shape $\mathbf{\Phi}_i$ is scaled by using the mass matrix $\mathbf{M}$ such that $\mathbf{\Phi}_i^T \mathbf{M} \mathbf{\Phi}_i = 1$.
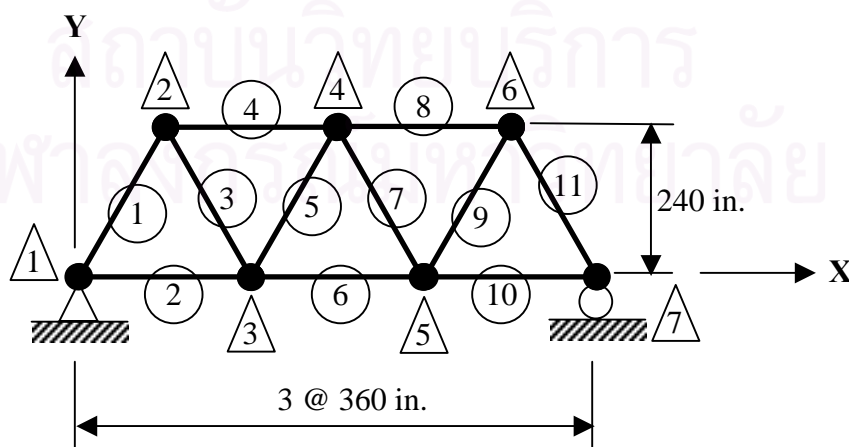
Figure 3.1 Geometry and topology of the simple-support truss.

Table 3.1 Baseline properties of the truss structure.

Member ID Number	Member Location	Cross-Sectional Area (in.^{2})	Stiffness Parameter $\hat{x}_b$ (kips)	Mass (kips-sec^2/ft/ft)
1	Diagonal	28.0	8.12×10^5	0.00298
2	Bottom	40.0	1.16×10^6	0.00425
3	Diagonal	28.0	8.12×10^5	0.00298
4	Top	32.0	9.28×10^5	0.00318
5	Diagonal	28.0	8.12×10^5	0.00298
6	Bottom	40.0	1.16×10^6	0.00425
7	Diagonal	28.0	8.12×10^5	0.00298
8	Top	32.0	9.28×10^5	0.00318
9	Diagonal	28.0	8.12×10^5	0.00298
10	Bottom	40.0	1.16×10^6	0.00425
11	Diagonal	28.0	8.12×10^5	0.00298

3.3 Statistical Damage Assessment

The simulation studies conducted in this section consist of single-damaged-member cases and two-damaged-member cases. For the single-damaged-member cases the damage of the structure is represented by a reduction of the stiffness of a single structural member whereas for the two-damaged-member cases the damage is due to the stiffness reduction of two structural members.
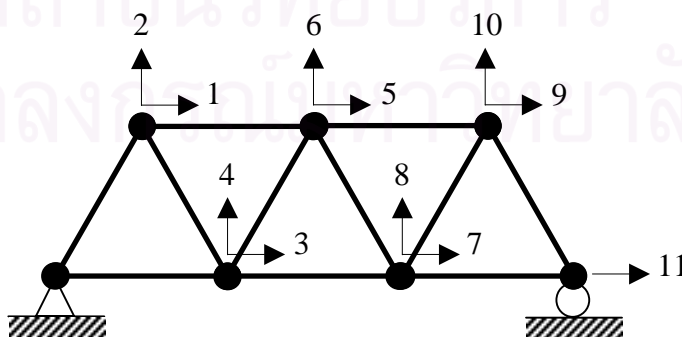
Figure 3.2 The set of measured degrees of freedom for the truss structure.

Table 3.2 Noise-free data for the baseline structure.

	1st Mode	2nd Mode	3rd Mode	4th Mode	5th Mode	6th Mode	7th Mode	8th Mode	9th Mode	10th Mode	11th Mode
Natural Frequency (Hz)	7.52	13.10	23.88	36.70	42.87	47.40	52.54	56.22	67.18	78.99	90.27
Mode Shape											
1st DOF	-0.24728	0.27596	-0.09842	0.74436	-0.16395	-0.11704	0.44056	0.46926	0.66564	-0.47303	-0.35455
2nd DOF	0.28023	-0.02279	0.54413	-0.12041	-0.66300	0.00321	0.96490	0.00484	-0.41867	-0.00360	0.11268
3rd DOF	-0.08799	0.29399	-0.09137	0.16103	0.37317	0.47314	0.00824	0.22963	-0.68011	-0.40920	0.45338
4th DOF	0.46840	0.16771	0.64623	-0.03952	-0.06496	0.30263	-0.61933	0.32096	0.28618	-0.21368	-0.05079
5th DOF	-0.15371	0.41119	0.21543	0.44232	-0.26596	-0.12822	-0.27599	-0.13535	-0.09732	0.83292	0.37072
6th DOF	0.53577	0.20150	0.00152	0.35877	0.78183	-0.13049	0.22752	-0.52007	0.09377	0.11138	-0.16068
7th DOF	-0.20394	0.41081	-0.01880	-0.38068	0.04657	0.47008	0.16375	0.04276	0.00479	0.33638	-0.84073
8th DOF	0.45965	0.25904	-0.59230	-0.23919	-0.09411	-0.42503	0.08437	0.63927	-0.17326	0.23701	0.03655
9th DOF	-0.05827	0.53964	0.00746	-0.17096	-0.26363	-0.68259	-0.29687	-0.47272	-0.35438	-0.79523	-0.27601
10th DOF	0.26210	0.14110	-0.56737	0.01723	-0.71742	0.72318	-0.09238	-0.53465	0.32129	-0.19434	0.25375
11th DOF	-0.25675	0.43094	0.19543	-0.65856	0.37925	-0.10094	0.38681	0.03838	0.82369	0.01781	1.05958

As previously discussed in Chapter 2, statistical parameter estimation is a key process in the current statistical damage assessment algorithm. In general, the modal response of a structure can be obtained through modal testing—by shaking the structure under certain resonance forces at the natural frequencies of the structure. For the current study, however, we model the measurement data of the structural response by using a computer simulation. The modal responses of the baseline structure in Table 3.2 are used as the noise-free measurement data $\hat{\mathbf{\Phi}}_b$ upon which the mean and the covariance matrix of the parameter estimates of the baseline structure, $\overline{\mathbf{x}}_b$ and $\mathbf{R}_b^{\mathbf{x}}$, are obtained by using different statistical parameter estimation algorithms. The statistical parameter estimation process for the baseline structure is illustrated in Figure 3.3. For the current structure the noise-free measurement data $\hat{\mathbf{\Phi}}_c$ are computed from an eigenvalue analysis of the structural model parameterized with the current stiffness parameters $\hat{\mathbf{x}}_c$ which are associated with each of the damage cases considered. The noise-free data $\hat{\mathbf{\Phi}}_c$ of the current structure are used to simulate the

$$\hat{\mathbf{x}}_b \longrightarrow \boxed{\text{FEM}} \longrightarrow \hat{\mathbf{\Phi}}_b \longrightarrow \boxed{\text{Statistical Parameter Estimation}} \longrightarrow \overline{\mathbf{x}}_b, \mathbf{R}_b^x$$
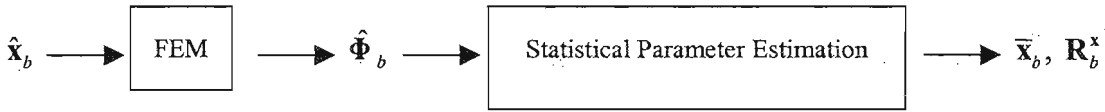
Figure 3.3 Statistical parameter estimation process for the baseline structure.

noisy measurement data $\hat{\mathbf{\Phi}}_c^\eta$ to account for the presence of noise in the measurements by using the data perturbation scheme of equation (2.35). With the simulated noisy measurements, the mean and the covariance matrix of the parameter estimates for the current structure, $\overline{\mathbf{x}}_c$ and $\mathbf{R}_c^x$, can be obtained from the statistical parameter estimation schemes. The schematic representation of this process is illustrated in Figure 3.4.

For the Monte Carlo method the statistical distribution of the parameter estimates can be obtained directly from the Monte Carlo sample of the parameter estimates. For the sensitivity-based and the optimum sensitivity-based methods, the statistical distribution of the parameter estimates for the baseline structure and the current structure is constructed by substituting the statistical indices from the statistical parameter estimation process into the probability density function of equation (2.88). By comparing the statistical distribution of the parameter estimates for the baseline and the current structures, the severity of damage for each structural member can be identified.

$$\hat{\mathbf{x}}_c \longrightarrow \boxed{\text{FEM}} \longrightarrow \hat{\mathbf{\Phi}}_c \longrightarrow \boxed{\hat{\mathbf{\Phi}}_c(1+\alpha\eta_{ij})} \longrightarrow \hat{\mathbf{\Phi}}_c^\eta$$

$$\overline{\mathbf{x}}_c, \mathbf{R}_c^x \longleftarrow \boxed{\text{Statistical Parameter Estimation}}$$
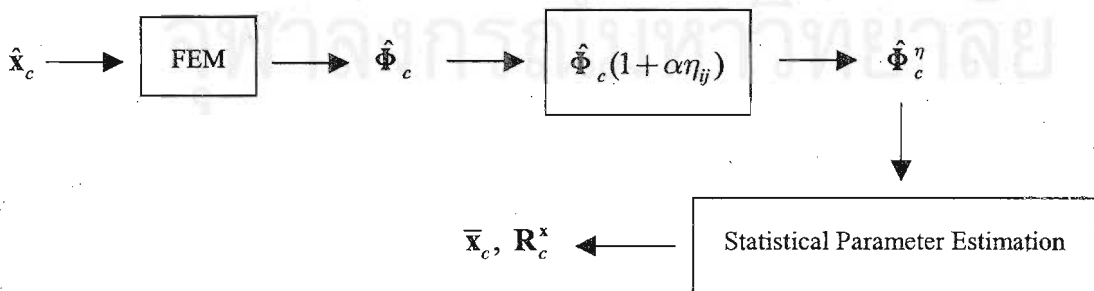
Figure 3.4 Statistical parameter estimation process for the current structure.

3.3.1　Single-Damaged-Member Cases

The single-damaged-member cases investigated herein consist of ten different combinations of the location and the severity of damage that are randomly generated as summarized in Table 3.3. In this table, the noise levels indicate different levels of noise amplitude a that are used in equation (2.35) to generate the noisy measurements. For each of the damage cases considered, three different statistical parameter estimation methods; i.e., the Monte Carlo simulation method, the sensitivity-based method, and the optimum sensitivity-based method, are used in conjunction with the OEE and ROEE algorithms to estimate the mean and the covariance matrix of parameters.

3.3.1.1 Monte Carlo Simulation with OEE Algorithm

The simulation studies conducted in this section are for the 10 different damage cases shown in Table 3.3 in which only a single member is damaged. The severity of damage is expressed in terms of the level of damage θ_m, as a percentage of reduction from the baseline parameters.

Table 3.3 Different damage scenarios with single damaged member

Damage Case	Damaged Member	Damage Level	Noise Levels
1	3	63.75%	1%, 3%, 5%, 10%, 15% and 20%
2	4	3.55%	1%, 3%, 5%, 10%, 15% and 20%
3	11	51.64%	1%, 3%, 5%, 10%, 15% and 20%
4	6	41.92%	1%, 3%, 5%, 10%, 15% and 20%
5	8	14.97%	1%, 3%, 5%, 10%, 15% and 20%
6	10	30.54%	1%, 3%, 5%, 10%, 15% and 20%
7	5	84.45%	1%, 3%, 5%, 10%, 15% and 20%
8	2	21.61%	1%, 3%, 5%, 10%, 15% and 20%
9	9	96.17%	1%, 3%, 5%, 10%, 15% and 20%
10	1	78.64%	1%, 3%, 5%, 10%, 15% and 20%

In the Monte Carlo simulation method, synthetic measurements are created from a single measurement set by using computer-generated random numbers. The mathematical expression for this process is shown in equation (2.35). The population of the parameter estimates is obtained by repeating the nonlinear least-squares minimization of equation (2.10) for each of the artificial measurements. The statistical distribution of the population of the estimated system parameters can be directly extracted from the computed Monte Carlo sample, from which the mean and the covariance matrix of the parameter estimates, $\overline{\mathbf{x}}$ and $\mathbf{R^x}$, can be obtained using the standard definition of the mean and the covariance matrix of a finite discrete data set. The concept behind Monte Carlo simulation is fairly simple and straightforward. Generally, the approximations can improve as the number of synthetic measurements increases.

In our simulation of the measurement data, only the mode shapes are taken as noise-polluted whereas the natural frequencies are noise-free. Moreover, the measurement information is assumed to be taken for all of the 11 structural vibration modes at all degrees of freedom of the structural model.

Following the work of Pothisiri and Hjelmstad (2003), we assess damage in a structural member by using the probability of the event that the value of the estimated parameter for that member is smaller than the value of the corresponding parameter estimate for the same member in the associated baseline structure to a certain extent (i.e., $X_{mc} < X_{mb}(1-\theta_m)$). By associating the probability value, $P(X_{mc} < X_{mb}(1-\theta_m))$, with each prescribed level of damage θ_m, we can plot the probability distribution for the range of 0-100% of the level of damage for all members in the structure as shown in the following illustrations. The plot of the probability distribution for a structural member can be divided into three parts starting from no damage to 100% damage. The constant unit probability value at low levels of damage indicates that the actual value of the member parameter is actually smaller than the parameter values associated with the damage at these levels. Likewise, the zero probability value at high levels of damage implies that there is no chance for the actual severity of damage to fall within these regions. Generally, the actual level of damage lies in the transition region between the unit probability and zero probability zones that appears as a slope

in the probability distribution. Note that the sensitivity of a member parameter to the measurement noise can be drawn from the probability distribution. A sharp drop in the probability values within the transition region indicates a low sensitivity of the member parameter to noise. A member parameter that is more sensitive to noise shows a more gradual decrease in the probability values within the transition zone. Hence, it might be difficult to identify a precise level of the actual damage from the probability distribution when the level of noise in the measurements is high. However, one can always describe the suspected level of damage in terms of probability to ensure the level of confidence in the results.

As previously discussed, the outcome of statistical parameter estimation by using the Monte Carlo simulation method can improve as the number of synthetic measurements, or the sample size for the parameter estimates, increases. This aspect of the algorithm is investigated by using different sample sizes to determine the values of the mean and the standard deviation of the parameter estimates. Figures 3.5 and 3.6 show the variation of the mean and the standard deviation of the parameter estimates for the baseline structural members with respect to different sample sizes for
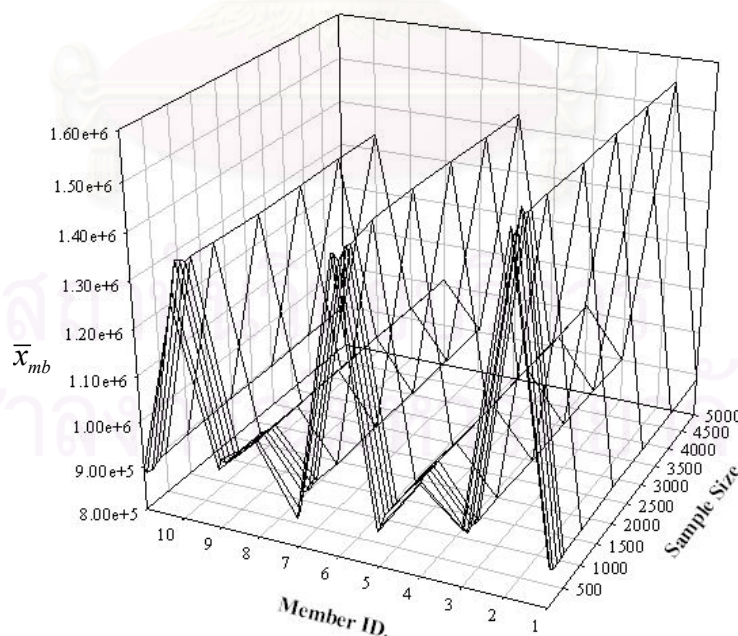
Figure 3.5 Variation of the mean of the parameter estimates for the baseline structural members with respect to different Monte Carlo sample sizes using 5% noisy measurements.
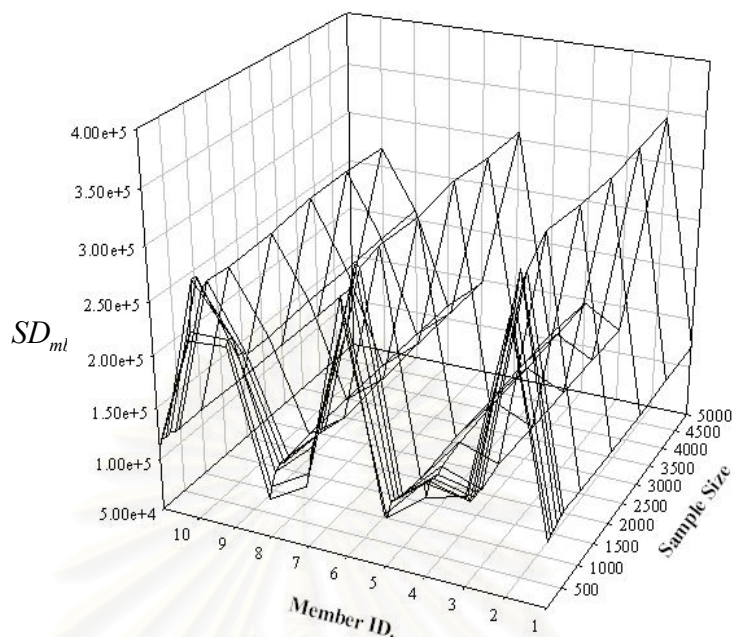
Figure 3.6 Variation of the standard deviation of the parameter estimates for the baseline structural members with respect to different Monte Carlo sample sizes using 5% noisy measurements.

the 5% noisy measurement case. It is seen from the figures that 1,000 samples are sufficient to ensure the accuracy of the mean and the standard deviation of the population of the parameter estimates. Therefore, we use 1,000 Monte Carlo samples to construct the statistical distribution of the parameter estimates for the assessment of damage in our simulation studies.

The damage assessment results are illustrated in Figure 3.7 for the ten damage cases with 1% noise in the measurements. It can be seen that the damage in all damage cases is successfully located and quantified. For example, from the plot of the probability distribution of damage case 1 (member 3 damaged with 63.75% severity), the severity of damage is suspected to fall in the range of 62.5-87.5%. The level of confidence in identifying a suspected level of damage as the actual damage severity is indicated by the value of the probability $P(X_{mc} < X_{mb}(1-\theta_m))$. For example, the probability value of 0.60 for 75% damage in member 3 indicates that it is 60% likely that the actual value of the member parameter is smaller than the value of the estimated parameter for the member with 75% damage. For the undamaged members,

Figure 3.7 Probability distribution with respect to different levels of damage for the single-damaged-member cases from 1,000 samples of parameter estimates (Monte Carlo simulation + OEE) using 1% noisy measurements.

it is seen that member 9 in damage cases 3 and 10 is also indicated a slight chance of the member being lightly damaged. Nonetheless, the probability of damage in member 9 for damage cases 3 and 10 is small compared with that of the actual damaged members.

The results from the damage cases in which 3%, 5%, 10%, 15% and 20% noisy measurements are used are shown in Figures 3.8, 3.9, 3.10, 3.11 and 3.12, respectively. It is seen that the actual damaged members are successfully identified for 3% and 5% noisy measurements. These members are, however, difficult to identify as being damaged when the level of noise in the measurements is increased to 10% and are unable to identify as being damaged at all for 15% and 20% noise levels. This observation leads to a conclusion that the performance of the current damage assessment algorithm may decrease as the level of noise in the measurements increases. In addition, it is observed that as the level of noise in the measurements increases, the decrease in the probability values for a structural member in the transition region becomes more gradual. Hence, it is more difficult to identify the actual level of damage in a structural member. Nevertheless, it is seen from the results of the current simulation that most undamaged members show significantly lower probability of being damaged compared with the actual damaged member for 3% and 5% noisy measurements. However, there is no constant unit-probability zone in the distribution of $P(X_{mc} < X_{mb}(1-\theta_m))$ for these members. Without the existence of this unit-probability zone for the assessed member, one cannot be absolutely certain that there is damage in that member. Hence, it is concluded that the deviation of the parameter estimate for these undamaged members is merely due to the measurement noise. For 10%, 15% and 20% noisy measurements, there is no clear distinction between the results for damaged and undamaged members. Hence, it is difficult to identify whether a member is damaged or undamaged by visual inspection of the simulation results.

From the results of the current simulation studies, it is evident that the performance of the proposed algorithm to assess damage in a structural system is limited by the level of noise in the measurements. However, the performance of the algorithm may also be affected by the severity of the damage in the structural

Figure 3.8 Probability distribution with respect to different levels of damage for the single-damaged-member cases from 1,000 samples of parameter estimates (Monte Carlo simulation + OEE) using 3% noisy measurements.

Figure 3.9 Probability distribution with respect to different levels of damage for the single-damaged-member cases from 1,000 samples of parameter estimates (Monte Carlo simulation + OEE) using 5% noisy measurements.

Figure 3.10 Probability distribution with respect to different levels of damage for the single-damaged-member cases from 1,000 samples of parameter estimates (Monte Carlo simulation + OEE) using 10% noisy measurements.

Figure 3.11 Probability distribution with respect to different levels of damage for the single-damaged-member cases from 1,000 samples of parameter estimates (Monte Carlo simulation + OEE) using 15% noisy measurements.

Figure 3.12 Probability distribution with respect to different levels of damage for the single-damaged-member cases from 1,000 samples of parameter estimates (Monte Carlo simulation + OEE) using 20% noisy measurements.

components. To examine the effect of the severity of damage in a structural member on the performance of the proposed algorithm, we compare the distribution of $P(X_{mc} < X_{mb}(1-\theta_m))$ for 10 different levels of damage ranging from 5% to 95% in member 2 and member 4 with 1%, 3% and 5% noises in the measurements.

The results for different severities of damage in member 4 are illustrated in Figures 3.13, 3.14 and 3.15, respectively, for 1%, 3% and 5% noisy measurements. Also, Figures 3.16-3.18 show the results for different damage severities of member 2. For the cases where member 4 is damaged, the lowest levels of damage severity which can be detected for 1%, 3% and 5% noisy measurements are 15%, 35% and 65%, respectively. For the cases where member 2 is damaged, the lowest levels of damage severity which can be detected are 25% and 35% for 1% and 3% noisy measurements, respectively, whereas the algorithm fails to identify damage at all for 5% noisy measurements. Thus, it is concluded that there is more chance for the proposed algorithm to successfully identify damage in a more severely damaged structural member.

3.3.1.2 The Sensitivity-Based Method with OEE Algorithm

In this section, the sensitivity-based method is used in conjunction with the OEE algorithm to obtain the statistical distribution of the parameter estimates. Again, the ten different damage cases in Table 3.3 are used to investigate the performance of the algorithm. The simulation results show that for all damage cases the maximum level of noise in which damage can be assessed is 10%. For the cases where the level of noise in the measurements is more than 10%, the statistical parameter estimation algorithm does not converge and hence the assessment of damage is not possible. Therefore, only 4 different noise levels—e = 1%, 3%, 5% and 10%—can be used to examine the performance of the current algorithm.

The results for the ten investigated damage cases with four different levels of noise in the measurements are shown in Figures 3.19-3.22. For 1% noisy measurements, as illustrated in Figure 3.19, it can be seen that the actual damage in all damage cases is successfully located and quantified. Nevertheless, there is no constant

Figure 3.13 Probability distribution with respect to different levels of damage for different severities of damage in member 4 from 1,000 samples of parameter estimates (Monte Carlo simulation + OEE) using 1% noisy measurements.
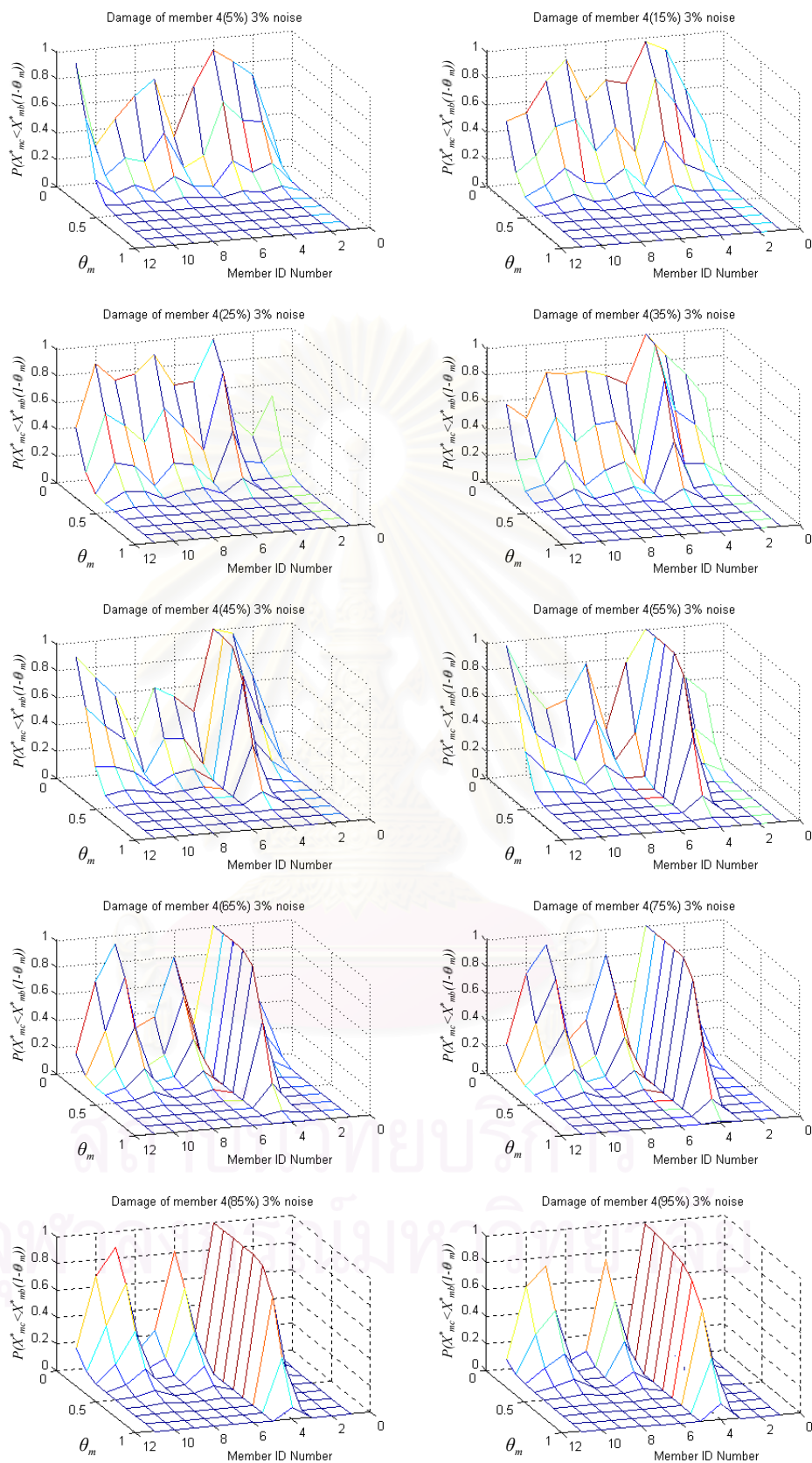
Figure 3.14 Probability distribution with respect to different levels of damage for different severities of damage in member 4 from 1,000 samples of parameter estimates (Monte Carlo simulation + OEE) using 3% noisy measurements.
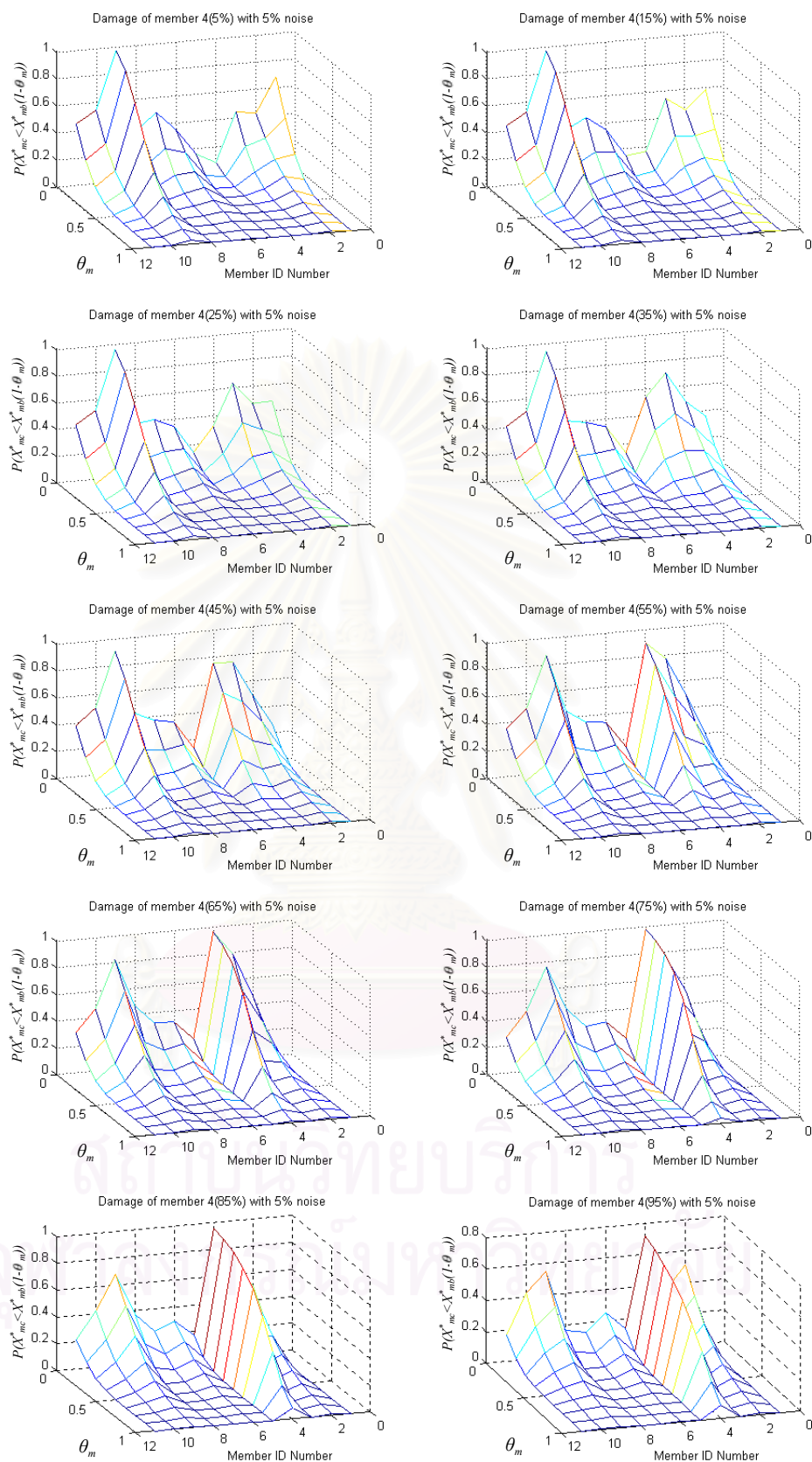
Figure 3.15 Probability distribution with respect to different levels of damage for different severities of damage in member 4 from 1,000 samples of parameter estimates (Monte Carlo simulation + OEE) using 5% noisy measurements.
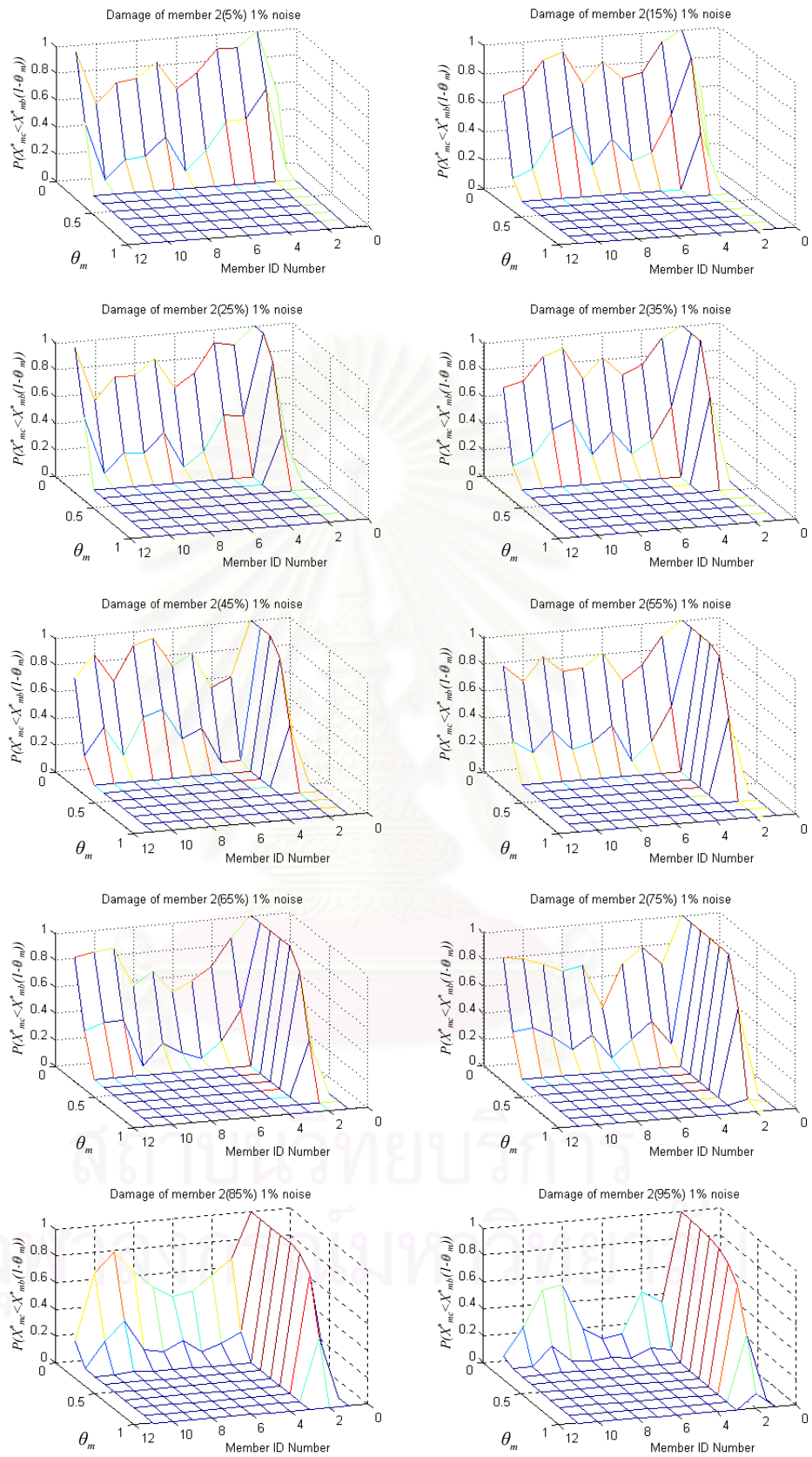
Figure 3.16 Probability distribution with respect to different levels of damage for different severities of damage in member 2 from 1,000 samples of parameter estimates (Monte Carlo simulation + OEE) using 1% noisy measurements.
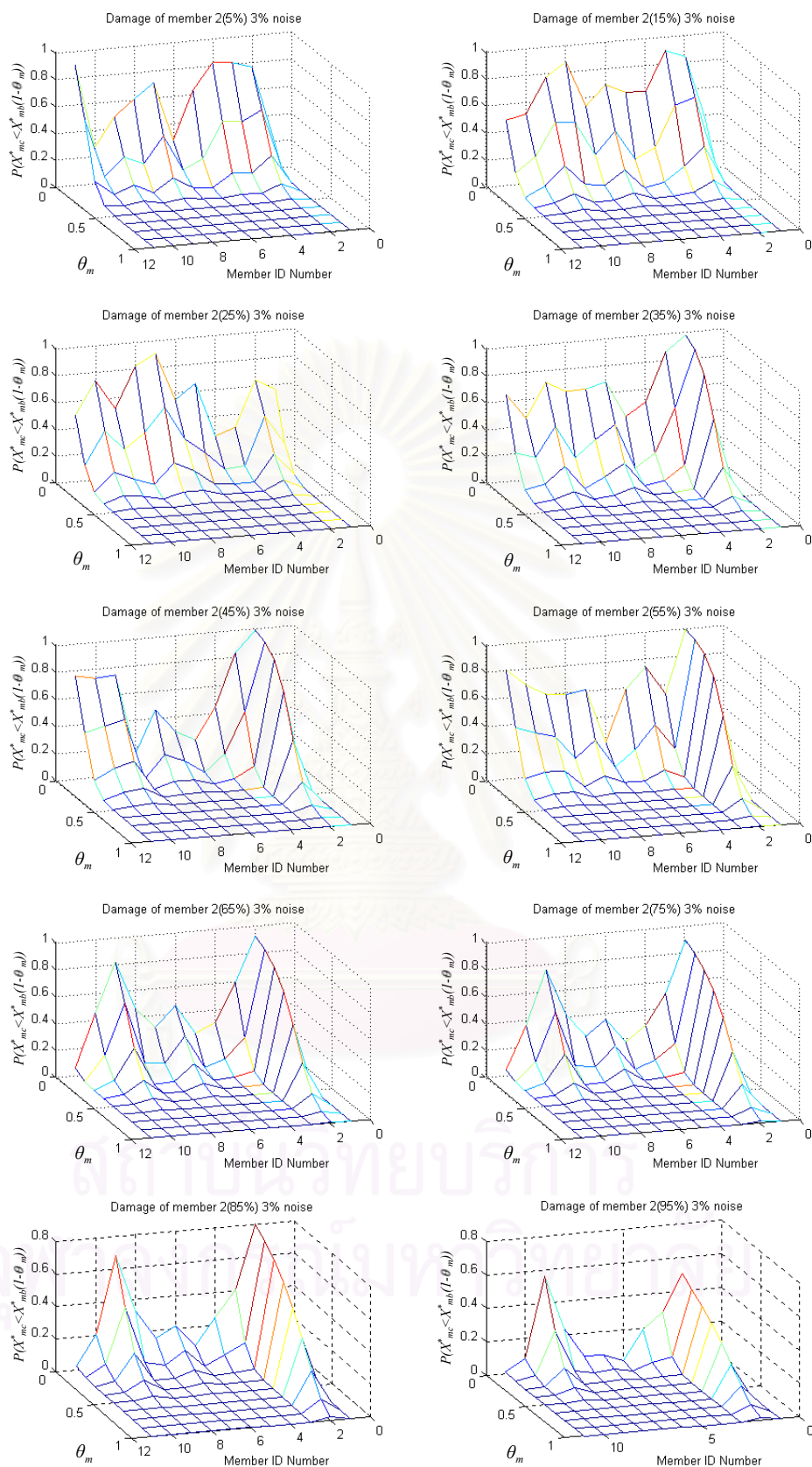
Figure 3.17 Probability distribution with respect to different levels of damage for different severities of damage in member 2 from 1,000 samples of parameter estimates (Monte Carlo simulation + OEE) using 3% noisy measurements.
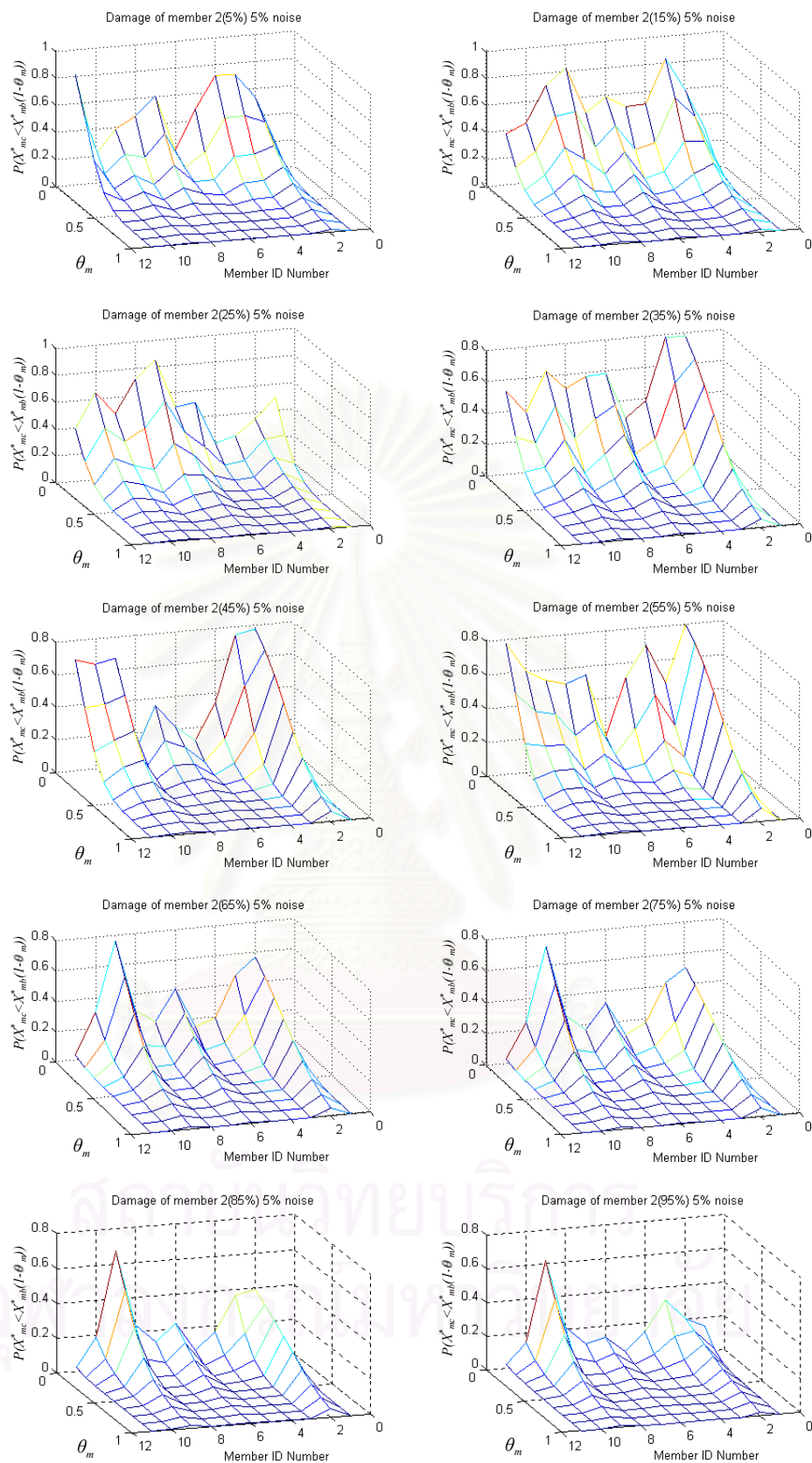
Figure 3.18 Probability distribution with respect to different levels of damage for different severities of damage in member 2 from 1,000 samples of parameter estimates (Monte Carlo simulation + OEE) using 5% noisy measurements.

Figure 3.19 Probability distribution with respect to different levels of damage for the single-damaged-member cases using the sensitivity-based method and OEE algorithm with 1% noisy measurements.

Figure 3.20 Probability distribution with respect to different levels of damage for the single-damaged-member cases using the sensitivity-based method and OEE algorithm with 3% noisy measurements.

Figure 3.21 Probability distribution with respect to different levels of damage for the single-damaged-member cases using the sensitivity-based method and OEE algorithm with 5% noisy measurements.

Figure 3.22 Probability distribution with respect to different levels of damage for the single-damaged-member cases using the sensitivity-based method and OEE algorithm with 10% noisy measurements.

unit-probability zone in the distribution of $P(X_{mc} < X_{mb}(1-\theta_m))$ for undamaged members in any of the damage cases considered. Hence, damage cannot be identified in these members. It is also noted that the performance of the damage assessment algorithm in this case is better compared to using the Monte Carlo simulation method and the OEE algorithm. For the same level of noise in the measurements, the results from the sensitivity-based method provide steeper slopes of the probability distribution within the transition zone for the damaged and undamaged members compared with the results from the Monte Carlo simulation method.

The results of the algorithm when the level of noise in the measurements is increased to 3%, 5%, and 10% are shown in Figures 3.20, 3.21, and 3.22, respectively. The actual damaged members are successfully identified for 3% and 5% noisy measurements. However, it is difficult to identify the actual damaged members from the probability distribution for 10% noisy measurements.

3.3.1.3 The Optimum Sensitivity-Based Method with OEE Algorithm

For the current section we examine the performance of the statistical damage assessment algorithm by using the optimum sensitivity-based method and the OEE algorithm to estimate the mean and the covariance matrix of the parameter estimates. The mean and the covariance matrix of the parameter estimates are used to construct the statistical distribution of the system parameters from which the damage is assessed. The results from the assessment of damage for all the damage cases of Table 3.3 show that the maximum level of noise permitting a damage assessment is 10%. As for the case of the sensitivity-based method, when the level of noise in the measurements is more than 10%, the statistical parameter estimation algorithm does not converge, making it impossible to assess damage. Hence, only the results from using four levels of measurement noise—i.e., e = 1%, 3%, 5% and 10%—are illustrated in the present section.

The results for the ten damage cases considered using four different levels of noise in the measurements are shown in Figures 3.23-3.26. For 1% noisy measurements, it can be seen that the actual damage in all damage cases is
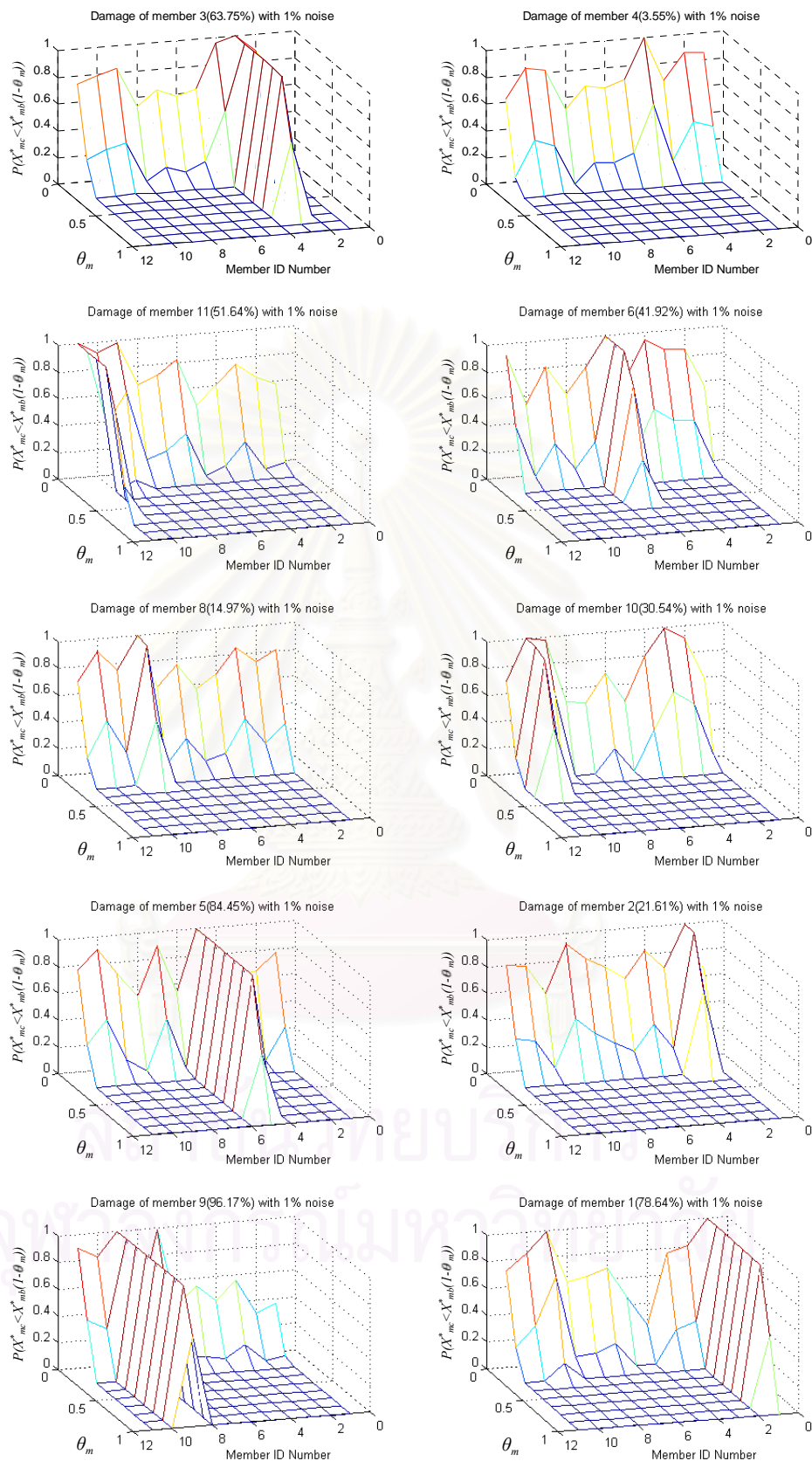
Figure 3.23 Probability distribution with respect to different levels of damage for the single-damaged-member cases using the optimum sensitivity-based method and OEE algorithm with 1% noisy measurements.

Figure 3.24 Probability distribution with respect to different levels of damage for the single-damaged-member cases using the optimum sensitivity-based method and OEE algorithm with 3% noisy measurements.

Figure 3.25 Probability distribution with respect to different levels of damage for the single-damaged-member cases using the optimum sensitivity-based method and OEE algorithm with 5% noisy measurements.

Figure 3.26 Probability distribution with respect to different levels of damage for the single-damaged-member cases using the optimum sensitivity-based method and OEE algorithm with 10% noisy measurements.

successfully located and quantified. Again, it is observed that there is no constant unit-probability zone in the distribution of $P(X_{mc} < X_{mb}(1-\theta_m))$ for undamaged members in any of the damage cases considered. Hence, damage cannot be identified in these members. It is also noted that the performance of the damage assessment algorithm in this case is better compared to using the Monte Carlo simulation method and the OEE algorithm.

The simulation studies of the current damage assessment algorithm for different damage cases with 3%, 5% and 10% noise in the measurements show similar trends to those of the sensitivity-based method with OEE. Hence, it is also concluded that the damage assessment results improve as the level of the measurement noise decreases. In addition, it is seen that the results using high levels of noise in the measurements exhibit higher variation in the parameter estimates compared with the results using lower levels of noise in the measurements as evident from a more gradual decrease in the probability distribution. Thus, it can be concluded that the sensitivity of the member parameters to noise increases with the noise level.

3.3.1.4 Monte Carlo Simulation with ROEE Algorithm

As previously discussed, the ROEE algorithm is improved from the OEE algorithm by adding a regularization function as the penalty term to the objective function to reduce the instabilities of the solutions in the parameter estimation process. The solutions of the ROEE algorithm are expected to be more clustered than those of the OEE algorithm. As before, we assume for our simulation studies that the natural frequency measurements are noise-free while the mode shape measurements are noise-polluted. We investigate six different levels of noise—e = 1%, 3%, 5%, 10%, 15% and 20%—in the measurements. Again, we use the ten damage cases in Table 3.3 as the model problems for examining the performance of the proposed algorithm.

The results of the algorithm when the levels of noise in the measurements are 1%, 3%, 5%, 10%, 15% and 20% are shown in Figures 3.27, 3.28, 3.29, 3.30, 3.31 and 3.32, respectively. From the results of the simulation study, it is seen that the actual
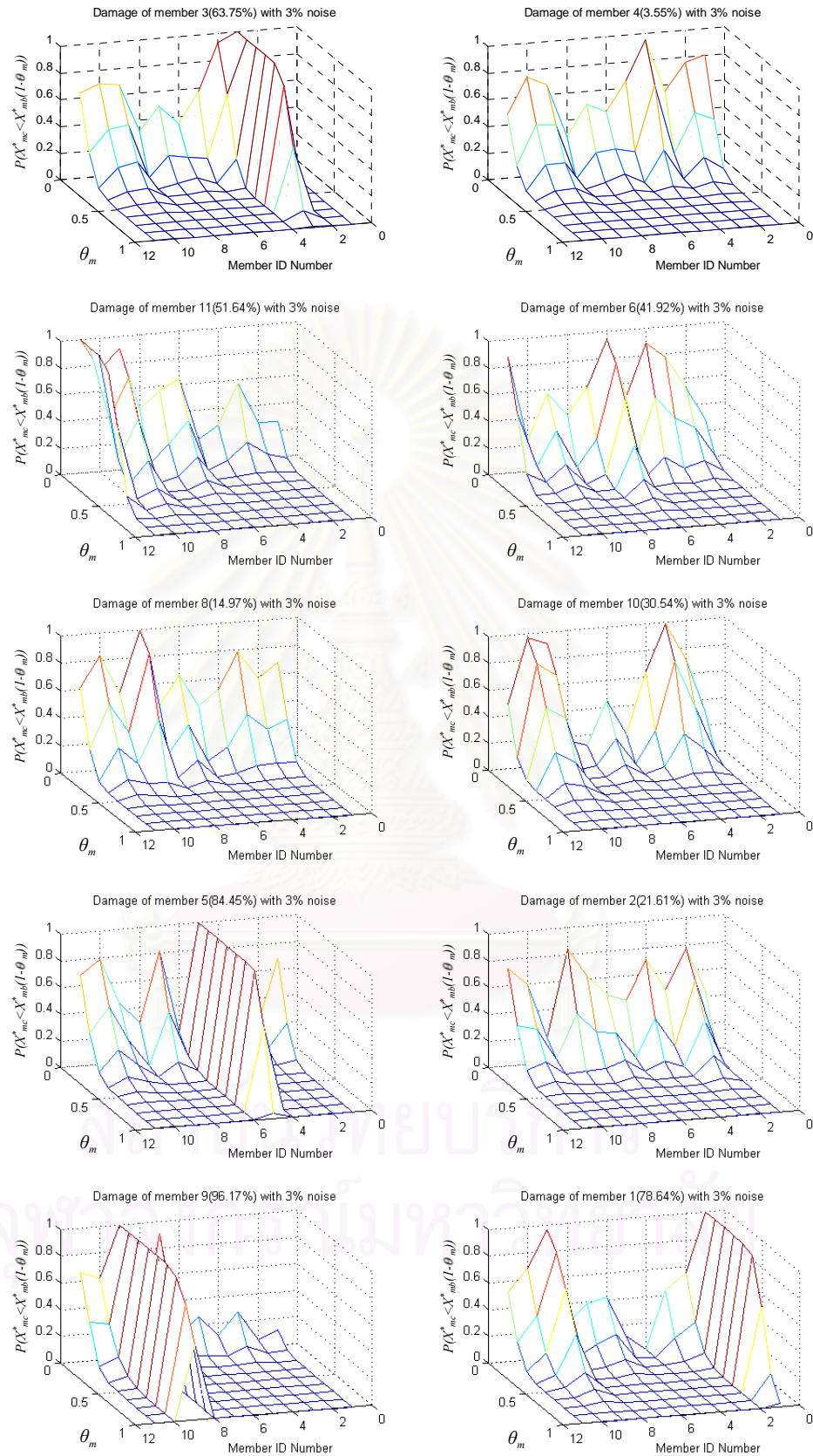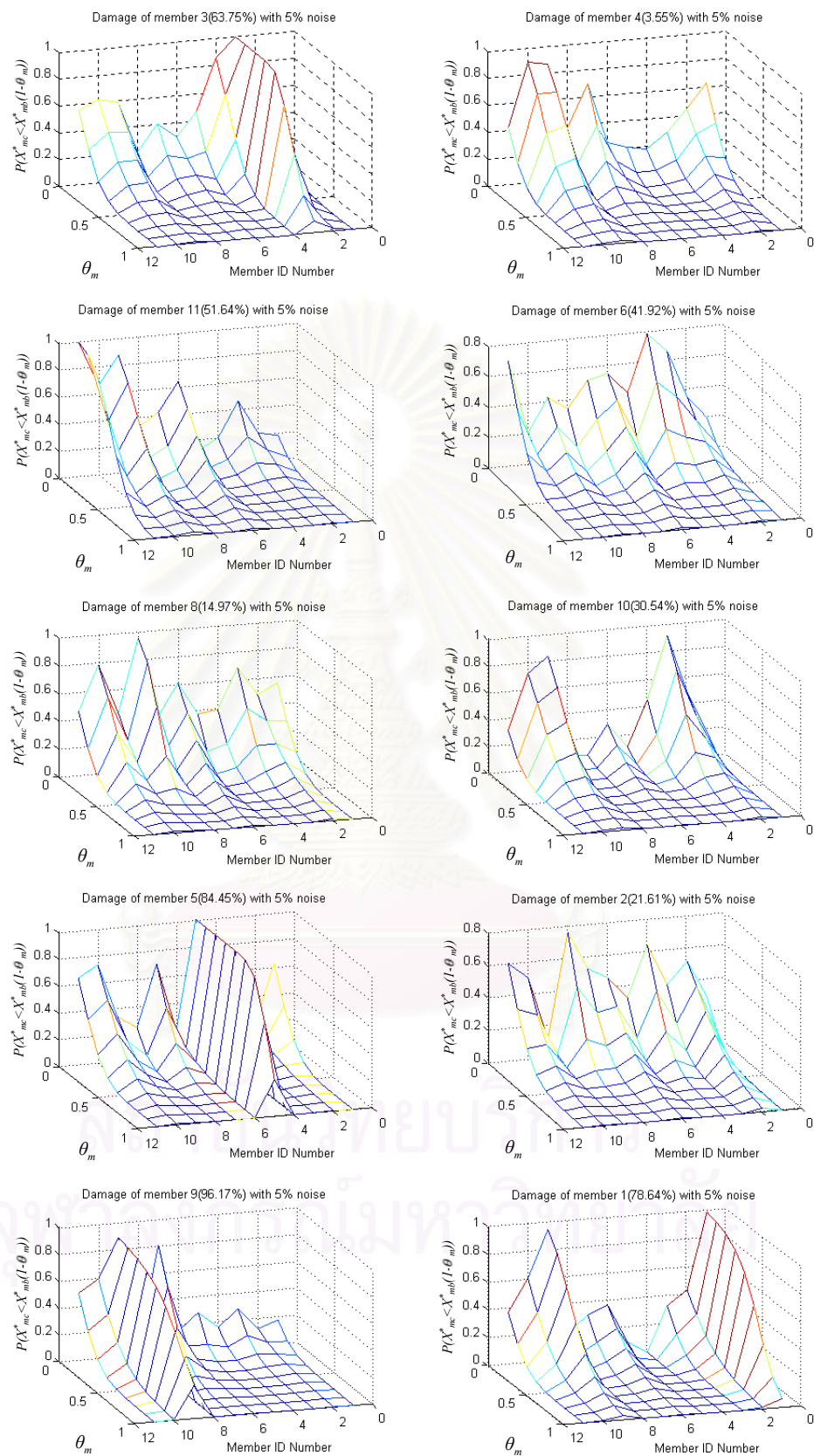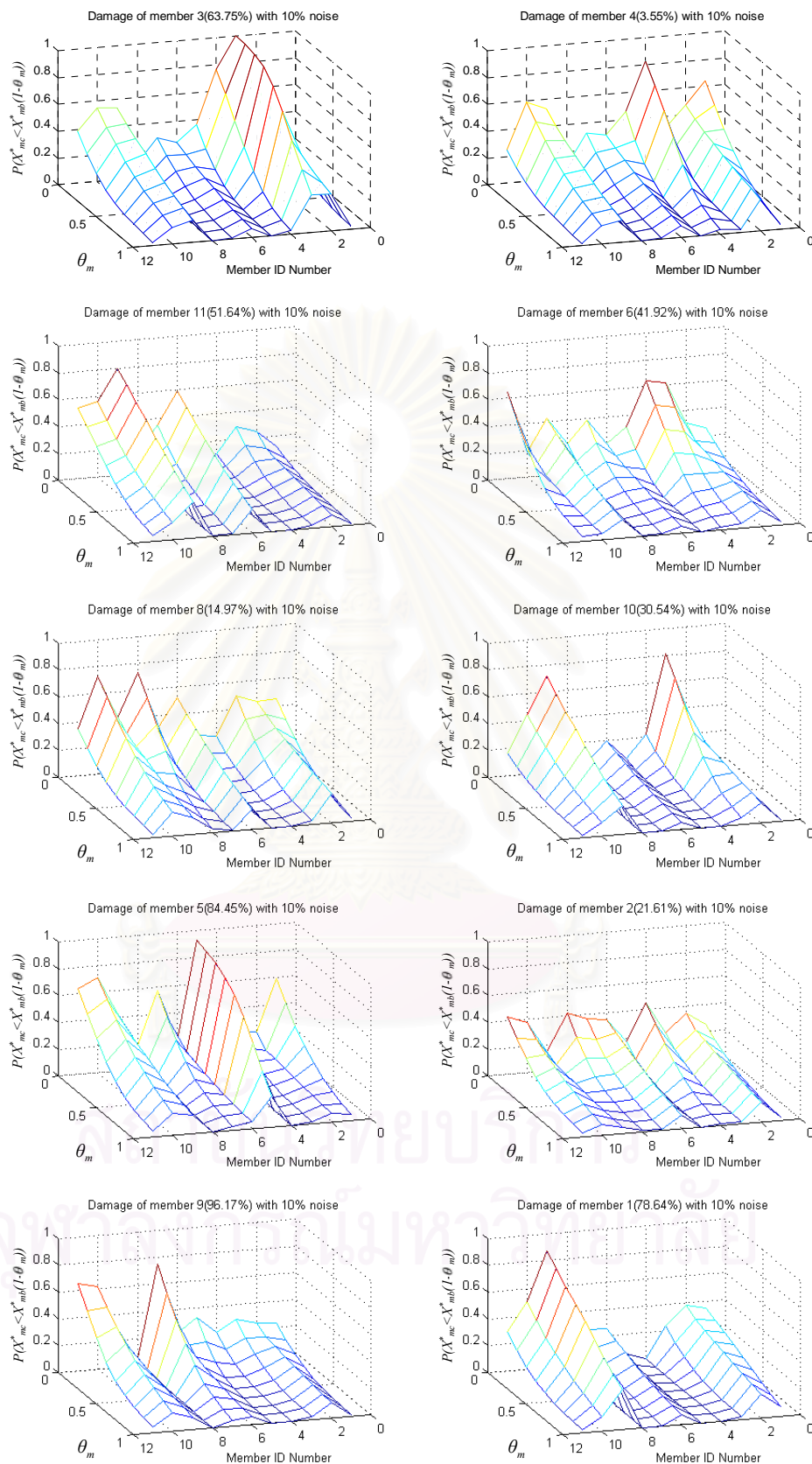
Figure 3.27 Probability distribution with respect to different levels of damage for the single-damaged-member cases from 1,000 samples of parameter estimates (Monte Carlo simulation + ROEE) using 1% noisy measurements.
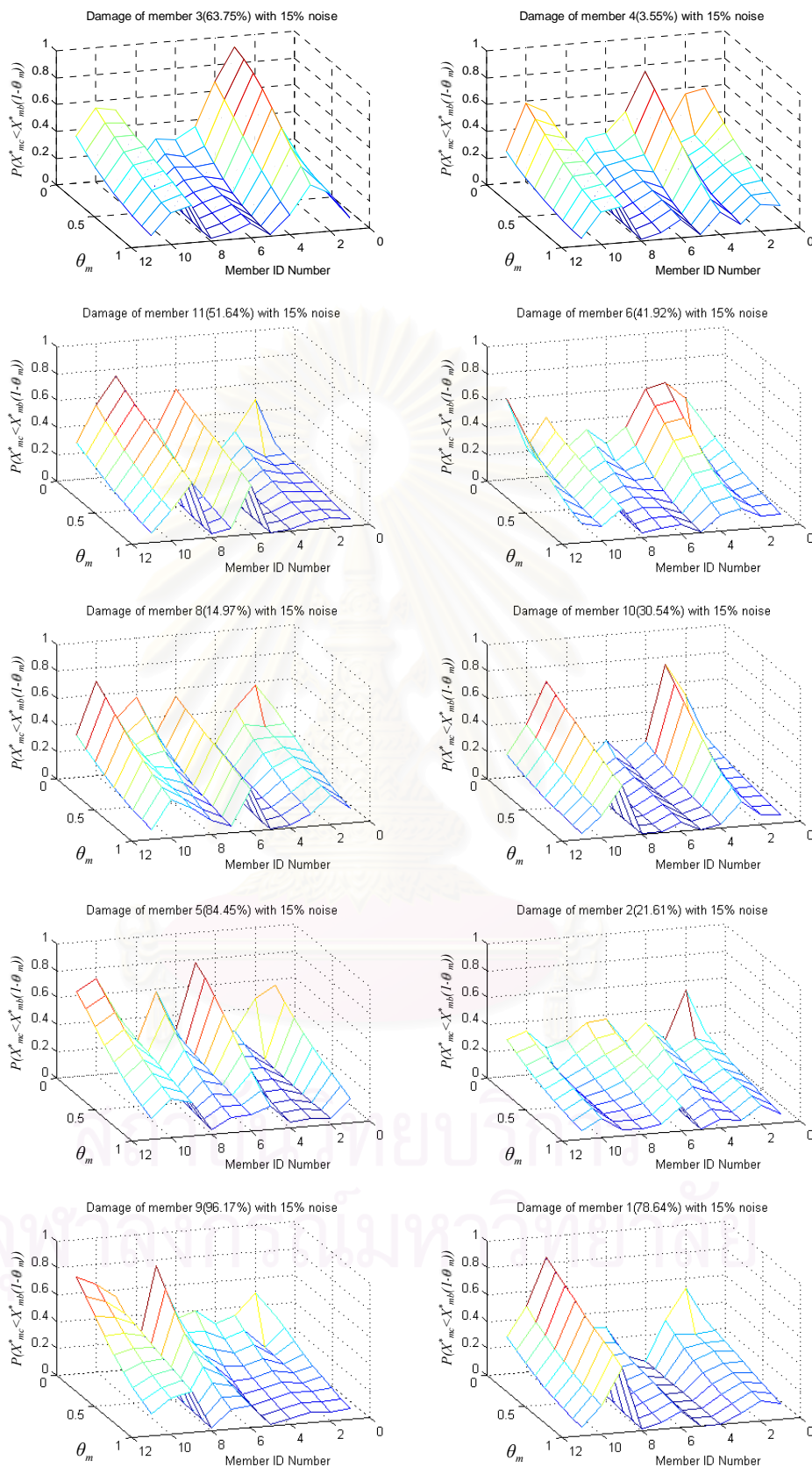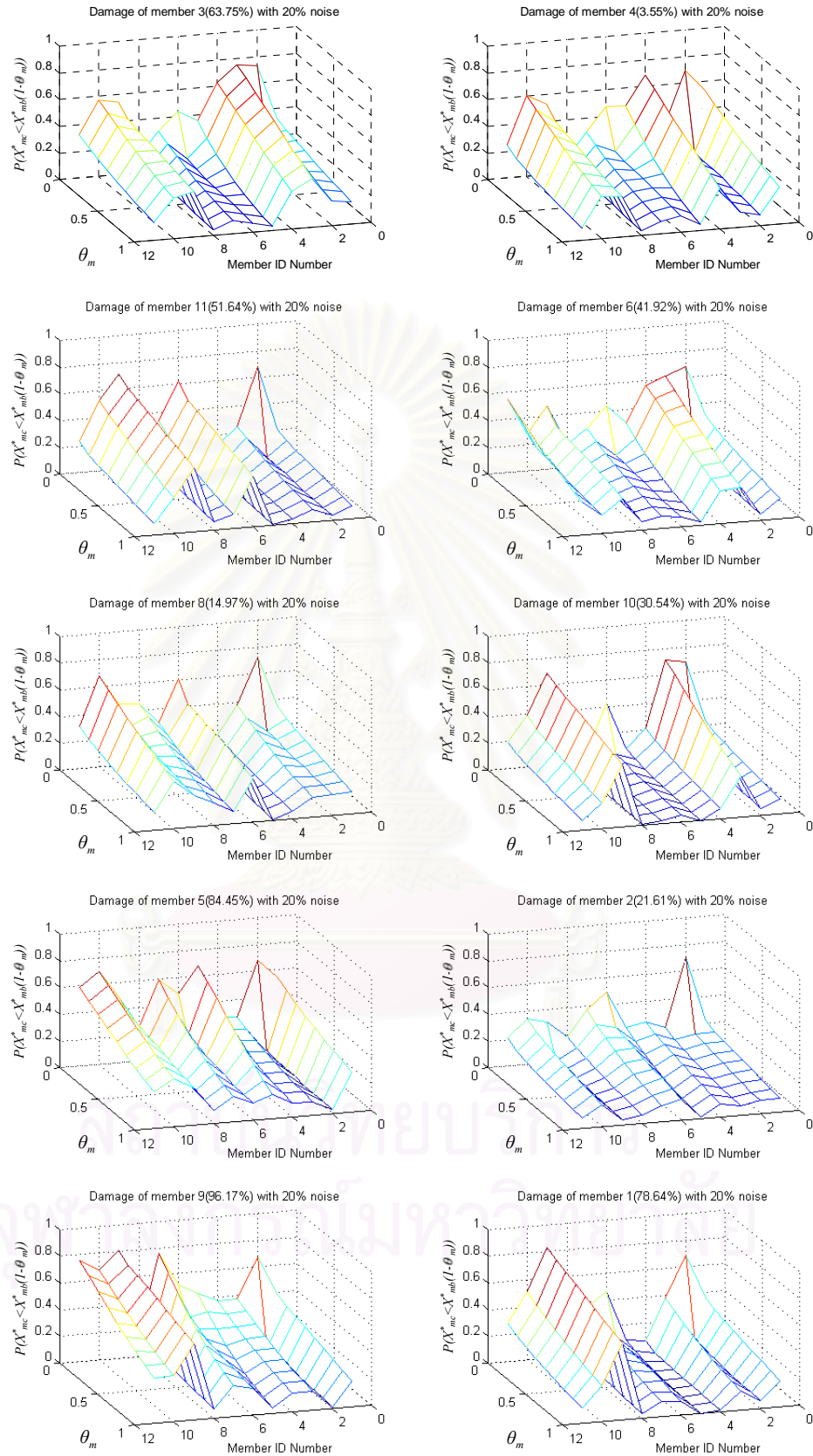
Figure 3.28 Probability distribution with respect to different levels of damage for the single-damaged-member cases from 1,000 samples of parameter estimates (Monte Carlo simulation + ROEE) using 3% noisy measurements.

Figure 3.29 Probability distribution with respect to different levels of damage for the single-damaged-member cases from 1,000 samples of parameter estimates (Monte Carlo simulation + ROEE) using 5% noisy measurements.

Figure 3.30 Probability distribution with respect to different levels of damage for the single-damaged-member cases from 1,000 samples of parameter estimates (Monte Carlo simulation + ROEE) using 10% noisy measurements.

Figure 3.31 Probability distribution with respect to different levels of damage for the single-damaged-member cases from 1,000 samples of parameter estimates (Monte Carlo simulation + ROEE) using 15% noisy measurements.
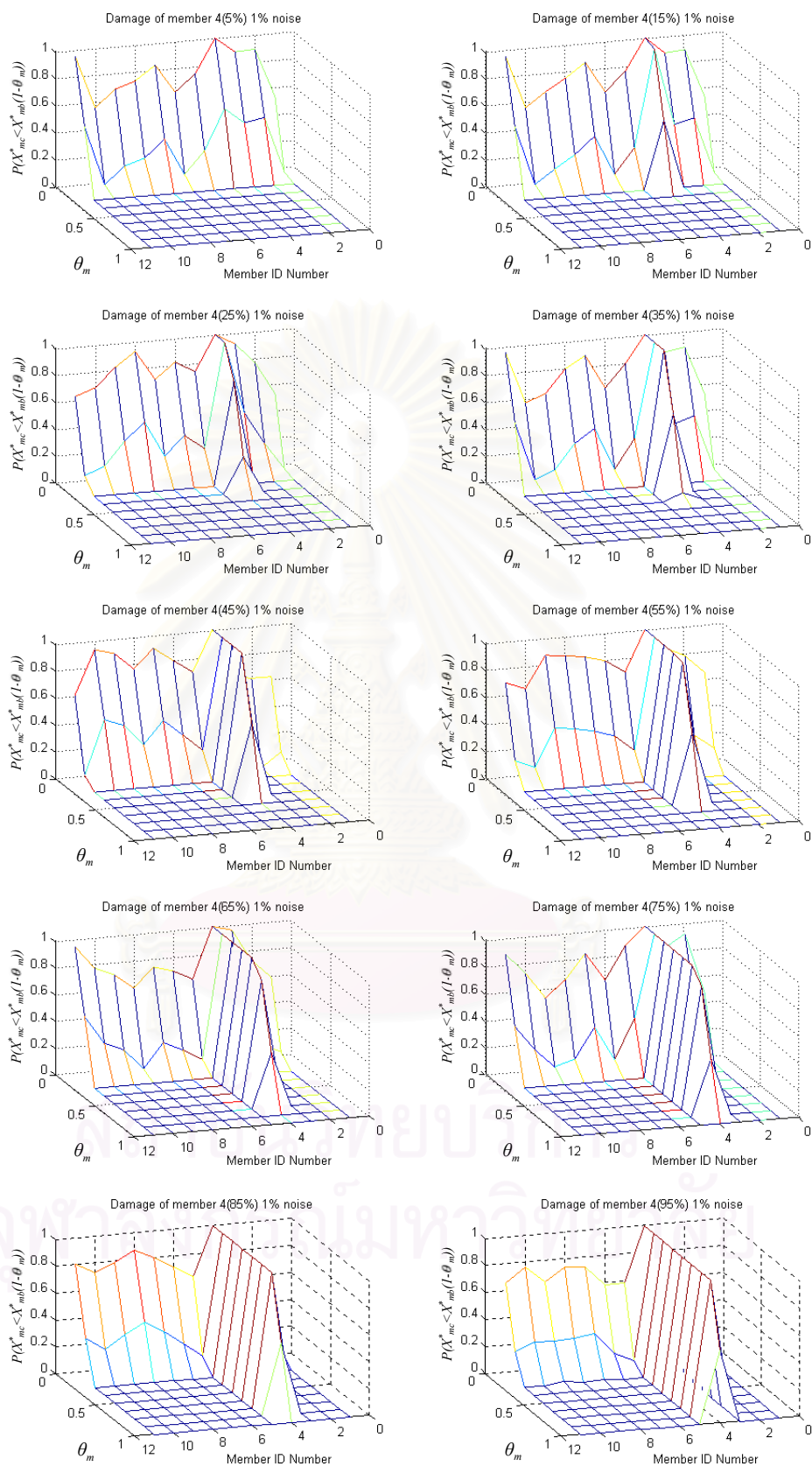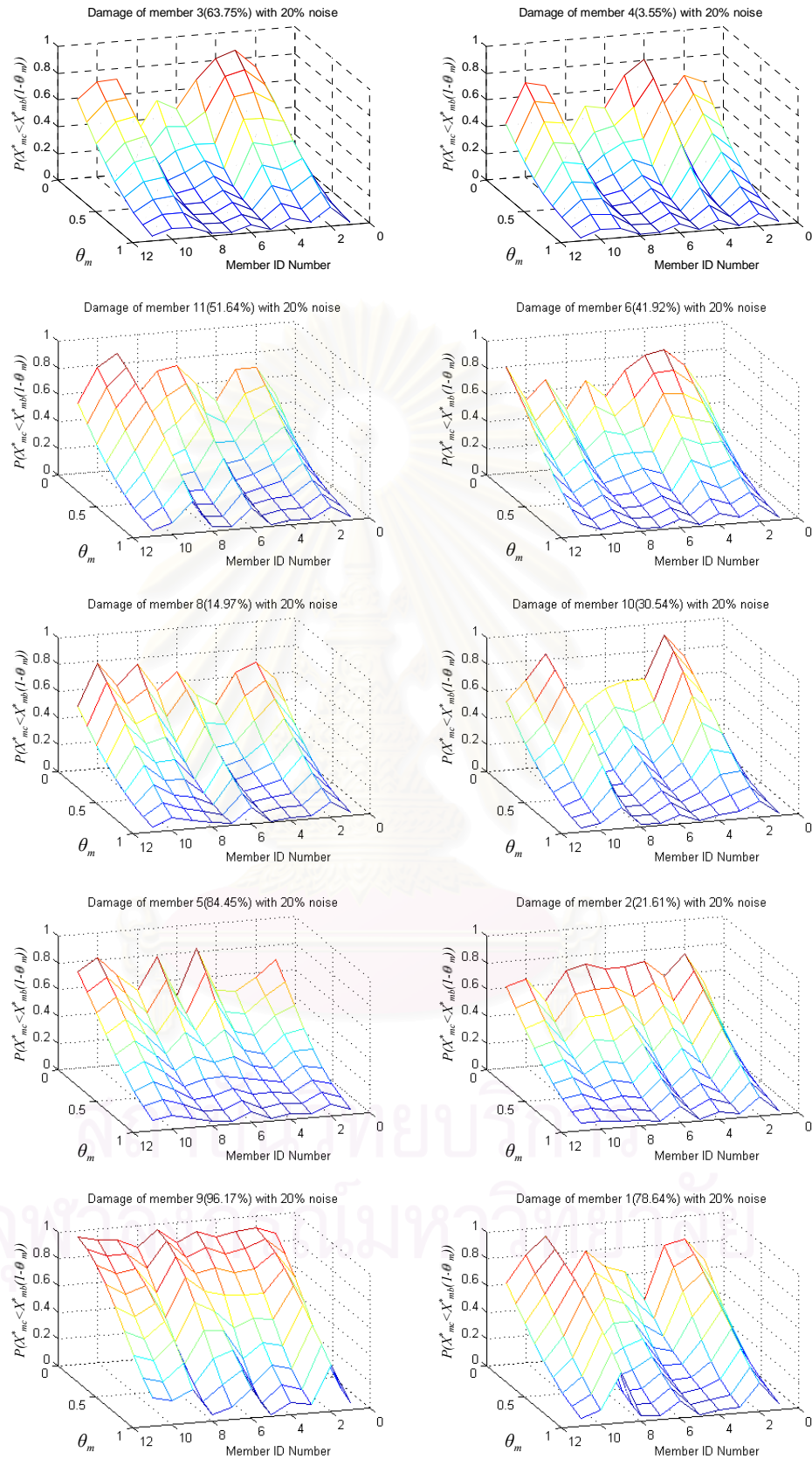
Figure 3.32 Probability distribution with respect to different levels of damage for the single-damaged-member cases from 1,000 samples of parameter estimates (Monte Carlo simulation + ROEE) using 20% noisy measurements.

damaged members are successfully located and quantified for all of the simulated damage cases with 1%, 3% and 5% noise in the measurements. For 10% and 15% noisy measurements, only the damaged members with high severity of damage can be successfully identified. Furthermore, the damage assessment algorithm fails to identify any damage at all for 20% noisy measurements. Therefore, it is evident from the current example that the performance of the proposed algorithm to assess damage in a structural system decreases as the level of noise in the measurements increases. Further, it is seen for all of the investigated damage cases that the maximum level of the measurement noise in which damage can be assessed is 20%, which is the same as when the Monte Carlo simulation method is used in conjunction with the OEE algorithm. It is also seen that the results of using Monte Carlo simulation with ROEE exhibit higher accuracy in assessing damage compared with those using Monte Carlo simulation with OEE, as observed from a more evident constant unit-probability zone in the probability distribution for damaged members. Hence, it may be concluded that the performance of the proposed algorithm in assessing damage can improve by using the regularization scheme.

3.3.1.5 The Sensitivity-Based Method with ROEE Algorithm

In this section, we investigate the performance of the statistical damage assessment algorithm by using the sensitivity-based method with OEE to evaluate the statistical distribution of the parameter estimates. As with the previous sections, we use the ten simulated damage cases of Table 3.3 as our model problems. The results show that for all of the damage cases considered the maximum level of noise permitting a damage assessment is 15%. This allows us to investigate five levels of noise (i.e., $e = 1\%, 3\%, 5\%, 10\%$ and 15%) in the simulated measurement data.

Figures 3.33-3.37 show the probability distribution, $P(X_{mc} < X_{mb}(1-\theta_m))$, for each level of damage θ_m in the structural members using different sets of simulated noisy measurements. It is seen that the results of the current algorithm are generally similar to those of the sensitivity-based method with OEE. Nevertheless, there are some differences in that the performance of the current algorithm to assess damage is

Figure 3.33 Probability distribution with respect to different levels of damage for the single-damaged-member cases using the sensitivity-based method and ROEE algorithm with 1% noisy measurements.

Figure 3.34 Probability distribution with respect to different levels of damage for the single-damaged-member cases using the sensitivity-based method and ROEE algorithm with 3% noisy measurements.

Figure 3.35 Probability distribution with respect to different levels of damage for the single-damaged-member cases using the sensitivity-based method and ROEE algorithm with 5% noisy measurements.

Figure 3.36 Probability distribution with respect to different levels of damage for the single-damaged-member cases using the sensitivity-based method and ROEE algorithm with 10% noisy measurements.

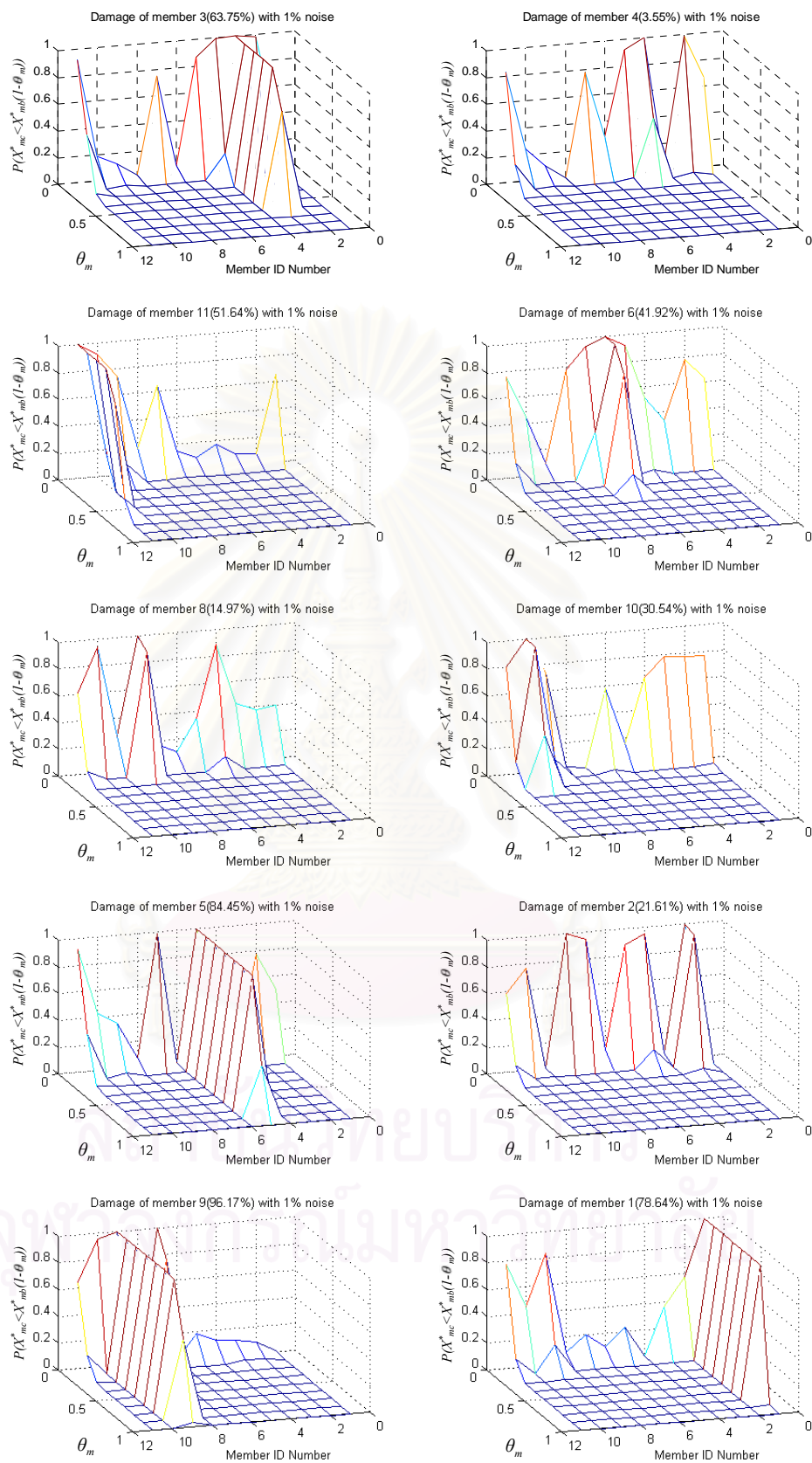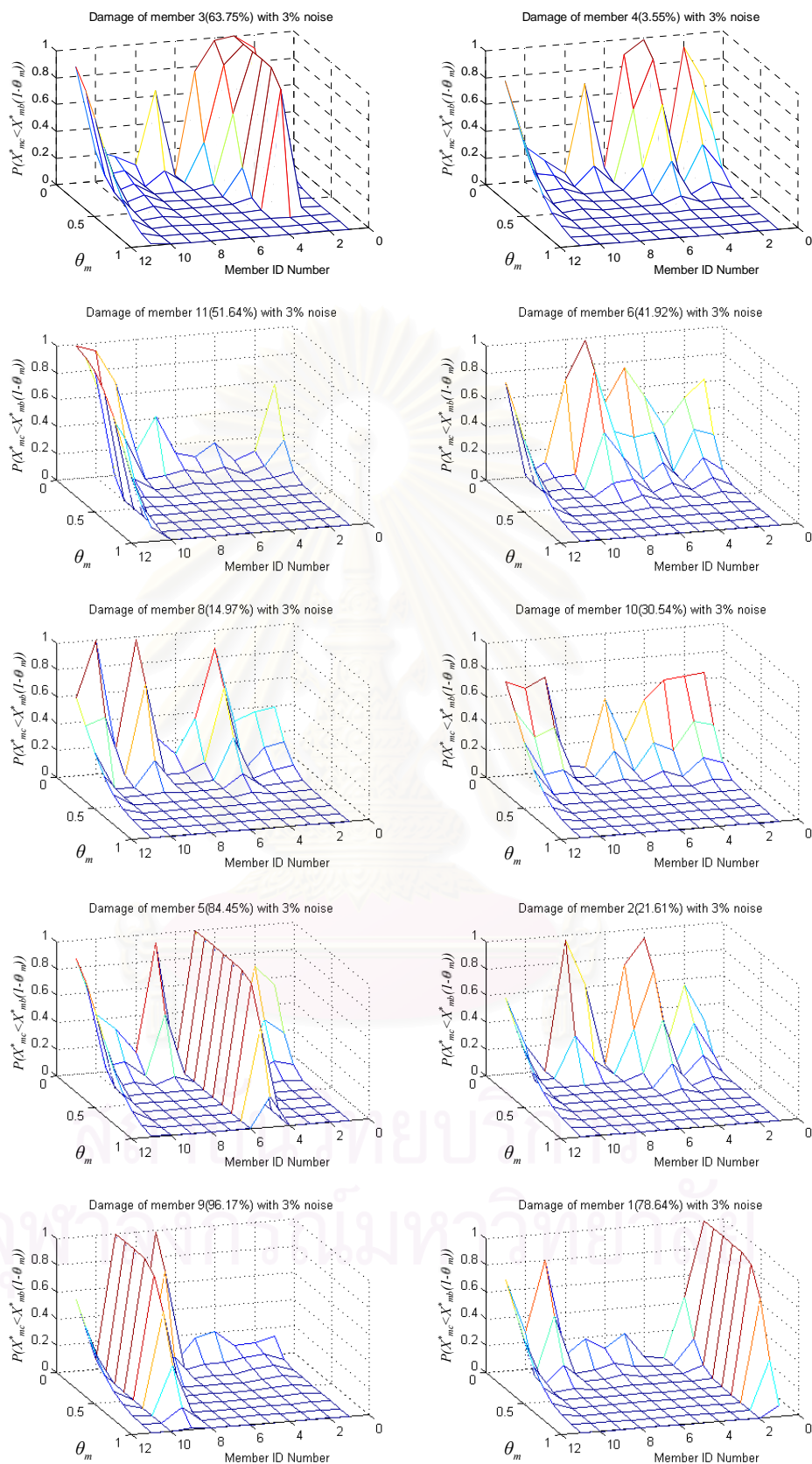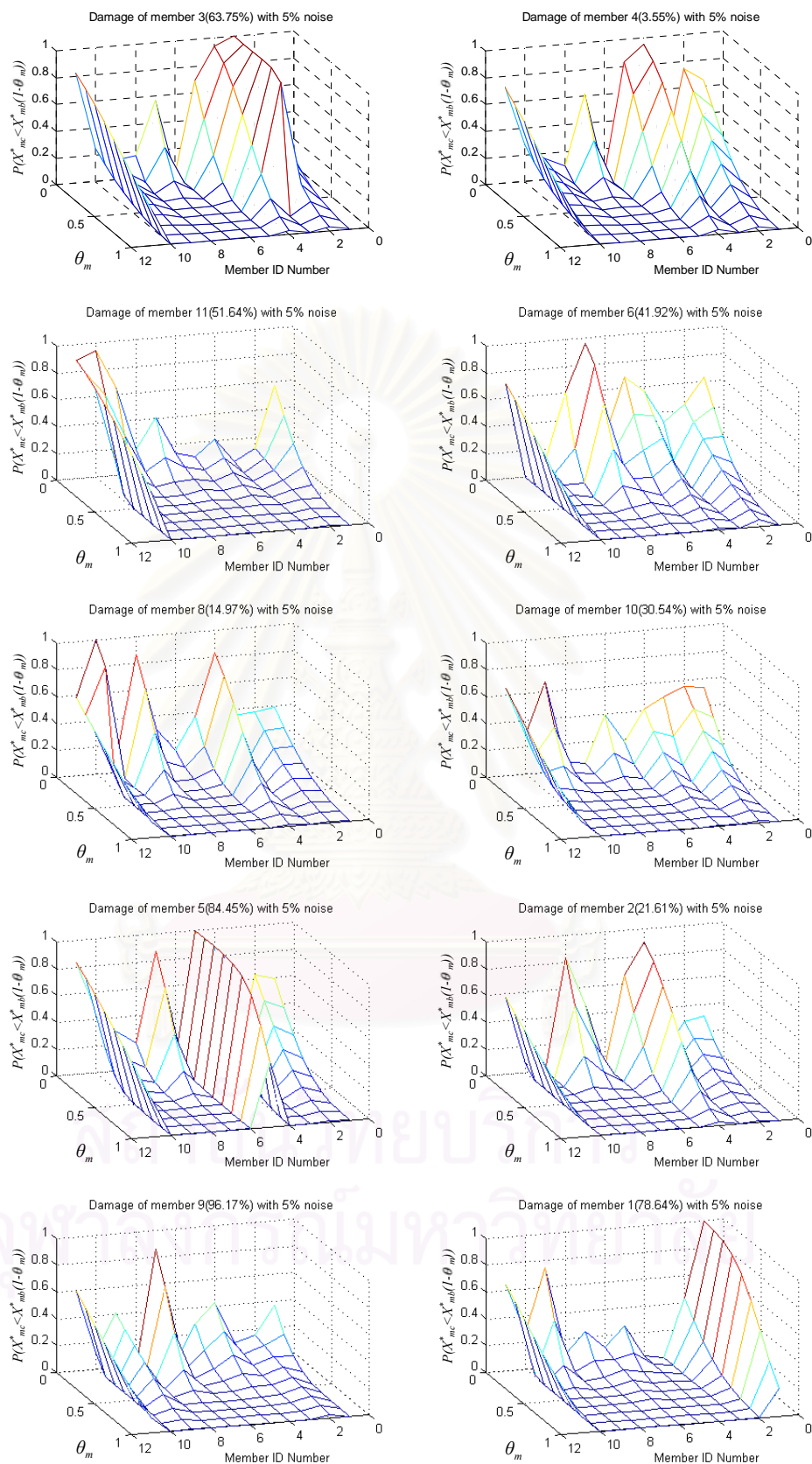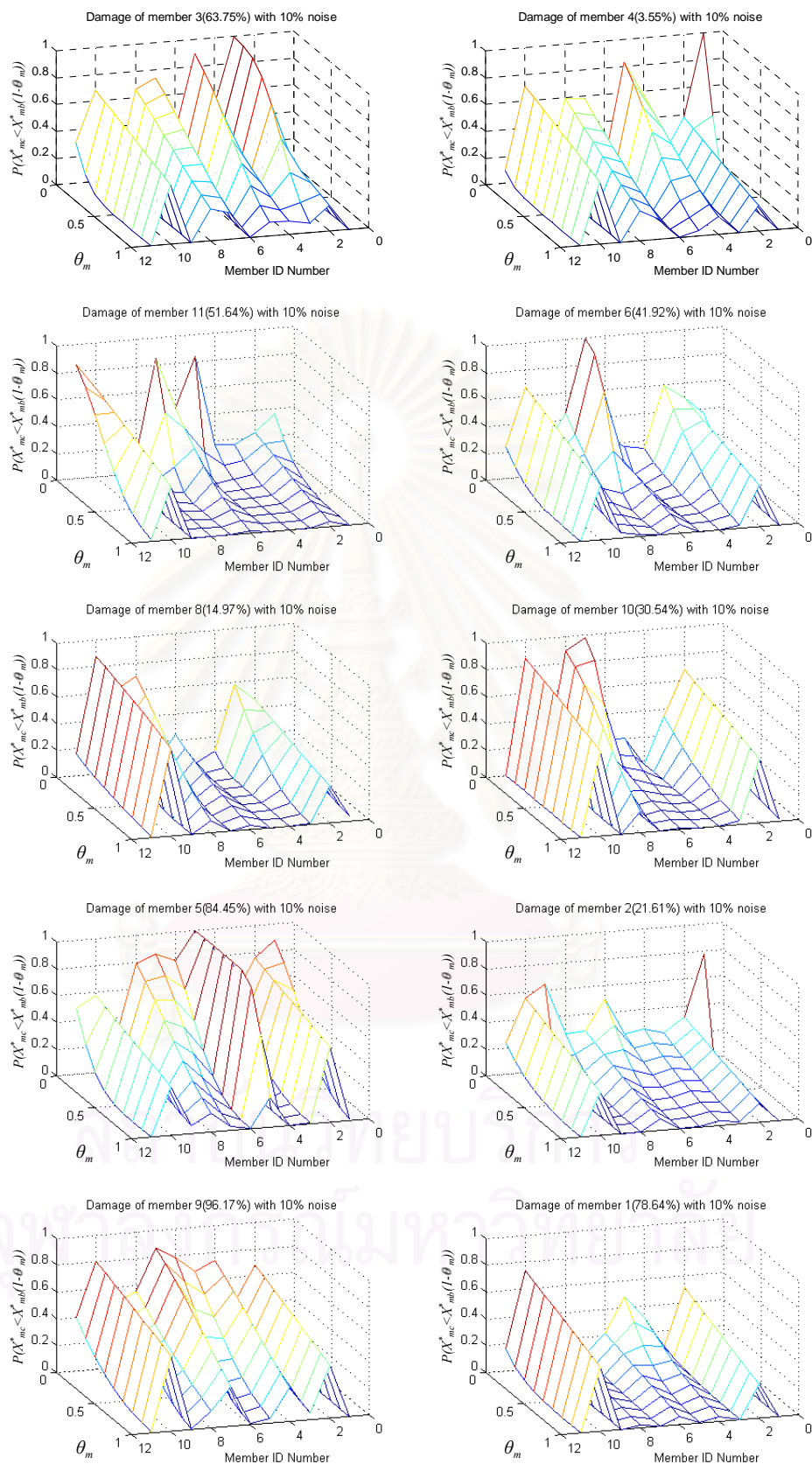Figure 3.37 Probability distribution with respect to different levels of damage for the single-damaged-member cases using the sensitivity-based method and ROEE algorithm with 15% noisy measurements.

improved as observed from a more evident constant unit-probability zone in the probability distribution for damaged members. In addition, for all of the investigated damage cases the maximum level of noise in which damage can be assessed is 15%, compared with 10% for the sensitivity-based method with OEE. Hence, it is concluded that the performance of the proposed method of assessing damage improves by using the ROEE algorithm.

3.3.1.6 The Optimum Sensitivity-Based Method with ROEE Algorithm

The ten damage cases in Table 3.3 are, again, used for evaluating the performance of the statistical damage assessment algorithm. For the simulation studies conducted in this section we use the ROEE method in conjunction with the optimum sensitivity-based scheme to obtain the statistical distribution of the parameter estimates. The results from the simulation studies show that for all damage cases the maximum level of noise permitting a damage assessment is 20%, and hence all of the six levels of the measurement noise in Table 3.3—e = 1%, 3%, 5%, 10%, 15% and 20%—are investigated in the present case.

Figures 3.38-3.43 show the probability distribution, $P(X_{mc} < X_{mb}(1-\theta_m))$, for each level of damage θ_m in the structural members using different levels of noisy incarnations in the simulated measurements. It is seen that the results of the current algorithm are generally similar to those obtained from using the optimum sensitivity-based method with OEE. However, we notice a better performance of the current algorithm to assess damage in the structural system, as observed from a more evident constant unit-probability zone in the probability distribution for damaged members. The maximum level of noise in which damage can be assessed is 20%, compared with 10% for the optimum sensitivity-based method with OEE. Hence, it is evident that the performance of the proposed damage assessment algorithm improves by implementing the ROEE algorithm in the statistical parameter estimation process.

Figure 3.38 Probability distribution with respect to different levels of damage for the single-damaged-member cases using the optimum sensitivity-based method and ROEE algorithm with 1% noisy measurements.
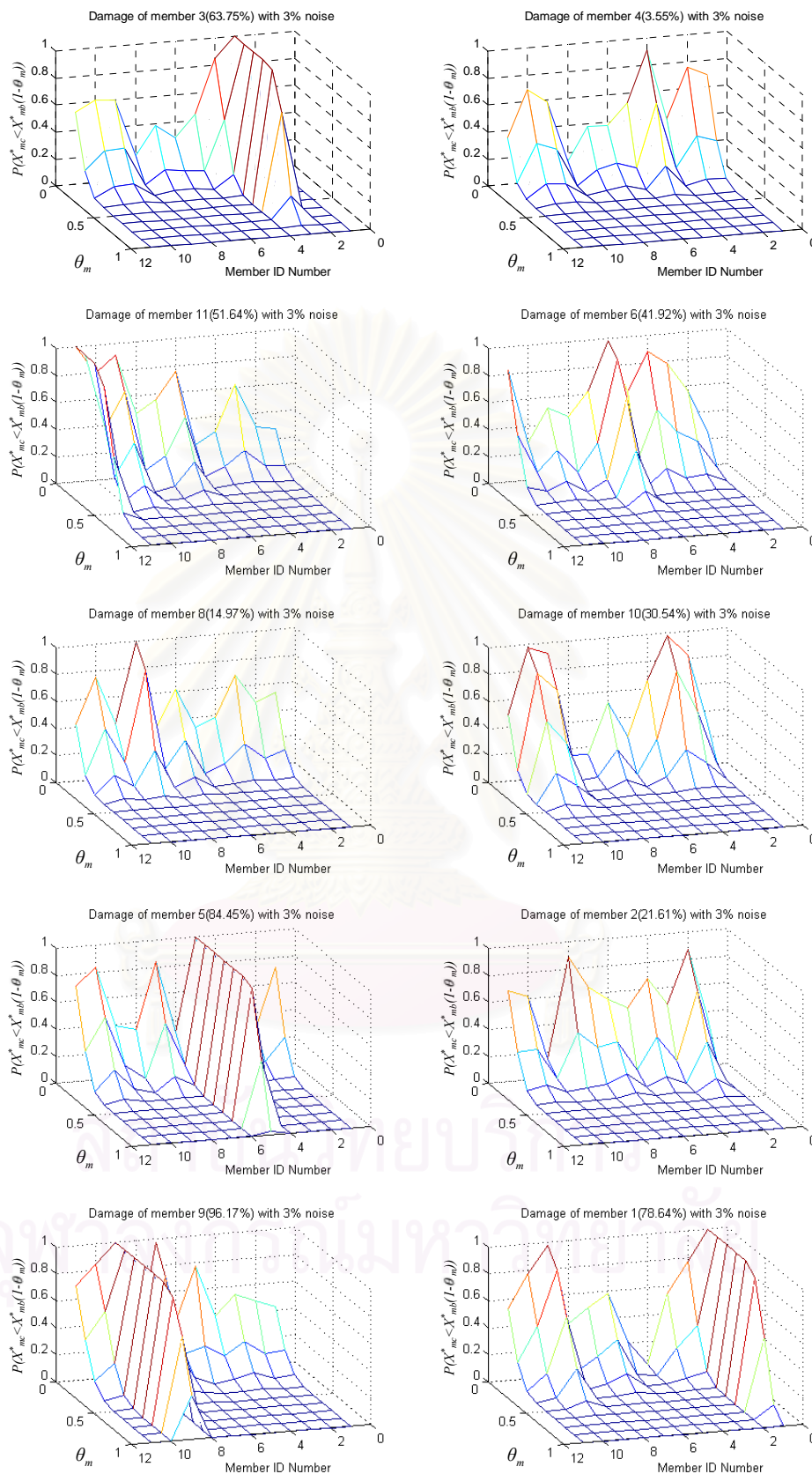
Figure 3.39 Probability distribution with respect to different levels of damage for the single-damaged-member cases using the optimum sensitivity-based method and ROEE algorithm with 3% noisy measurements.
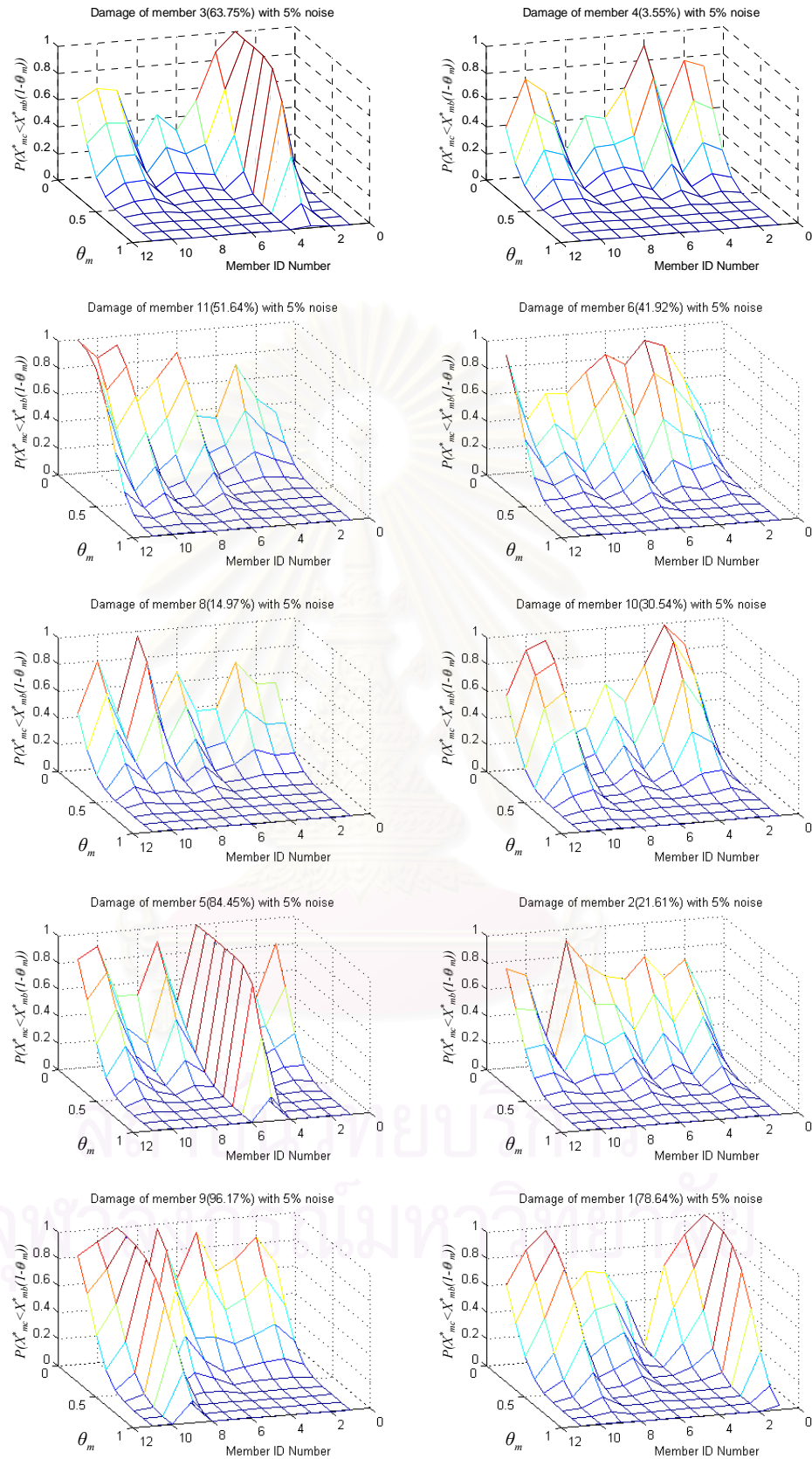
Figure 3.40 Probability distribution with respect to different levels of damage for the single-damaged-member cases using the optimum sensitivity-based method and ROEE algorithm with 5% noisy measurements.
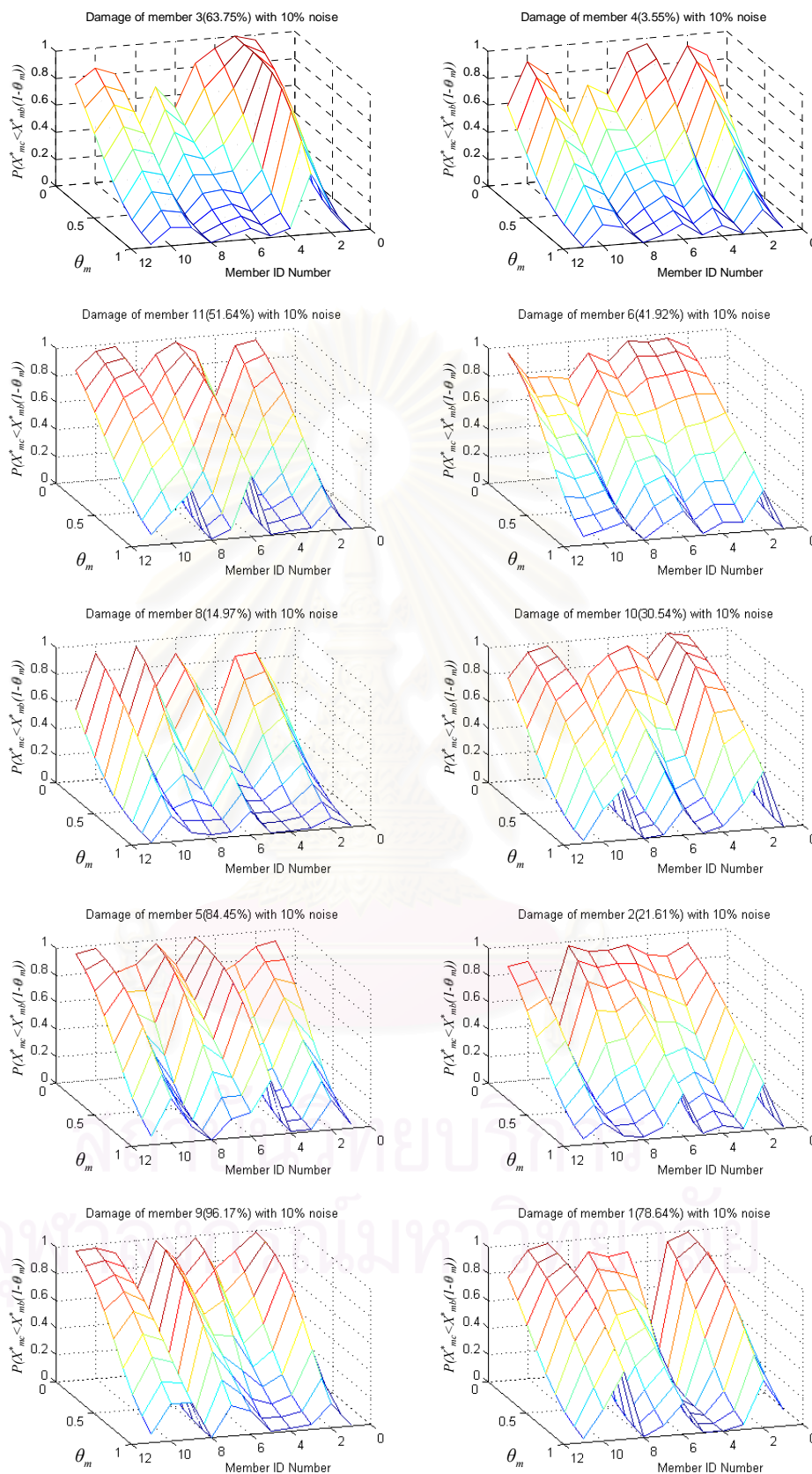
Figure 3.41 Probability distribution with respect to different levels of damage for the single-damaged-member cases using the optimum sensitivity-based method and ROEE algorithm with 10% noisy measurements.
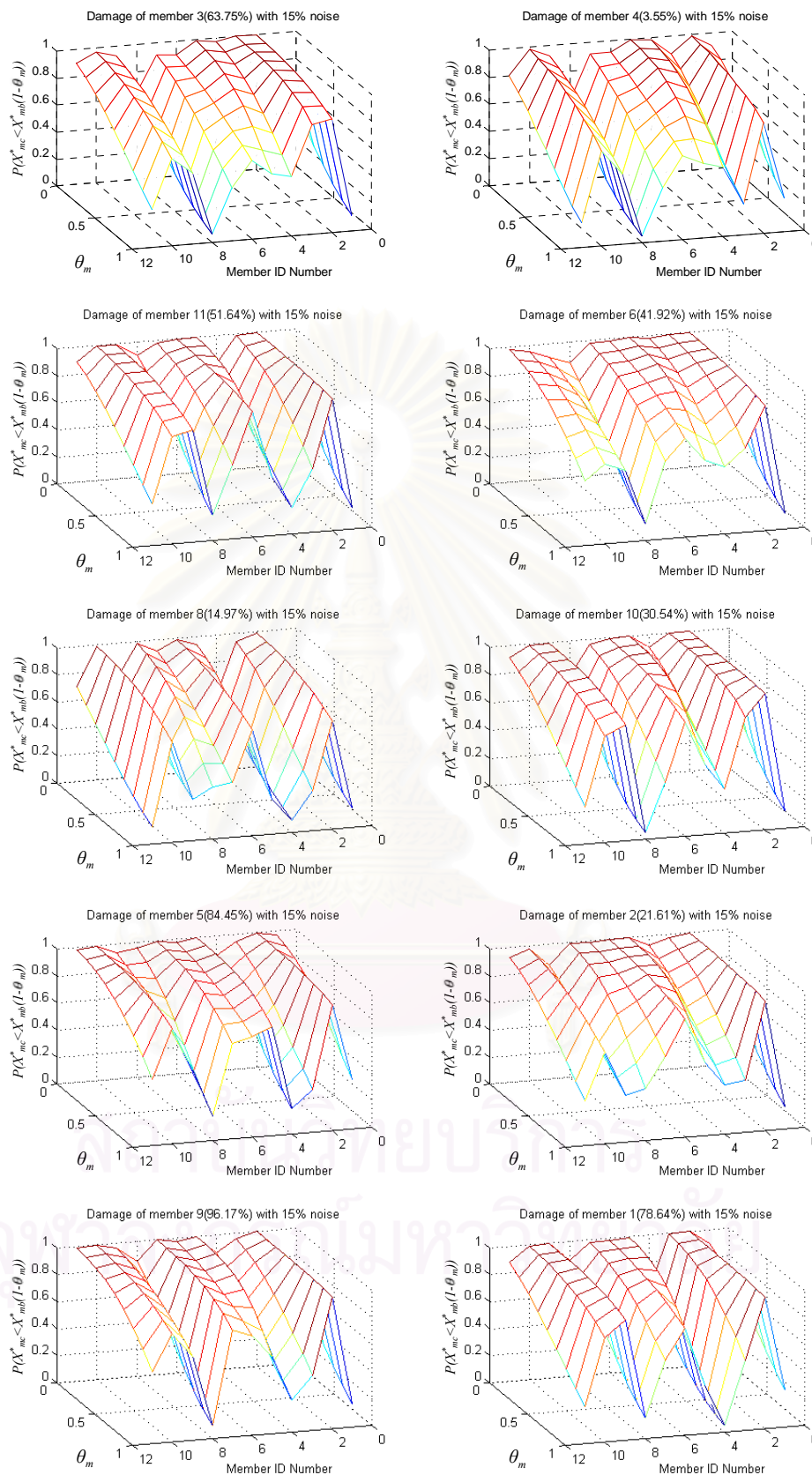
Figure 3.42 Probability distribution with respect to different levels of damage for the single-damaged-member cases using the optimum sensitivity-based method and ROEE algorithm with 15% noisy measurements.
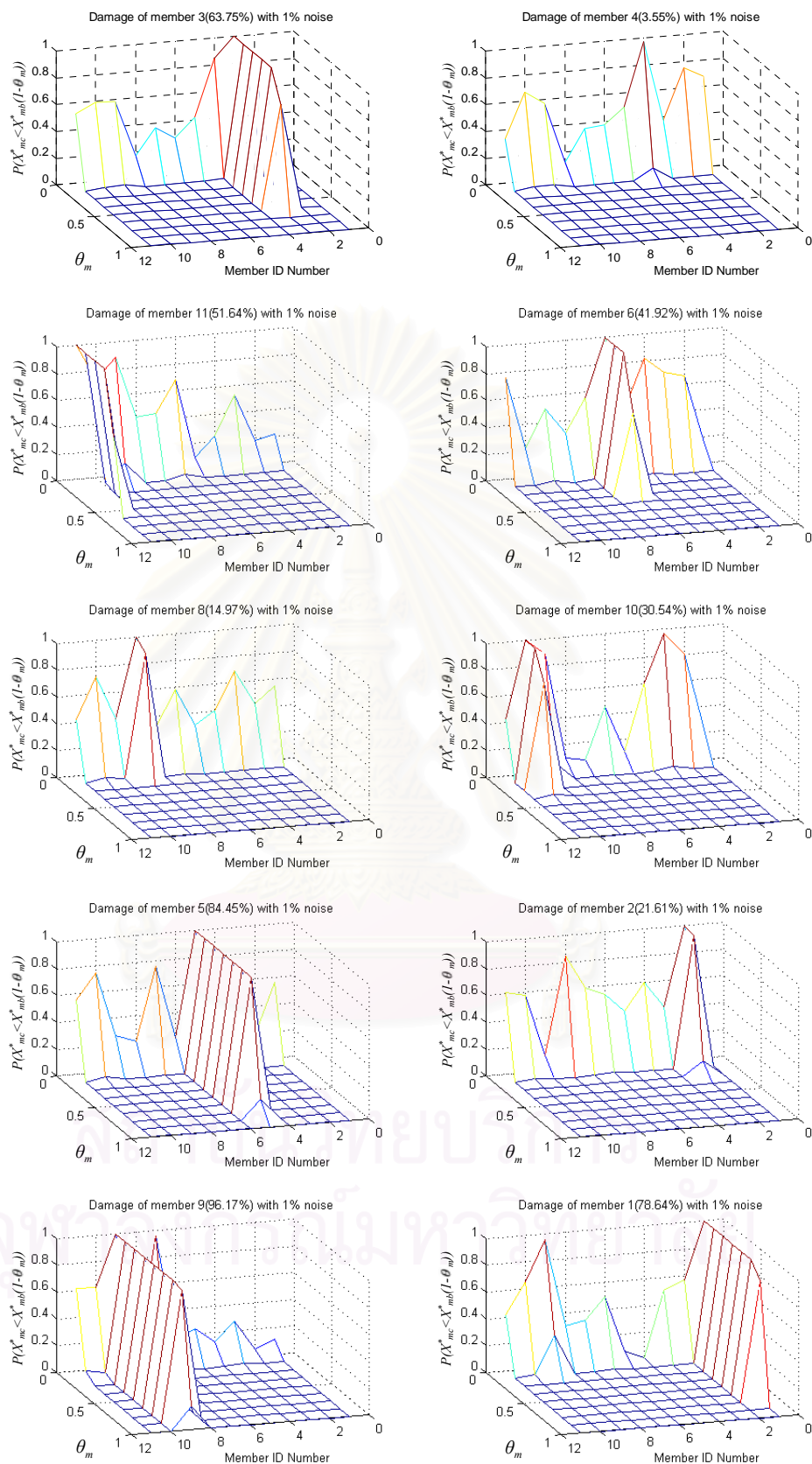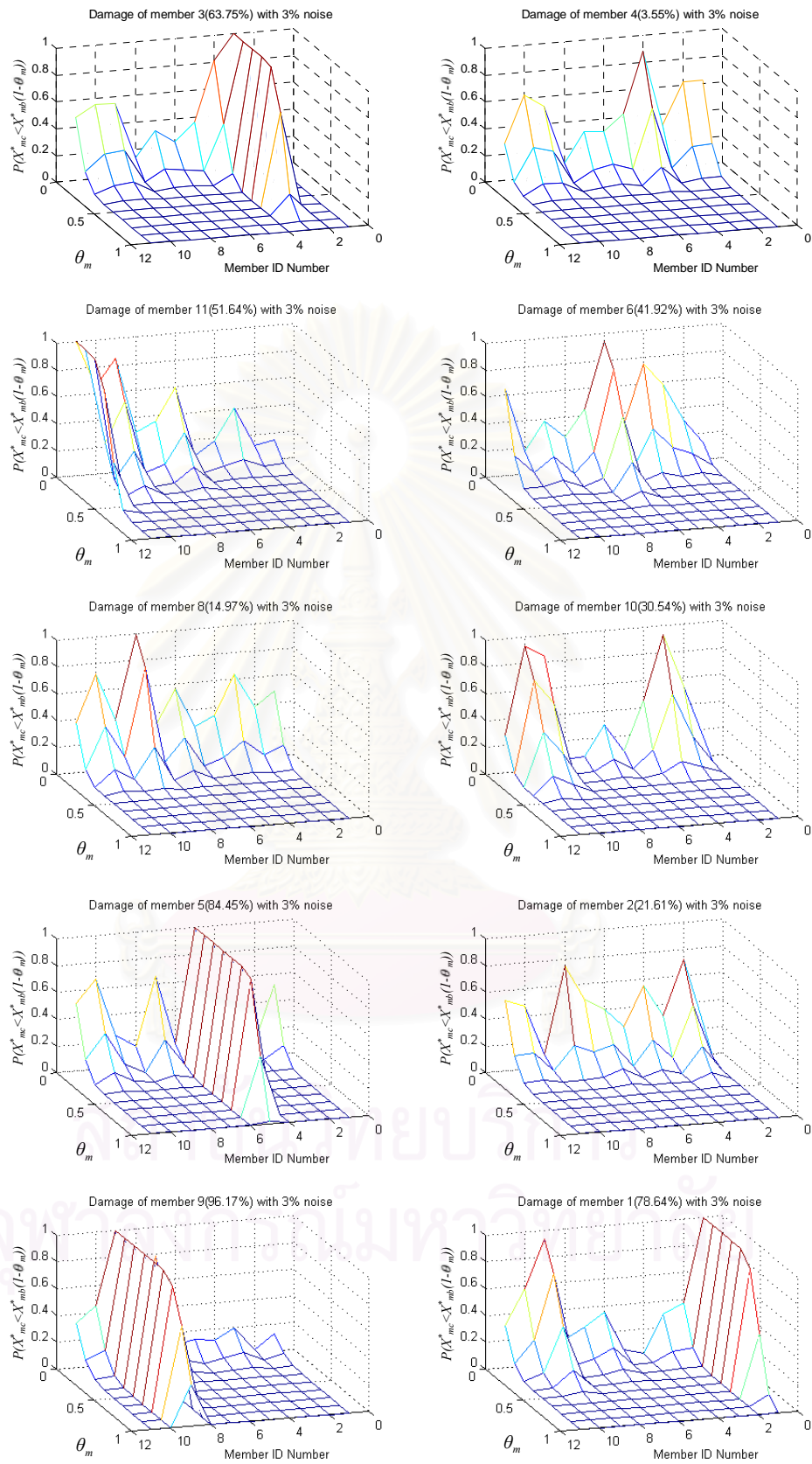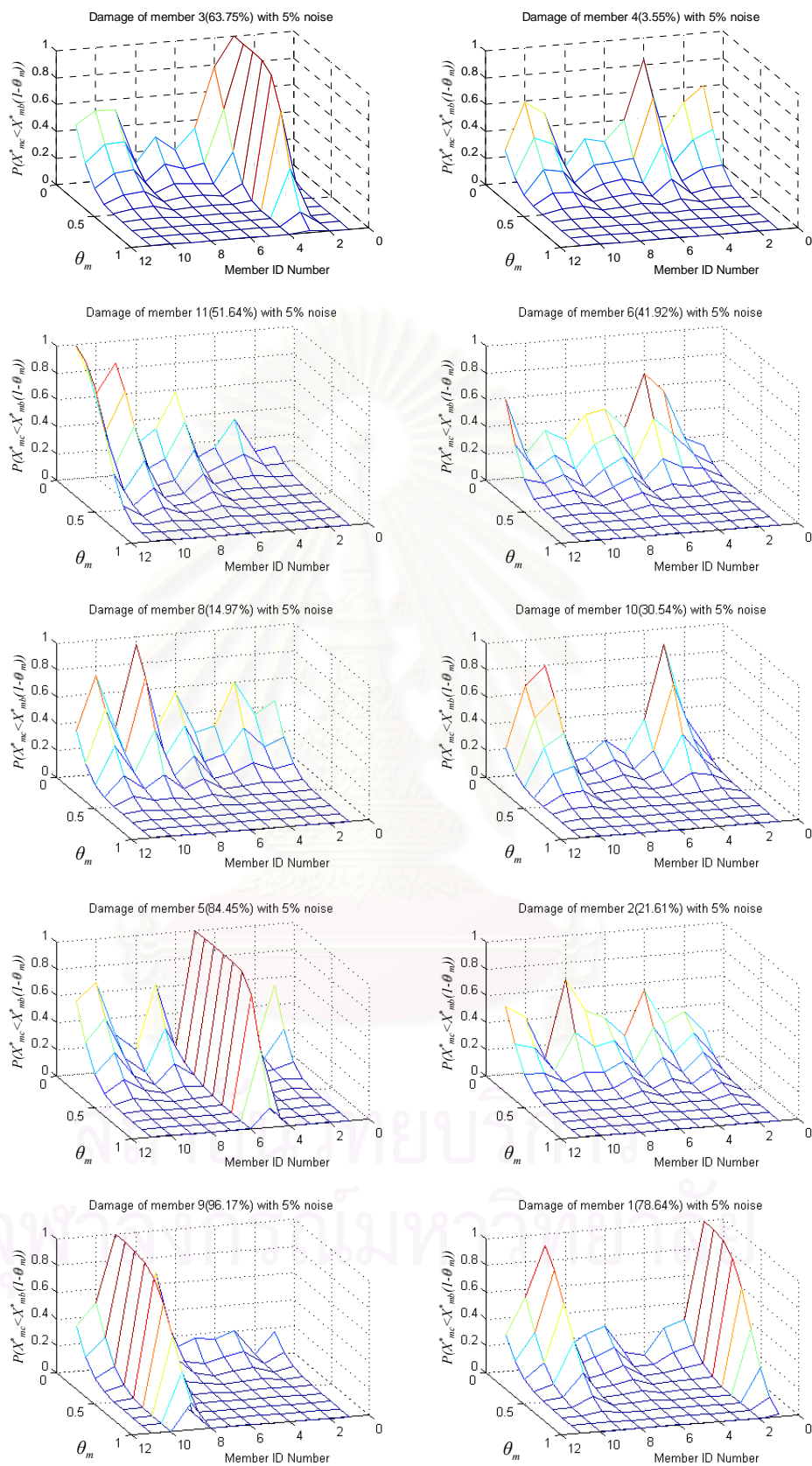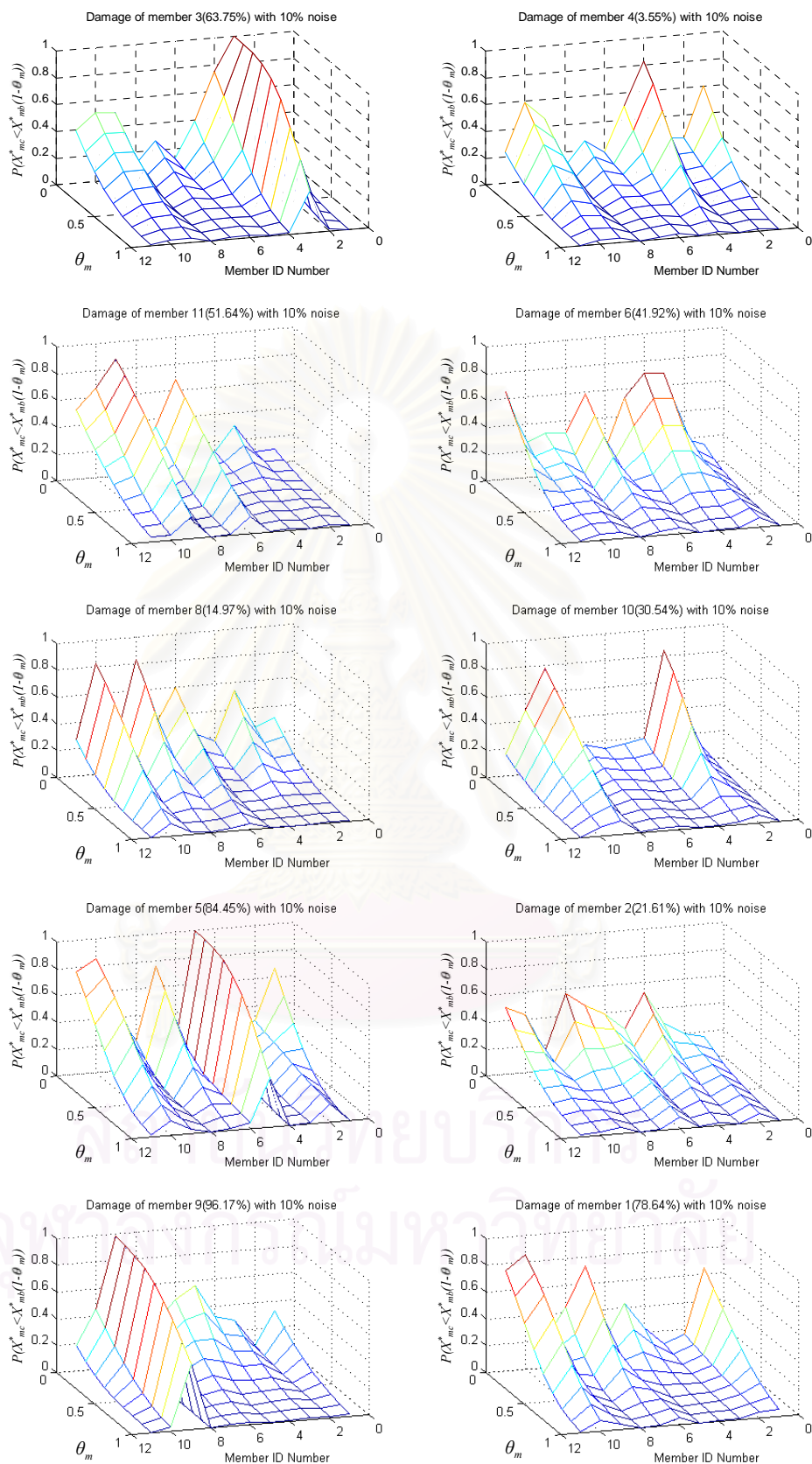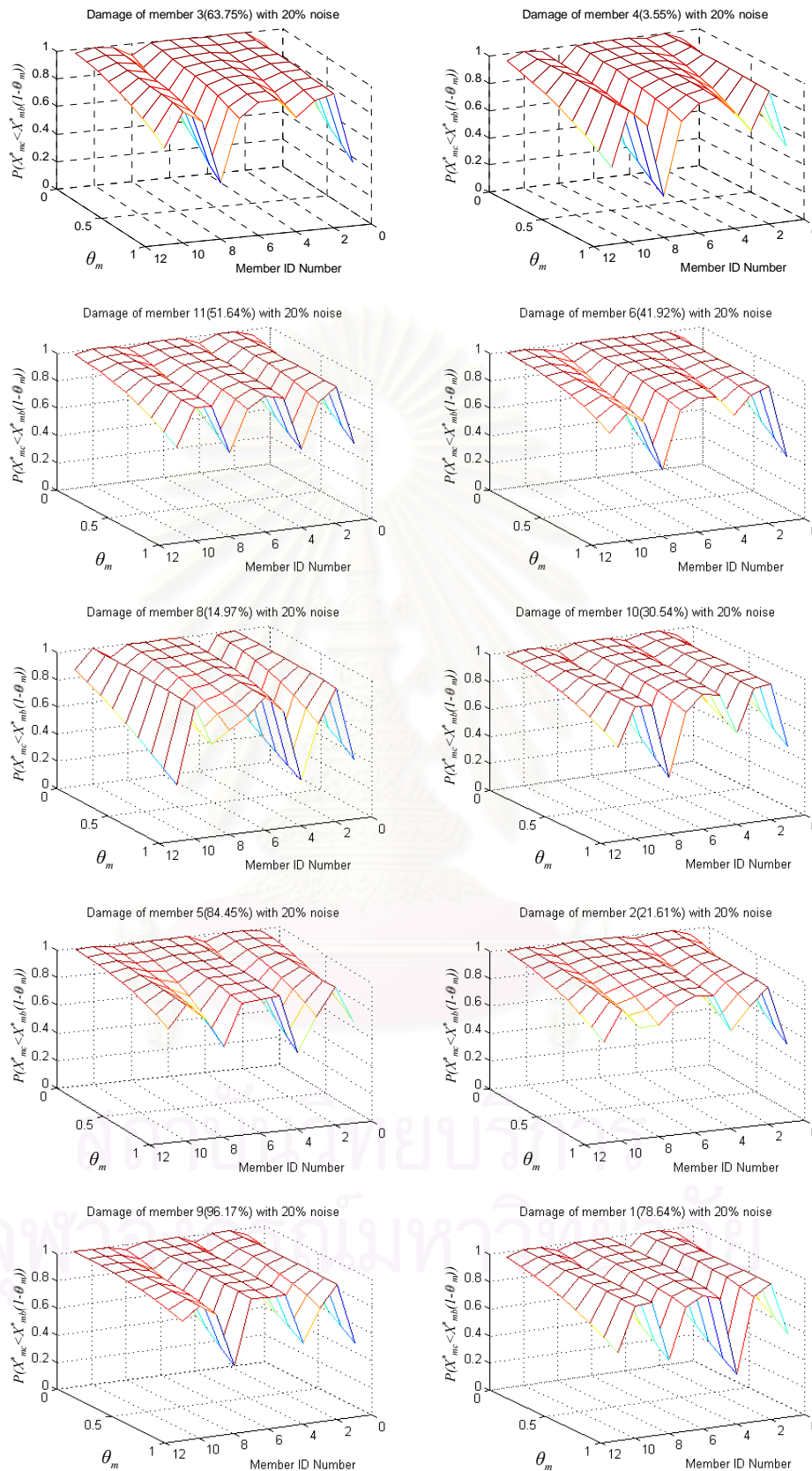
Figure 3.43 Probability distribution with respect to different levels of damage for the single-damaged-member cases using the optimum sensitivity-based method and ROEE algorithm with 20% noisy measurements.

3.3.2 Two-Damaged-Member Cases

The two-damaged-member cases investigated herein consist of ten randomly generated combinations of the location and the severity of damage as summarized in Table 3.4. In this table, the noise levels indicate different levels of noise that are used to investigate the performance of the current damage assessment algorithm from using different statistical parameter estimation schemes. As for the single-damaged-member cases, three different statistical parameter estimation schemes—i.e., the Monte Carlo simulation method, the sensitivity-based method and the optimum sensitivity-based method—are used in conjunction with the OEE and ROEE algorithms to estimate the mean and the covariance matrix of the parameter estimates for the construction of the statistical distribution of the system parameters.

Table 3.4 Different damage scenarios with two damaged members.

Damage Case	Damaged Members	Damage Levels (%)	Noise Levels (%)
1	3	55.15	1%, 3%, 5%, 10%, 15% and 20%
	8	78.98	
2	4	37.18	1%, 3%, 5%, 10%, 15% and 20%
	8	48.51	
3	2	90.31	1%, 3%, 5%, 10%, 15% and 20%
	11	51.64	
4	6	41.92	1%, 3%, 5%, 10%, 15% and 20%
	8	14.97	
5	9	48.12	1%, 3%, 5%, 10%, 15% and 20%
	5	84.45	
6	6	54.81	1%, 3%, 5%, 10%, 15% and 20%
	2	21.61	
7	7	19.65	1%, 3%, 5%, 10%, 15% and 20%
	10	48.95	
8	6	5.93	1%, 3%, 5%, 10%, 15% and 20%
	10	17.26	
9	9	96.17	1%, 3%, 5%, 10%, 15% and 20%
	3	63.75	
10	1	78.64	1%, 3%, 5%, 10%, 15% and 20%
	4	64.18	

The results of the ten simulated damage cases are shown, respectively, in Figures 3.44-3.49 for the Monte Carlo simulation method with OEE, Figures 3.50-3.53 for the sensitivity-based method with OEE, Figures 3.54-3.57 for the optimum sensitivity-based method with OEE, Figures 3.58-3.63 for the Monte Carlo simulation method with ROEE, Figures 3.64-3.68 for the sensitivity-based method with ROEE and Figures 3.69-3.74 for the optimum sensitivity-based method with ROEE.

The results of the current simulation studies are similar to those of the single-damaged-member cases. It is seen that the damage assessment results can become less accurate as the level of noise in the measurements increases. Also, it is observed that as the level of noise in the measurements increases, the decrease in the probability values for a structural member in the transition region becomes more gradual. Therefore, we reach the same conclusion that the performance of the proposed algorithm to assess damage in a structural system is limited by the level of noise in the measurements.

It is noted from the results of the damage assessment algorithm by using the ROEE algorithm comparing to using the OEE algorithm in the parameter estimation process that the maximum level of noise permitting a damage assessment is increased from 10% to 15% for the sensitivity-based method and from 10% to 20% for the optimum sensitivity-based method, while remaining unchanged for the Monte Carlo simulation method. This observation suggests that the ROEE algorithm is somewhat more effective when using in conjunction with the optimum sensitivity-based method compared to when using with the sensitivity-based and the Monte Carlo simulation methods.
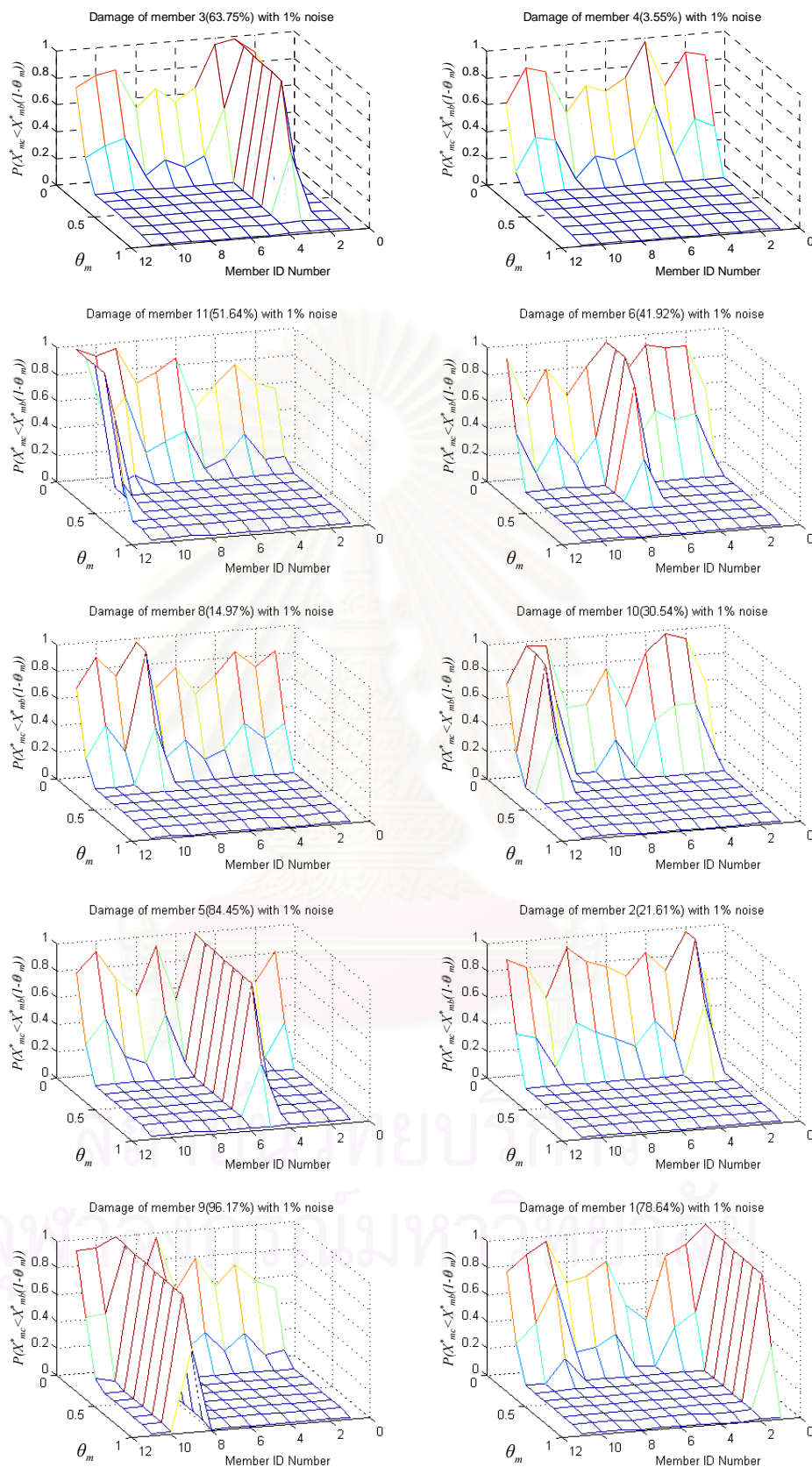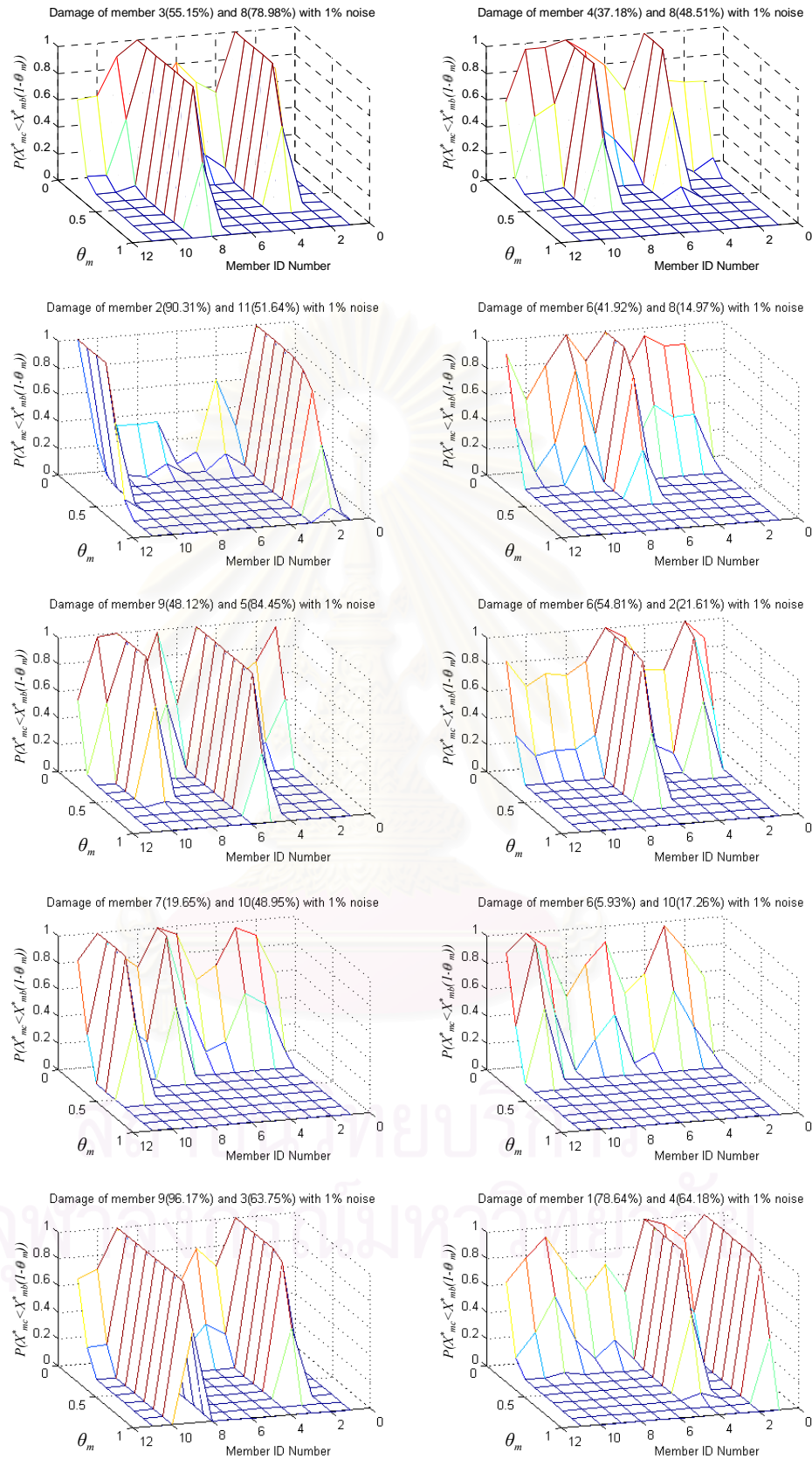
Figure 3.44 Probability distribution with respect to different levels of damage for the two-damaged-members cases from 1,000 samples of parameter estimates (Monte Carlo simulation + OEE) using 1% noisy measurements.
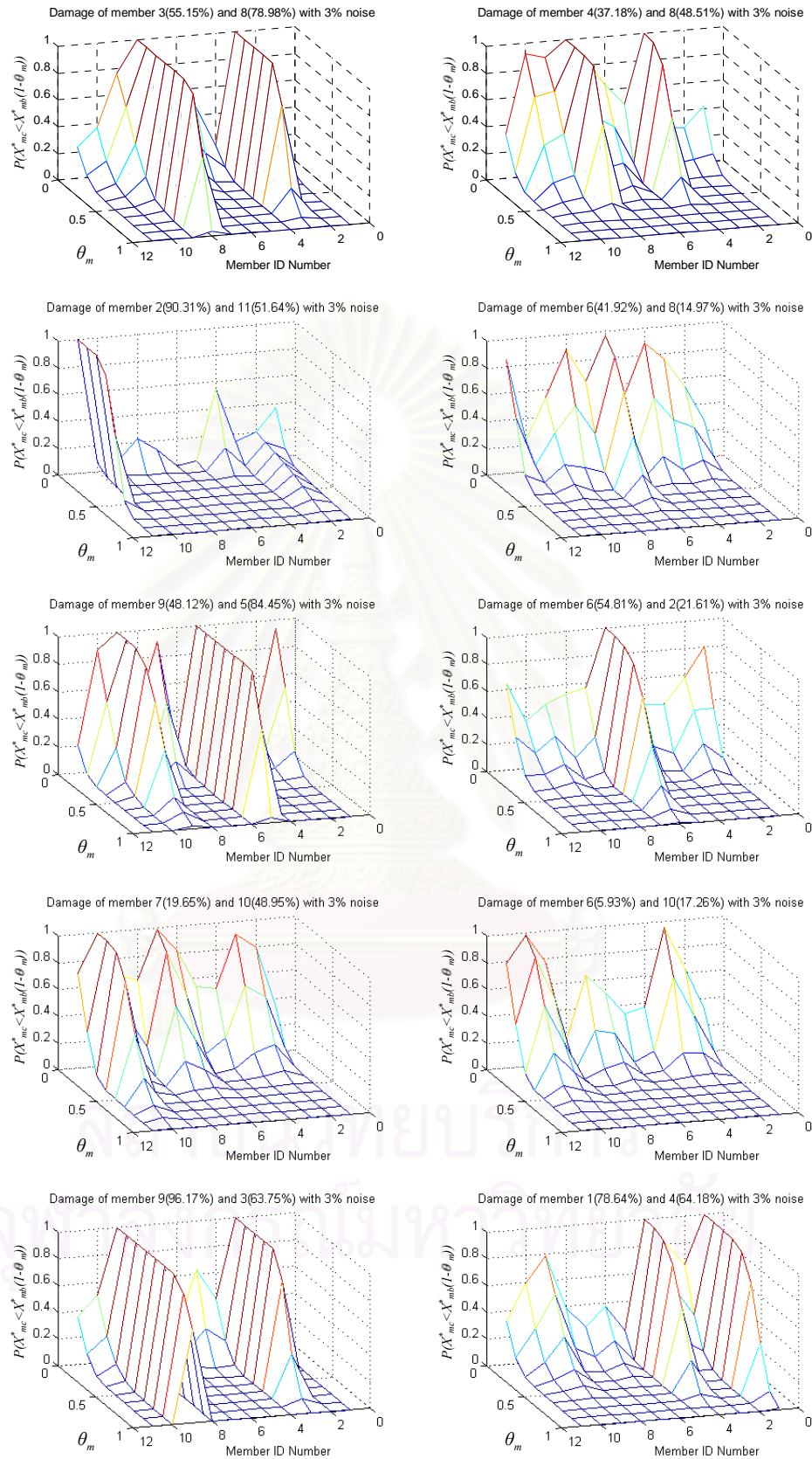
Figure 3.45 Probability distribution with respect to different levels of damage for the two-damaged-members cases from 1,000 samples of parameter estimates (Monte Carlo simulation + OEE) using 3% noisy measurements.
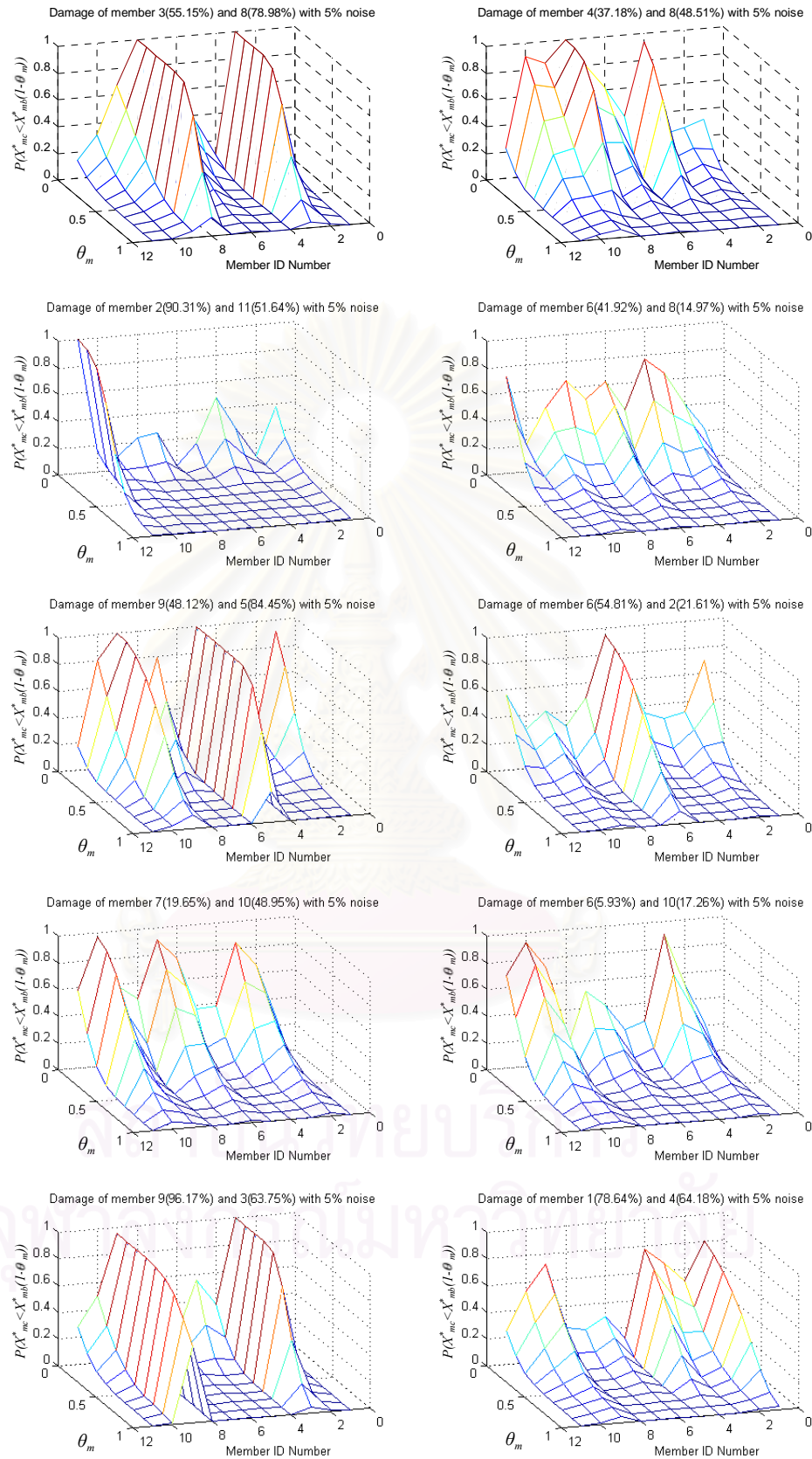
Figure 3.46 Probability distribution with respect to different levels of damage for the two-damaged-members cases from 1,000 samples of parameter estimates (Monte Carlo simulation + OEE) using 5% noisy measurements.
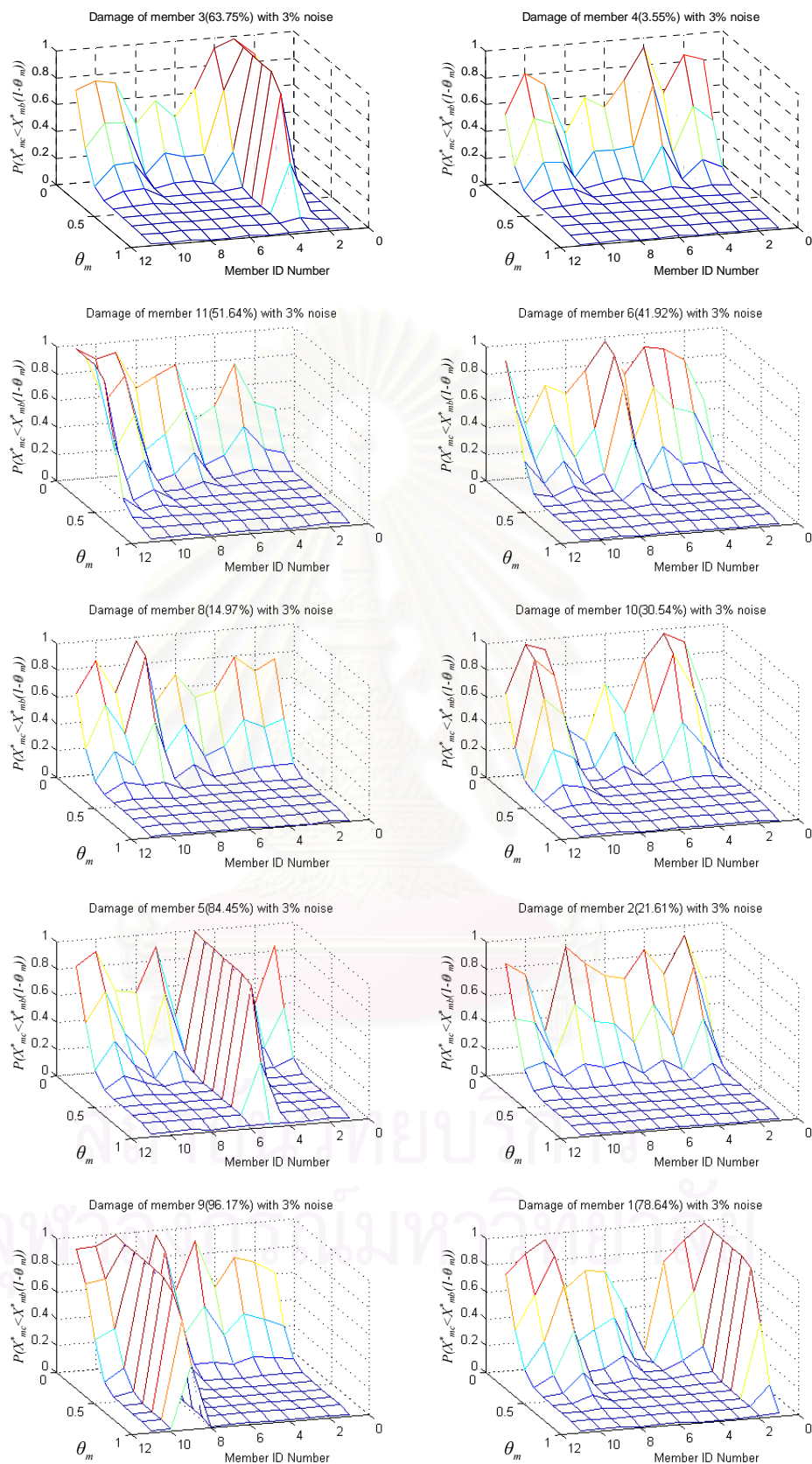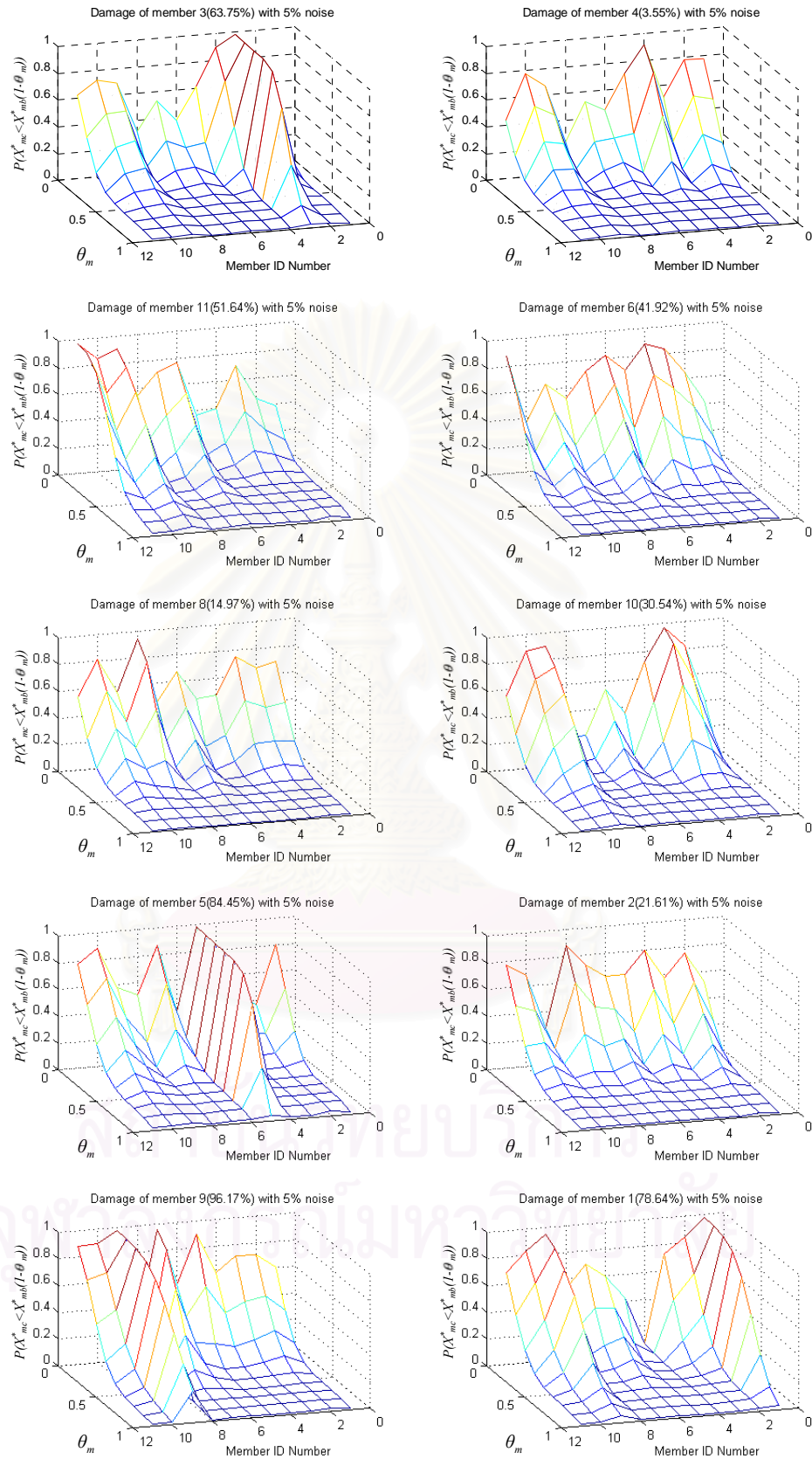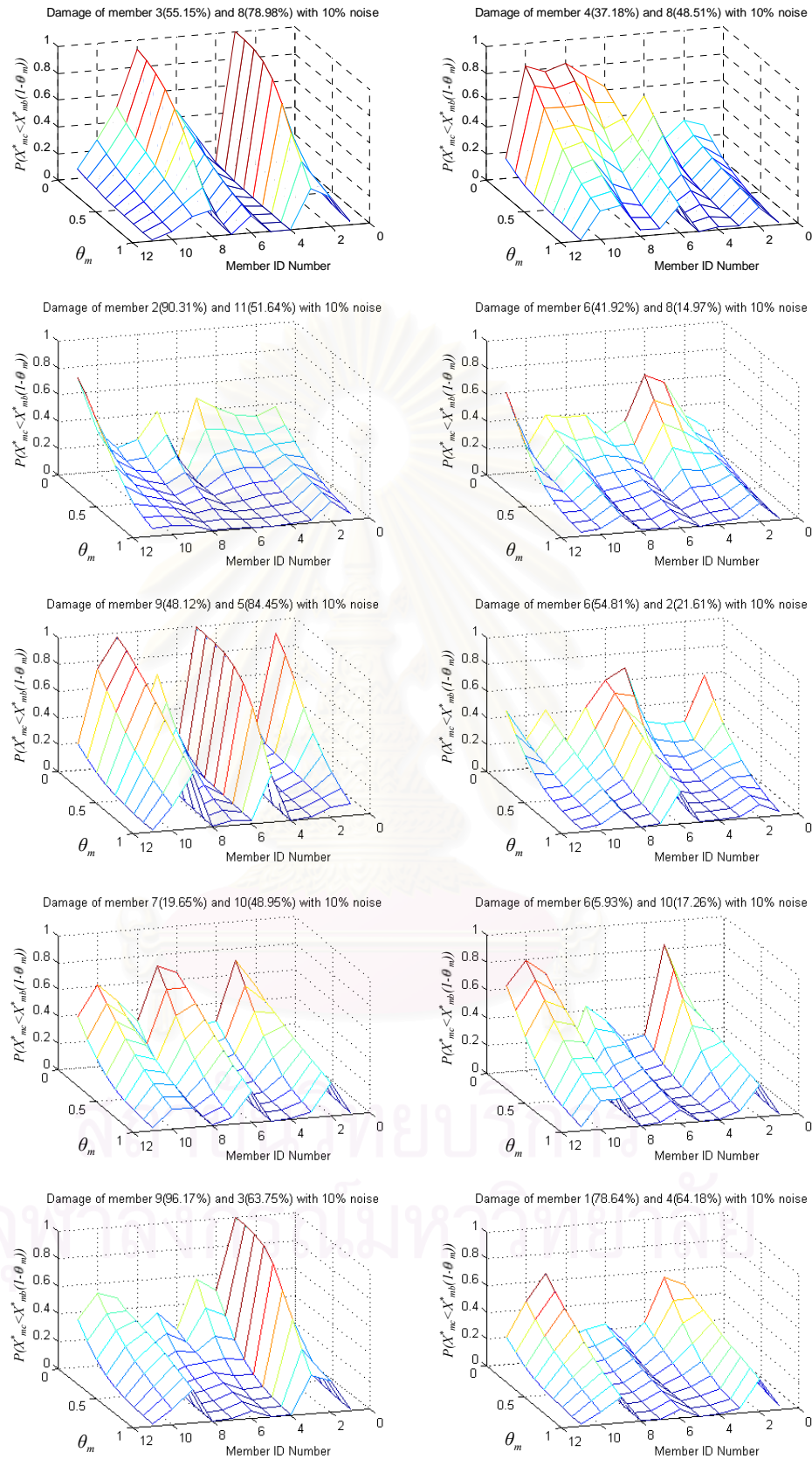
Figure 3.47 Probability distribution with respect to different levels of damage for the two-damaged-members cases from 1,000 samples of parameter estimates (Monte Carlo simulation + OEE) using 10% noisy measurements.
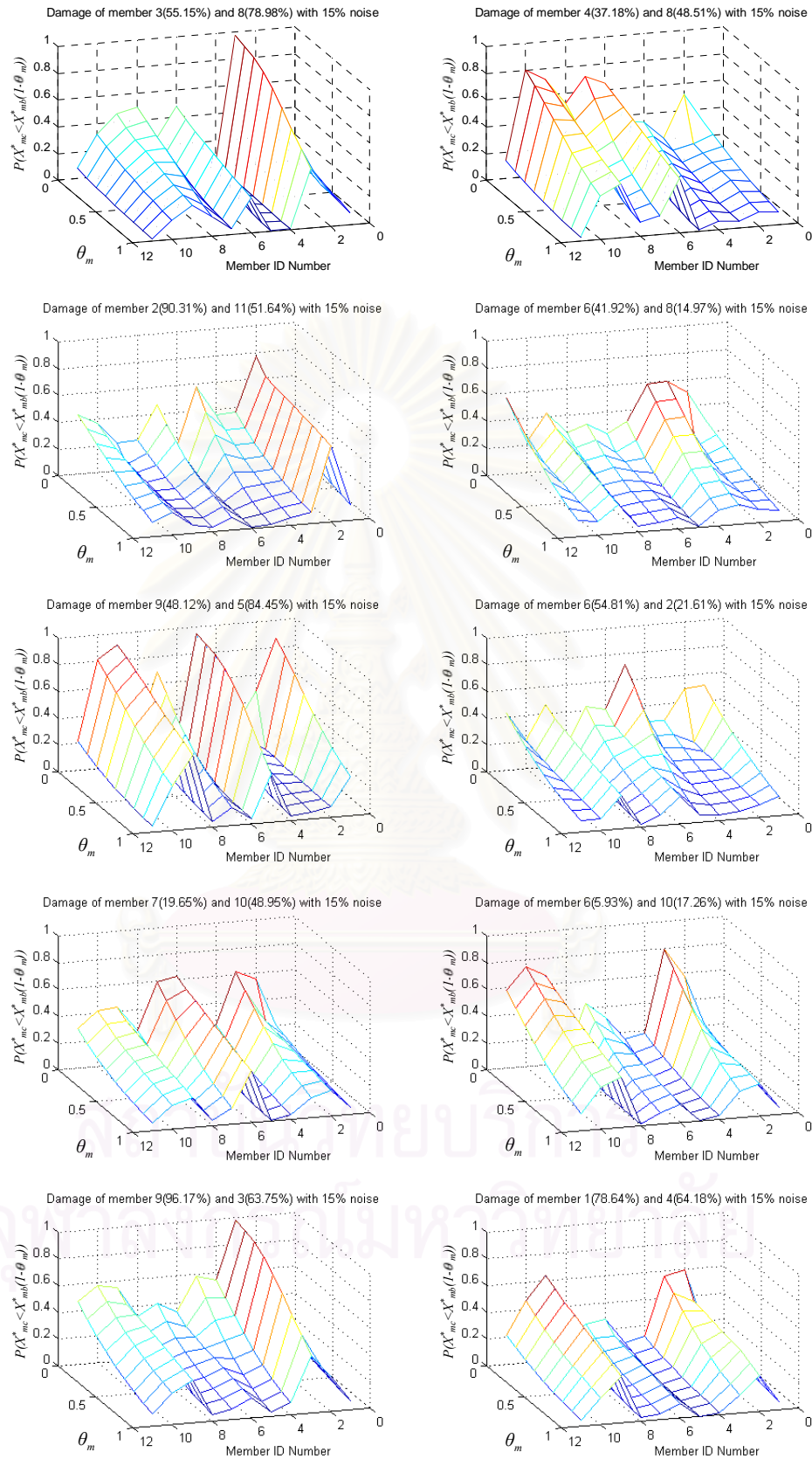
Figure 3.48 Probability distribution with respect to different levels of damage for the two-damaged-members cases from 1,000 samples of parameter estimates (Monte Carlo simulation + OEE) using 15% noisy measurements.
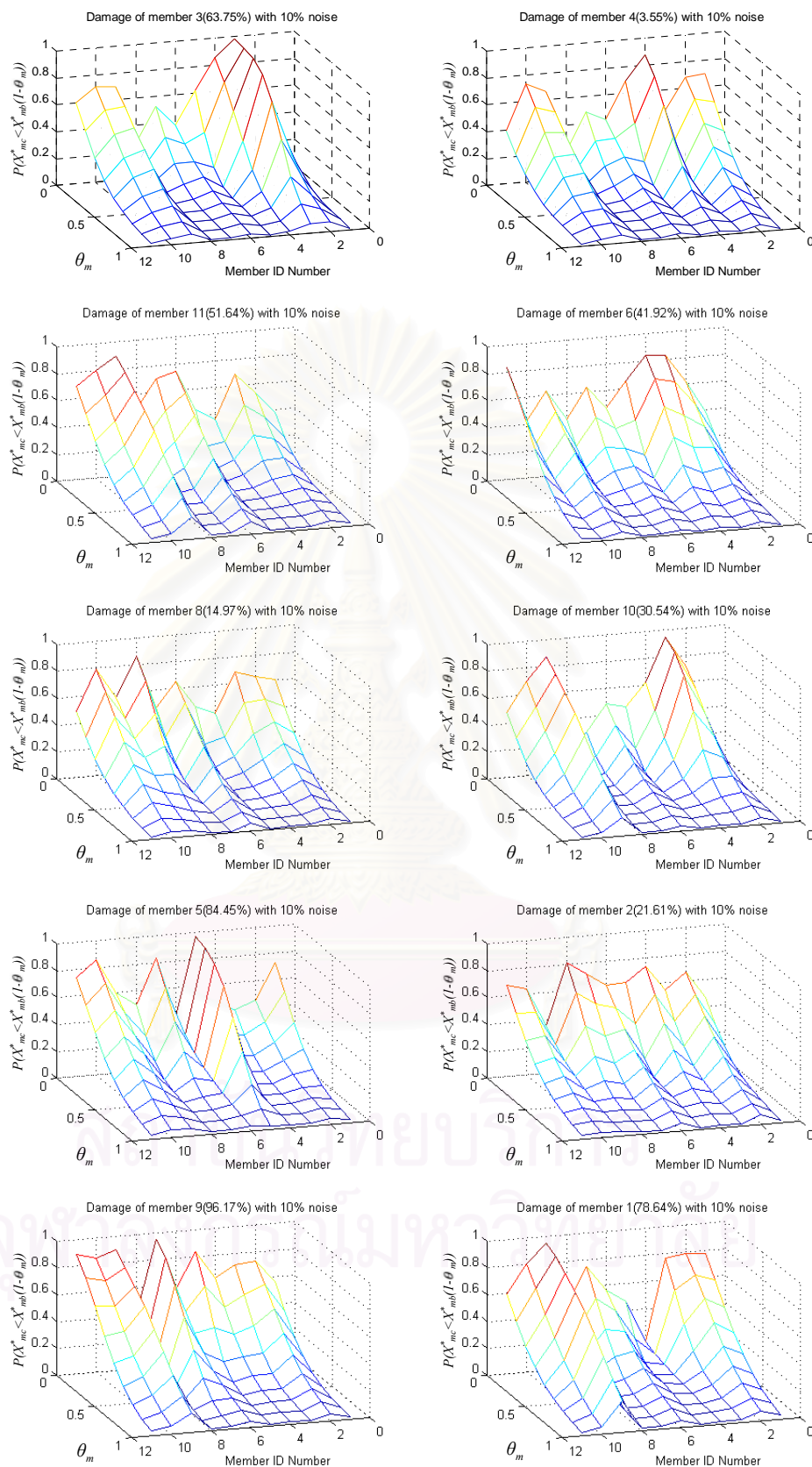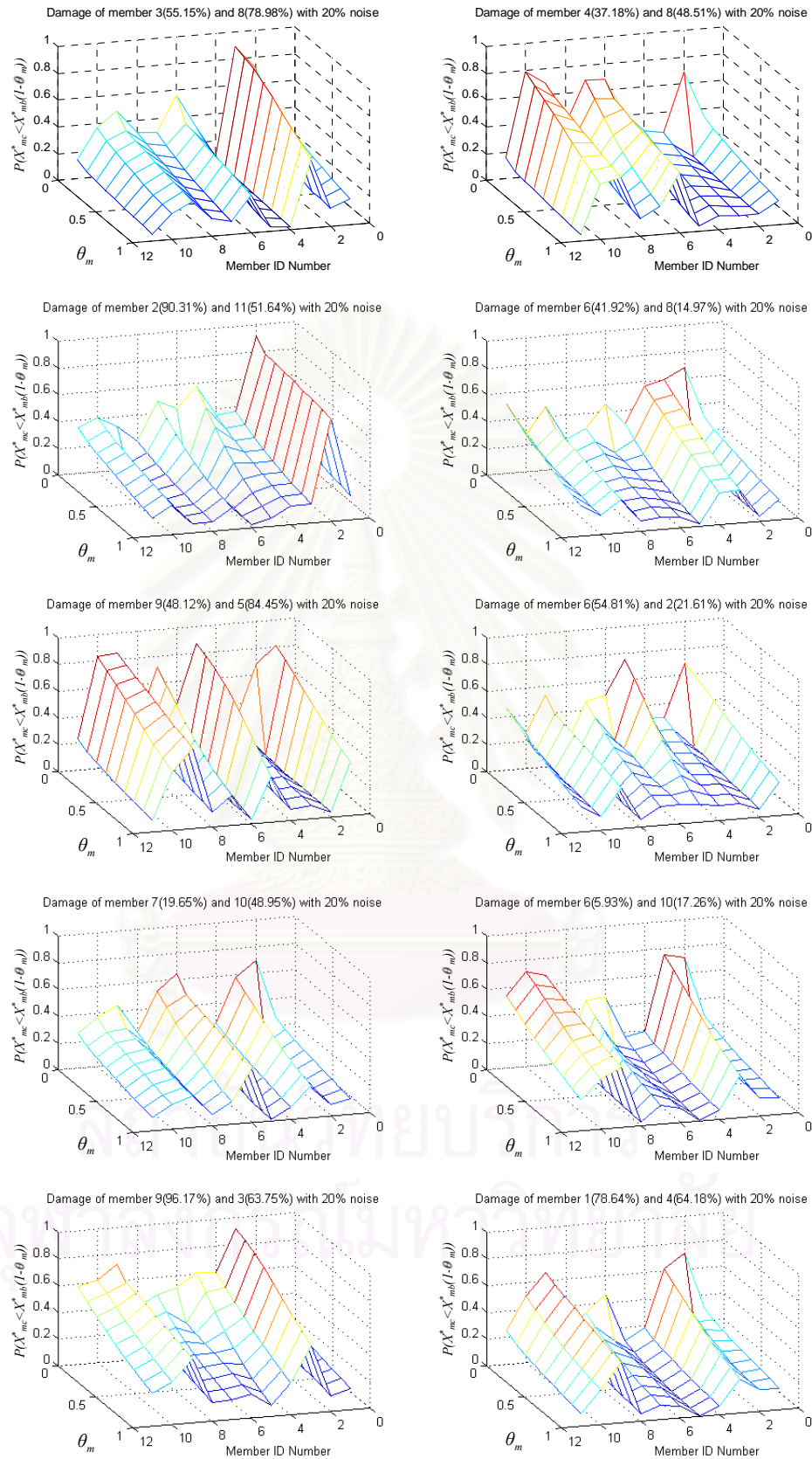
Figure 3.49 Probability distribution with respect to different levels of damage for the two-damaged-members cases from 1,000 samples of parameter estimates (Monte Carlo simulation + OEE) using 20% noisy measurements.
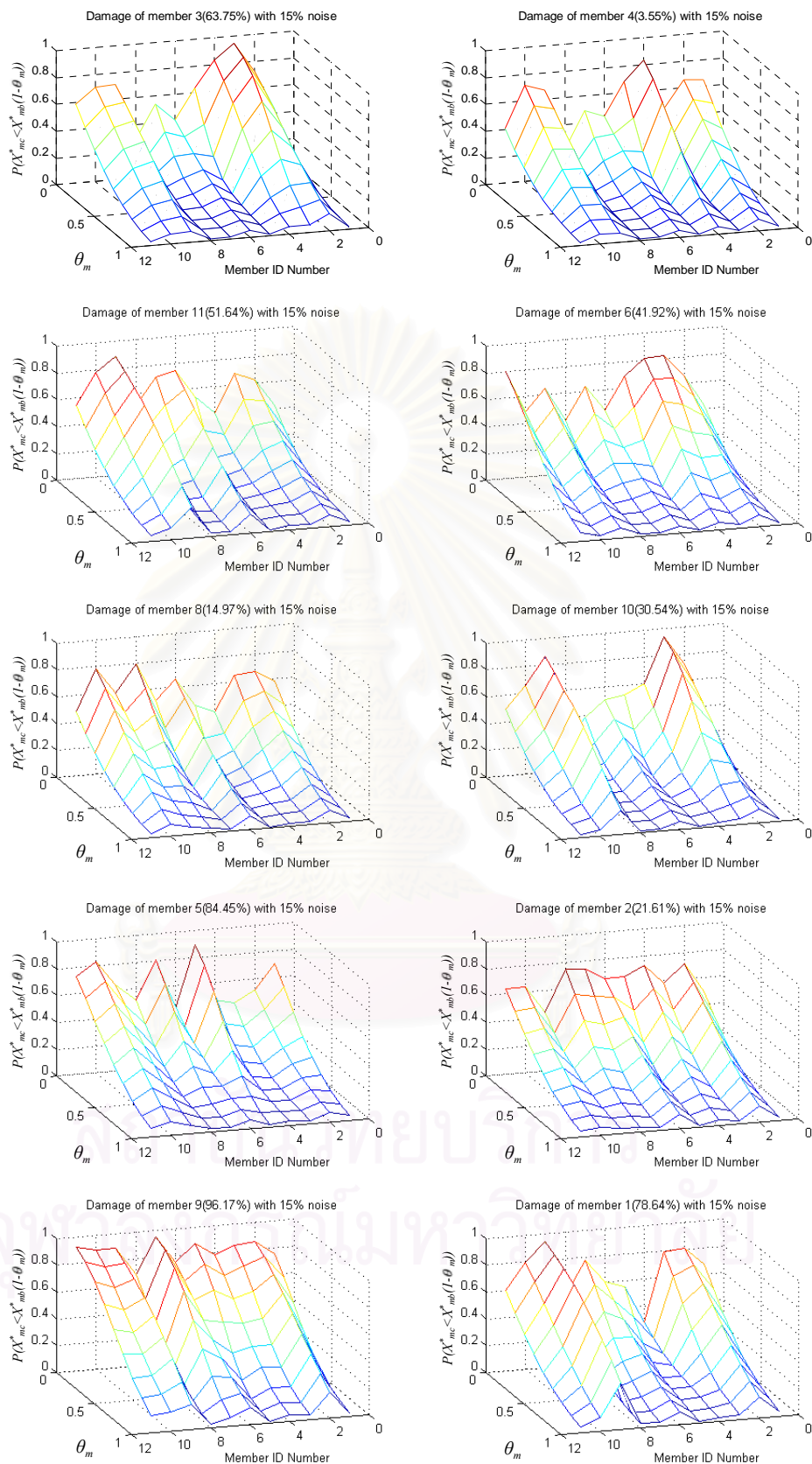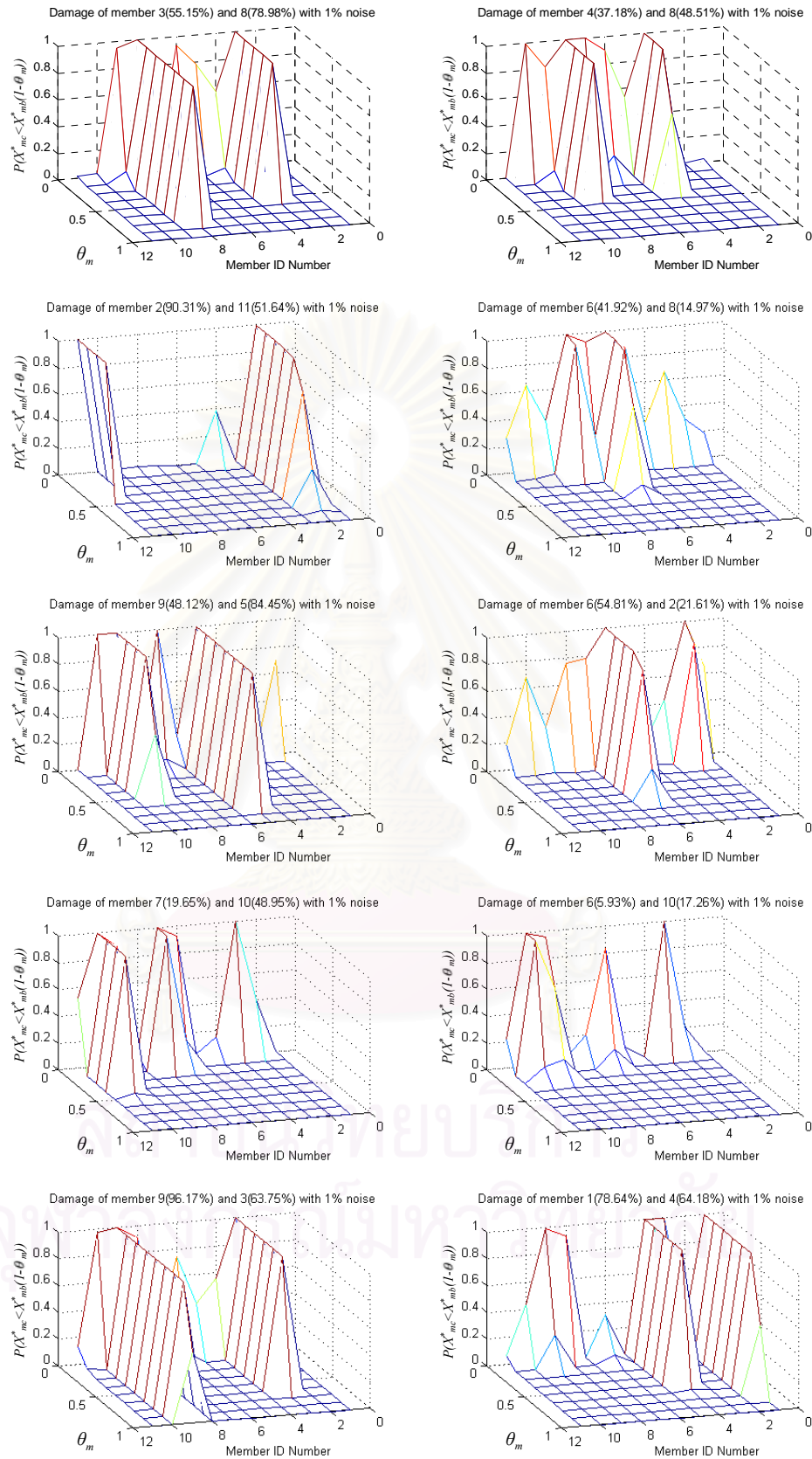
Figure 3.50 Probability distribution with respect to different levels of damage for the two-damaged-members cases using the sensitivity-based method and OEE algorithm with 1% noisy measurements.
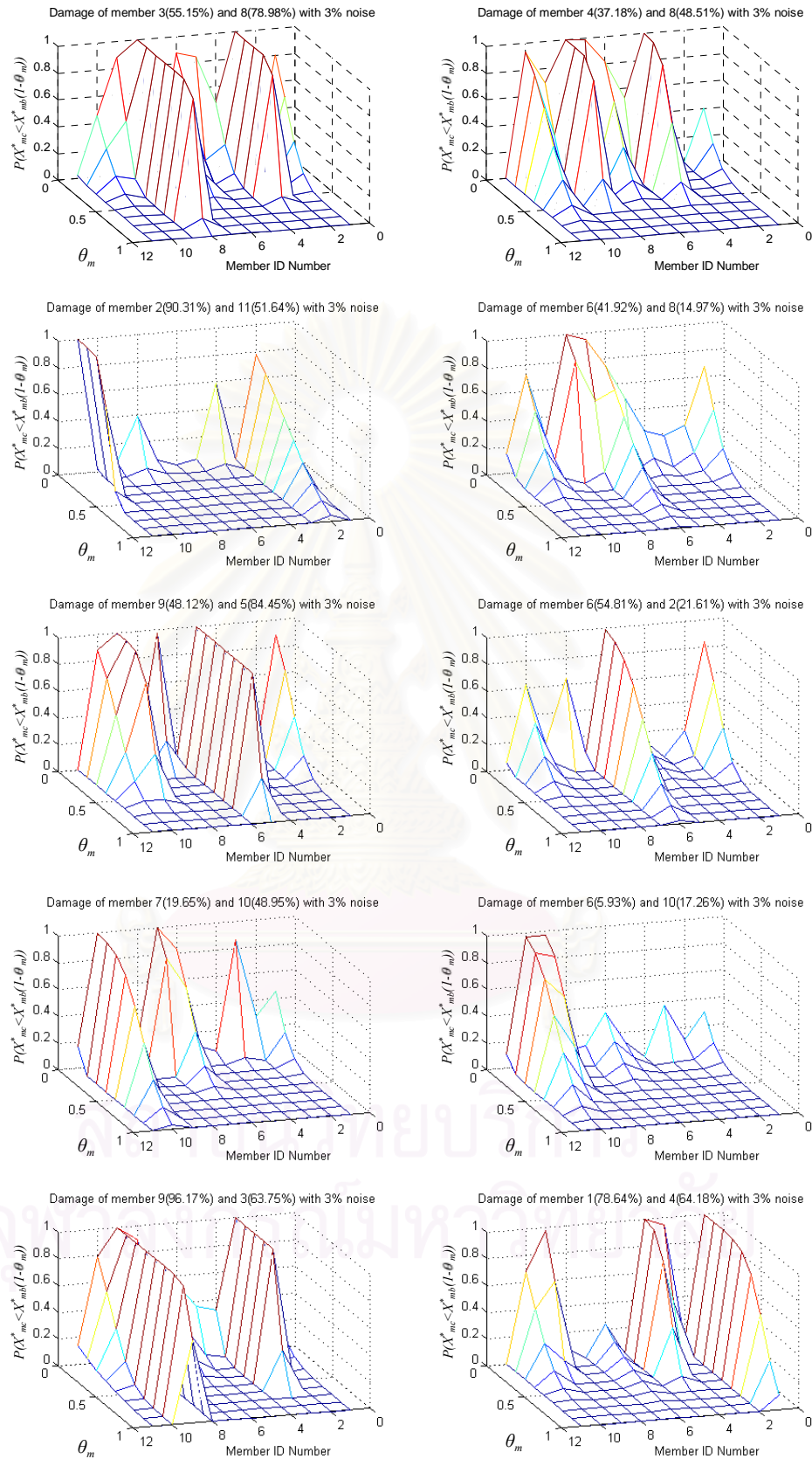
Figure 3.51 Probability distribution with respect to different levels of damage for the two-damaged-members cases using the sensitivity-based method and OEE algorithm with 3% noisy measurements.
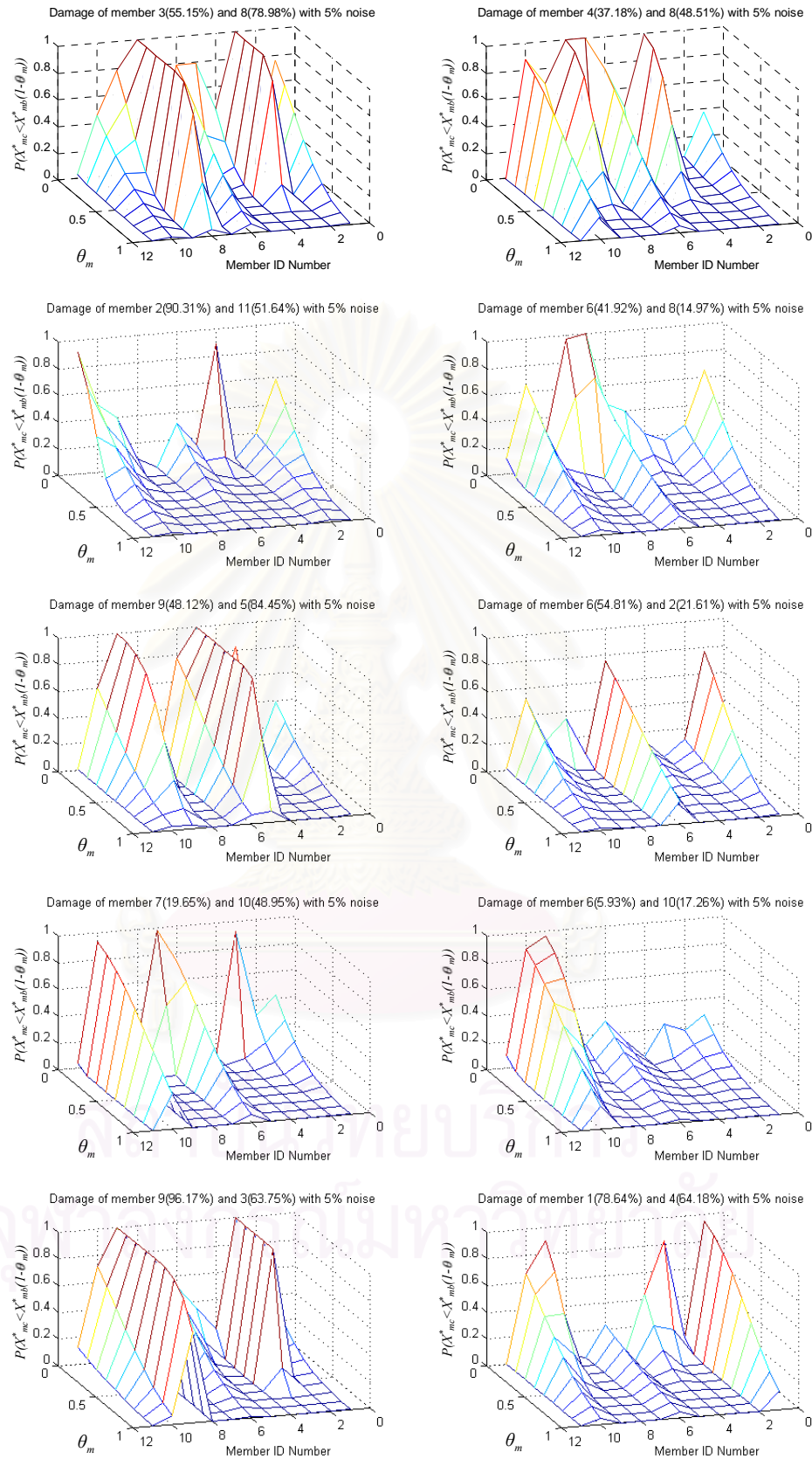
Figure 3.52 Probability distribution with respect to different levels of damage for the two-damaged-members cases using the sensitivity-based method and OEE algorithm with 5% noisy measurements.

Figure 3.53 Probability distribution with respect to different levels of damage for the two-damaged-members cases using the sensitivity-based method and OEE algorithm with 10% noisy measurements.
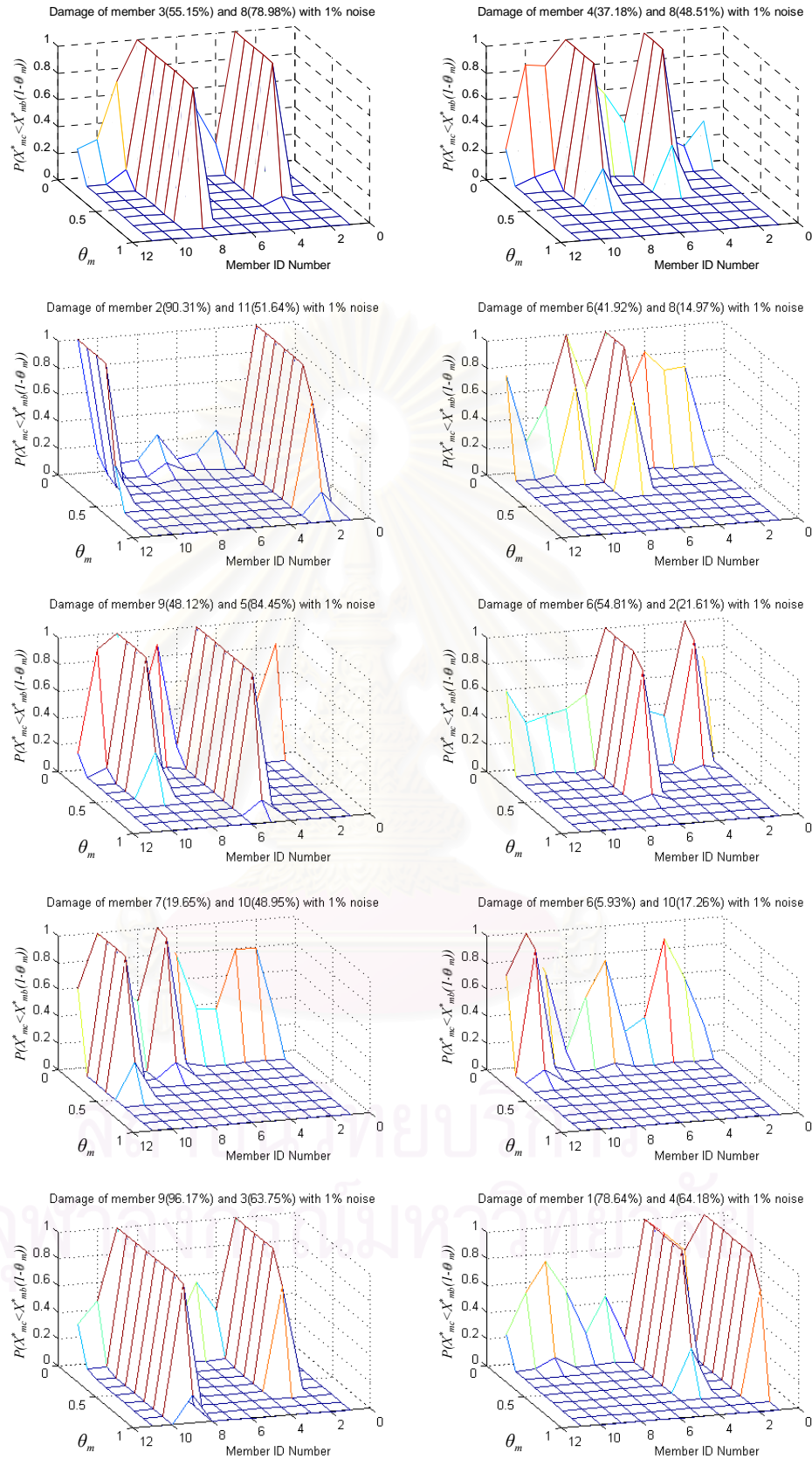
Figure 3.54 Probability distribution with respect to different levels of damage for the two-damaged-members cases using the optimum sensitivity-based method and OEE algorithm with 1% noisy measurements.
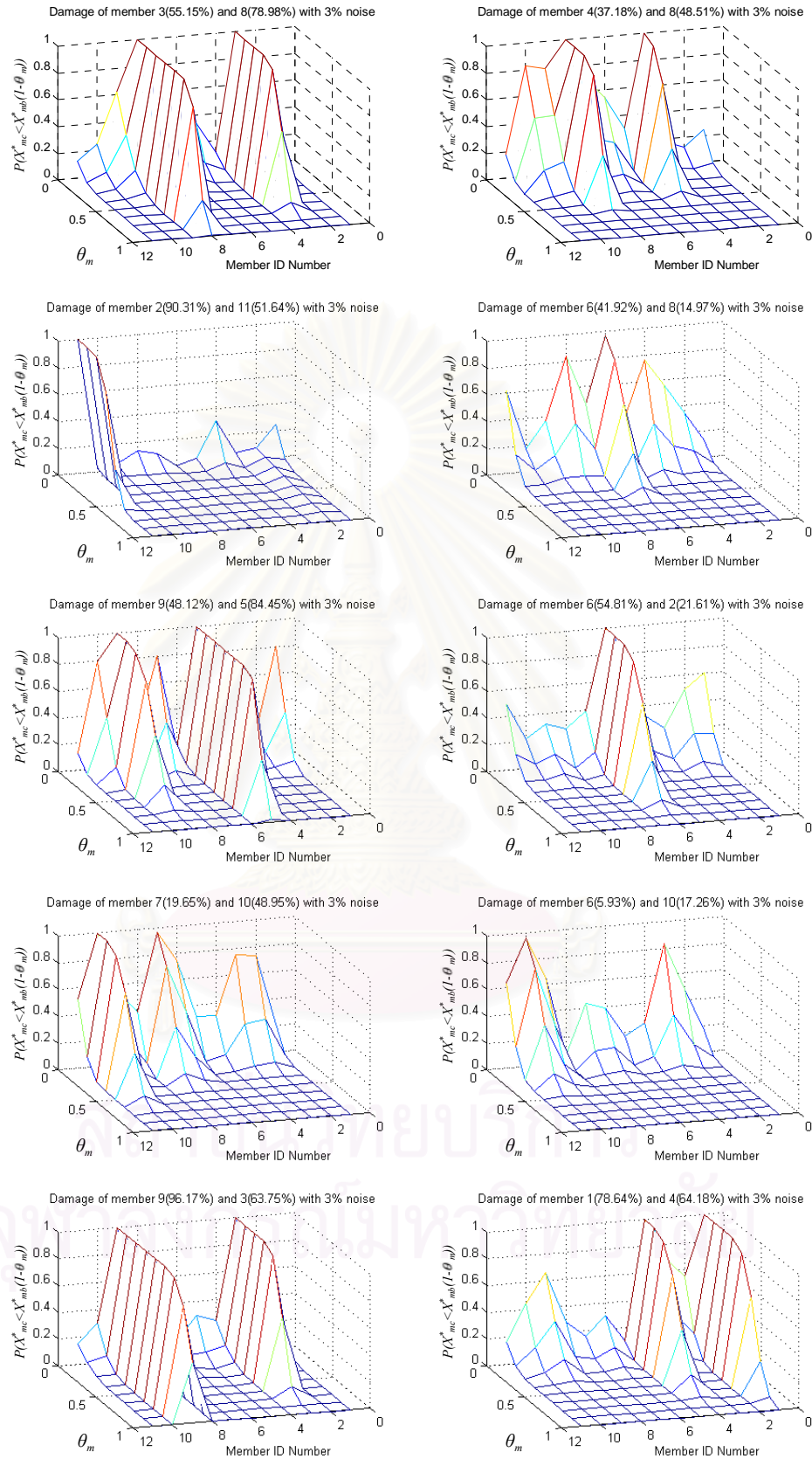
Figure 3.55 Probability distribution with respect to different levels of damage for the two-damaged-members cases using the optimum sensitivity-based method and OEE algorithm with 3% noisy measurements.
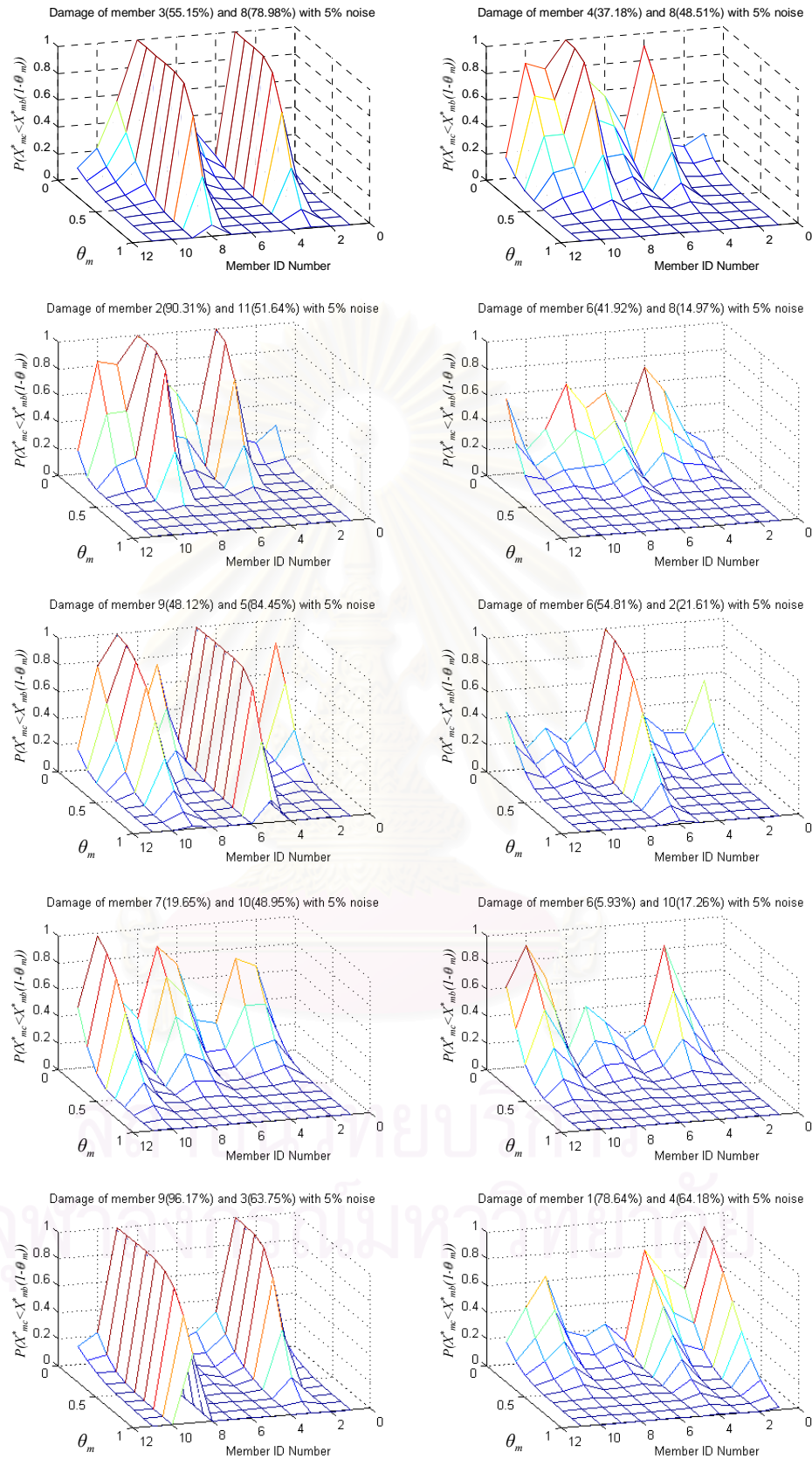
Figure 3.56 Probability distribution with respect to different levels of damage for the two-damaged-members cases using the optimum sensitivity-based method and OEE algorithm with 5% noisy measurements.
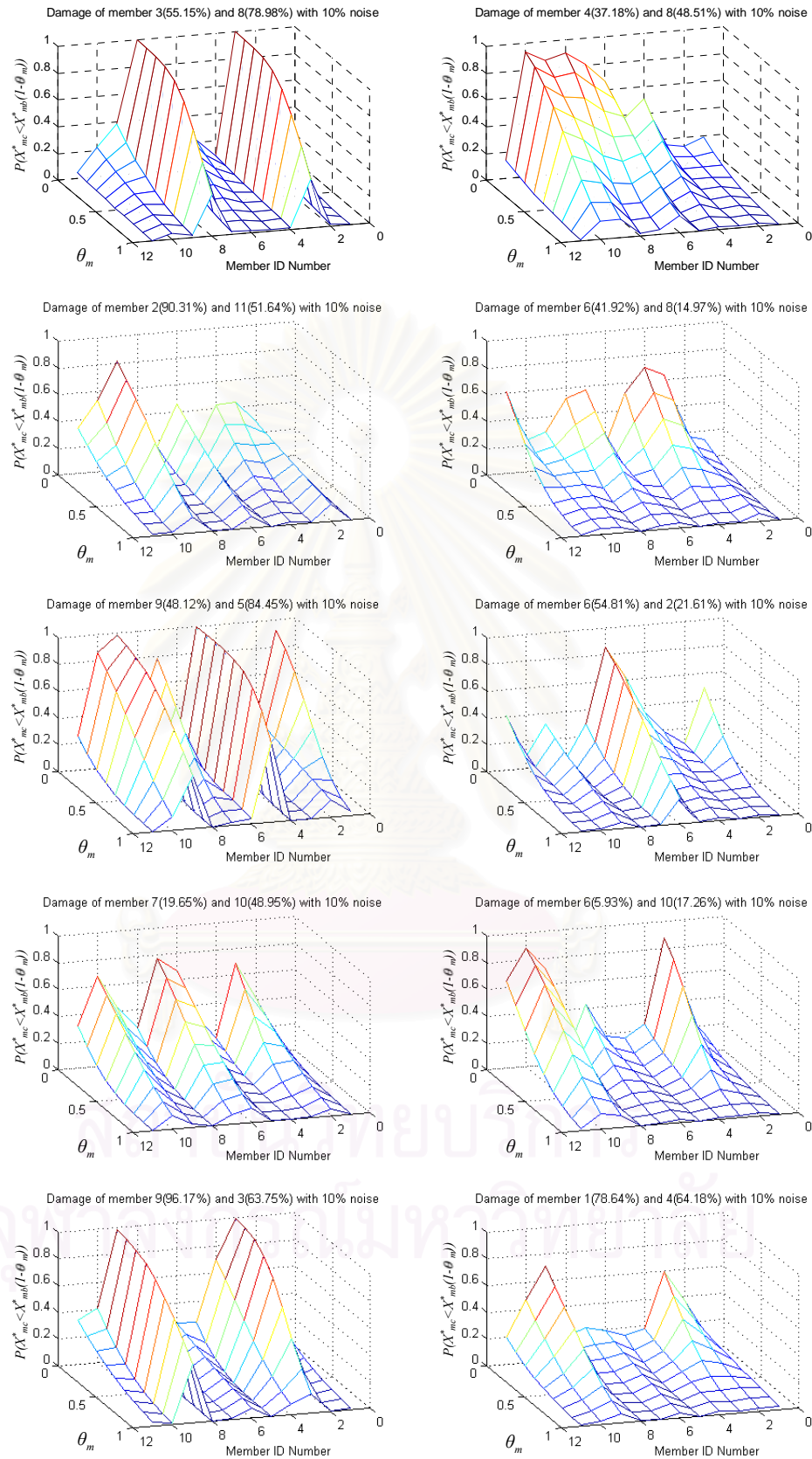
Figure 3.57 Probability distribution with respect to different levels of damage for the two-damaged-members cases using the optimum sensitivity-based method and OEE algorithm with 10% noisy measurements.
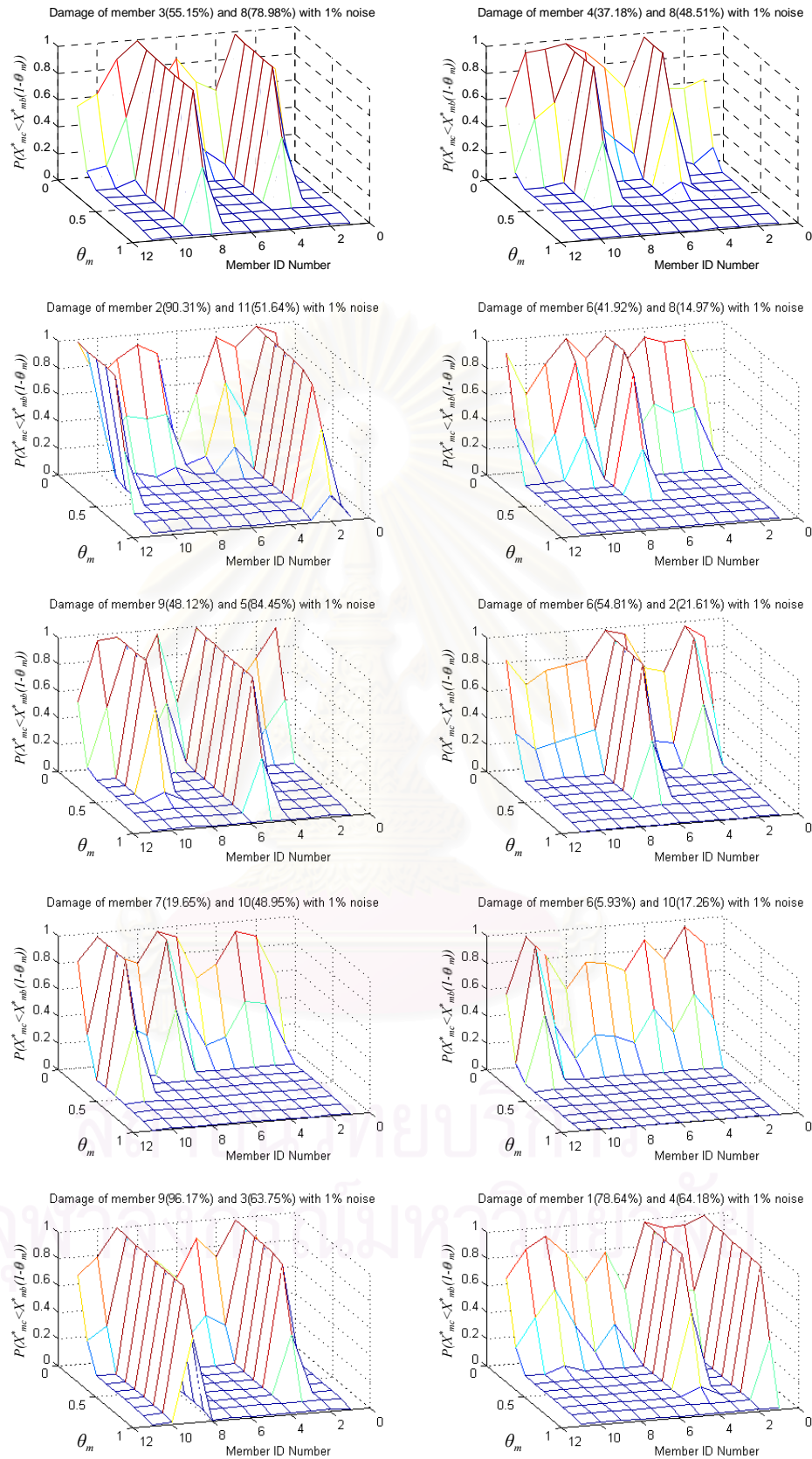
Figure 3.58 Probability distribution with respect to different levels of damage for the two-damaged-members cases from 1,000 samples of parameter estimates (Monte Carlo simulation + ROEE) using 1% noisy measurements.
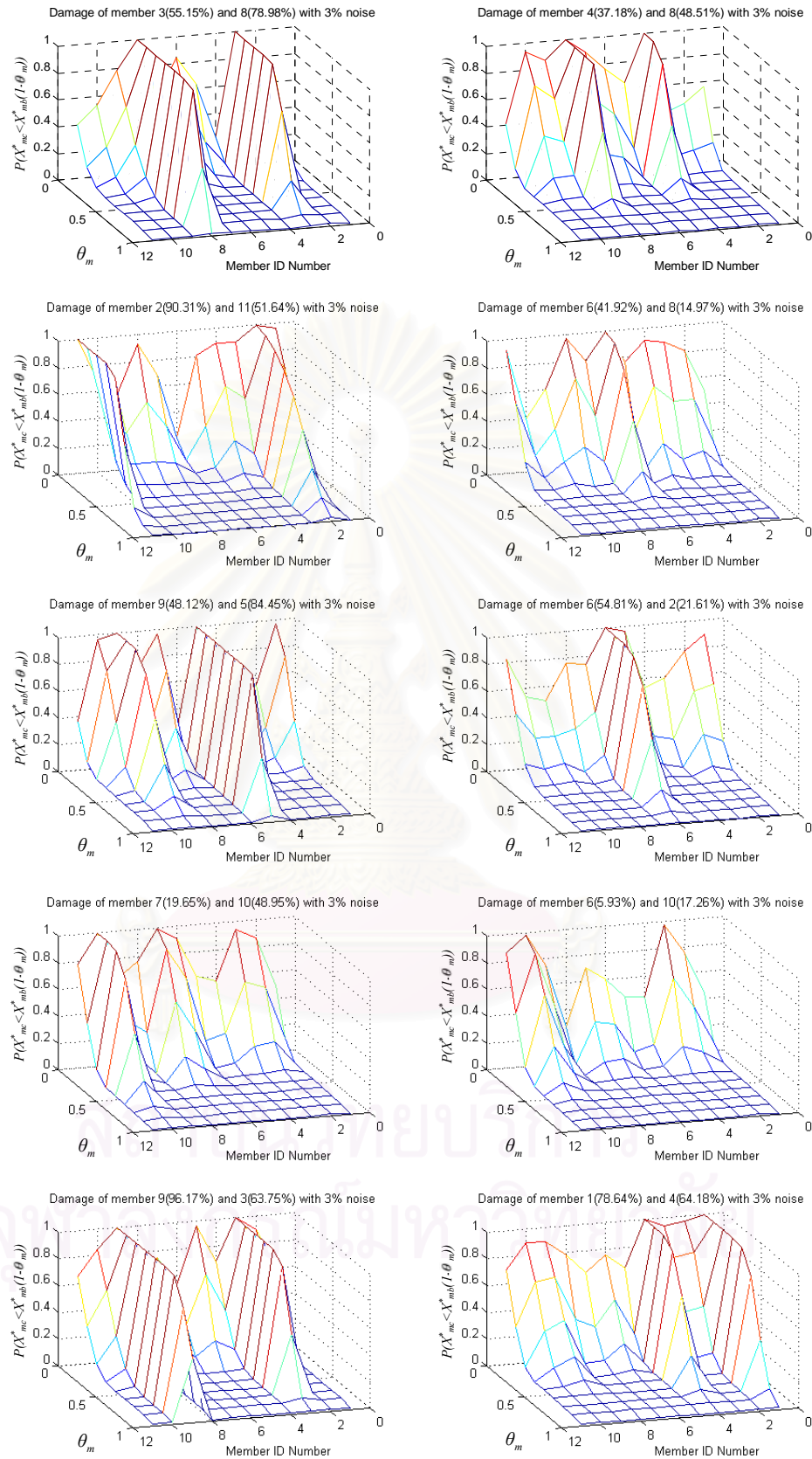
Figure 3.59 Probability distribution with respect to different levels of damage for the two-damaged-members cases from 1,000 samples of parameter estimates (Monte Carlo simulation + ROEE) using 3% noisy measurements.
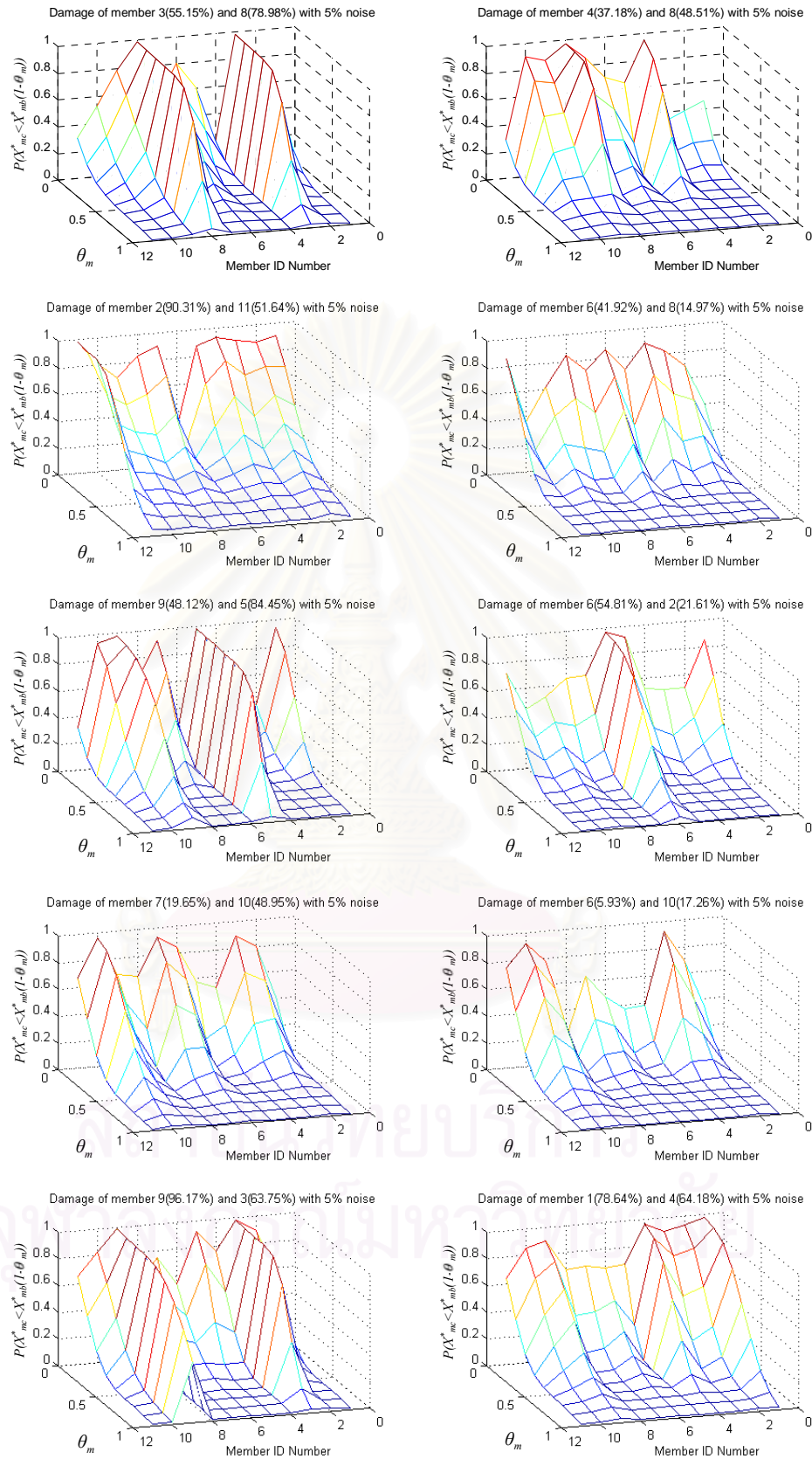
Figure 3.60 Probability distribution with respect to different levels of damage for the two-damaged-members cases from 1,000 samples of parameter estimates (Monte Carlo simulation + ROEE) using 5% noisy measurements.
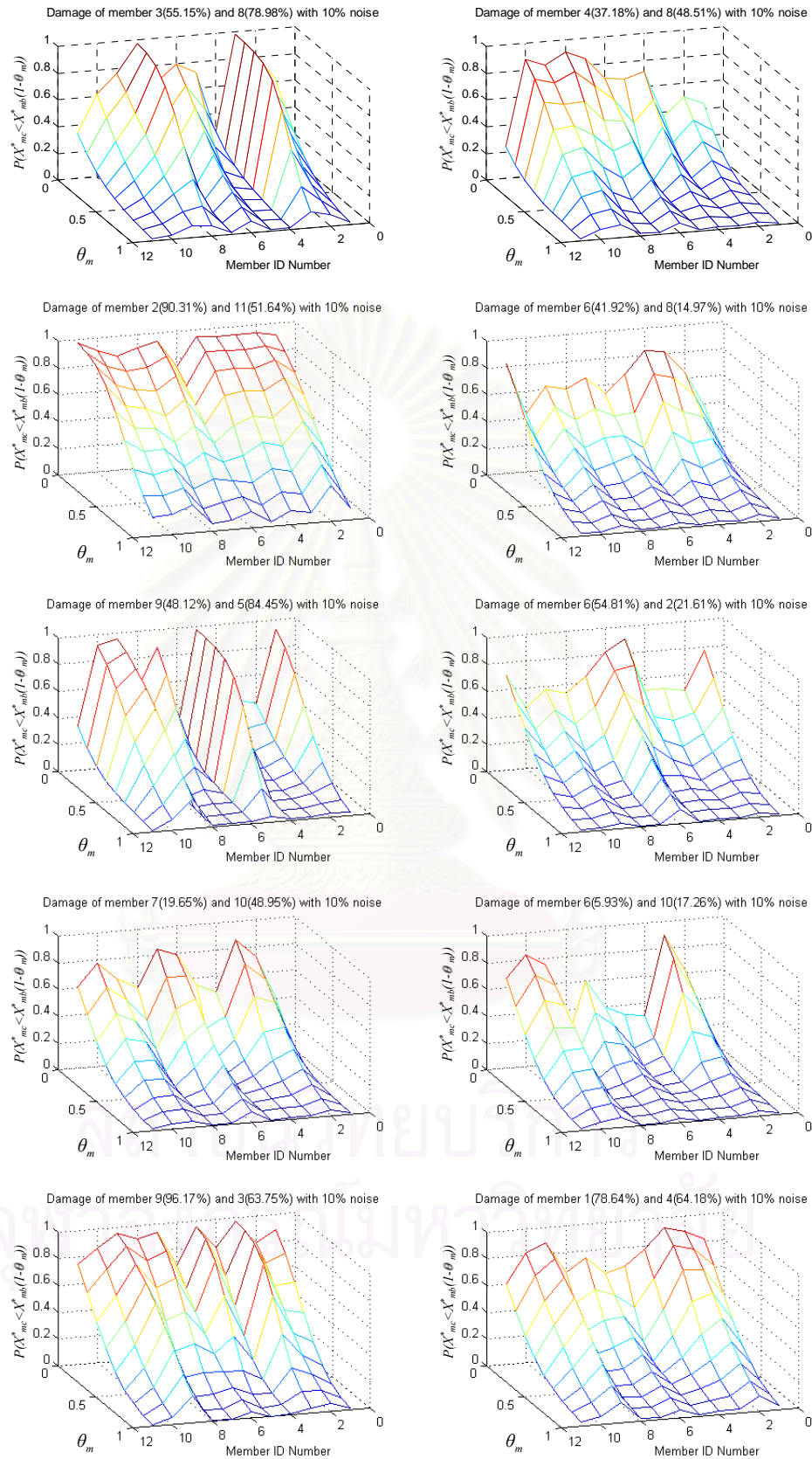
Figure 3.61 Probability distribution with respect to different levels of damage for the two-damaged-members cases from 1,000 samples of parameter estimates (Monte Carlo simulation + ROEE) using 10% noisy measurements.
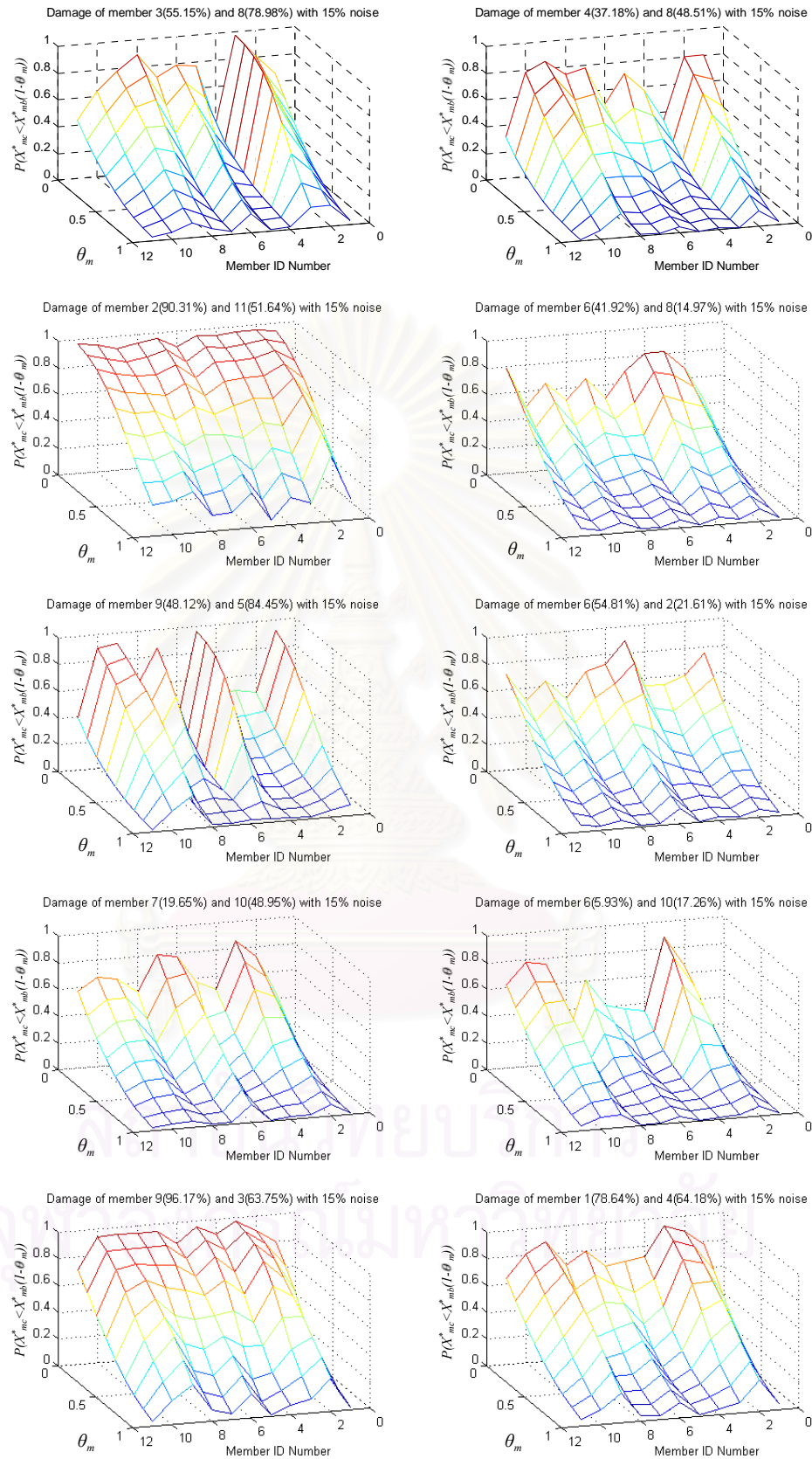
Figure 3.62 Probability distribution with respect to different levels of damage for the two-damaged-members cases from 1,000 samples of parameter estimates (Monte Carlo simulation + ROEE) using 15% noisy measurements.
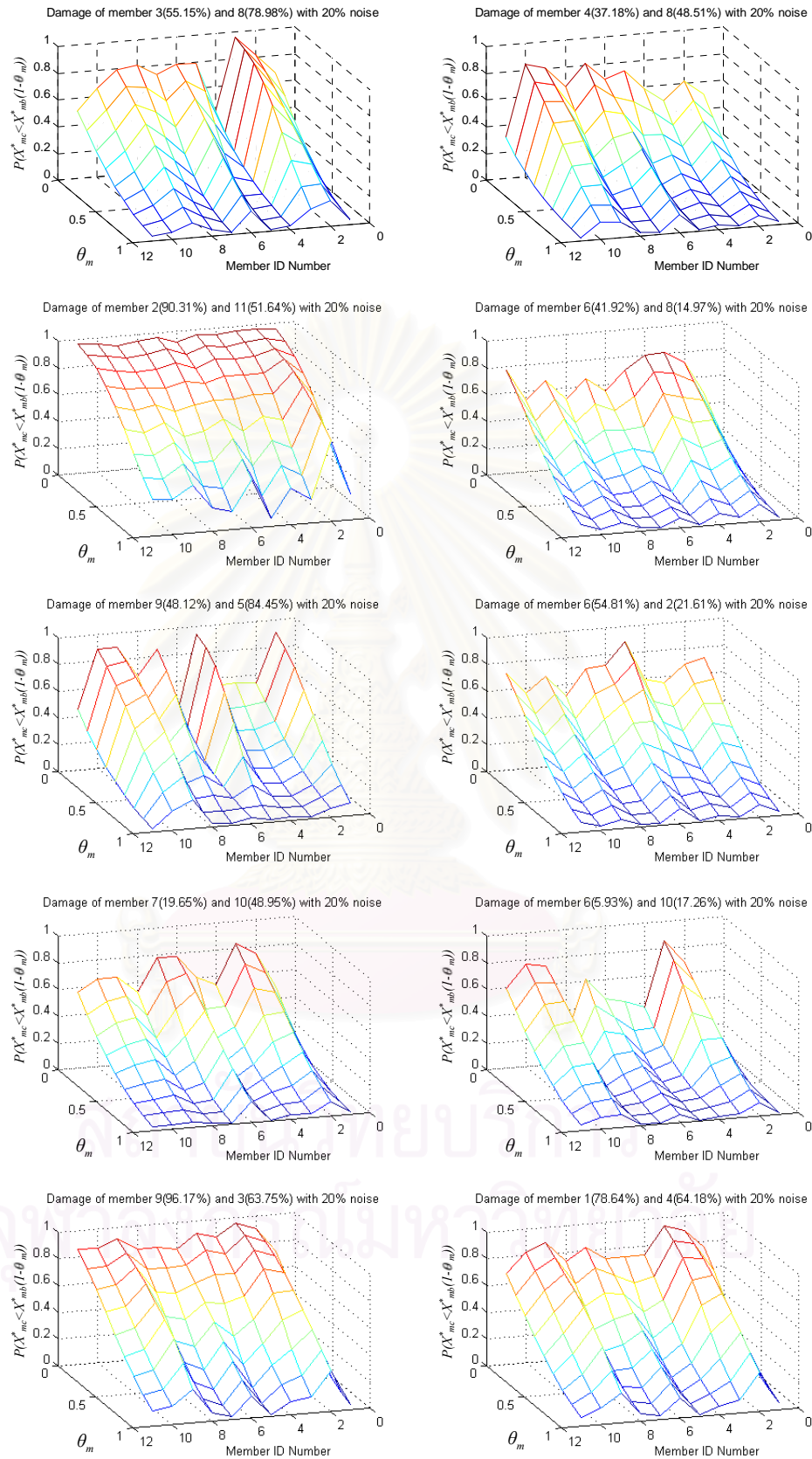
Figure 3.63 Probability distribution with respect to different levels of damage for the two-damaged-members cases from 1,000 samples of parameter estimates (Monte Carlo simulation + ROEE) using 20% noisy measurements.
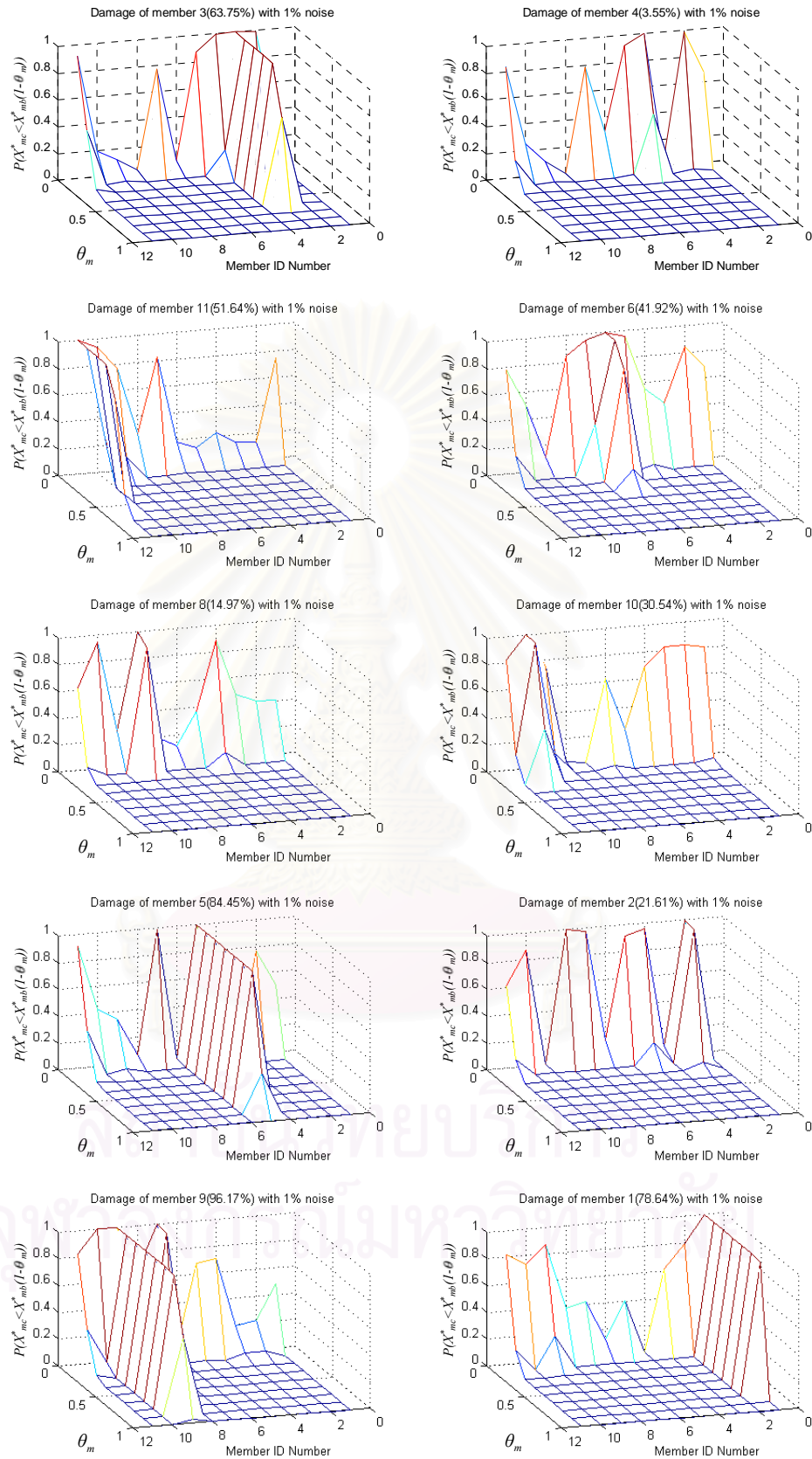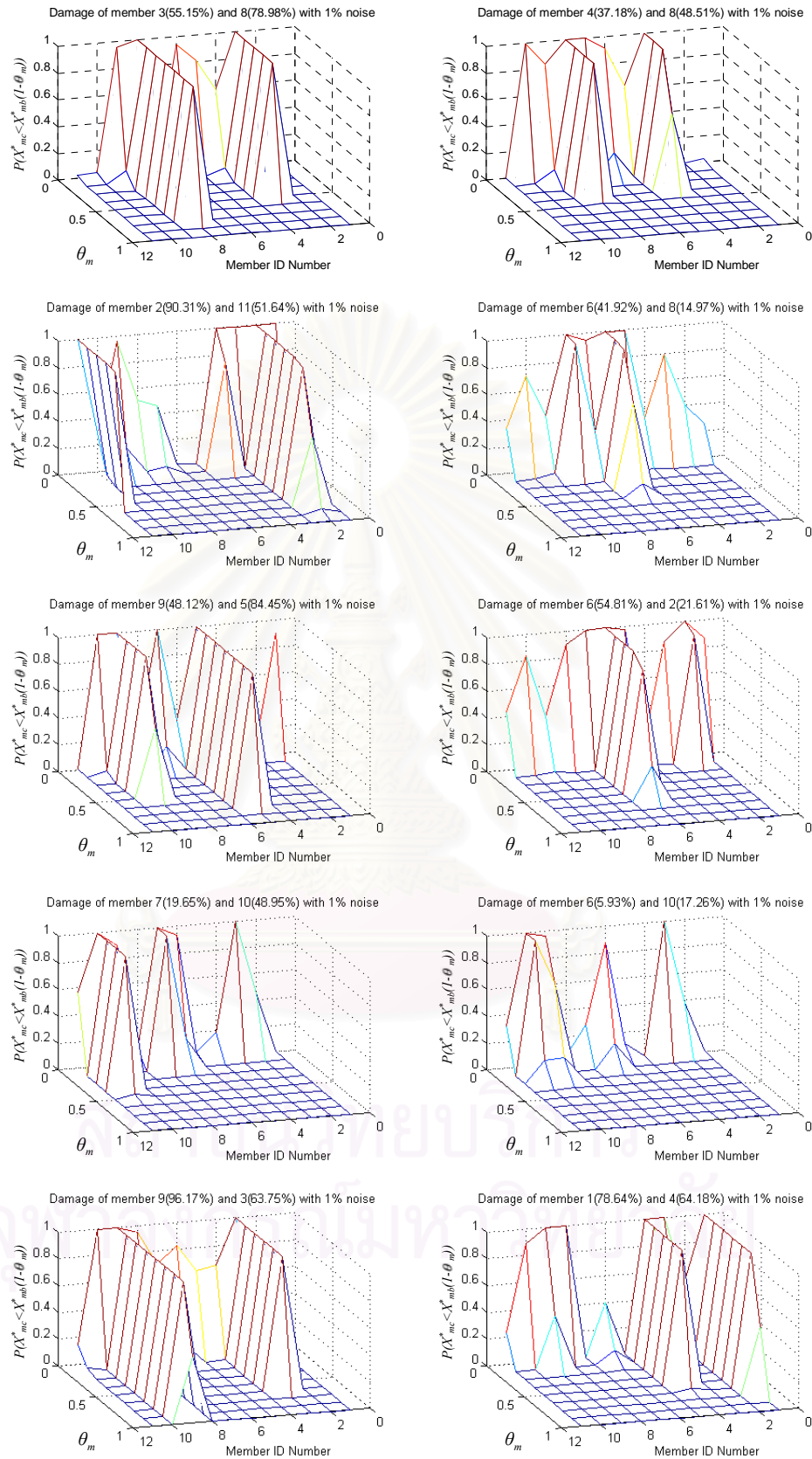
Figure 3.64 Probability distribution with respect to different levels of damage for the two-damaged-members cases using the sensitivity-based method and ROEE algorithm with 1% noisy measurements.
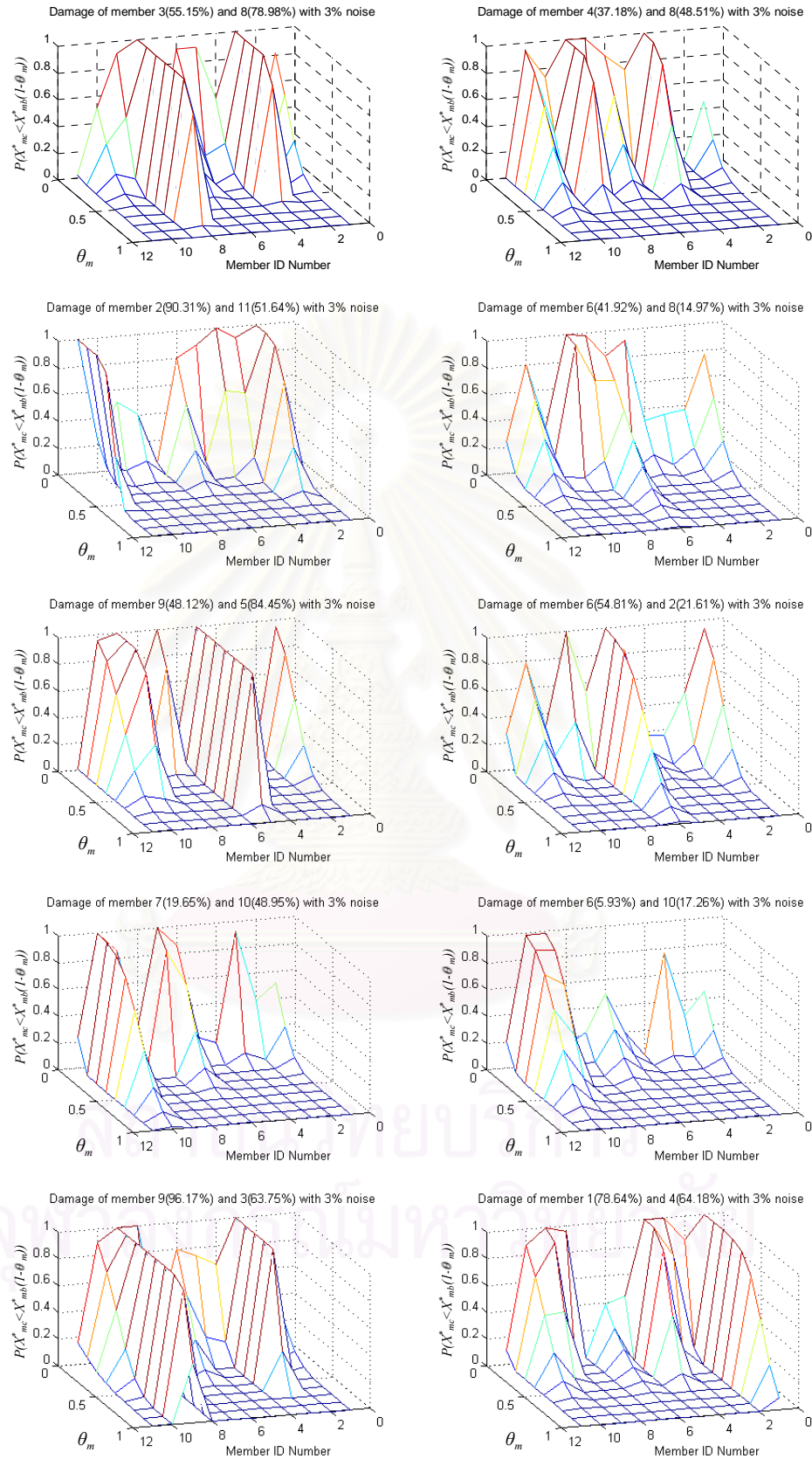
Figure 3.65 Probability distribution with respect to different levels of damage for the two-damaged-members cases using the sensitivity-based method and ROEE algorithm with 3% noisy measurements.
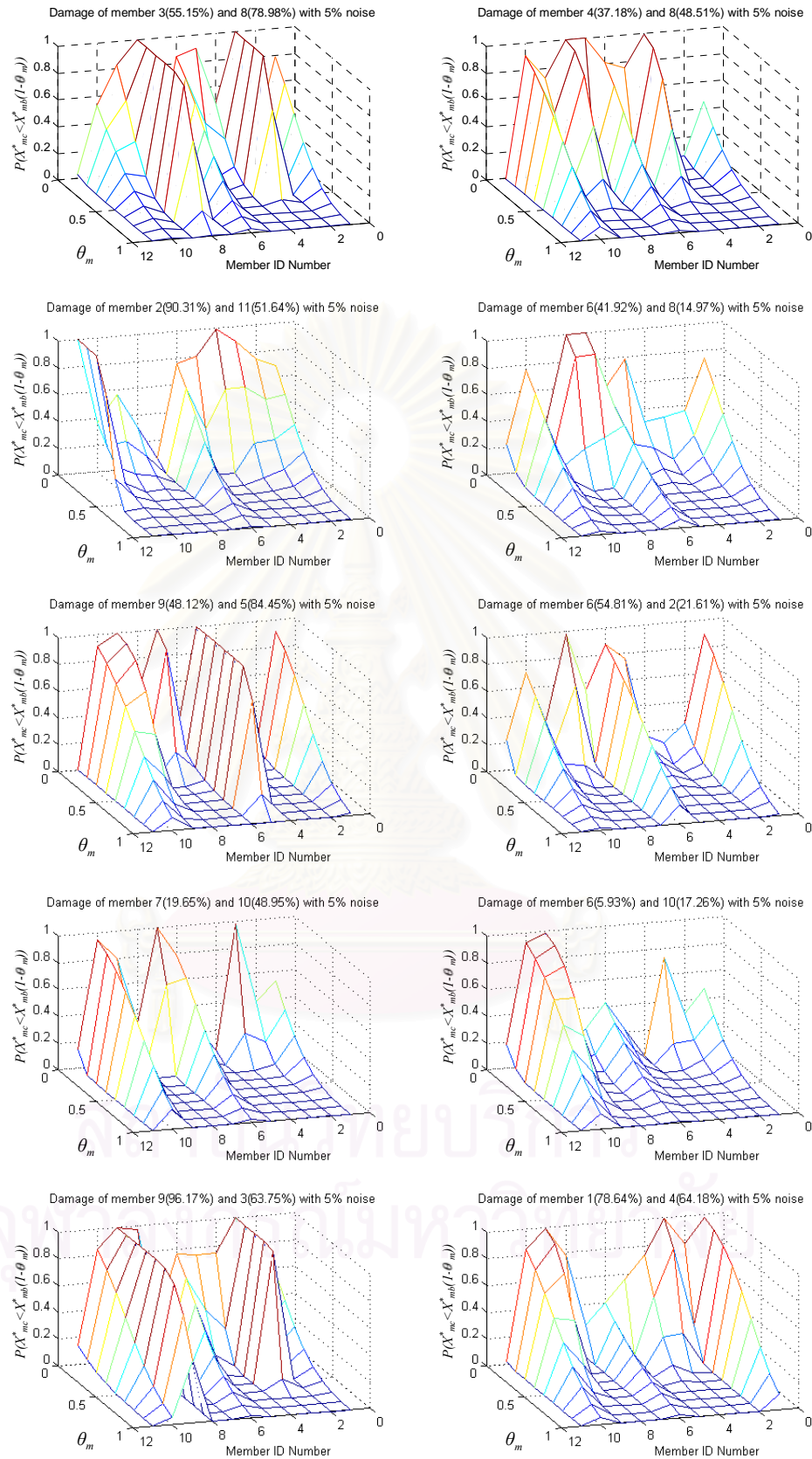
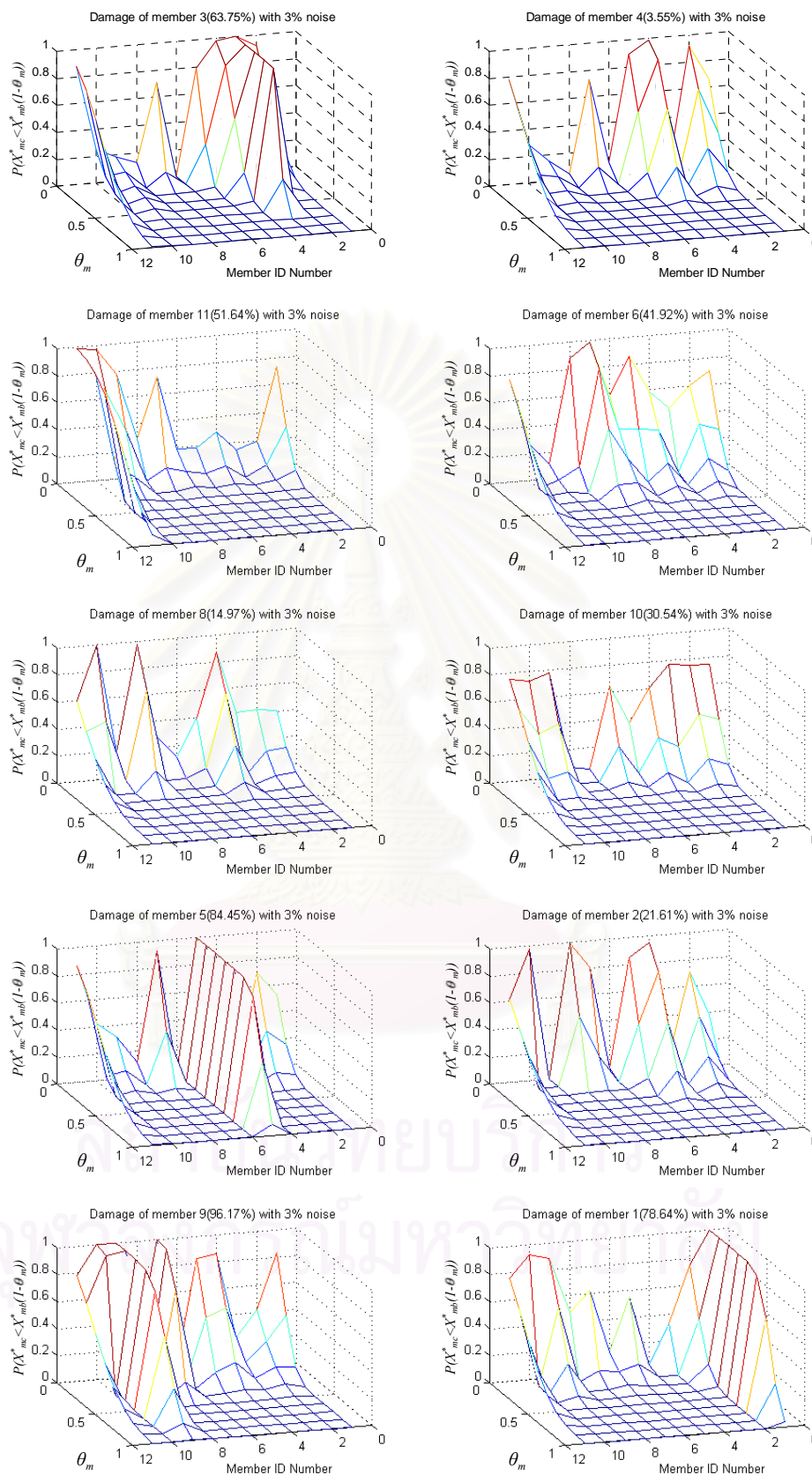Figure 3.66 Probability distribution with respect to different levels of damage for the two-damaged-members cases using the sensitivity-based method and ROEE algorithm with 5% noisy measurements.
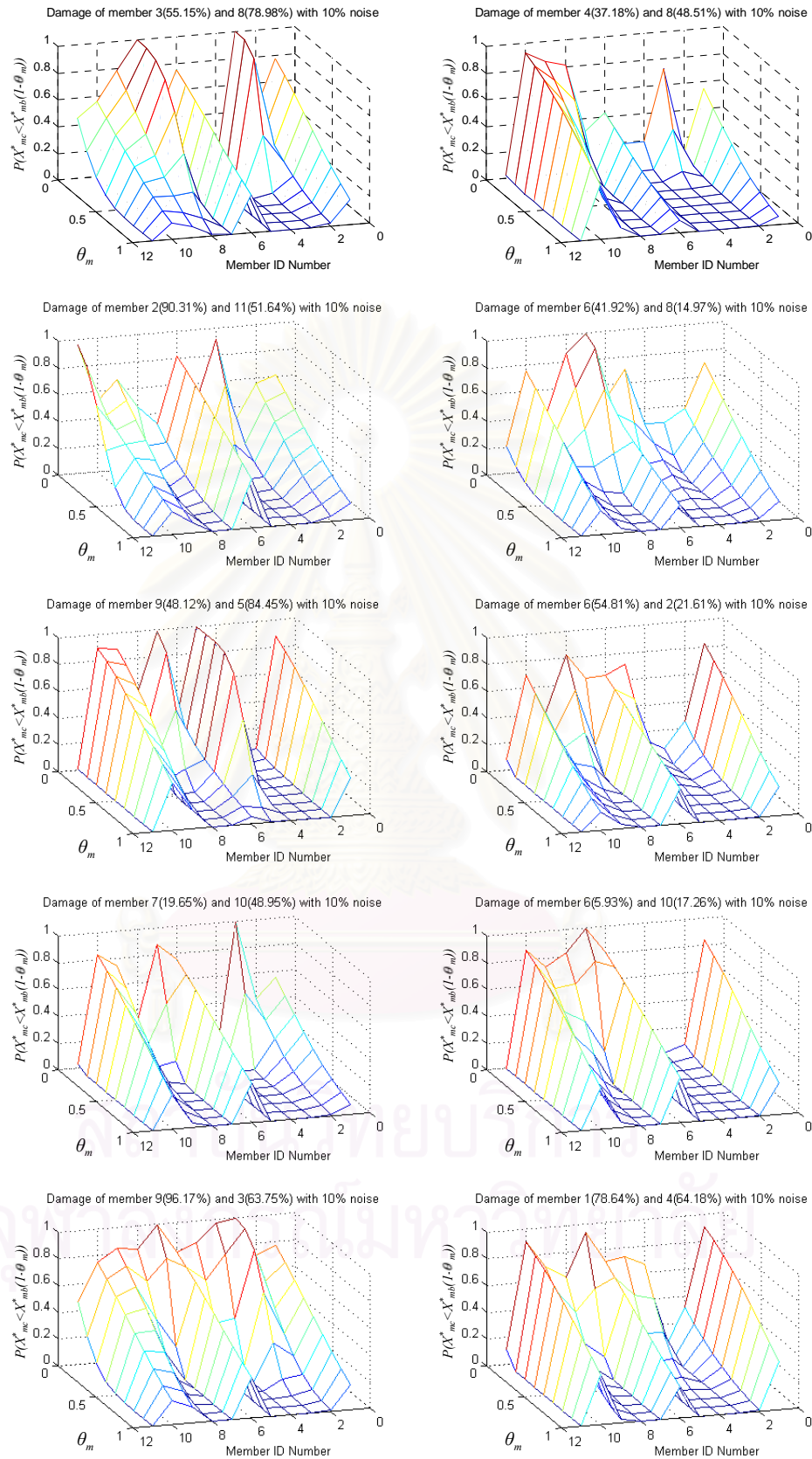
Figure 3.67 Probability distribution with respect to different levels of damage for the two-damaged-members cases using the sensitivity-based method and ROEE algorithm with 10% noisy measurements.
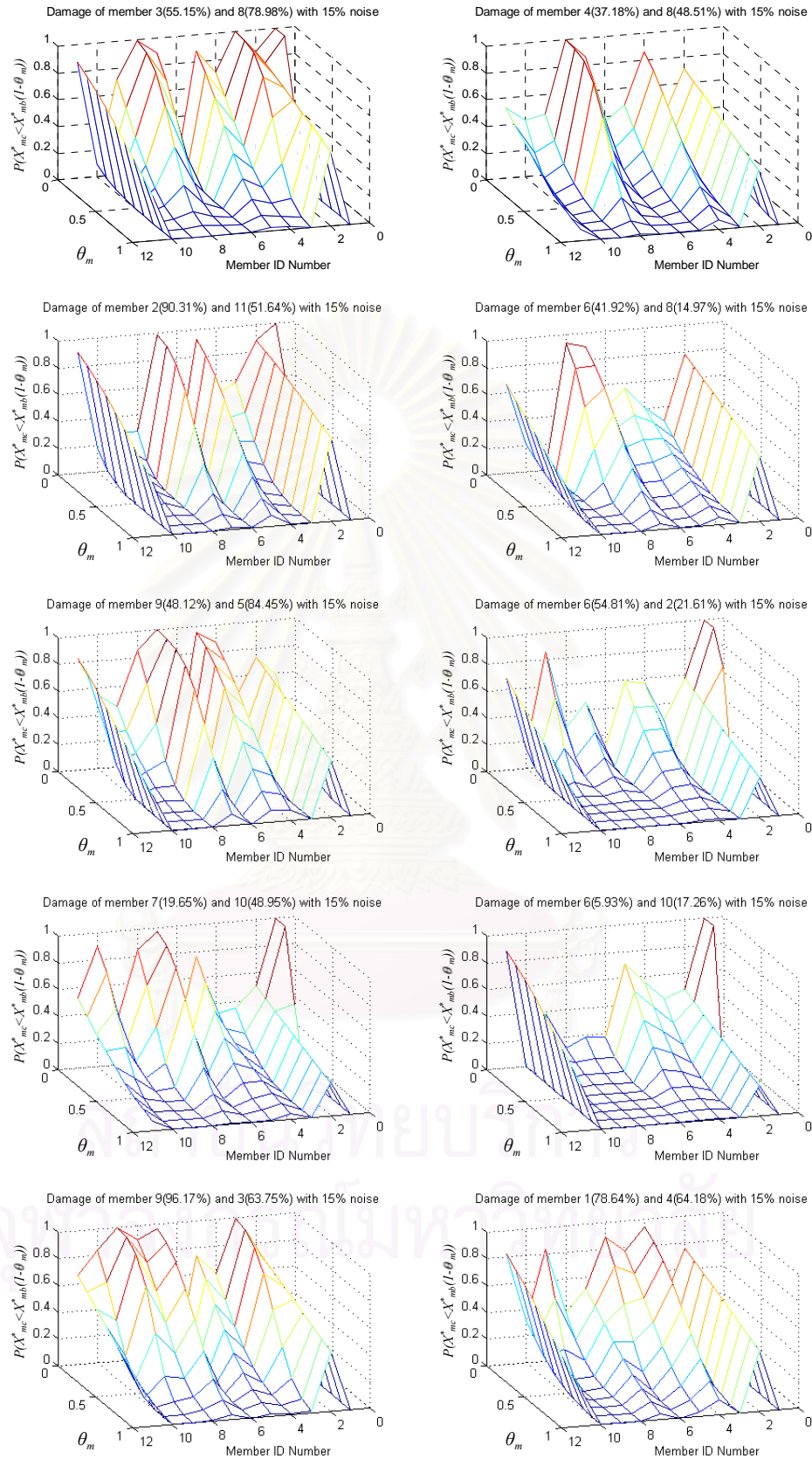
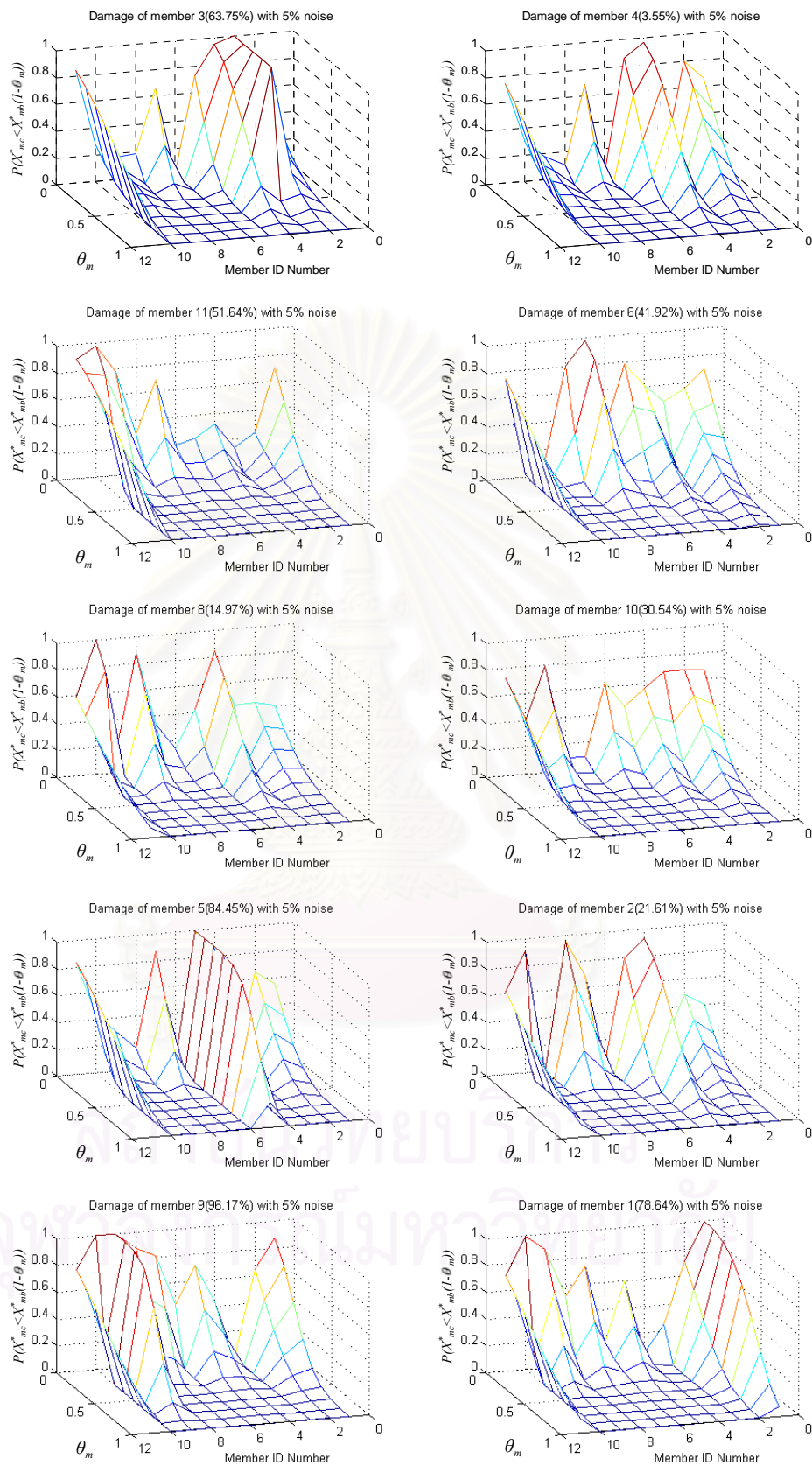Figure 3.68 Probability distribution with respect to different levels of damage for the two-damaged-members cases using the sensitivity-based method and ROEE algorithm with 15% noisy measurements.
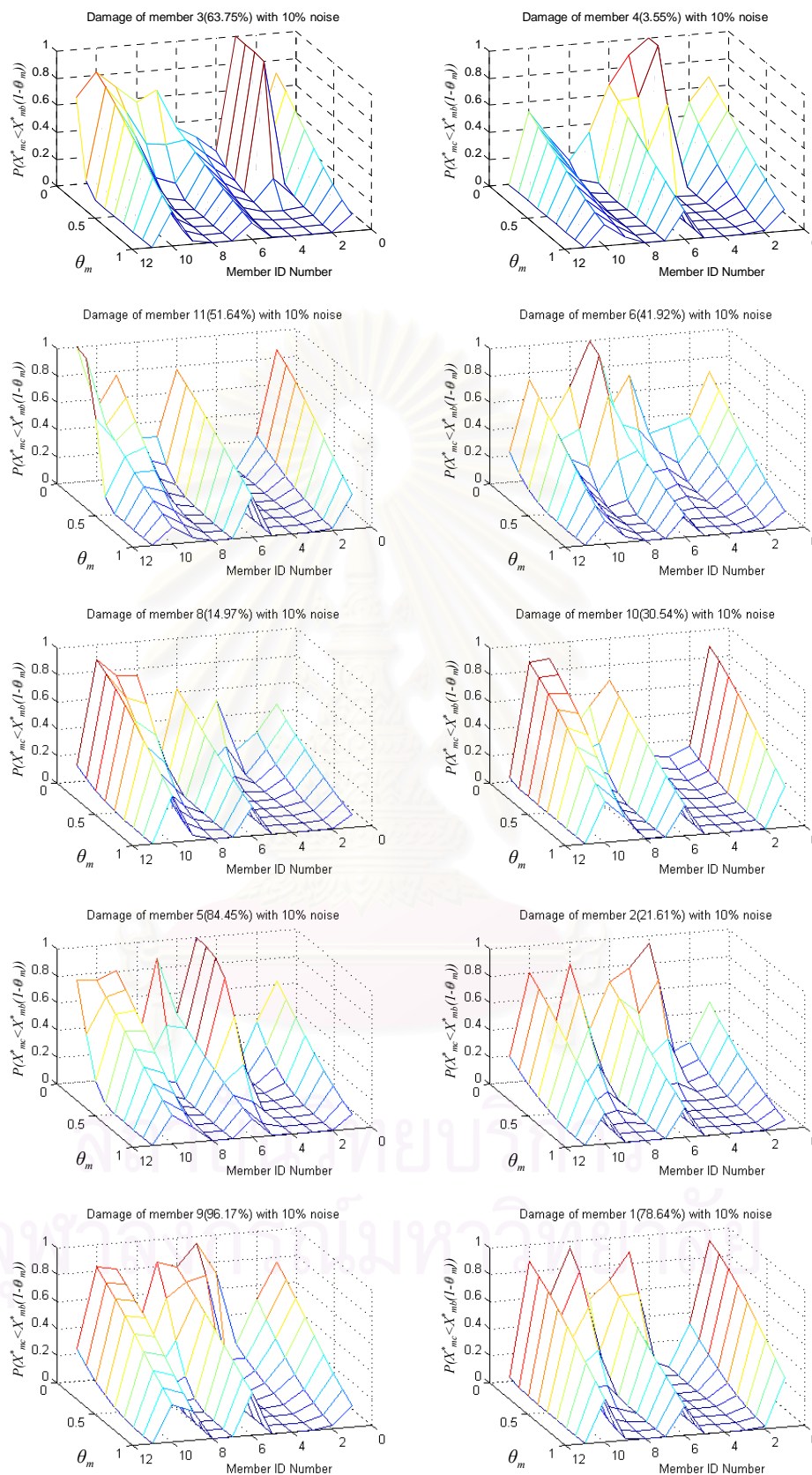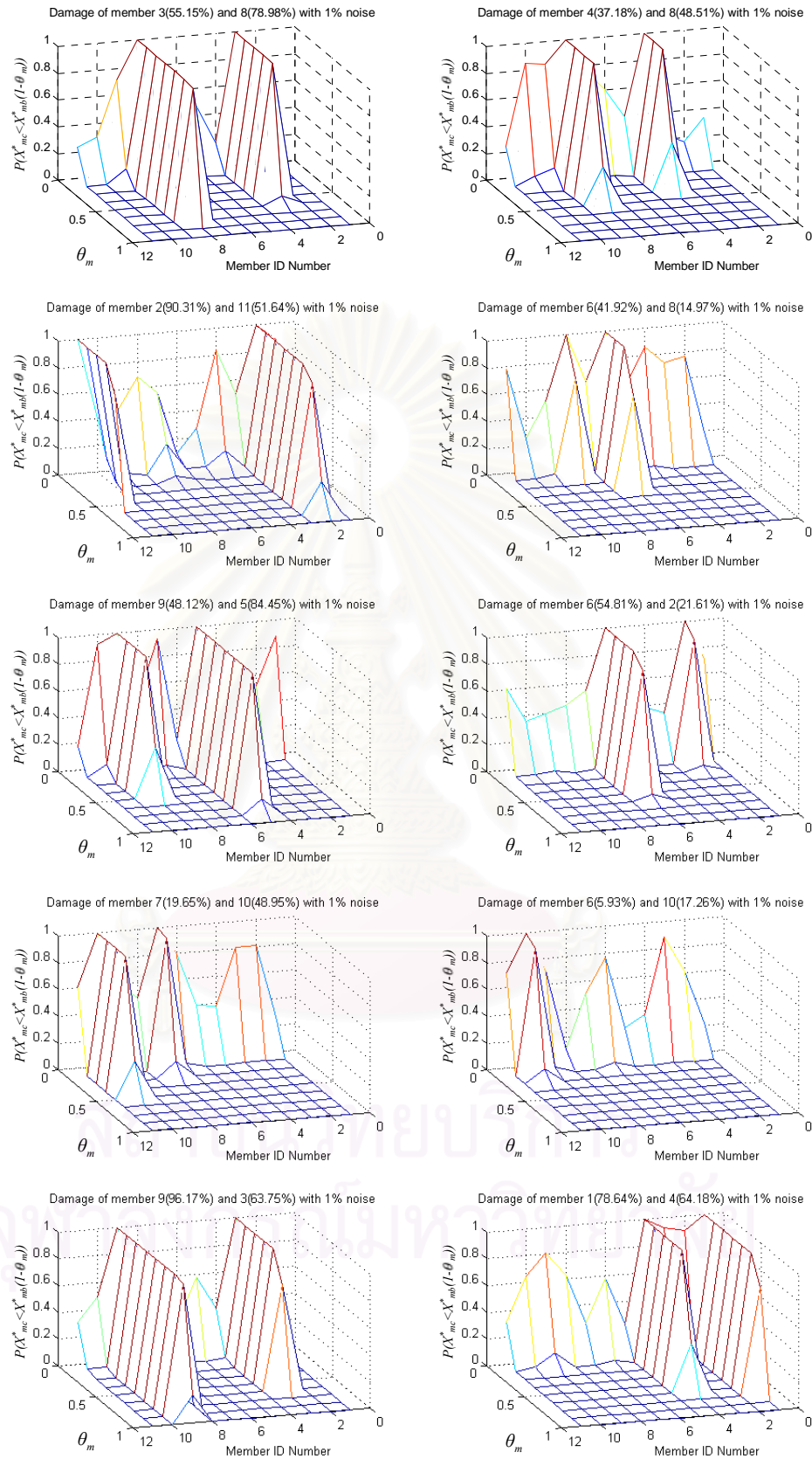
Figure 3.69 Probability distribution with respect to different levels of damage for the two-damaged-members cases using the optimum sensitivity-based method and ROEE algorithm with 1% noisy measurements.
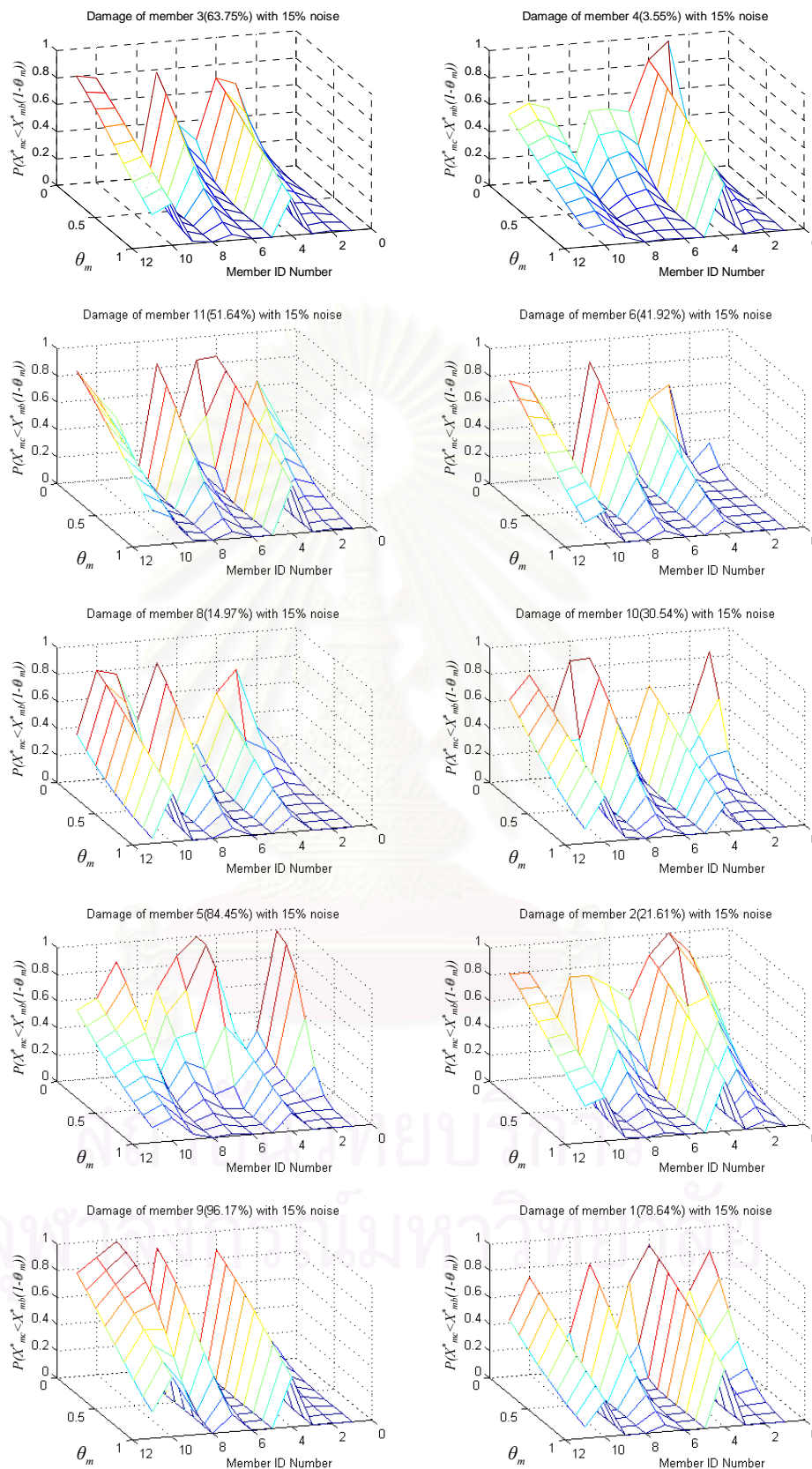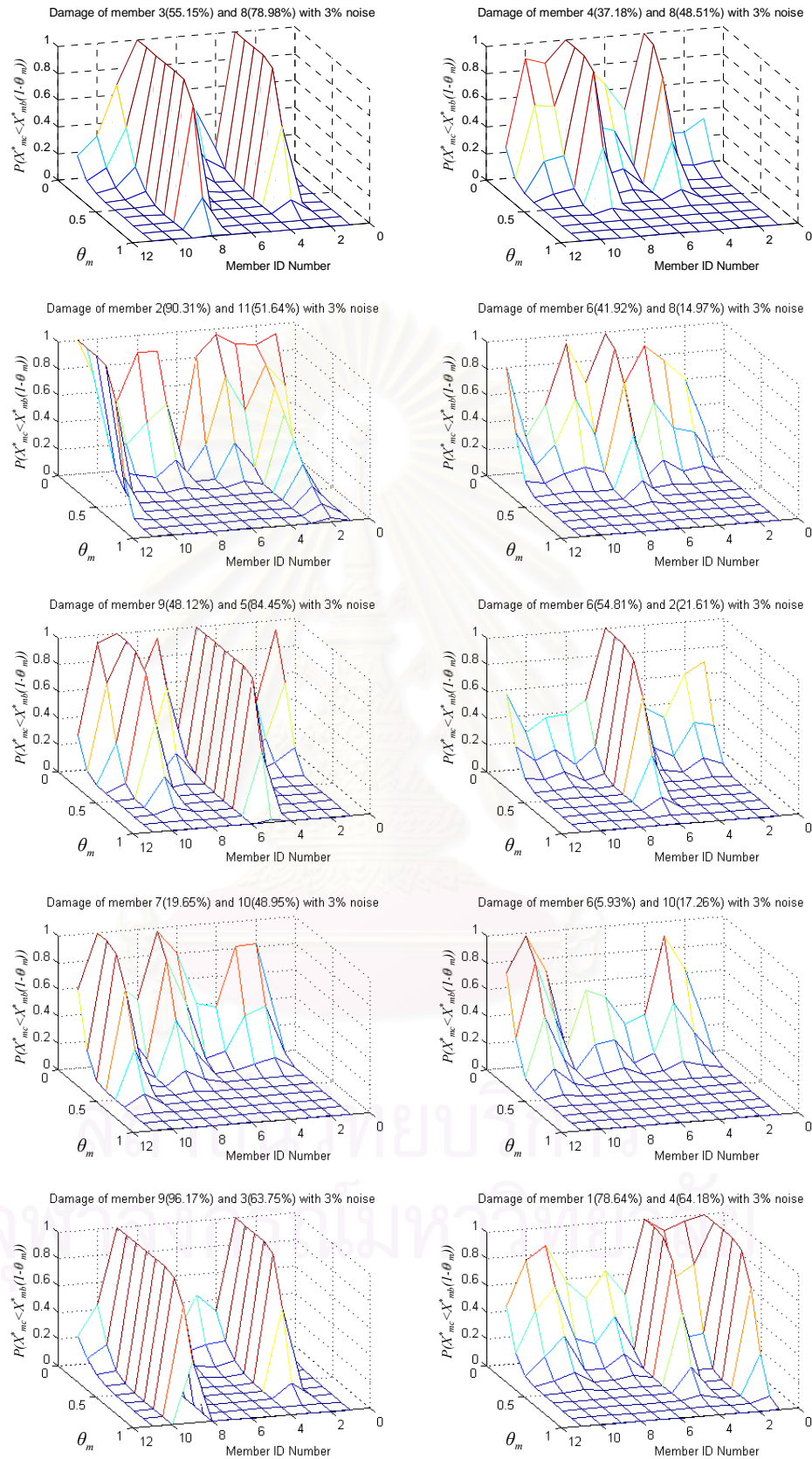
Figure 3.70 Probability distribution with respect to different levels of damage for the two-damaged-members cases using the optimum sensitivity-based method and ROEE algorithm with 3% noisy measurements.
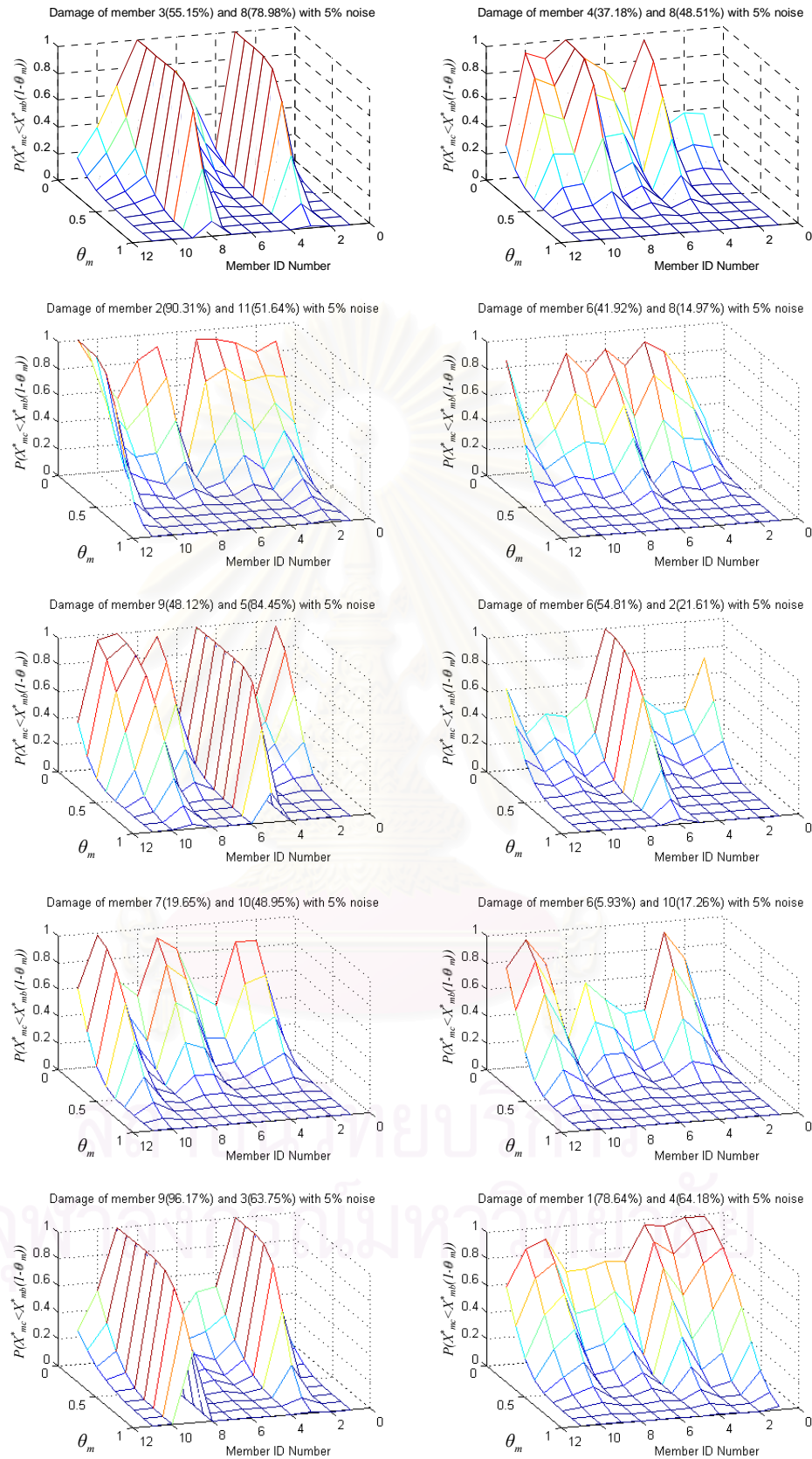
Figure 3.71 Probability distribution with respect to different levels of damage for the two-damaged-members cases using the optimum sensitivity-based method and ROEE algorithm with 5% noisy measurements.
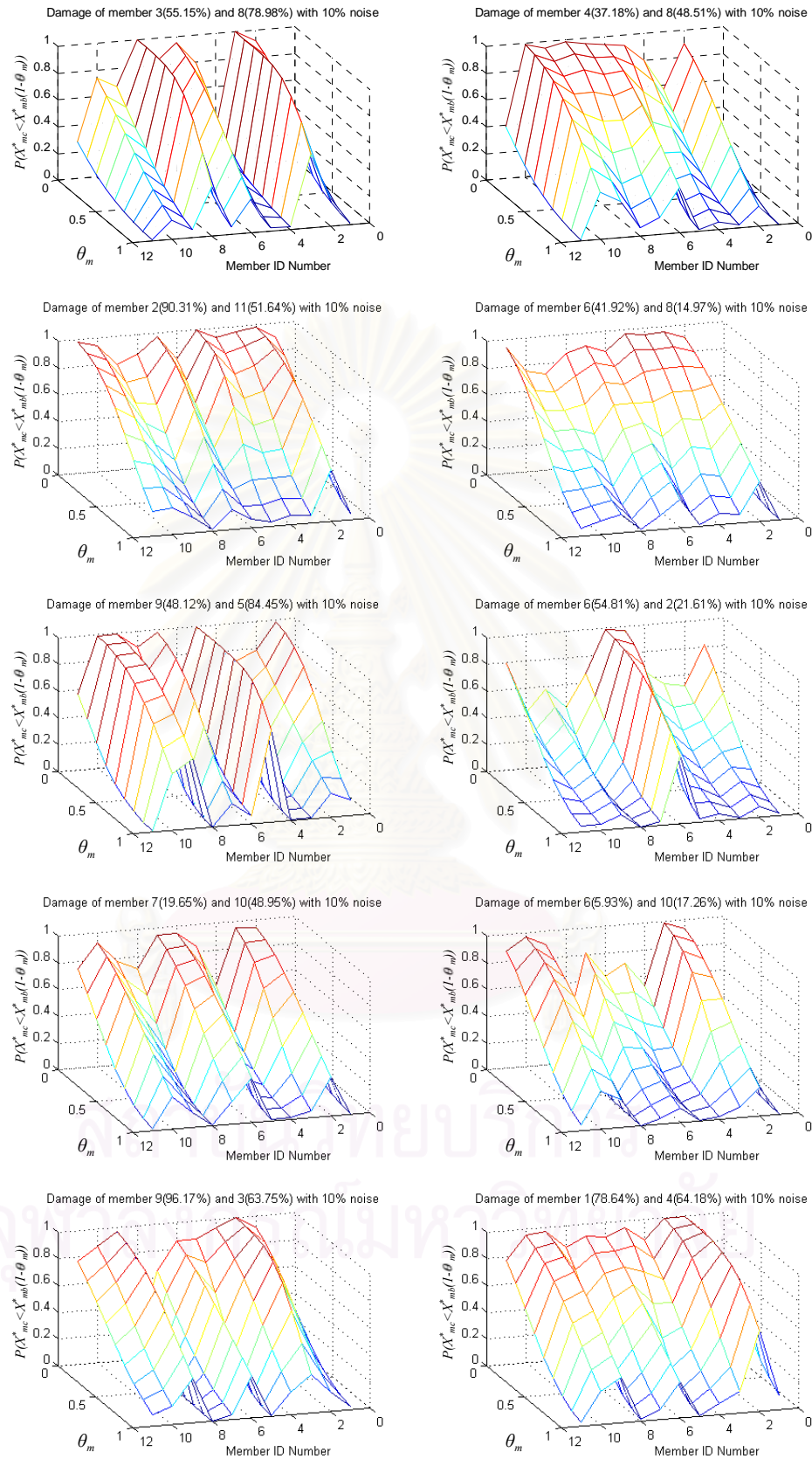
Figure 3.72 Probability distribution with respect to different levels of damage for the two-damaged-members cases using the optimum sensitivity-based method and ROEE algorithm with 10% noisy measurements.
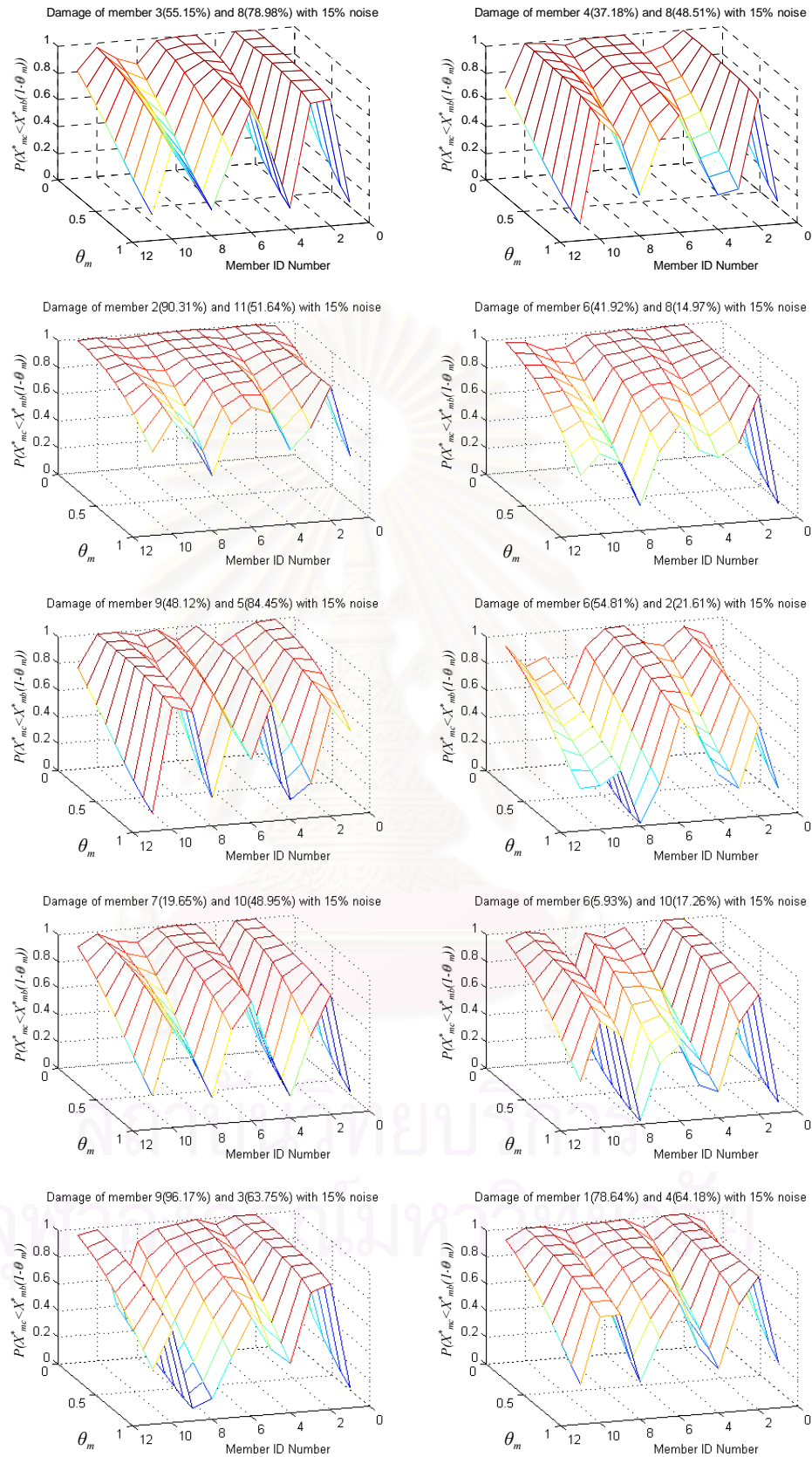
Figure 3.73 Probability distribution with respect to different levels of damage for the two-damaged-members cases using the optimum sensitivity-based method and ROEE algorithm with 15% noisy measurements.
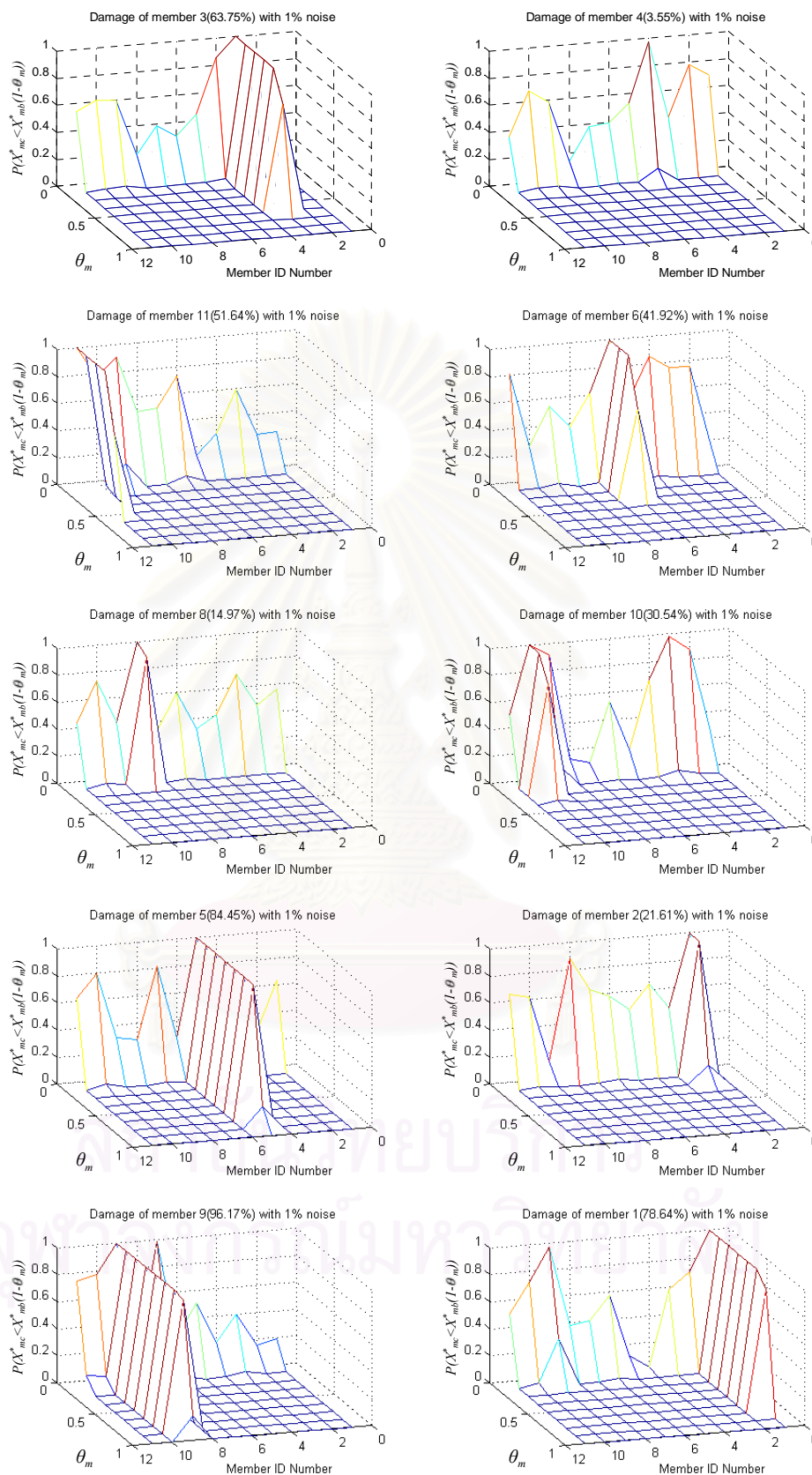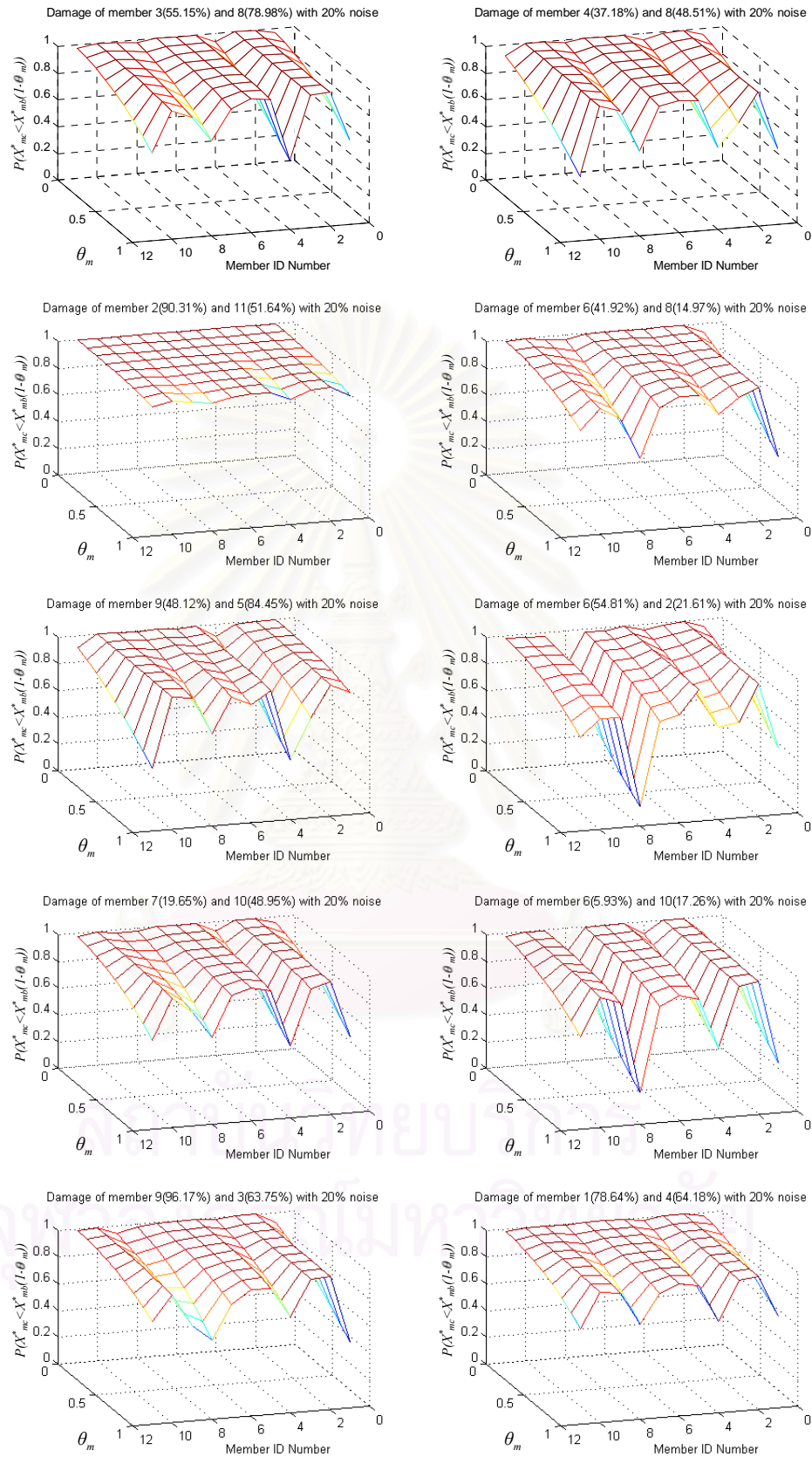
Figure 3.74 Probability distribution with respect to different levels of damage for the two-damaged-members cases using the optimum sensitivity-based method and ROEE algorithm with 20% noisy measurements.

3.4 Chapter Summary

The damage assessment procedure developed in the previous chapter has been tested with the single-damaged-member cases and the two-damaged-member cases of 10 different simulated damage cases for a simply supported truss structure. Through simulation studies, the procedure of assessing damage in the presence of the measurement noise was illustrated. To account for the sensitivity of the parameter estimates to the measurement noise, we adopt the technique of statistical parameter estimation. In particular, we use three different methods of statistical parameter estimation—the Monte Carlo simulation method, the sensitivity-based method and the optimum sensitivity-based method—to obtain the statistical distribution of the parameter estimates that is used as an input to the statistical damage assessment algorithm. Evaluation of the statistical distribution of the parameter estimates at the potential damage locations has proved reliable as a method for assessing whether damage is detectable above the noise in the measurements. From the simulation results, it is concluded that the proposed algorithm can assess damage effectively at low levels of noise in the measurements. For higher levels of noise in the measurements, there are always cases where actually damaged elements are identified as undamaged or actually undamaged elements are identified as damaged. However, the results have been shown to improve dramatically when the level of noise in the measurements decreases. In addition to the level of noise in the measurements, the severity of the damage in the structural components also limits the ability of the proposed algorithm to assess damage in a structural system.

From the simulation results, it can be concluded that the performance of the proposed statistical damage assessment method is improved by using the regularization method on the parameter estimation problem (ROEE) for all of the statistical parameter estimation schemes considered. Furthermore, the ROEE algorithm is more effective when using with the optimum sensitivity-based method compared to when using with the Monte Carlo simulation method and the sensitivity-based method.

CHAPTER 4

STATISTICAL SIMULATION STUDY—A BRIDGE TRUSS

4.1 Introduction

In the previous chapter, we have used different statistical parameter estimation algorithms in conjunction with the proposed damage assessment scheme to quantify damage in a simple-support bridge truss by using 10 simulated damage scenarios. In this chapter, we use the same truss structure in our simulation studies, but a larger number of damage cases is considered to obtain a clearer picture of the performance of the proposed algorithm in the statistical sense. A statistical identification error (SIE) is devised to quantify the level of accuracy of the damage assessment algorithm. We consider three distinct cases of damage: the single-damaged-member cases, the two-damaged-member cases, and the three-damaged-member cases. For each of these damage cases, we generate 100 different damage scenarios by randomly varying the location and the severity of damage.

As for the previous chapter, we examine three methods of statistical parameter estimation; i.e., the Monte Carlo simulation method, the sensitivity-based method, and the optimum sensitivity-based method. We use these methods in conjunction with the output error estimator (OEE) and the regularized output error estimator (ROEE) to investigate the performance of the present statistical damage assessment scheme from using different statistical evaluation schemes and estimators by using the statistical identification error (SIE) of the damaged member parameters.

Through statistical simulation studies, the procedures of each of the investigated algorithms in assessing damage by using the plot of the SIE value of the damage member parameters and the probability of successfully detecting damage with respect to different levels of noise in the measurements are illustrated.

4.2 Statistical Identification Error

The performance of the investigated algorithms is evaluated by using a statistical identification error (SIE) index. For the single-damaged-member cases, the SIE index for the damaged member m is defined as

$$SIE_m = \sqrt{\left(1 - \frac{\overline{x}_{mb}}{\hat{x}_{mb}}\right)^2 + \left(1 - \frac{\overline{x}_{mc}}{\hat{x}_{mc}}\right)^2 + \left(1 - \frac{(\overline{x}_{mb} - \overline{x}_{mc})}{(\hat{x}_{mb} - \hat{x}_{mc})}\right)^2 + \left(\frac{\sigma_{x_{mb}}}{\hat{x}_{mb}}\right)^2 + \left(\frac{\sigma_{x_{mb}}}{\hat{x}_{mb}}\right)^2 + \left(\frac{\sigma_{(x_{mb}-x_{mc})}}{\hat{x}_{mb}}\right)^2}$$

$$(4.1)$$

in which

$\hat{x}_{mb}$ is the actual value of the baseline parameter for member m;

$\hat{x}_{mc}$ is the actual value of the current parameter for member m;

$\overline{x}_{mb}$ is the mean of the baseline parameter estimates for member m;

$\overline{x}_{mc}$ is the mean of the current parameter estimates for member m;

$\sigma_{x_{mb}}$ is the standard deviation of the baseline parameter estimates for member m;

$\sigma_{x_{mc}}$ is the standard deviation of the current parameter estimates for member m;

and $\sigma_{(x_{mb}-x_{mc})}$ is the standard deviation of the changes of the value of the current parameter estimate from the baseline parameter estimate for member m.

The level of success of the damage assessment is identified by the SIE value of the damaged members. Note that equation (4.1) consists of six terms: (1) deviation of the baseline parameter estimate from the actual value; (2) deviation of the current parameter estimate from the actual value; (3) deviation of the estimated change of the parameter values from the actual change; (4) the scatter of (1); (5) the scatter of (2); and (6) the scatter of (3). The assessment of damage is considered effective when the SIE value approaches zero. For the current study we use the plot of SIE index with

respect to the levels of noise in the measurements to illustrate the performance of each of the algorithms under consideration.

For the two-damaged-member cases and three-damaged-member cases, the SIE values are computed, respectively, as

$$SIE_2 = \frac{(SIE_l + SIE_m)}{2}; \quad \text{and} \quad SIE_3 = \frac{(SIE_l + SIE_m + SIE_n)}{3} \tag{4.2}$$

whereas the subscripts l, m, and n represent the quantity being associated with damaged members l, m, and n, respectively.

4.3 Simulation Studies

In our simulation studies, we investigate the performance of each of the investigated algorithms in assessing damage by plotting the SIE value with respect to different levels of noise in the measurements. The key objective of the present study is to examine the efficacy of using the regularization scheme to improve the performance of the statistical damage assessment scheme. Again, we use synthetic measurements that are generated in accord with equation (2.35). Three statistical parameter estimation methods, i.e. the Monte Carlo simulation method, the optimum sensitivity-based method and the sensitivity-based method are used in conjunction with the OEE and ROEE algorithms to obtain the required statistics of parameter estimates for the damage assessment algorithm. The same truss structure of Chapter 3 is used as our model problem.

The simulation studies conducted in this section consist of single-damaged-member cases, two-damaged-member cases and three-damaged-member cases. As in Chapter 3, for the single-damaged-member cases the damage of the structure is represented by a reduction of the stiffness of a single structural member. For the two-damaged-member and three-damaged-member cases, the damage is due to the stiffness reduction of two and three structural members, respectively. For each of the

damage cases considered, we generate 100 different damage scenarios by randomly varying the location and the severity of damage.

4.3.1 Single-Damaged-Member Cases

The single-damaged-member cases investigated herein consist of 100 different combinations of the location and the severity of damage that are randomly generated. As mentioned previously, we use the Monte-Carlo simulation method, the optimum sensitivity-based method and the sensitivity-based method in conjunction with the OEE and the ROEE algorithms for the statistical parameter estimation from noisy responses. The performance of each algorithm in the statistical damage assessment scheme is investigated by examining the SIE values. The level of success in the detection of damage is indicated by the probability of success in detecting damage P_s, which is defined as

$$P_s = \frac{\sum_{i=1}^{100} N_i^S}{\sum_{i=1}^{100} N_i^{AD}} \tag{4.3}$$

in which

N_i^S is the number of the successfully detected damages for damage case i;

and N_i^{AD} is the number of the actual damages for damage case i.

The accuracy of the statistical evaluation of the performance of the proposed damage assessment algorithm can improve as the number of damage cases, or the sample size, increases. This aspect of the algorithm is investigated by examining the variation of the average SIE values associated with the successfully-detected damaged members for all damage scenarios which are obtained from using different numbers of simulated damage cases. Figure 4.1 shows the results from using the Monte-Carlo
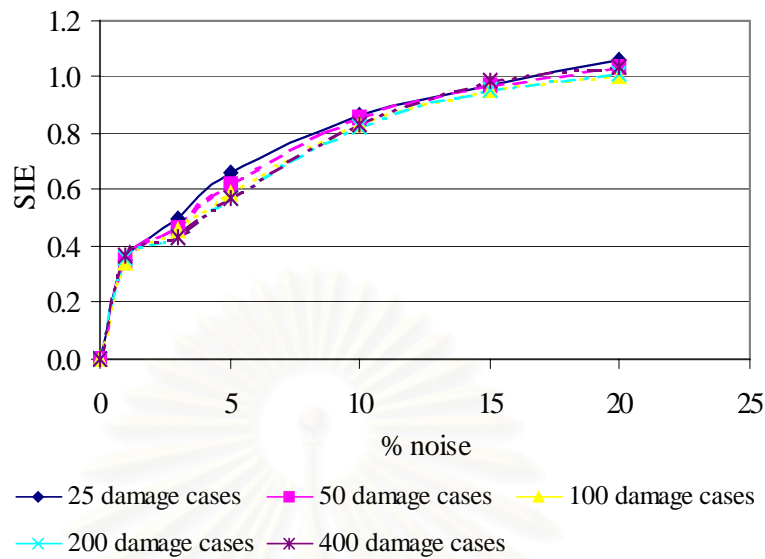
Figure 4.1 Variation of the average SIE values associated with the successfully-detected damaged members with respect to different levels of noise in the measurements using the Monte Carlo simulation method in conjunction with the ROEE algorithm for different numbers of damage cases.

simulation method in conjunction with ROEE with respect to different levels of noise in the measurements for different numbers of damage cases. It is seen from the figure that 100 samples are sufficient to carry out the performance assessment in the range of noise levels considered. Therefore, we use 100 damage cases in order to evaluate the performance of the statistical damage assessment in our simulation studies.

Figure 4.2 summarizes the performance of the investigated algorithms with the increasing level of noise for the single-damaged-member cases. Figures 4.2(a), 4.2(c) and 4.2(e) on the left column show the results from using the OEE algorithm in conjunction with the Monte-Carlo simulation method, the optimum sensitivity-based method and the sensitivity-based method, respectively. On the right column, figures 4.2(b), 4.2(d) and 4.2(f) show the results from using the ROEE algorithm in conjunction with different statistical parameter estimation methods in the same order. Note that each of these plots show the average SIE values for the successfully-detected damaged members in all of the damage cases considered.
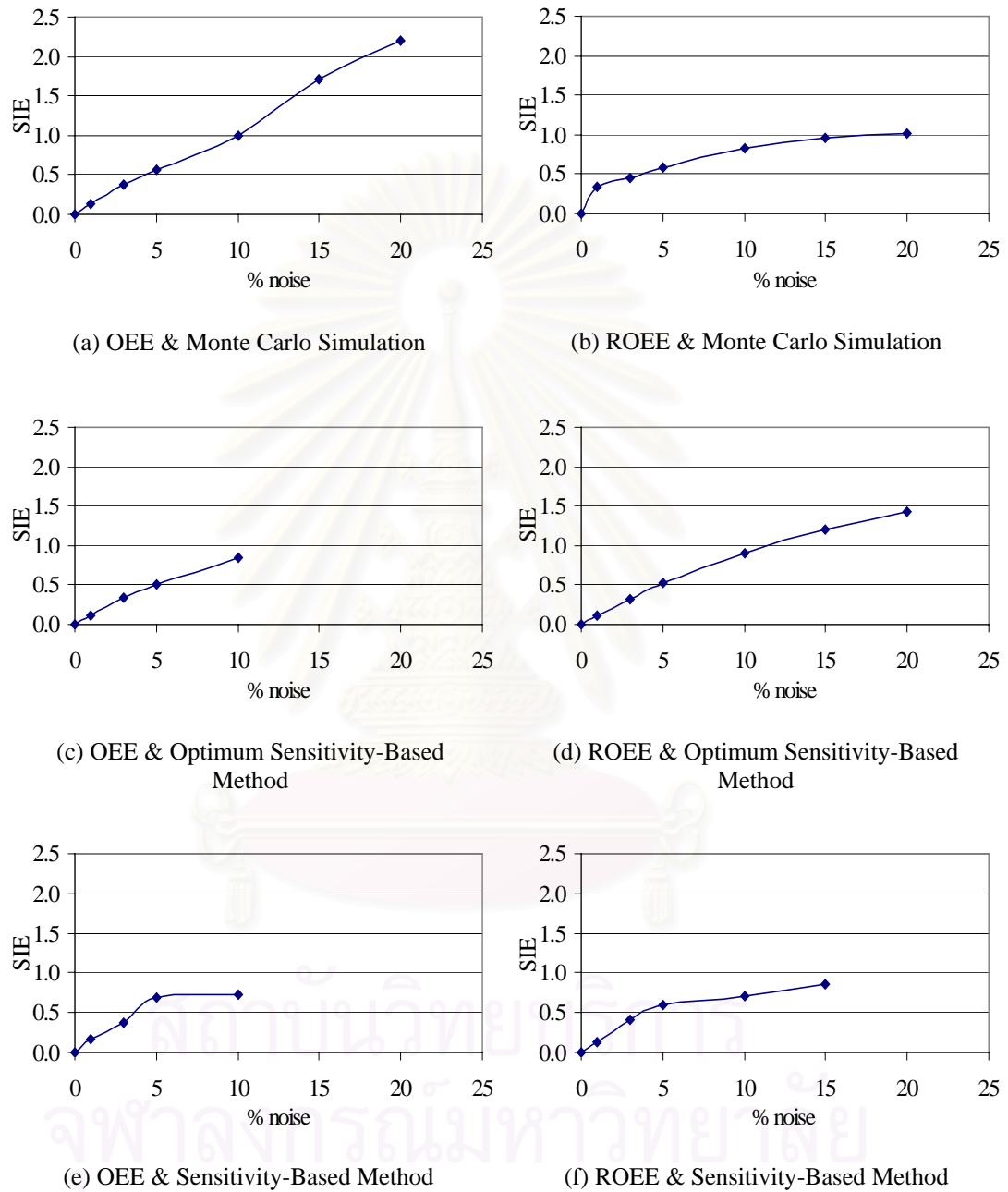
Figure 4.2 Variation of the average SIE values associated with the successfully-detected damaged members with respect to different levels of noise in the measurements for 100 single-damaged-member cases using different methods of statistical parameter estimation with the OEE and ROEE algorithms.

It is seen from the illustration that the average SIE value increases as the level of noise in the measurements increases. The results from using the three statistical parameter estimation methods with the OEE algorithm show that the maximum level of noise permitting a damage assessment is 10% for the optimum sensitivity-based method and the sensitivity-based method, and 20% for the Monte Carlo simulation method. With the ROEE method, the maximum level of noise is increased to 20% for the Monte Carlo simulation and the optimum sensitivity-based methods. For the sensitivity-based method, the maximum level of noise is increased to 15%. Moreover, the performance of the proposed damage assessment method is somewhat stabilized by the regularization effect when using the Monte Carlo simulation method as evident from the lower, and less fluctuated, SIE values.

Figure 4.3 summarizes the probability of success in detecting damage with respect to different levels of noise in the measurements for the single-damaged-member cases. The format of the illustration follows Figure 4.2 in which the left and right columns show the results from using the OEE and the ROEE algorithms, respectively, in conjunction with different statistical parameter estimation schemes.

The results from using all three statistical parameter estimation methods with the OEE and the ROEE algorithms show that the probability of success in detecting damage decreases as the level of noise in the measurements increases. The decrease in the probability of success in detecting damage is more gradual for the results using the ROEE algorithm. The probability of failing to detect damage increases as the level of noise in the measurements increases. Again, we observe a more gradual increase in the probability values for the results from using the ROEE algorithm.

Figure 4.4 is the plot of the distribution of the SIE values which success in detecting damage with respect to different levels of noise in the measurements for each of the single-damaged-member cases. In the illustration, the left and right columns show the results from using the OEE and the ROEE algorithms, respectively, in conjunction with different statistical parameter estimation schemes.

It is seen from the illustration that the variation of the SIE values at each noise level is small when the level of noise in the measurements is low due to high success in detecting damage. The variation of the SIE values is large when the level of noise
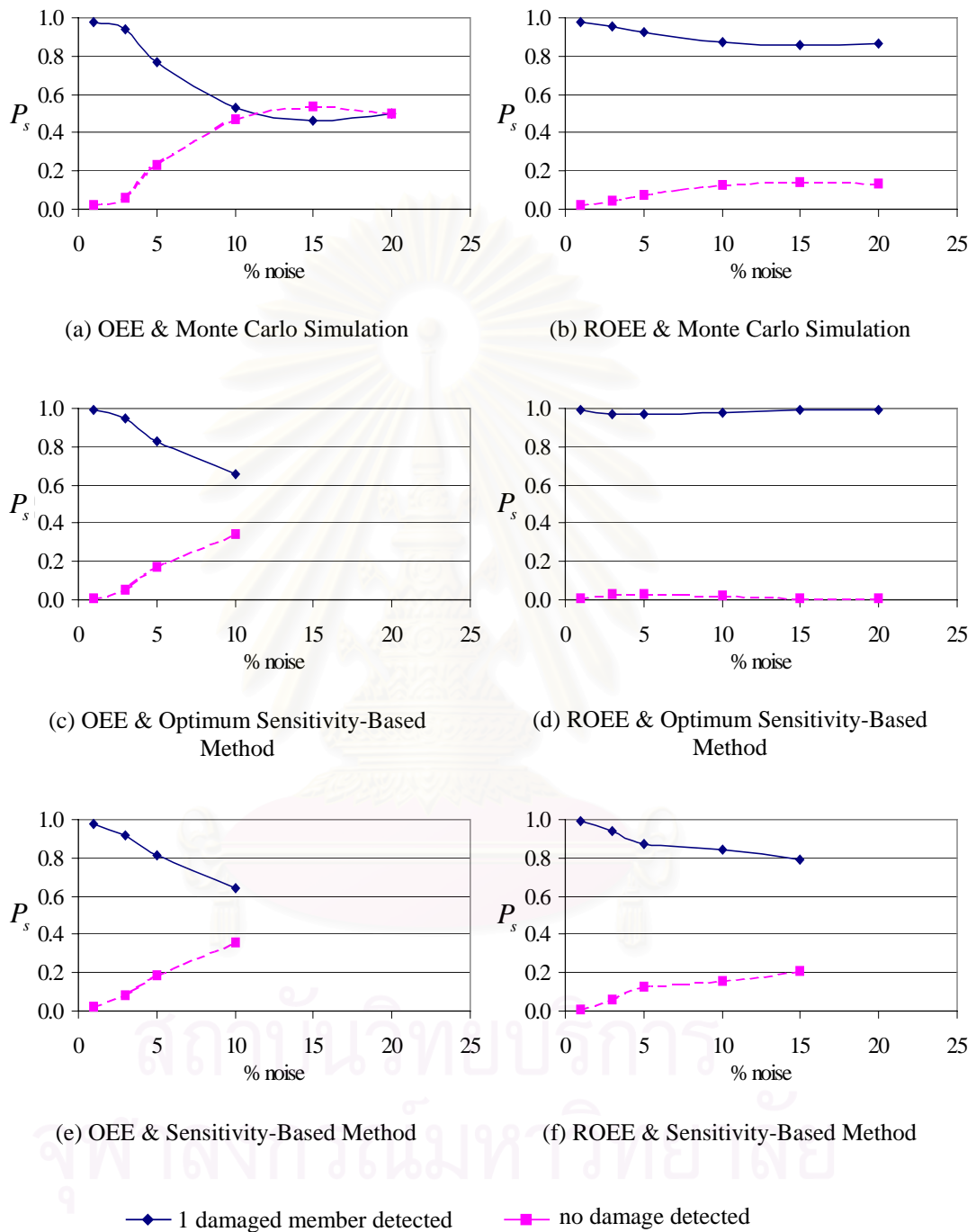
Figure 4.3 Probability of success in detecting damage with respect to different levels of noise in the measurements for 100 single-damaged-member cases using different methods of statistical parameter estimation with the OEE and ROEE algorithms.
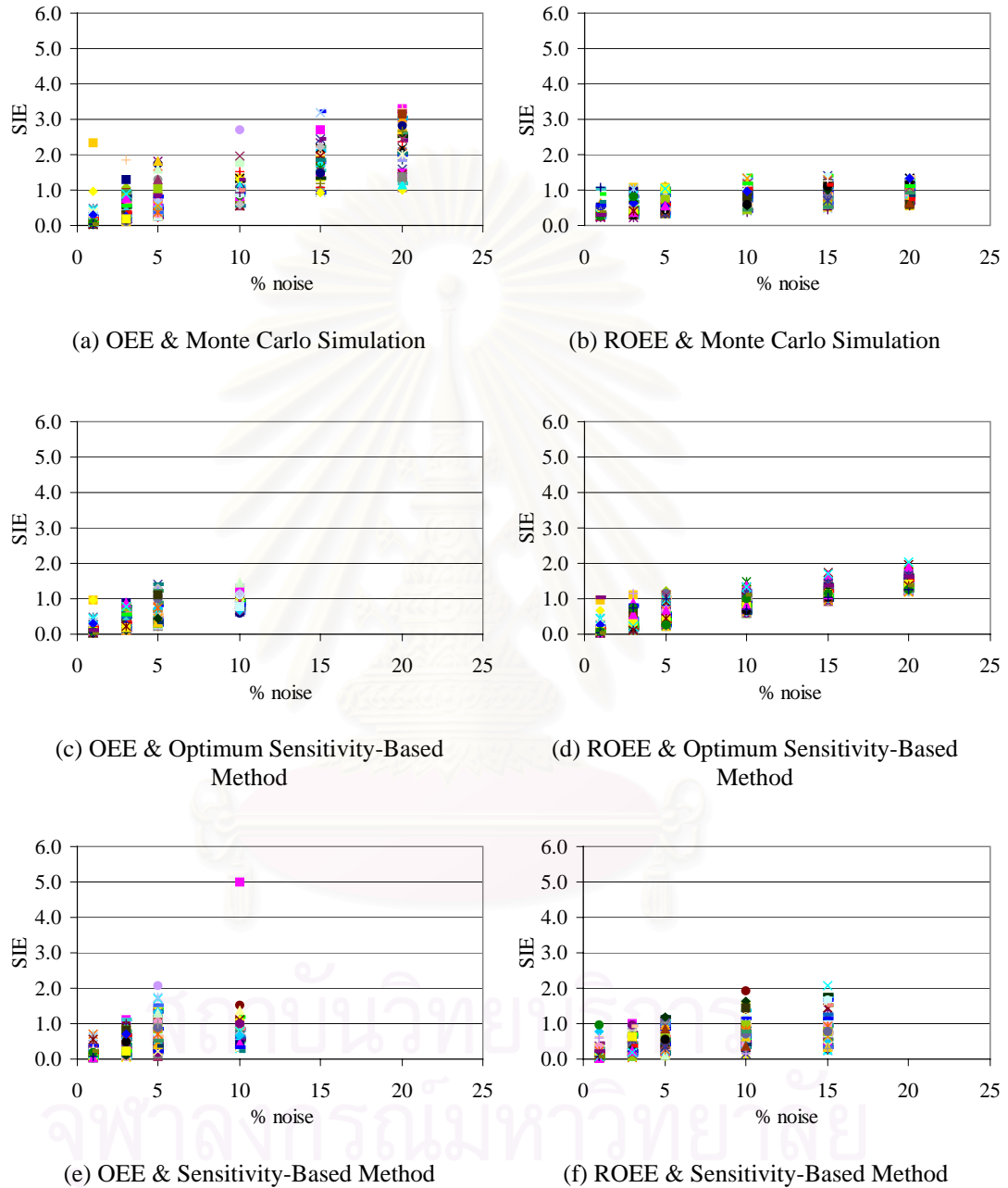
Figure 4.4 Variation of the SIE values for each of the successfully-detected damaged members with respect to different levels of noise in the measurements from 100 single-damaged-member cases using different methods of statistical parameter estimation with the OEE and ROEE algorithms.

is high due to low success in detecting damage. Moreover, the fluctuation in the performance of the proposed damage assessment method is somewhat stabilized by the regularization effect as evident from the smaller variation of the SIE values.

4.3.2 Two-Damaged-Member Cases

The two-damaged-member cases investigated herein consist of 100 different combinations of the location and the severity of damage that are randomly generated. As for the single-damaged-member cases, three statistical parameter estimation methods, i.e. the Monte-Carlo simulation method, the optimum sensitivity-based method and the sensitivity-based method, are used in conjunction with the OEE and the ROEE algorithms to investigate the performance of the proposed damage assessment scheme. The SIE index, as computed from equation (4.2), is used to quantify this performance. The level of success of the damage detection is indicated by the value of P_s, which is the ratio of the number of damages detected to the number of actual damages in the structure. We plot the average SIE values, the P_s values, and the distribution of the SIE values for the 100 damage cases under consideration with respect to different levels of noise in the measurements for each of the investigated algorithms.

Figure 4.5 illustrates the overall performance of the presented algorithms with respect to the level of the measurement noise for the two-damaged-member cases. The format of the illustration follows Figure 4.2 in which the left and right columns show the results from using the OEE and the ROEE algorithms, respectively, in conjunction with different statistical parameter estimation schemes. Note that the SIE values in Figure 4.5 are plotted as the average SIE values for the successfully-detected damaged members for the cases in which one and two damaged members are detected as well as for all of the 100 damage cases.

The same sort of results as for the single-damaged-member cases are again seen for the two-damage-member cases. The SIE value increases as the level of noise in the measurements increases. For all of the investigated damage cases, the ROEE method out-performs the OEE method in the assessment of damage using all the
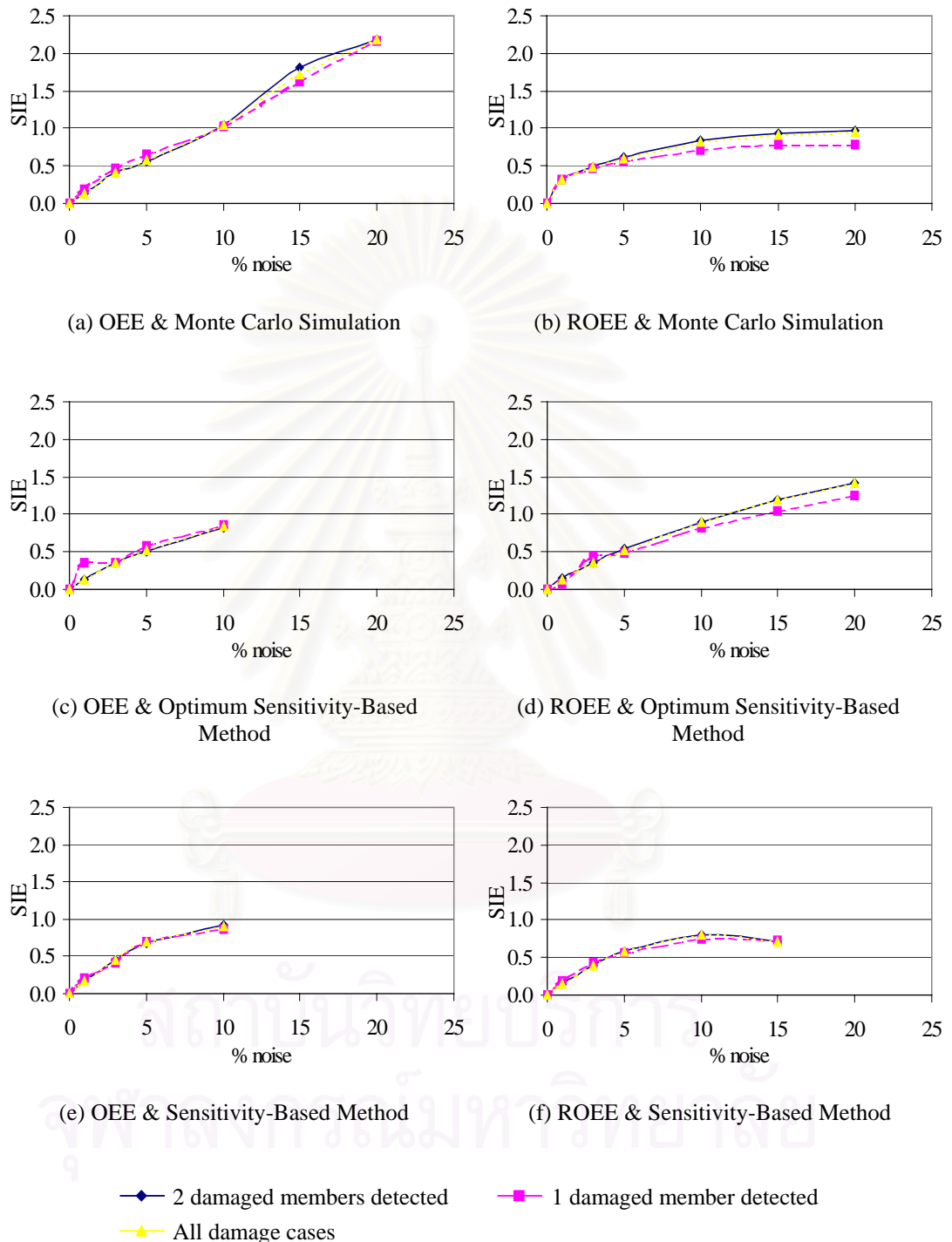
Figure 4.5 Variation of the average SIE values for the successfully-detected damaged members with respect to different levels of noise in the measurements for the cases in which one and two damaged members are detected, and for all 100 damage cases using different methods of statistical parameter estimation with the OEE and ROEE algorithms.

statistical parameter estimation schemes considered with higher levels of measurement noise permitting a damage assessment.

Figure 4.6 summarizes the probability of success in detecting damage with respect to different levels of noise in the measurements for the two-damaged-member cases. The results from using all three statistical parameter estimation methods with the OEE and the ROEE algorithms show that the probability of success in detecting both damaged members decreases as the level of noise in the measurements increases. However, the probability distribution for the cases using the ROEE algorithm shows a more gradual decrease. Moreover, the probability of detecting only a single damaged member as well as the probability of detecting no damage at all increases with the level of noise in the measurements. Again, a more gradual increase is observed for the results from the ROEE algorithm.

Figures 4.7 and 4.8 show the distribution of the SIE values for the cases in which one damaged member and two damaged members are successfully detected, respectively, with respect to the level of noise in the measurements. It is seen from the illustration for all three statistical parameter estimation methods with the OEE algorithm that the variation of the SIE values is small at low levels of noise. This is due to the comparatively high success in detecting damage. However, the variation of the SIE values becomes quite large at higher levels of noise. The performance of the proposed damage assessment method is somewhat improved when the ROEE algorithm is used as evident from the smaller variation of the SIE values at all noise levels.

4.3.3 Three-Damaged-Member Cases

In this section, we investigate 100 damage cases in which three truss members are damaged. We randomly select the locations and the severities of damage for the truss. As for the previous cases, we examine three statistical parameter estimation methods, i.e. the Monte-Carlo simulation method, the optimum sensitivity-based method and the sensitivity-based method, in conjunction with the OEE and the ROEE algorithms for the proposed damage assessment scheme.

(a) OEE & Monte Carlo Simulation

(b) ROEE & Monte Carlo Simulation

(c) OEE & Optimum Sensitivity-Based Method

(d) ROEE & Optimum Sensitivity-Based Method

(e) OEE & Sensitivity-Based Method

(f) ROEE & Sensitivity-Based Method

— ♦ — 2 damaged members detected   — ■ — 1 damaged member detected
— ▲ — no damage detected
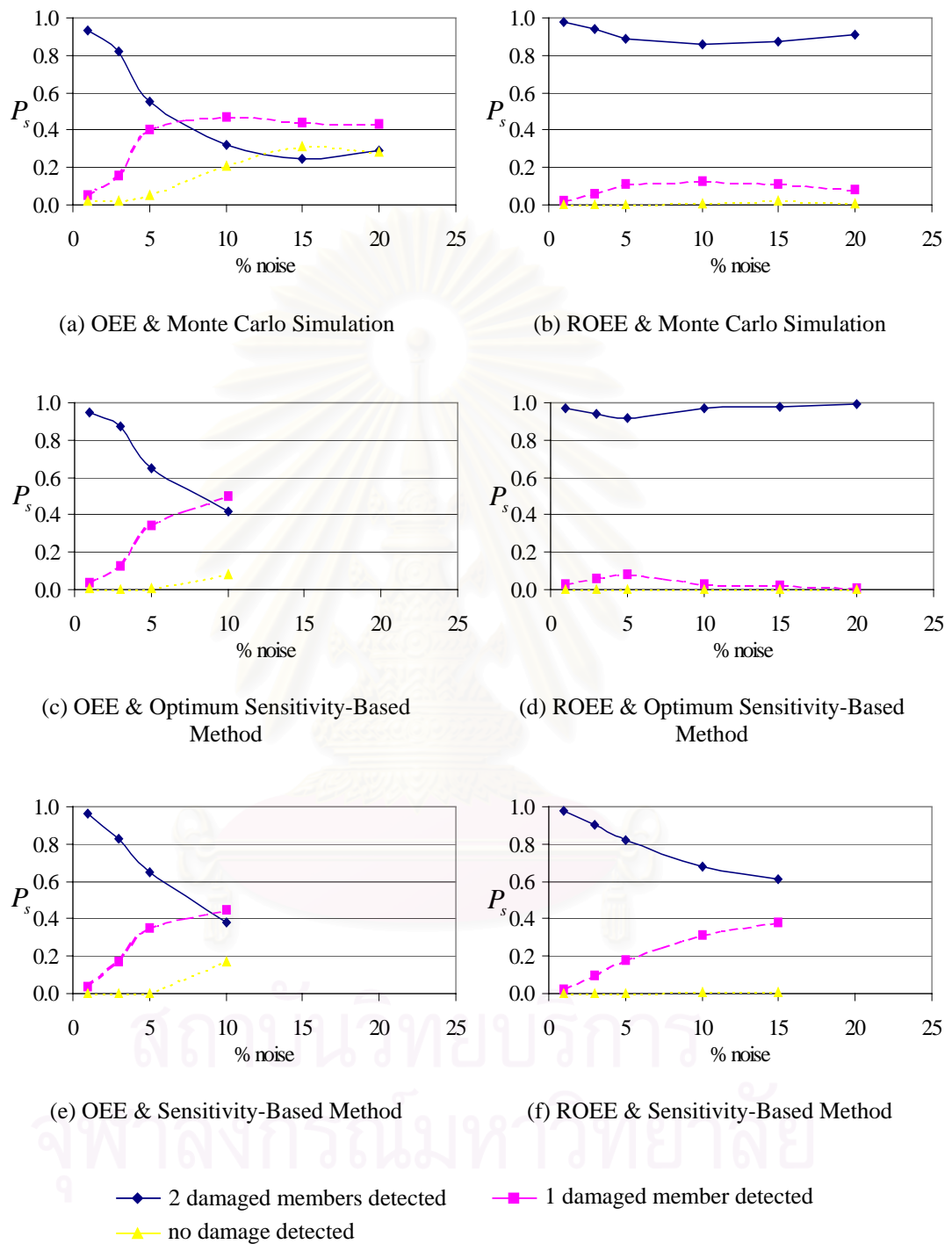
Figure 4.6 Probability of success in detecting damage with respect to different levels of noise in the measurements for 100 two-damaged-member cases using different methods of statistical parameter estimation with the OEE and ROEE algorithms.

(a) OEE & Monte Carlo Simulation

(b) ROEE & Monte Carlo Simulation

(c) OEE & Optimum Sensitivity-Based Method

(d) ROEE & Optimum Sensitivity-Based Method

(e) OEE & Sensitivity-Based Method

(f) ROEE & Sensitivity-Based Method
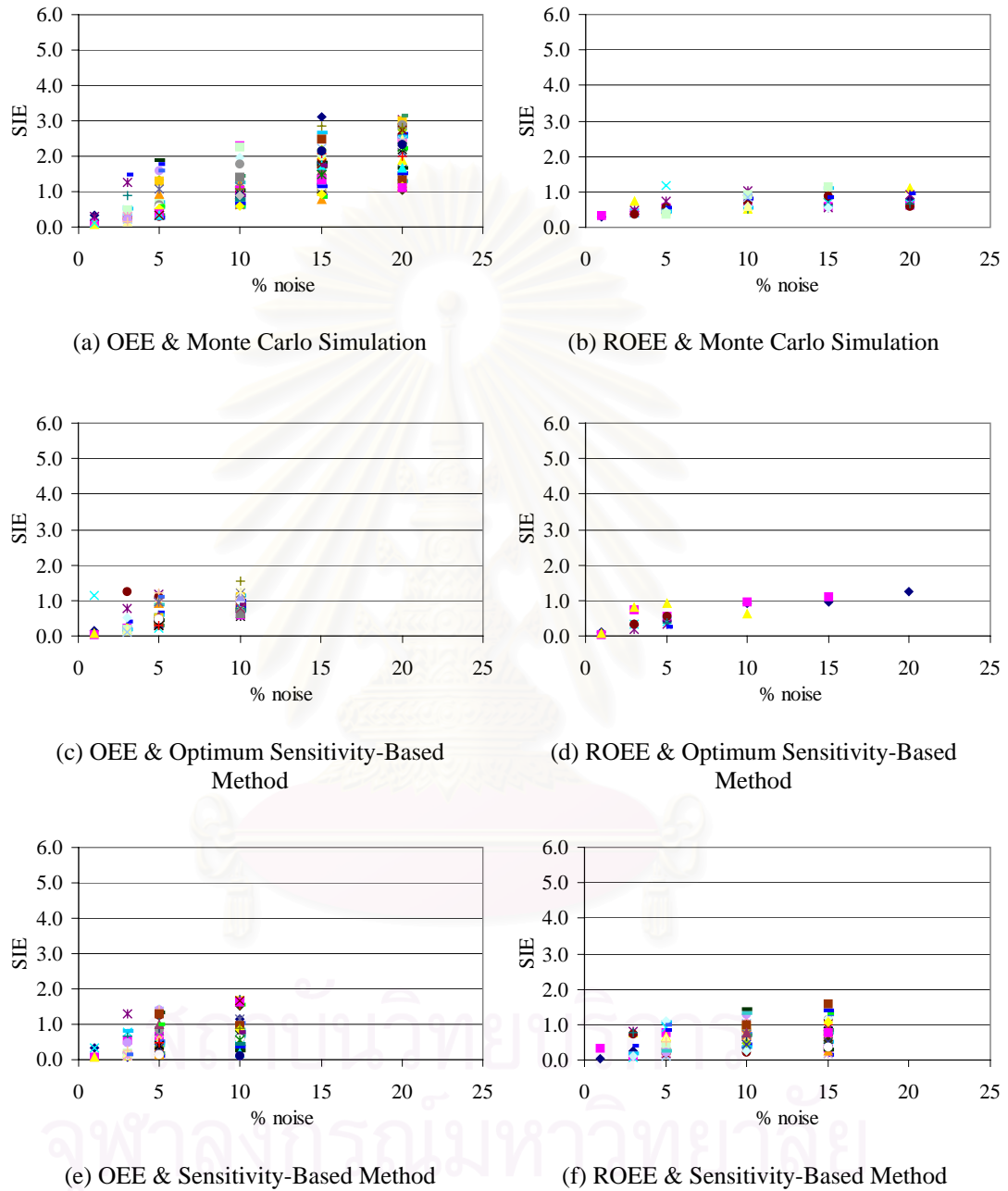
Figure 4.7 Variation of the SIE values with respect to different levels of noise for the two-damaged-member cases in which only one member is successfully detected as damaged using different methods of statistical parameter estimation with the OEE and ROEE algorithms.

(a) OEE & Monte Carlo Simulation

(b) ROEE & Monte Carlo Simulation

(c) OEE & Optimum Sensitivity-Based Method

(d) ROEE & Optimum Sensitivity-Based Method

(e) OEE & Sensitivity-Based Method

(f) ROEE & Sensitivity-Based Method
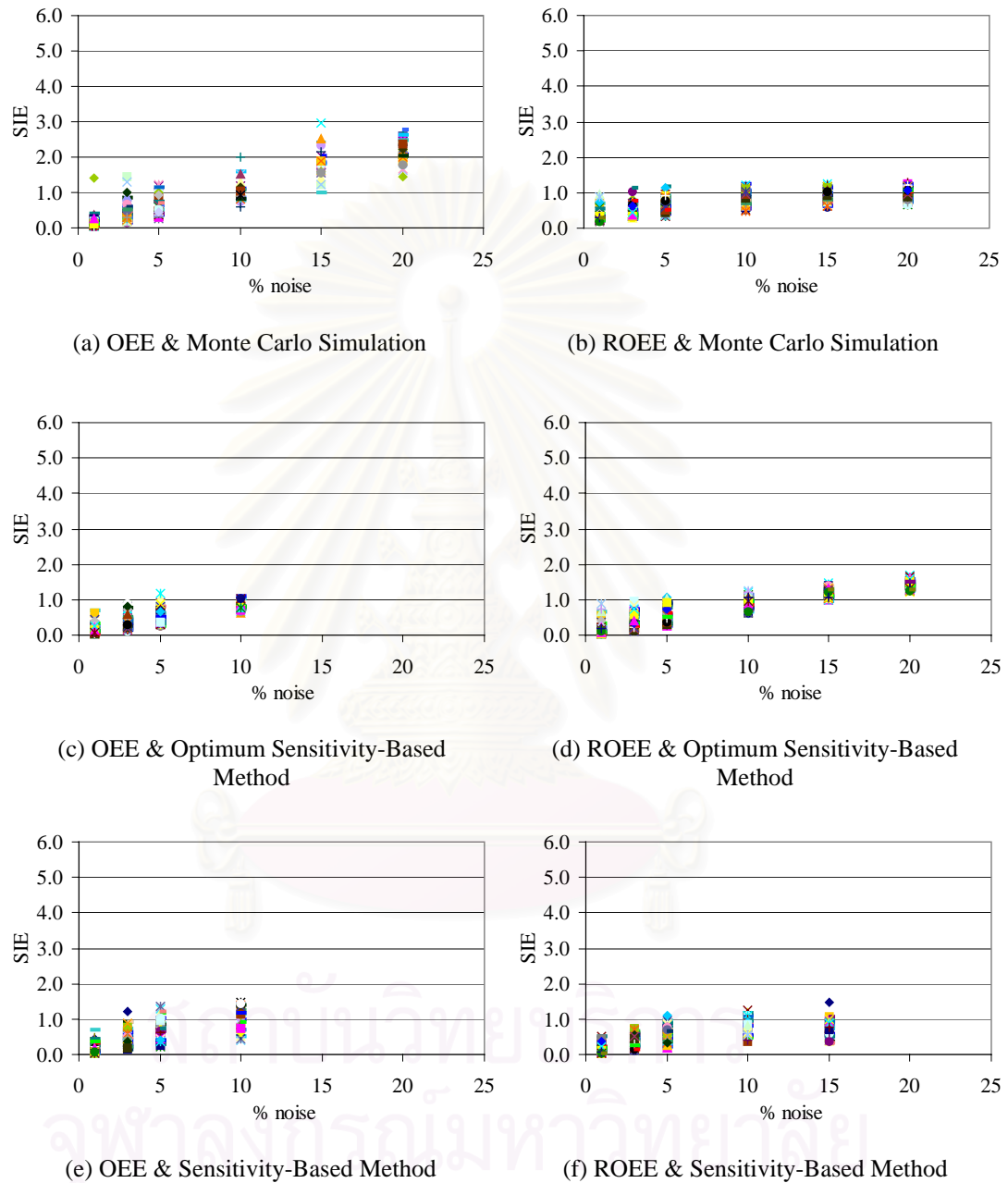
Figure 4.8 Variation of the SIE values with respect to different levels of noise for the two-damaged-member cases in which both damaged members are successfully detected using different methods of statistical parameter estimation with the OEE and ROEE algorithms.

Figure 4.9 shows the performance of the algorithms under consideration with respect to different levels of noise in the measurements. The SIE values in this figure are plotted as the average of the SIE values for the members whose damage can be detected for the cases in which one, two, and three damaged members are detected and for all of the investigated damage cases.

It is seen from the illustration that the SIE value increases as the level of noise in the measurements increases. For all of the investigated damage cases, the ROEE method out-performs the OEE method in the assessment of damage using all the statistical parameter estimation schemes considered with higher levels of noise permitting a damage assessment.

Figure 4.10 shows the probability of success in detecting damage with respect to different levels of noise in the measurements for the three-damaged-member cases. The results from using all three statistical parameter estimation methods with the OEE and the ROEE algorithms show that the probability of successfully detecting all damaged members as damaged decreases as the level of noise in the measurements increases, with a more gradual decrease when the ROEE algorithm is used. In addition, the probability of detecting two members, one member and no member as damaged increases with the level of noise in the measurements. Again, the increase in the probability values for the results obtained from using the ROEE algorithm is more gradual.

Figures 4.11, 4.12 and 4.13 summarize the variation of the SIE values for the cases in which one, two and three damaged members are successfully detected, respectively. The same sort of results as for the previous damage cases are again seen for the three-damaged-member cases. For all three statistical parameter estimation methods with the OEE and the ROEE algorithms, the variation of the SIE values is small for low levels of noise. The variation of the SIE values becomes larger for higher levels of noise. At the same level of noise, the variation of the SIE values is smaller when the ROEE algorithm is used, which confirms the improvement of the assessment of damage by using the regularization method on the statistical parameter estimation schemes considered.
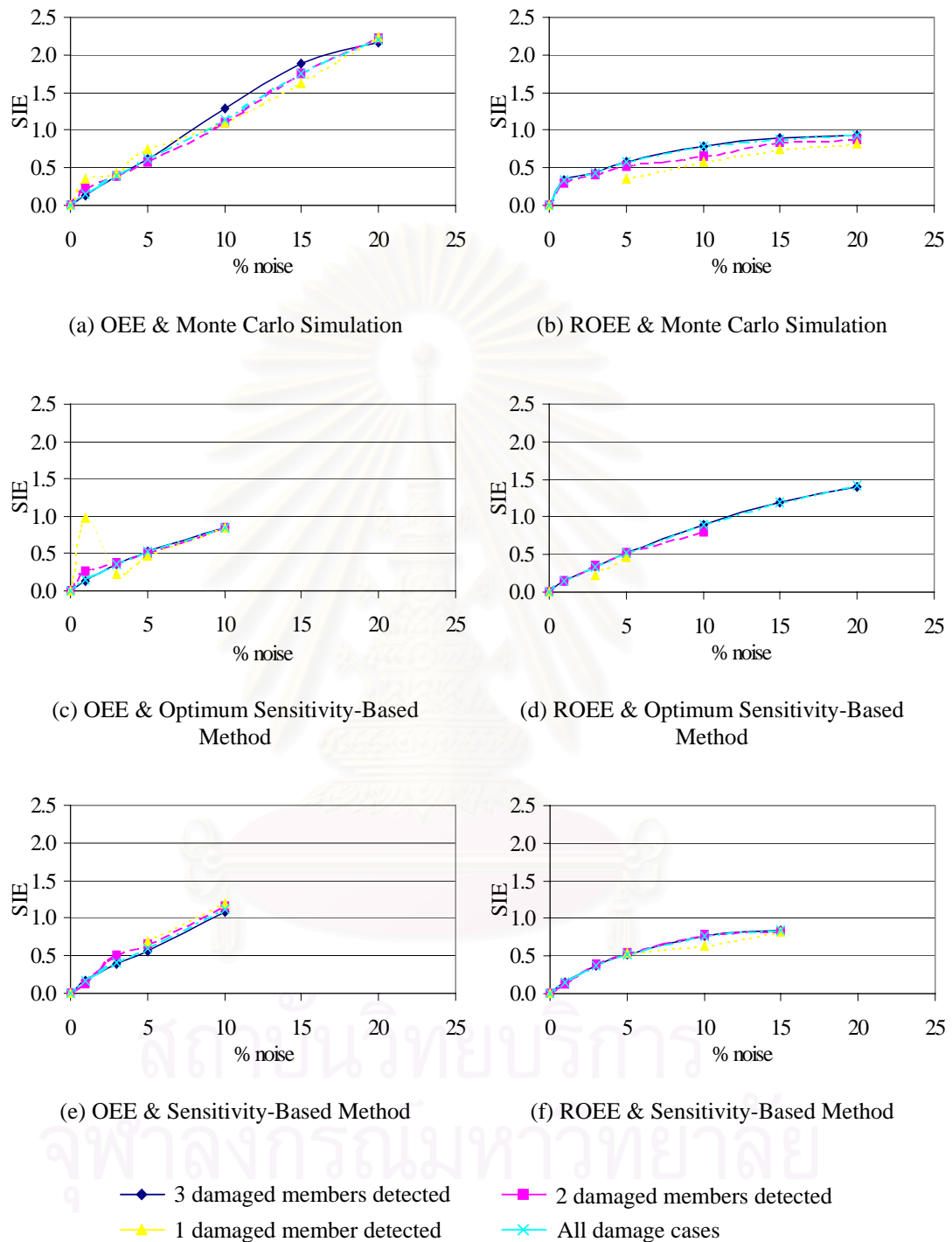
Figure 4.9 Variation of the average SIE values for the successfully-detected damaged members with respect to different levels of noise in the measurements for the cases in which one, two, and three damaged members are detected and for all 100 damage cases using different methods of statistical parameter estimation with the OEE and ROEE algorithms.
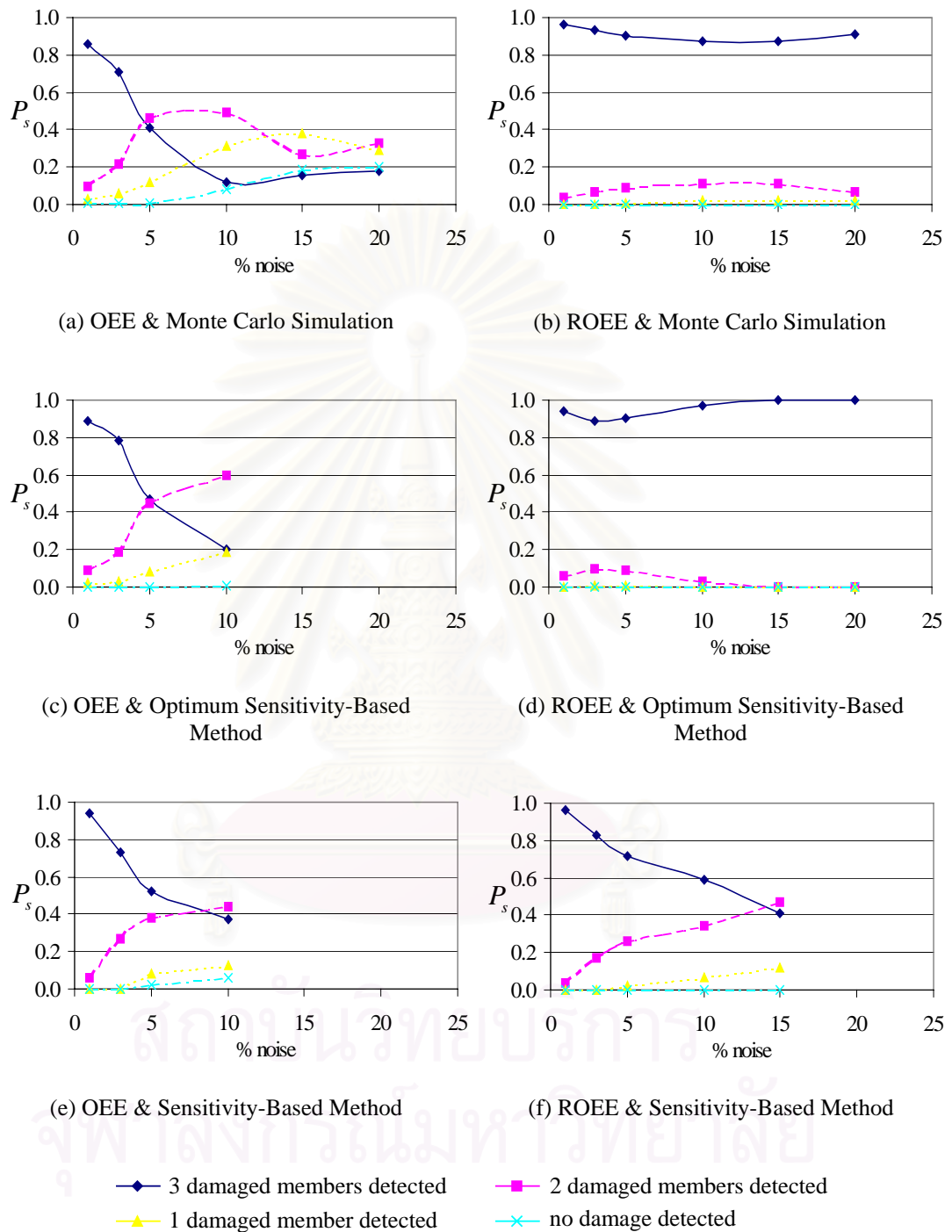
Figure 4.10 Probability of success in detecting damage with respect to different levels of noise in the measurements for 100 three-damaged-member cases using different methods of statistical parameter estimation with the OEE and ROEE algorithms.
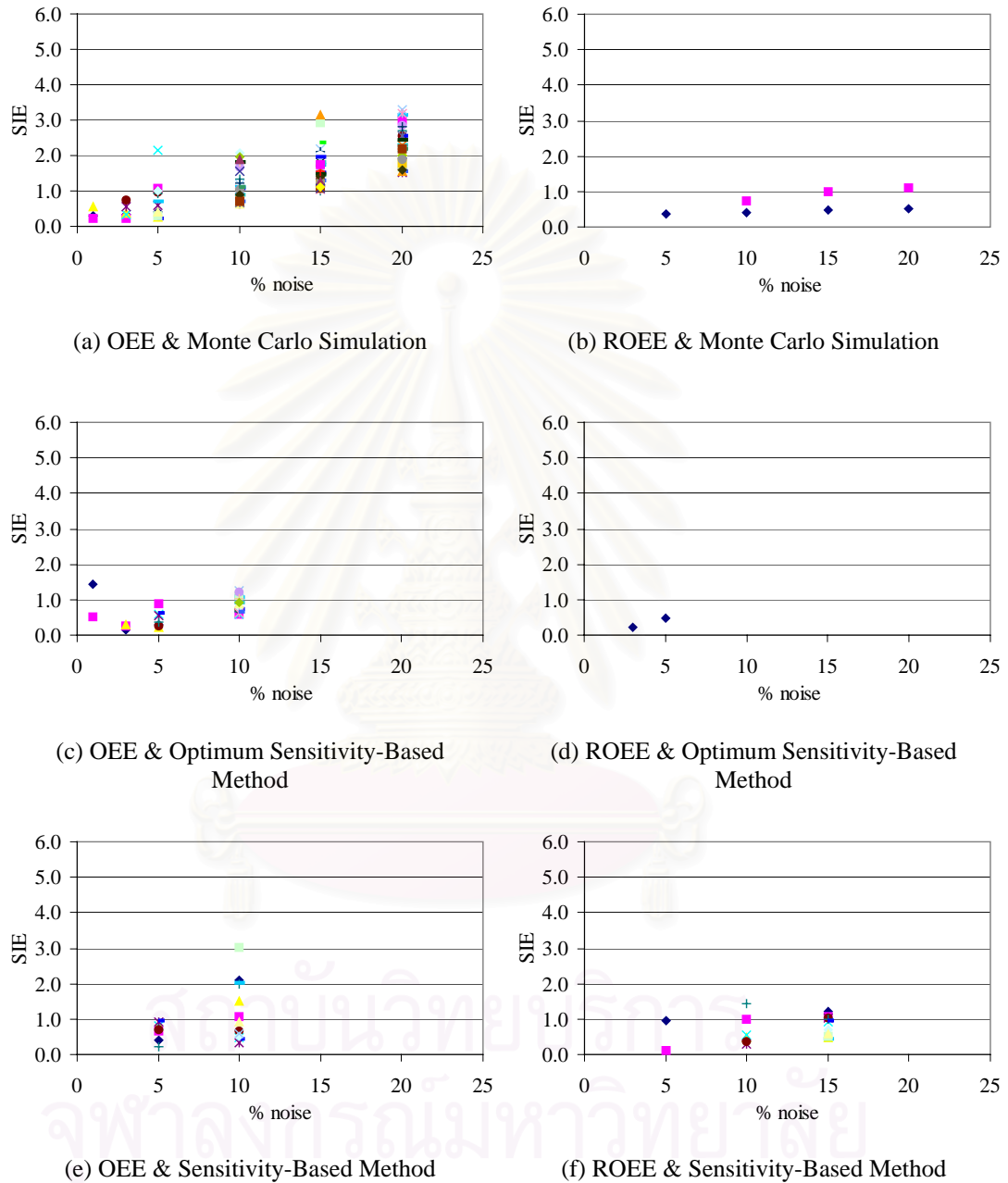
Figure 4.11 Variation of the SIE values with respect to different levels of noise for the three-damaged-member cases in which only one member is successfully detected as damaged using different methods of statistical parameter estimation with the OEE and ROEE algorithms.
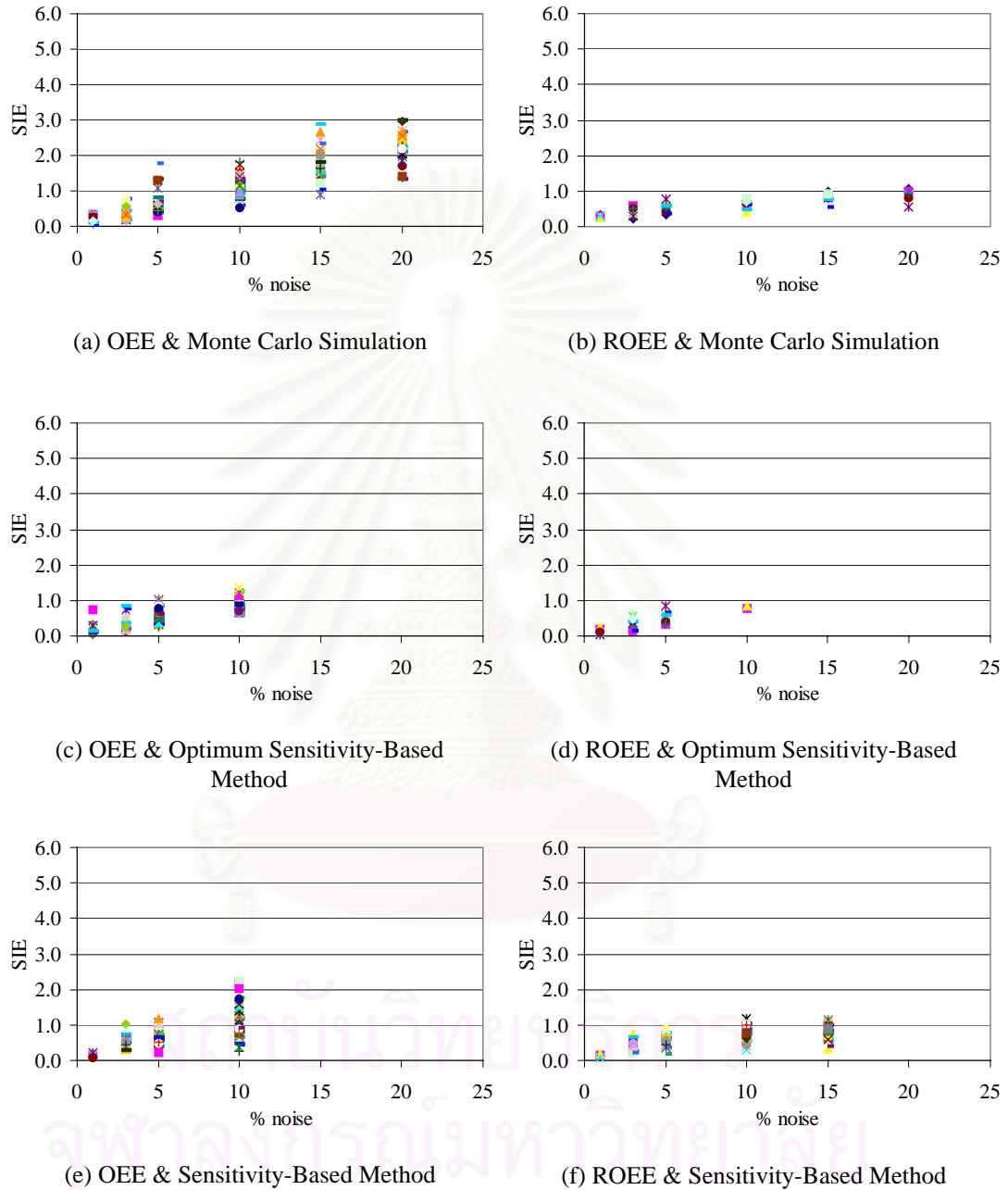
Figure 4.12 Variation of the SIE values with respect to different levels of noise for the three-damaged-member cases in which two members are successfully detected as damaged using different methods of statistical parameter estimation with the OEE and ROEE algorithms.

(a) OEE & Monte Carlo Simulation

(b) ROEE & Monte Carlo Simulation

(c) OEE & Optimum Sensitivity-Based Method

(d) ROEE & Optimum Sensitivity-Based Method

(e) OEE & Sensitivity-Based Method

(f) ROEE & Sensitivity-Based Method
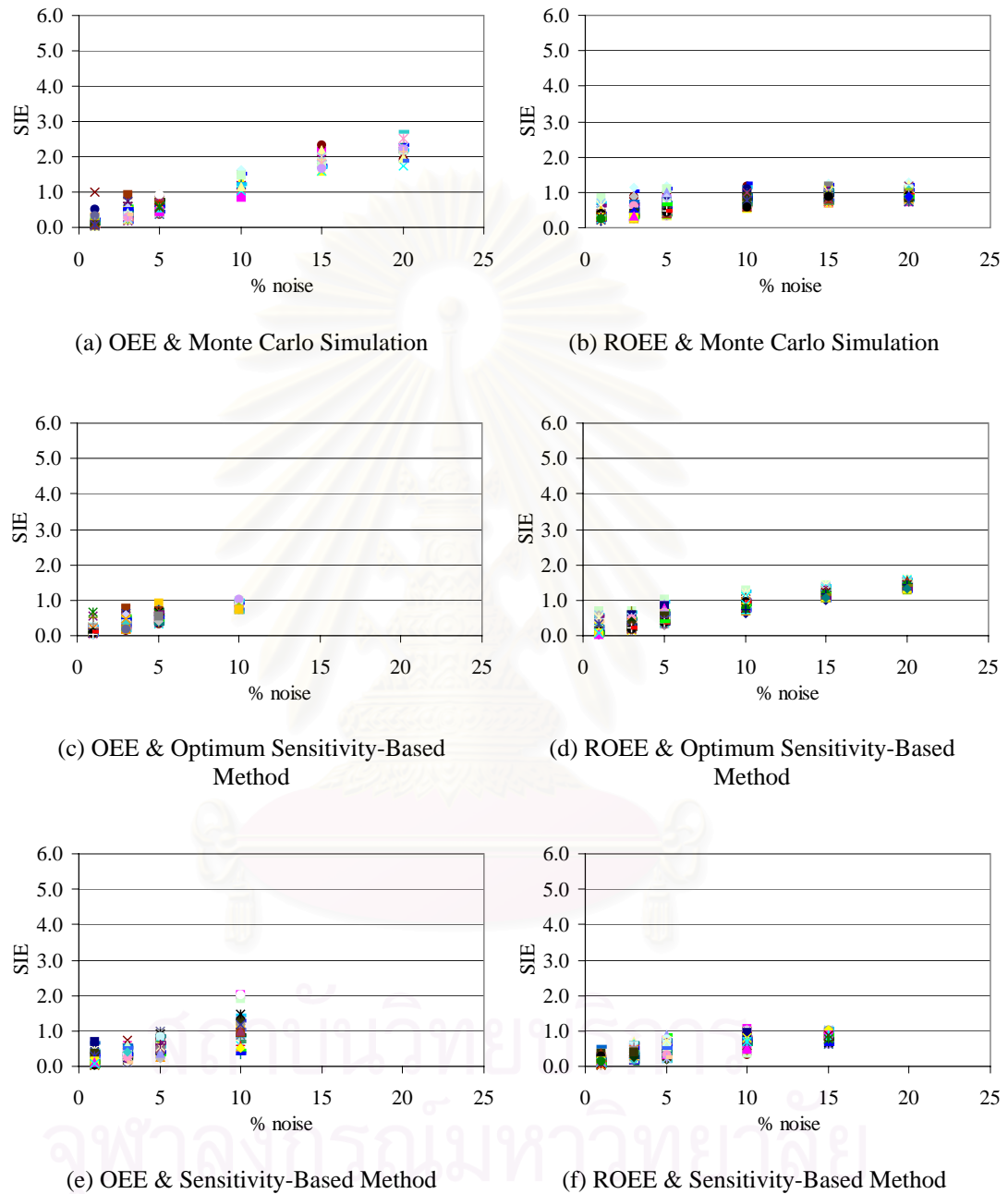
Figure 4.13 Variation of the SIE values with respect to different levels of noise for the three-damaged-member cases in which all of the three damaged members are successfully detected using different methods of statistical parameter estimation with the OEE and ROEE algorithms.

4.4 Chapter Summary

The performance of the statistical damage assessment scheme was investigated through a simulation study using a truss structure as the model problem. Various damage cases with different locations and severities of damage of the truss were randomly selected for the single-damaged-member cases, the two-damaged-member cases and the three-damaged-member cases, respectively. The statistics of the structural parameters are obtained by using three methods of statistical parameter estimation, i.e. the Monte-Carlo simulation method, the optimum sensitivity-based method and the sensitivity-based method. The performance of the damage assessment is identified by using a statistical identification error (SIE) index that approaches zero when the assessment is effective. The level of success of the damage detection is indicated by the probability of success in detecting damage (P_s). The performance of damage assessment with respect to the level of noise in the measurements is illustrated by the variation of the SIE values for all damage cases. The results of the simulation study showed that the performance of the present statistical damage assessment method can be improved by using the regularization method on the parameter estimation scheme for all of the damage cases considered.

CHAPTER 5

SIMULATION STUDY—A BRACED FRAME WITH MULTI-PARAMETER MEMBERS

5.1 Introduction

It has been shown in Chapter 3 and Chapter 4 that the proposed statistical damage assessment scheme in conjunction with the OEE and the ROEE algorithms can be used to assess damage in a simple-support bridge truss effectively even when the measured data are noise-polluted. In this chapter, the optimum sensitivity-based method are used in conjunction with the ROEE algorithm in the simulation study of a two-story braced frame with members consisting of multiple stiffness parameters. The method of damage assessment for multi-parameter structural members proposed in Chapter 2 is used in the current study.

A two-story braced frame is used as our model problem. We consider two distinct cases of damage: the damage of the single-parameter frame members and the damage of the multiple-parameter frame members. The performance of the proposed algorithm is assessed in terms of the probability of the damage P_d^m for member m. The performance of the algorithm is illustrated through the variation of the probability of the damage P_d^m with respect to different levels of damage in percentage of reduction of the corresponding stiffness parameters, coupled with the effect of noise in the measurements. In addition, the values of the probability of the damage P_d^m associated with the identified damaged members are also ranked in order to identify the accuracy of the outcome of the damage assessment scheme.

5.2 Description of the Example Structure

The structure we investigate herein is a two-story braced frame. The geometry and the topology of the frame are shown in Figure 5.1. In the figure the numbers in circles
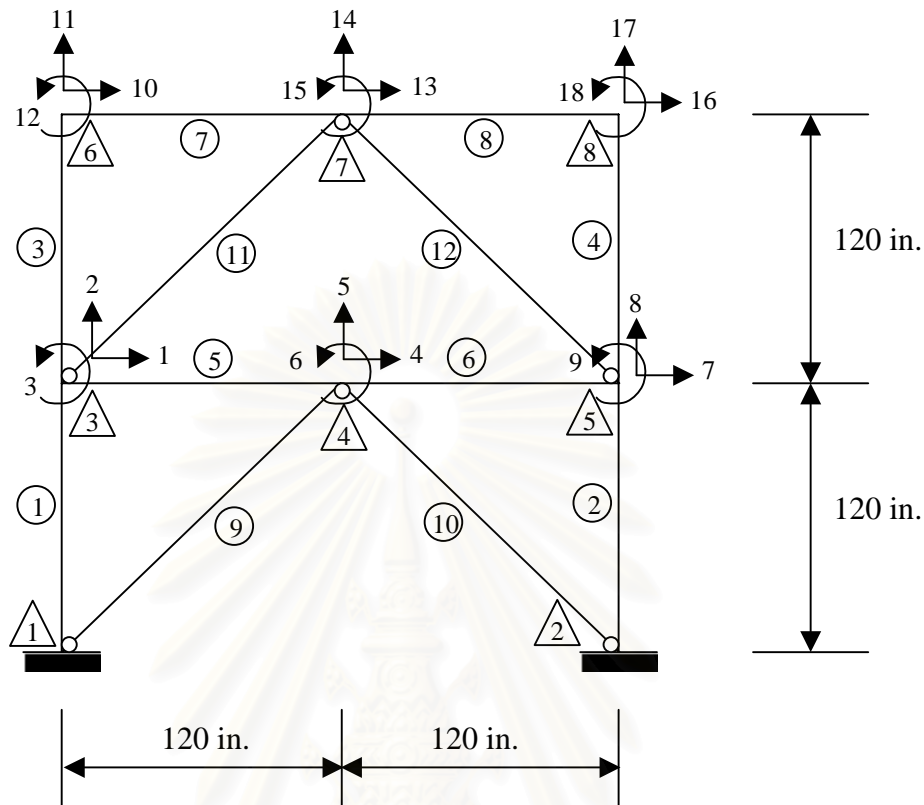
Figure 5.1 Geometry and topology of the two-story braced frame.

represent the member identification numbers and the numbers in triangles represent the nodal identification numbers. The finite-element model of the braced frame consists of 12 elements and 8 nodes with 18 degrees of freedom. The braced-frame members can be categorized into two types: (1) the two-parameter members (column members 1 – 4 and beam members 5 – 8); and (2) the single-parameter members (bracing members 9 – 12). The stiffness parameters for the two-parameter members are the axial stiffness (EA) and the bending stiffness (EI). The stiffness parameter for the single-parameter members is the axial stiffness (EA). The baseline properties for each of the braced frame members are listed in Table 5.1. Note that the self-weight of the structural members is calculated based on the unit weight $w = 0.145$ kips/ft^3. In addition to the self-weight of the structural members shown in the table, we assume that the dead load being imposed upon the structure is uniformly distributed along the length of all 12 members with a value of 0.017 kips-sec^2/ft/ft. Moreover, all members are assumed to have a modulus of elasticity of $E = 582,768$ kips/ft^2.

Table 5.1 Baseline properties of the two-story braced frame.

Member	Location	Cross Section (in.× in.)	Cross-Sectional Area, A (in.^{2})	I (ft.^{4})	EA (kips)	EI (kips-ft^2)	Self Weight (kips-sec^2/ft/ft)	Total Weight (kips-sec^2/ft/ft)
1	1st-story left column	24.×24	576	1.33333	2321573	773858	0.01801	0.03501
2	1st-story right column	24.×24	576	1.33333	2321573	773858	0.01801	0.03501
3	2nd-story left column	22.×22	484	0.94142	1950766	546395	0.01514	0.03214
4	2nd-story right column	22.×22	484	0.94142	1950766	546395	0.01514	0.03214
5	1st-story left beam	10.×18	180	0.23438	725492	136030	0.00563	0.02263
6	1st-story right beam	10.×18	180	0.23438	725492	136030	0.00563	0.02263
7	2nd-story left beam	10.×18	180	0.23438	725492	136030	0.00563	0.02263
8	2nd-story right beam	10.×18	180	0.23438	725492	136030	0.00563	0.02263
9	1st-story bracing member	-	57.6	-	232157	-	0.00180	0.01880
10	1st-story bracing member	-	57.6	-	232157	-	0.00180	0.01880
11	2nd-story bracing member	-	48.4	-	195077	-	0.00151	0.01851
12	2nd-story bracing member	-	48.4	-	195077	-	0.00151	0.01851

In the current study we assume that the natural frequencies and mode shapes of the structure for all of the 18 vibration modes are available as our measurement information. Each of the mode shapes are assumed to be measured at all 18 degrees of freedom of the structural model as shown in Figure 5.1. The free-vibration responses obtained from an eigenvalue analysis of the baseline structure are shown in Table 5.2, in which the ith mode shape $\mathbf{\Phi}_i$ is scaled by using the mass matrix $\mathbf{M}$ such that $\mathbf{\Phi}_i^T \mathbf{M} \mathbf{\Phi}_i = 1$.

5.3 Statistical Damage Assessment of Multi-Parameter Structural Members

The simulation studies conducted in this section consist of the damage cases of the single-parameter members and the damage cases of the two-parameter members. For the damage cases of the single-parameter members the damage of the structure is

Table 5.2 Noise-free data for the baseline structure.

Mode	1st Mode	2nd Mode	3rd Mode	4th Mode	5th Mode	6th Mode	7th Mode	8th Mode	9th Mode
Natural Frequency (Hz)	12.76	30.84	37.26	37.98	61.50	66.25	68.49	90.30	93.82
Mode Shape									
1st DOF	0.44850	0.18191	-0.02103	-0.71037	0.19426	-0.78431	-0.06250	-0.32238	-0.66131
2nd DOF	0.01225	0.07540	0.02934	0.03990	-0.18820	0.10030	-0.25800	0.60586	-0.34312
3rd DOF	-0.05712	-0.2763	0.04427	0.01449	0.09431	0.15383	-0.19249	-0.12324	-0.26246
4th DOF	0.40961	0.00000	0.00000	-0.74302	0.26993	0.00000	-0.09867	0.00000	0.00000
5th DOF	0.00000	-0.02763	1.67188	0.00000	0.00000	-0.18882	0.00000	-0.06293	0.25037
6th DOF	0.02844	0.00000	0.00000	-0.02402	-0.06015	0.00000	1.13441	0.00000	0.00000
7th DOF	0.44850	-0.18191	0.02103	-0.71037	0.19426	0.78431	-0.06250	0.32238	0.66131
8th DOF	-0.01225	0.07540	0.02934	-0.03990	0.18820	0.10030	0.25800	0.60586	-0.34312
9th DOF	-0.05712	0.02763	-0.04427	0.01449	0.09431	-0.15383	-0.19249	0.12324	0.26246
10th DOF	0.85216	-0.00417	-0.01992	0.75068	-0.03422	-0.38479	-0.05179	0.34389	0.69799
11th DOF	0.01266	0.09901	0.03203	0.03249	-0.35167	0.12121	-0.32390	0.94714	-0.49965
12th DOF	-0.02252	0.10519	-0.02186	-0.21814	-0.29388	-0.27840	0.10940	0.18921	0.16008
13th DOF	0.83334	0.00000	0.00000	0.70794	-0.02480	0.00000	-0.13857	0.00000	0.00000
14th DOF	0.00000	1.57599	0.03666	0.00000	0.00000	0.41602	0.00000	-0.57257	0.25085
15th DOF	0.00994	0.00000	0.00000	0.17913	0.97308	0.00000	0.04095	0.00000	0.00000
16th DOF	0.85216	0.00417	0.01992	0.75068	-0.03422	0.38479	-0.05179	-0.34389	-0.69799
17th DOF	-0.01266	0.09901	0.03203	-0.03249	0.35167	0.12121	0.32390	0.94714	-0.49965
18th DOF	-0.02252	-0.10519	0.02186	-0.21814	-0.29388	0.27840	0.10940	-0.18921	-0.16008

Mode	10th Mode	11th Mode	12th Mode	13th Mode	14th Mode	15th Mode	16th Mode	17th Mode	18th Mode
Natural Frequency (Hz)	101.01	118.33	131.31	140.54	187.32	194.07	243.10	267.05	284.54
Mode Shape									
1st DOF	0.03057	0.03182	0.03474	-0.67861	-0.00693	-0.30072	-0.27322	0.15961	-0.35870
2nd DOF	0.67677	0.11961	0.16442	-0.00837	0.01640	-0.50018	-0.75456	-0.80445	0.53696
3rd DOF	-0.00232	-0.38530	0.37452	-0.14345	0.56552	0.69371	0.43687	-0.10531	0.38597
4th DOF	0.18272	-0.29946	0.00000	1.46676	0.00590	0.00000	0.14525	0.00000	0.15614
5th DOF	0.00000	0.00000	-0.22691	0.00000	0.00000	-0.22460	0.00000	0.18651	0.00000
6th DOF	0.75329	-0.60728	0.00000	-0.19806	0.58876	0.00000	0.10519	0.00000	0.52724
7th DOF	0.03057	0.03182	-0.03474	-0.67861	-0.00693	0.30072	-0.27322	-0.15961	-0.35871
8th DOF	-0.67677	-0.11961	0.16442	0.00837	-0.01640	-0.50018	0.75456	-0.80445	-0.53696
9th DOF	-0.00232	-0.38530	-0.37452	-0.14345	0.56552	-0.69371	0.43687	0.10531	0.38597
10th DOF	-0.05123	0.05952	1.63098	0.30299	1.28311	-0.25028	-0.55904	0.65413	-1.10109
11th DOF	0.98983	0.10993	-0.01900	-0.02385	-0.07663	-0.05301	0.82129	1.51725	-1.28722
12th DOF	-0.19181	0.48520	-0.62122	-0.05053	-0.05579	0.91248	0.79733	-0.81503	1.32400
13th DOF	0.06618	-0.70342	0.00000	-0.06469	-1.09501	0.00000	0.41534	0.00000	0.59337
14th DOF	0.00000	0.00000	0.26684	0.00000	0.00000	-0.25237	0.00000	0.30368	0.00000
15th DOF	0.56484	0.95347	0.00000	-0.08131	-0.09041	0.00000	1.03320	0.00000	0.66415
16th DOF	-0.05123	0.05952	-1.63098	0.30299	1.28311	0.25028	-0.55904	-0.65413	-1.10109
17th DOF	-0.98983	-0.10993	-0.01900	0.02385	0.07663	-0.05301	-0.82129	1.51725	1.28722
18th DOF	-0.19181	0.48520	0.62122	-0.05053	-0.05579	-0.91248	0.79733	0.81503	1.32400

represented by the reduction of a single stiffness parameter of a structural member whereas for the damage cases of the two-parameter member the damage is due to the reduction of two stiffness parameters of a structural member. The stiffness parameters for the two-parameter members are the axial stiffness (*EA*) and the bending stiffness (*EI*), respectively, whereas the stiffness parameter for the single-parameter members is the axial stiffness (*EA*).

As for Chapter 3, we model the measurement data of the structural response by using a computer simulation. The modal responses of the baseline structure in Table 5.2 are used as the noise-free measurement data upon which the mean and the covariance matrix of the parameter estimates of the baseline structure are obtained by using the optimum sensitivity-based method in conjunction with the ROEE algorithm.

In the statistical damage assessment process, the probability of the damage P_d^m for member *m* can be computed directly—as a function of the distance of the limit-state line to the origin of the reduced variates; that is, the distance b_m—by substituting the statistical indices from the statistical parameter estimation process into equation (2.101). Moreover, to investigate the effect of a_i^m's in equation (2.101) on the damage assessment results, two alternatives of a_i^m's from equations (2.104) and (2.105) are examined.

5.3.1   Single-Parameter Member Damage Cases

For the cases in which the single-parameter members are damaged, we model damage of the bracing members 10 and 12 with 10%, 50% and 90% reduction of the axial stiffness parameter (*EA*) and we examine four different levels of noise in the measurements: 0.1%, 0.3% 0.5% and 1%. The optimum sensitivity-based method is used in conjunction with the ROEE algorithm to estimate the mean and the covariance matrix of the stiffness parameters.

Tables 5.3 and 5.4 summarize the five structural members with the highest probability of damage P_d^m for 10%, 50% and 90% reduction of the axial stiffness

Table 5.3 Ranking of the identified damaged members by P_d^m value for different percentages of reduction of the stiffness parameter of members 10 and 12 using noisy measurements and a_i^m's from equation (2.104).

Actual Damaged Member	% noise	% Reduction of Parameter Value (EA)	Ranking of Identified Damaged Members (by P_d^m value)				
			1st	2nd	3rd	4th	5th
10	0.1	10	10 (1.00000)	7 (0.826392)	6 (0.799546)	5 (0.791031)	8 (0.640577)
10	0.1	50	10 (1.00000)	7 (0.838914)	6 (0.833977)	5 (0.680823)	8 (0.644309)
10	0.1	90	10 (1.00000)	7 (0.853142)	6 (0.810571)	8 (0.644309)	5 (0.567495)
10	0.3	10	10 (0.85083)	7 (0.823815)	6 (0.802338)	5 (0.776373)	8 (0.629300)
10	0.3	50	10 (1.00000)	6 (0.836458)	7 (0.828945)	5 (0.636831)	8 (0.621720)
10	0.3	90	10 (1.00000)	7 (0.823815)	6 (0.823815)	8 (0.598706)	5 (0.511966)
10	0.5	10	7 (0.818589)	6 (0.813268)	5 (0.767305)	8 (0.617912)	4 (0.531881)
10	0.5	50	10 (0.999739)	6 (0.848496)	7 (0.818589)	5 (0.606420)	8 (0.602568)
10	0.5	90	10 (1.000000)	6 (0.836458)	7 (0.799546)	8 (0.567495)	4 (0.539828)
10	1.0	10	7 (0.823815)	6 (0.793893)	5 (0.782305)	4 (0.742154)	2 (0.742154)
10	1.0	50	6 (0.886861)	7 (0.821214)	4 (0.776373)	2 (0.738914)	10 (0.625516)
10	1.0	90	6 (0.859930)	4 (0.821214)	7 (0.807850)	2 (0.698469)	10 (0.662758)
12	0.1	10	12 (0.999998)	7 (0.821214)	5 (0.807850)	6 (0.779351)	8 (0.648028)
12	0.1	50	12 (1.000000)	5 (0.826392)	7 (0.785237)	6 (0.751748)	8 (0.651732)
12	0.1	90	12 (1.000000)	5 (0.846136)	6 (0.666402)	7 (0.633072)	8 (0.575345)
12	0.3	10	12 (0.866501)	7 (0.815941)	5 (0.799546)	6 (0.776373)	8 (0.636831)
12	0.3	50	12 (1.000000)	5 (0.805106)	7 (0.776373)	6 (0.708841)	8 (0.640577)
12	0.3	90	12 (1.000000)	5 (0.779351)	1 (0.644309)	7 (0.587064)	8 (0.551717)
12	0.5	10	7 (0.813268)	5 (0.793893)	6 (0.779351)	12 (0.659097)	8 (0.625516)
12	0.5	50	12 (0.999993)	5 (0.785237)	7 (0.767305)	6 (0.662758)	8 (0.625516)
12	0.5	90	12 (1.000000)	1 (0.751748)	5 (0.705402)	7 (0.583166)	8 (0.547758)
12	1.0	10	5 (0.823815)	7 (0.815941)	2 (0.758037)	4 (0.712261)	1 (0.698469)
12	1.0	50	12 (0.962462)	1 (0.925067)	2 (0.857691)	5 (0.807850)	7 (0.767305)
12	1.0	90	12 (0.997364)	1 (0.963273)	2 (0.929220)	3 (0.785237)	5 (0.764238)

Table 5.4 Ranking of the identified damaged members by P_d^m value for different percentages of reduction of the stiffness parameter of members 10 and 12 using noisy measurements and a_i^m's from equation (2.105).

Actual Damaged Member	% noise	% Reduction of Parameter Value (EA)	Ranking of Identified Damaged Members (by P_d^m value)				
			1st	2nd	3rd	4th	5th
10	0.1	10	10 (1.000000)	7 (0.826392)	5 (0.810571)	6 (0.802338)	8 (0.640577)
10	0.1	50	10 (1.000000)	7 (0.836458)	6 (0.831473)	5 (0.735653)	8 (0.644309)
10	0.1	90	10 (1.000000)	7 (0.853142)	6 (0.793893)	8 (0.644309)	5 (0.629300)
10	0.3	10	10 (0.850831)	7 (0.823815)	6 (0.805106)	5 (0.796731)	8 (0.629300)
10	0.3	50	10 (1.000000)	6 (0.831473)	7 (0.826392)	5 (0.691463)	8 (0.621720)
10	0.3	90	10 (1.000000)	7 (0.823815)	6 (0.810571)	8 (0.594835)	5 (0.583166)
10	0.5	10	7 (0.818589)	6 (0.813268)	5 (0.776373)	8 (0.617912)	4 (0.547758)
10	0.5	50	10 (0.999739)	6 (0.833977)	7 (0.818589)	5 (0.655422)	8 (0.602568)
10	0.5	90	10 (1.000000)	6 (0.810571)	7 (0.799546)	4 (0.633072)	8 (0.567495)
10	1.0	10	4 (0.872857)	7 (0.826392)	6 (0.785237)	3 (0.785237)	2 (0.748572)
10	1.0	50	4 (0.906583)	6 (0.838914)	7 (0.821214)	3 (0.779351)	2 (0.751748)
10	1.0	90	4 (0.957284)	3 (0.828945)	7 (0.807850)	6 (0.751748)	2 (0.719043)
12	0.1	10	12 (0.999998)	5 (0.823815)	7 (0.821214)	6 (0.785237)	8 (0.648028)
12	0.1	50	12 (1.000000)	5 (0.836458)	7 (0.788145)	6 (0.748572)	8 (0.651732)
12	0.1	90	12 (1.000000)	5 (0.846136)	7 (0.644309)	6 (0.621720)	8 (0.579260)
12	0.3	10	12 (0.866501)	7 (0.815941)	5 (0.813268)	6 (0.782305)	8 (0.636831)
12	0.3	50	12 (1.000000)	5 (0.805106)	7 (0.779351)	6 (0.687933)	8 (0.640577)
12	0.3	90	12 (1.000000)	5 (0.722405)	1 (0.629300)	7 (0.598706)	8 (0.555670)
12	0.5	10	7 (0.813268)	5 (0.793893)	6 (0.779351)	12 (0.659097)	8 (0.625516)
12	0.5	50	12 (0.999993)	7 (0.767305)	5 (0.751748)	8 (0.625516)	6 (0.621720)
12	0.5	90	12 (1.000000)	1 (0.748572)	7 (0.594835)	3 (0.587064)	5 (0.579260)
12	1.0	10	4 (0.857691)	7 (0.815941)	3 (0.796731)	2 (0.764238)	5 (0.742154)
12	1.0	50	12 (0.962462)	1 (0.923642)	3 (0.868644)	2 (0.859930)	4 (0.821214)
12	1.0	90	12 (0.997364)	3 (0.977250)	1 (0.964852)	2 (0.929220)	4 (0.767305)

parameter (*EA*) of members 10 and 12 using the 0.1%, 0.3%, 0.5% and 1.0% noisy measurements. The results in the tables are obtained from using the coefficients a_i^m's in equations (2.104) and (2.105), respectively. Note that even though the coefficient a_1^m obtained from both equations (2.104) and (2.105) has the unit value, the coefficients a_i^m's from these equations are still different for other multi-parameter members that are examined. Therefore, the rankings in Tables 5.3 and 5.4 are different. The unit P_d^m value indicates that the probability that the member under consideration is damaged is 100%. Likewise, the zero P_d^m value implies that there is no chance that the investigated member is damaged.

It is seen from the tables that there is no clear distinction between the results using a_i^m's from equations (2.104) and (2.105). This is due to the same unit value of a_1^m from the two equations for the actual damaged members. Members 10 and 12 are successfully identified with the highest probability of damage at high levels of damage and at low levels of noise in the measurements. These members are, however, not identified with the highest probability of damage when the level of noise in the measurements increases. For 1% noisy measurements, the actual damaged member 10 is ranked with the fifth highest probability of damage in Table 5.3 for 50% and 90% reduction of *EA*. Similar results are observed in Table 5.4 in which member 12 is not ranked within the five highest probability of damage for 1% noisy measurements. In other words, there is more chance for the proposed algorithm to successfully identify damage for higher level of damage and lower level of noise in the measurements. Note that the maximum level of noise permitting a damage assessment is 1%.

Figure 5.2 summarizes the damage assessment results for the damage cases in which the single-parameter bracing members 10 and 12 are damaged with different percentages of reduction of the axial stiffness parameter (*EA*) and levels of noise in the measurements. Figures 5.2(a) and 5.2(b) show the results for the cases in which members 10 and 12 are damaged, respectively. In these figures, the results from using different levels of noise in the measurements are compared with the reference value of P_d^m which is obtained by substituting the actual value of $\bar{H}_i^m$ and the $SD^{H_i^m}$ value for
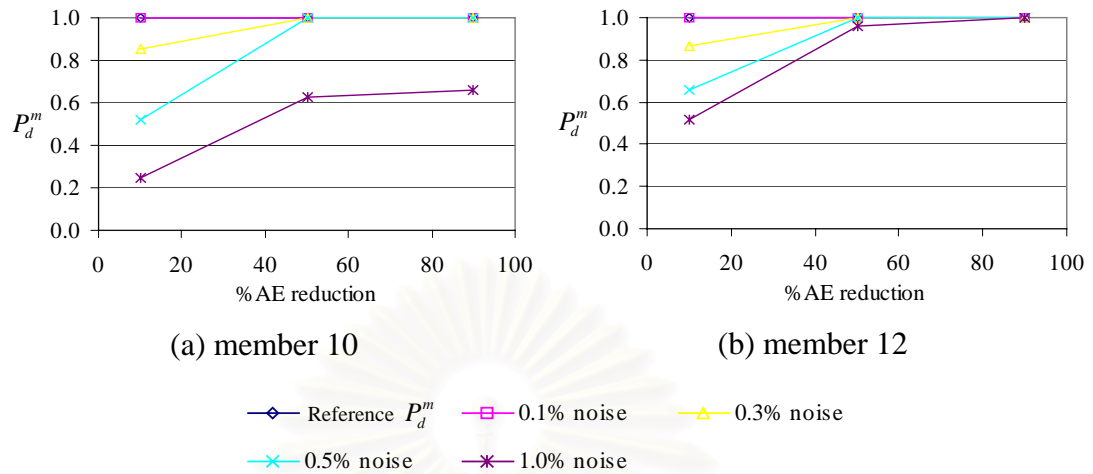
Figure 5.2 Variation of the P_d^m values of the actual damaged members 10 and 12 with respect to different percentages of *EA* reduction for different levels of noise in the measurements.

0.1% noisy measurements in equation (2.101). In addition, the values of the probability of damage P_d^m for the actual damaged members are plotted in the range 0–1. The unit P_d^m value indicates that the probability of detecting damage is 100%. Likewise, the zero P_d^m value implies that there is no chance to detect damage.

It is seen from the illustration that the P_d^m value increases by approaching to the unit value as the percentage of *EA* reduction increases. Thus, it is concluded that there is more chance for the proposed algorithm to successfully identify damage in a more severely damaged structural member. Moreover, for the same level of damage the P_d^m value decreases as the level of noise in the measurements increases. Hence, it is evident that the performance of the proposed algorithm to assess damage is limited by the level of noise in the measurements.

5.3.2 Two-Parameter Member Damage Cases

For the present case, we model damage in the column member 4 and the beam member 6 with 0%, 10%, 50% and 90% reduction of the axial stiffness parameter

(*EA*) and the bending stiffness parameter (*EI*) using four different levels of noise in the measurements: 0.1%, 0.3% 0.5% and 1%. As for the cases with damage in the single-parameter members, the optimum sensitivity-based method is used in conjunction with the ROEE algorithm to estimate the mean and the covariance matrix of the stiffness parameters.

Tables 5.5-5.8 summarize the five frame members with the highest probability of damage for different percentages of reduction of *EA* and *EI* using a_i^m's in equation (2.104) for 0.1%, 0.3%, 0.5% and 1.0% noisy measurements, respectively. Tables 5.9-5.12 summarize the damage assessment results from using the coefficient a_i^m's in equation (2.105) for 0.1%, 0.3%, 0.5% and 1.0% noisy measurements, respectively. As for the cases with the single-parameter members, the frame members are ranked in the descending order of the value of the probability of damage P_d^m. Note that the reduction of *EA* and *EI* are assumed to be independent in the current study.

It can be seen that the actual damaged members are successfully identified with the highest probability of damage in most cases. However, for the cases in which the level of damage is low and the level of noise is high, the actual damaged members are not ranked with the highest probability of damage. In addition, for the same levels of reduction in *EA* and *EI* the P_d^m values associated with the reduction of *EA* are closer to the unit value than those with the reduction of *EI*. Thus, the damage assessment results are more sensitive with the reduction of *EA* compared with the reduction of *EI*. Moreover, the number of cases in which the actual damaged member is identified with the highest probability of damage when the coefficients a_i^m's from equation (2.105) are used is higher than when using a_i^m's from equation (2.104). Again, the maximum level of noise permitting a damage assessment is 1%.

Figures 5.3 and 5.4 summarize the variation of the P_d^m values for the actual damaged member 4 by using a_i^m's from equations (2.104) and (2.105), respectively. The results from using the four different levels of noise in the measurements are again compared with the reference value of P_d^m. Figures 5.3(a), 5.3(c), 5.3(e) and 5.3(g) on the left column show the results in which the percentage of reduction of the bending

Table 5.5 Ranking of the identified damaged members by P_d^m value for different percentages of reduction of the stiffness parameter of members 4 and 6 using 0.1% noisy measurements and a_i^m's from equation (2.104).

| % noise = 0.1% | | | Ranking of Identified Damaged Members (by P_d^m value) | | | | |
| Actual Damaged Member | % Reduction of Parameter Value | | 1ˢᵗ | 2ⁿᵈ | 3ʳᵈ | 4ᵗʰ | 5ᵗʰ |
	EA	EI					
4	10	0	4 (0.999997)	7 (0.882977)	5 (0.868644)	6 (0.758037)	8 (0.610261)
4	50	0	4 (1.000000)	6 (0.864335)	7 (0.857691)	11 (0.785237)	5 (0.785237)
4	90	0	4 (1.000000)	6 (0.948450)	5 (0.882977)	11 (0.862144)	7 (0.745374)
4	0	10	4 (0.999998)	5 (0.896166)	7 (0.850831)	6 (0.764238)	8 (0.614092)
4	10	10	4 (1.000000)	5 (0.936992)	7 (0.899728)	6 (0.719043)	11 (0.598706)
4	50	10	4 (1.000000)	5 (0.941793)	7 (0.857691)	11 (0.841345)	6 (0.807850)
4	90	10	4 (1.000000)	6 (0.938220)	11 (0.859930)	5 (0.848496)	7 (0.764238)
4	0	50	4 (1.000000)	5 (0.967116)	6 (0.886861)	7 (0.857691)	11 (0.742154)
4	10	50	4 (1.000000)	5 (0.976148)	7 (0.884931)	6 (0.841345)	11 (0.831473)
4	50	50	4 (1.000000)	5 (0.948450)	11 (0.908241)	6 (0.846136)	7 (0.828945)
4	90	50	4 (1.000000)	7 (0.855428)	11 (0.805106)	5 (0.779351)	6 (0.779351)
4	0	90	4 (1.000000)	5 (0.973197)	6 (0.881001)	7 (0.862144)	11 (0.831473)
4	10	90	4 (1.000000)	5 (0.977250)	7 (0.876976)	11 (0.866501)	6 (0.853142)
4	50	90	4 (1.000000)	5 (0.950529)	11 (0.923642)	6 (0.850831)	7 (0.793893)
4	90	90	4 (1.000000)	7 (0.846136)	11 (0.821214)	6 (0.779351)	5 (0.779351)
6	10	0	6 (0.999950)	7 (0.823815)	5 (0.807850)	8 (0.640577)	4 (0.405164)
6	50	0	6 (1.000000)	5 (0.833977)	7 (0.799546)	8 (0.659097)	4 (0.409045)
6	90	0	6 (1.000000)	5 (0.813268)	7 (0.788145)	8 (0.633072)	4 (0.440382)
6	0	10	6 (0.999954)	7 (0.826392)	5 (0.807850)	8 (0.636831)	4 (0.409045)
6	10	10	6 (1.000000)	7 (0.826392)	5 (0.813268)	8 (0.636831)	4 (0.409045)
6	50	10	6 (1.000000)	5 (0.841345)	7 (0.802338)	8 (0.655422)	4 (0.412935)
6	90	10	6 (1.000000)	5 (0.826392)	7 (0.788145)	8 (0.629300)	4 (0.444329)
6	0	50	6 (1.000000)	7 (0.833977)	5 (0.833977)	8 (0.629300)	4 (0.420740)
6	10	50	6 (1.000000)	5 (0.836458)	7 (0.833977)	8 (0.629300)	4 (0.420740)
6	50	50	6 (1.000000)	5 (0.848496)	7 (0.810571)	8 (0.644309)	4 (0.432504)
6	90	50	6 (1.000000)	5 (0.859930)	7 (0.793893)	8 (0.617912)	4 (0.464143)
6	0	90	6 (1.000000)	7 (0.841345)	5 (0.807850)	8 (0.621720)	4 (0.448283)
6	10	90	6 (1.000000)	7 (0.841345)	5 (0.810571)	8 (0.621720)	4 (0.452241)
6	50	90	6 (1.000000)	5 (0.823815)	7 (0.818589)	8 (0.640577)	4 (0.460172)
6	90	90	6 (1.000000)	5 (0.862144)	7 (0.796731)	8 (0.610261)	4 (0.492021)

Table 5.6 Ranking of the identified damaged members by P_d^m value for different percentages of reduction of the stiffness parameter of members 4 and 6 using 0.3% noisy measurements and a_i^m's from equation (2.104).

% noise = 0.3%			Ranking of Identified Damaged Members (by P_d^m value)				
Actual Damaged Member	% Reduction of Parameter Value		1st	2nd	3rd	4th	5th
	EA	EI					
4	10	0	4 (0.942947)	7 (0.882977)	5 (0.864335)	6 (0.735653)	8 (0.590954)
4	50	0	4 (1.000000)	7 (0.855428)	6 (0.815941)	11 (0.751748)	5 (0.715662)
4	90	0	4 (1.000000)	6 (0.908241)	11 (0.833977)	5 (0.807850)	7 (0.738914)
4	0	10	4 (0.940620)	5 (0.892513)	7 (0.848496)	6 (0.745374)	8 (0.602568)
4	10	10	4 (0.999698)	5 (0.933193)	7 (0.899728)	6 (0.659097)	11 (0.579260)
4	50	10	4 (1.000000)	5 (0.913086)	7 (0.853142)	11 (0.815941)	6 (0.680823)
4	90	10	4 (1.000000)	6 (0.890652)	11 (0.838914)	7 (0.758037)	5 (0.754903)
4	0	50	4 (1.000000)	5 (0.959071)	7 (0.853142)	6 (0.799546)	11 (0.725747)
4	10	50	4 (1.000000)	5 (0.969258)	7 (0.881001)	11 (0.831473)	6 (0.708841)
4	50	50	4 (1.000000)	5 (0.917736)	11 (0.909878)	7 (0.818589)	6 (0.691463)
4	90	50	4 (1.000000)	7 (0.853142)	11 (0.810571)	5 (0.708841)	6 (0.680823)
4	0	90	4 (1.000000)	5 (0.964852)	7 (0.853142)	11 (0.841345)	6 (0.742154)
4	10	90	4 (1.000000)	5 (0.969946)	11 (0.884931)	7 (0.868644)	6 (0.691463)
4	50	90	4 (1.000000)	11 (0.936992)	5 (0.923642)	7 (0.782305)	6 (0.680823)
4	90	90	4 (1.000000)	11 (0.843753)	7 (0.841345)	5 (0.715662)	6 (0.673645)
6	10	0	6 (0.971934)	7 (0.821214)	5 (0.802338)	8 (0.629300)	4 (0.460172)
6	50	0	6 (1.000000)	5 (0.831473)	7 (0.796731)	8 (0.648028)	4 (0.460172)
6	90	0	6 (1.000000)	5 (0.810571)	7 (0.782305)	8 (0.614092)	4 (0.456204)
6	0	10	6 (0.970621)	7 (0.823815)	5 (0.799546)	8 (0.625516)	4 (0.464143)
6	10	10	6 (0.998777)	7 (0.823815)	5 (0.805106)	8 (0.625516)	4 (0.468118)
6	50	10	6 (1.000000)	5 (0.836458)	7 (0.799546)	8 (0.644309)	4 (0.468118)
6	90	10	6 (1.000000)	5 (0.821214)	7 (0.782305)	8 (0.610261)	4 (0.460172)
6	0	50	6 (1.000000)	7 (0.831473)	5 (0.815941)	8 (0.614092)	4 (0.484046)
6	10	50	6 (1.000000)	7 (0.831473)	5 (0.818589)	8 (0.614092)	4 (0.484046)
6	50	50	6 (1.000000)	5 (0.833977)	7 (0.807850)	8 (0.629300)	4 (0.492021)
6	90	50	6 (1.000000)	5 (0.846136)	7 (0.788145)	8 (0.594835)	4 (0.480061)
6	0	90	6 (1.000000)	7 (0.836458)	5 (0.767305)	8 (0.606420)	4 (0.519939)
6	10	90	6 (1.000000)	7 (0.836458)	5 (0.770351)	8 (0.606420)	4 (0.519939)
6	50	90	6 (1.000000)	7 (0.813268)	5 (0.785237)	8 (0.625516)	4 (0.527903)
6	90	90	6 (1.000000)	5 (0.833977)	7 (0.788145)	8 (0.583166)	4 (0.503989)

Table 5.7 Ranking of the identified damaged members by P_d^m value for different percentages of reduction of the stiffness parameter of members 4 and 6 using 0.5% noisy measurements and a_i^m's from equation (2.104).

% noise = 0.5%			Ranking of Identified Damaged Members (by P_d^m value)				
Actual Damaged Member	% Reduction of Parameter Value		1st	2nd	3rd	4th	5th
	EA	EI					
4	10	0	7 (0.882977)	4 (0.879000)	5 (0.859930)	6 (0.701944)	8 (0.575345)
4	50	0	4 (1.000000)	7 (0.855428)	6 (0.751748)	11 (0.715662)	2 (0.617912)
4	90	0	4 (1.000000)	6 (0.826392)	11 (0.802338)	7 (0.738914)	2 (0.648028)
4	0	10	5 (0.888768)	4 (0.876976)	7 (0.848496)	6 (0.712261)	8 (0.590954)
4	10	10	4 (0.991106)	5 (0.925067)	7 (0.899728)	6 (0.567495)	11 (0.559618)
4	50	10	4 (1.000000)	5 (0.853142)	7 (0.850831)	11 (0.776373)	2 (0.633072)
4	90	10	4 (1.000000)	6 (0.810571)	11 (0.807850)	7 (0.758037)	2 (0.659097)
4	0	50	4 (1.000000)	5 (0.941793)	7 (0.850831)	11 (0.701944)	6 (0.598706)
4	10	50	4 (1.000000)	5 (0.950529)	7 (0.876976)	11 (0.815941)	2 (0.496010)
4	50	50	4 (1.000000)	11 (0.892513)	5 (0.859930)	7 (0.815941)	2 (0.644309)
4	90	50	4 (1.000000)	7 (0.853142)	11 (0.802338)	8 (0.670032)	2 (0.655422)
4	0	90	4 (1.000000)	5 (0.946301)	7 (0.848496)	11 (0.841345)	8 (0.547758)
4	10	90	4 (1.000000)	5 (0.952541)	11 (0.892513)	7 (0.864335)	8 (0.507978)
4	50	90	4 (1.000000)	11 (0.933193)	5 (0.879000)	7 (0.779351)	2 (0.583166)
4	90	90	4 (1.000000)	11 (0.843753)	7 (0.841345)	8 (0.680823)	5 (0.651732)
6	10	0	6 (0.935745)	7 (0.818589)	5 (0.799546)	8 (0.617912)	4 (0.531881)
6	50	0	6 (0.999993)	5 (0.831473)	7 (0.793893)	8 (0.636831)	4 (0.531881)
6	90	0	6 (1.000000)	5 (0.802338)	7 (0.776373)	8 (0.598706)	4 (0.500000)
6	0	10	6 (0.930564)	7 (0.821214)	5 (0.796731)	8 (0.614092)	4 (0.535856)
6	10	10	6 (0.986447)	7 (0.821214)	5 (0.799546)	8 (0.614092)	4 (0.539828)
6	50	10	6 (0.999999)	5 (0.833977)	7 (0.796731)	8 (0.633072)	4 (0.539828)
6	90	10	6 (1.000000)	5 (0.813268)	7 (0.779351)	8 (0.594835)	4 (0.507978)
6	0	50	6 (0.999988)	7 (0.826392)	5 (0.802338)	8 (0.598706)	4 (0.563559)
6	10	50	6 (0.999999)	7 (0.826392)	5 (0.805106)	8 (0.598706)	4 (0.567495)
6	50	50	6 (1.000000)	7 (0.818589)	5 (0.802338)	8 (0.617912)	4 (0.571424)
6	90	50	6 (1.000000)	5 (0.828945)	7 (0.782305)	8 (0.575345)	4 (0.527903)
6	0	90	6 (1.000000)	7 (0.831473)	5 (0.729070)	4 (0.606420)	8 (0.590954)
6	10	90	6 (1.000000)	7 (0.831473)	5 (0.732372)	4 (0.610261)	8 (0.587064)
6	50	90	6 (1.000000)	7 (0.807850)	5 (0.745374)	4 (0.614092)	8 (0.606420)
6	90	90	6 (1.000000)	5 (0.791031)	7 (0.785237)	8 (0.559618)	4 (0.555670)

Table 5.8 Ranking of the identified damaged members by P_d^m value for different percentages of reduction of the stiffness parameter of members 4 and 6 using 1.0% noisy measurements and a_i^m's from equation (2.104).

| % noise = 1.0% | | | Ranking of Identified Damaged Members (by P_d^m value) | | | | |
| Actual Damaged Member | % Reduction of Parameter Value | | | | | | |
	EA	EI	1st	2nd	3rd	4th	5th
4	10	0	1 (0.935745)	2 (0.892513)	4 (0.892513)	7 (0.888768)	5 (0.886861)
4	50	0	4 (0.999834)	2 (0.992240)	1 (0.987775)	7 (0.884931)	3 (0.810571)
4	90	0	4 (1.000000)	2 (0.991106)	1 (0.984997)	11 (0.848496)	3 (0.815941)
4	0	10	1 (0.936992)	5 (0.911493)	4 (0.884931)	7 (0.853142)	2 (0.841345)
4	10	10	1 (0.975002)	2 (0.973810)	4 (0.968557)	7 (0.904903)	5 (0.872857)
4	50	10	4 (0.999930)	2 (0.987126)	1 (0.978822)	7 (0.886861)	5 (0.810571)
4	90	10	4 (1.000000)	2 (0.990862)	1 (0.985738)	3 (0.846136)	11 (0.838914)
4	0	50	4 (0.999982)	2 (0.969946)	1 (0.925067)	7 (0.881001)	5 (0.838914)
4	10	50	4 (0.999999)	2 (0.976148)	1 (0.954486)	7 (0.903200)	5 (0.897958)
4	50	50	4 (1.000000)	2 (0.987454)	1 (0.984997)	11 (0.864335)	7 (0.857691)
4	90	50	4 (1.000000)	2 (0.988089)	1 (0.983414)	3 (0.888768)	7 (0.876976)
4	0	90	4 (1.000000)	2 (0.967843)	1 (0.958185)	5 (0.901475)	7 (0.879000)
4	10	90	4 (1.000000)	2 (0.971934)	1 (0.965621)	5 (0.920731)	7 (0.888768)
4	50	90	4 (1.000000)	2 (0.984222)	1 (0.982997)	11 (0.896166)	5 (0.831473)
4	90	90	4 (1.000000)	2 (0.984997)	1 (0.981237)	3 (0.892513)	7 (0.866501)
6	10	0	6 (0.838914)	5 (0.826392)	7 (0.823815)	2 (0.738914)	4 (0.735653)
6	50	0	6 (0.991344)	5 (0.853142)	7 (0.796731)	1 (0.758037)	4 (0.748572)
6	90	0	6 (0.999904)	1 (0.923642)	5 (0.782305)	7 (0.776373)	4 (0.758037)
6	0	10	7 (0.828945)	5 (0.826392)	6 (0.815941)	2 (0.758037)	4 (0.738914)
6	10	10	6 (0.897958)	7 (0.826392)	5 (0.826392)	2 (0.751748)	4 (0.742154)
6	50	10	6 (0.995975)	5 (0.853142)	7 (0.799546)	1 (0.770351)	4 (0.758037)
6	90	10	6 (0.999971)	1 (0.931888)	5 (0.785237)	7 (0.779351)	4 (0.767305)
6	0	50	6 (0.971284)	5 (0.831473)	7 (0.831473)	2 (0.818589)	4 (0.773373)
6	10	50	6 (0.988396)	7 (0.831473)	5 (0.828945)	2 (0.813268)	4 (0.776373)
6	50	50	6 (0.999947)	5 (0.828945)	7 (0.807850)	1 (0.805106)	4 (0.799546)
6	90	50	6 (1.000000)	1 (0.957284)	4 (0.807850)	7 (0.785237)	5 (0.770351)
6	0	90	6 (0.999730)	2 (0.886861)	7 (0.841345)	4 (0.826392)	1 (0.708841)
6	10	90	6 (0.999943)	2 (0.888768)	7 (0.841345)	4 (0.831473)	1 (0.732372)
6	50	90	6 (1.000000)	2 (0.848496)	4 (0.848496)	7 (0.815941)	1 (0.802338)
6	90	90	6 (1.000000)	1 (0.972571)	4 (0.848496)	7 (0.791031)	2 (0.779351)

Table 5.9 Ranking of the identified damaged members by P_d^m value for different percentages of reduction of the stiffness parameter of members 4 and 6 using 0.1% noisy measurements and a_i^m's from equation (2.105).

% noise = 0.1%			Ranking of Identified Damaged Members (by P_d^m value)				
Actual Damaged Member	% Reduction of Parameter Value						
	EA	EI	1st	2nd	3rd	4th	5th
4	10	0	4 (1.000000)	5 (0.888768)	7 (0.882977)	6 (0.758037)	8 (0.610261)
4	50	0	4 (1.000000)	6 (0.862144)	7 (0.859930)	5 (0.833977)	11 (0.785237)
4	90	0	4 (1.000000)	6 (0.949498)	5 (0.914657)	11 (0.862144)	7 (0.745374)
4	0	10	4 (0.998411)	5 (0.908241)	7 (0.848496)	6 (0.779351)	8 (0.614092)
4	10	10	4 (1.000000)	5 (0.948450)	7 (0.899728)	6 (0.729070)	11 (0.598706)
4	50	10	4 (1.000000)	5 (0.958185)	7 (0.857691)	11 (0.841345)	6 (0.823815)
4	90	10	4 (1.000000)	6 (0.939430)	5 (0.888768)	11 (0.859930)	7 (0.764238)
4	0	50	4 (1.000000)	5 (0.976705)	6 (0.896166)	7 (0.855428)	11 (0.742154)
4	10	50	4 (1.000000)	5 (0.984222)	7 (0.882977)	6 (0.848496)	11 (0.831473)
4	50	50	4 (1.000000)	5 (0.965621)	11 (0.908241)	6 (0.857691)	7 (0.828945)
4	90	50	4 (1.000000)	7 (0.859930)	5 (0.831473)	11 (0.805106)	6 (0.782305)
4	0	90	4 (1.000000)	5 (0.982571)	6 (0.886861)	7 (0.857691)	11 (0.831473)
4	10	90	4 (1.000000)	5 (0.985738)	7 (0.872857)	11 (0.866501)	6 (0.857691)
4	50	90	4 (1.000000)	5 (0.969946)	11 (0.923642)	6 (0.855428)	7 (0.793893)
4	90	90	4 (1.000000)	7 (0.848496)	5 (0.833977)	11 (0.821214)	6 (0.776373)
6	10	0	6 (1.000000)	5 (0.828945)	7 (0.823815)	8 (0.640577)	11 (0.401293)
6	50	0	6 (1.000000)	5 (0.857691)	7 (0.799546)	8 (0.659097)	11 (0.382088)
6	90	0	6 (1.000000)	5 (0.853142)	7 (0.785237)	8 (0.633072)	2 (0.440382)
6	0	10	6 (0.999499)	7 (0.826392)	5 (0.826392)	8 (0.636831)	11 (0.401293)
6	10	10	6 (1.000000)	5 (0.831473)	7 (0.826392)	8 (0.636831)	11 (0.401293)
6	50	10	6 (1.000000)	5 (0.862144)	7 (0.802338)	8 (0.655422)	11 (0.385907)
6	90	10	6 (1.000000)	5 (0.864335)	7 (0.785237)	8 (0.629300)	2 (0.436440)
6	0	50	6 (1.000000)	5 (0.853142)	7 (0.833977)	8 (0.625516)	11 (0.378280)
6	10	50	6 (1.000000)	5 (0.857691)	7 (0.833977)	8 (0.625516)	11 (0.378280)
6	50	50	6 (1.000000)	5 (0.868644)	7 (0.810571)	8 (0.644309)	11 (0.389738)
6	90	50	6 (1.000000)	5 (0.888768)	7 (0.791031)	8 (0.614092)	2 (0.424654)
6	0	90	6 (1.000000)	5 (0.841345)	7 (0.838914)	8 (0.621720)	2 (0.385907)
6	10	90	6 (1.000000)	5 (0.846136)	7 (0.838914)	8 (0.621720)	11 (0.385907)
6	50	90	6 (1.000000)	5 (0.853142)	7 (0.815941)	8 (0.640577)	11 (0.401293)
6	90	90	6 (1.000000)	5 (0.894351)	7 (0.793893)	8 (0.606420)	11 (0.428576)

Table 5.10 Ranking of the identified damaged members by P_d^m value for different percentages of reduction of the stiffness parameter of members 4 and 6 using 0.3% noisy measurements and a_i^m's from equation (2.105).

| % noise = 0.3% | | | Ranking of Identified Damaged Members (by P_d^m value) | | | | |
| Actual Damaged Member | % Reduction of Parameter Value | | | | | | |
	EA	EI	1st	2nd	3rd	4th	5th
4	10	0	4 (0.999784)	7 (0.882977)	5 (0.881001)	6 (0.729070)	8 (0.594835)
4	50	0	4 (1.000000)	7 (0.857691)	6 (0.773373)	11 (0.751748)	5 (0.745374)
4	90	0	4 (1.000000)	6 (0.872857)	11 (0.833977)	5 (0.823815)	7 (0.738914)
4	0	10	5 (0.899728)	7 (0.848496)	4 (0.846136)	6 (0.758037)	8 (0.602568)
4	10	10	4 (0.999999)	5 (0.940620)	7 (0.899728)	6 (0.655422)	11 (0.579260)
4	50	10	4 (1.000000)	5 (0.911493)	7 (0.853142)	11 (0.815941)	6 (0.659097)
4	90	10	4 (1.000000)	6 (0.848496)	11 (0.838914)	5 (0.773373)	7 (0.758037)
4	0	50	4 (1.000000)	5 (0.965621)	7 (0.850831)	6 (0.799546)	11 (0.725747)
4	10	50	4 (1.000000)	5 (0.974412)	7 (0.876976)	11 (0.831473)	6 (0.694975)
4	50	50	4 (1.000000)	5 (0.917736)	11 (0.909878)	7 (0.818589)	6 (0.655422)
4	90	50	4 (1.000000)	7 (0.857691)	11 (0.810571)	5 (0.725747)	8 (0.655422)
4	0	90	4 (1.000000)	5 (0.970621)	7 (0.850831)	11 (0.841345)	6 (0.732372)
4	10	90	4 (1.000000)	5 (0.975002)	11 (0.884931)	7 (0.866501)	6 (0.677242)
4	50	90	4 (1.000000)	11 (0.936992)	5 (0.930564)	7 (0.782305)	6 (0.644309)
4	90	90	4 (1.000000)	7 (0.846136)	11 (0.843753)	5 (0.745374)	8 (0.659097)
6	10	0	6 (0.995060)	7 (0.821214)	5 (0.818589)	8 (0.629300)	4 (0.405164)
6	50	0	6 (1.000000)	5 (0.853142)	7 (0.796731)	8 (0.648028)	4 (0.416833)
6	90	0	6 (1.000000)	5 (0.838914)	7 (0.779351)	8 (0.614092)	2 (0.460172)
6	0	10	6 (0.955435)	7 (0.823815)	5 (0.815941)	8 (0.625516)	4 (0.412935)
6	10	10	6 (0.999758)	7 (0.823815)	5 (0.821214)	8 (0.625516)	4 (0.416833)
6	50	10	6 (1.000000)	5 (0.855428)	7 (0.799546)	8 (0.644309)	4 (0.420740)
6	90	10	6 (1.000000)	5 (0.848496)	7 (0.782305)	8 (0.610261)	2 (0.456204)
6	0	50	6 (1.000000)	5 (0.838914)	7 (0.828945)	8 (0.614092)	4 (0.444329)
6	10	50	6 (1.000000)	5 (0.841345)	7 (0.828945)	8 (0.614092)	4 (0.452241)
6	50	50	6 (1.000000)	5 (0.853142)	7 (0.805106)	8 (0.629300)	4 (0.448283)
6	90	50	6 (1.000000)	5 (0.870763)	7 (0.785237)	8 (0.594835)	4 (0.460172)
6	0	90	6 (1.000000)	7 (0.833977)	5 (0.810571)	8 (0.602568)	4 (0.492021)
6	10	90	6 (1.000000)	7 (0.833977)	5 (0.813268)	8 (0.602568)	4 (0.492021)
6	50	90	6 (1.000000)	5 (0.821214)	7 (0.810571)	8 (0.625516)	4 (0.488033)
6	90	90	6 (1.000000)	5 (0.866501)	7 (0.788145)	8 (0.583166)	4 (0.488033)

Table 5.11 Ranking of the identified damaged members by P_d^m value for different percentages of reduction of the stiffness parameter of members 4 and 6 using 0.5% noisy measurements and a_i^m's from equation (2.105).

% noise = 0.5%			Ranking of Identified Damaged Members (by P_d^m value)				
Actual Damaged Member	% Reduction of Parameter Value						
	EA	EI	1st	2nd	3rd	4th	5th
4	10	0	4 (0.994297)	7 (0.882977)	5 (0.855428)	6 (0.687933)	8 (0.579260)
4	50	0	4 (1.000000)	7 (0.859930)	11 (0.715662)	3 (0.666402)	6 (0.659097)
4	90	0	4 (1.000000)	3 (0.823815)	11 (0.802338)	7 (0.738914)	6 (0.722405)
4	0	10	5 (0.879000)	4 (0.853142)	7 (0.846136)	6 (0.719043)	8 (0.590954)
4	10	10	4 (0.999863)	5 (0.909878)	7 (0.899728)	11 (0.559618)	6 (0.559618)
4	50	10	4 (1.000000)	7 (0.850831)	5 (0.776373)	11 (0.776373)	3 (0.770351)
4	90	10	4 (1.000000)	3 (0.843753)	11 (0.807850)	7 (0.761148)	6 (0.698469)
4	0	50	4 (1.000000)	5 (0.922197)	7 (0.846136)	11 (0.701944)	6 (0.598706)
4	10	50	4 (1.000000)	5 (0.927855)	7 (0.874929)	11 (0.815941)	3 (0.625516)
4	50	50	4 (1.000000)	11 (0.892513)	3 (0.841345)	7 (0.818589)	5 (0.782305)
4	90	50	4 (1.000000)	7 (0.857691)	3 (0.836458)	11 (0.802338)	8 (0.673645)
4	0	90	4 (1.000000)	5 (0.925067)	7 (0.846136)	11 (0.841345)	3 (0.633072)
4	10	90	4 (1.000000)	5 (0.930564)	11 (0.892513)	7 (0.862144)	3 (0.666402)
4	50	90	4 (1.000000)	11 (0.933193)	3 (0.855428)	5 (0.823815)	7 (0.779351)
4	90	90	4 (1.000000)	7 (0.846136)	3 (0.846136)	11 (0.843753)	8 (0.684387)
6	10	0	6 (0.974412)	7 (0.818589)	5 (0.805106)	8 (0.617912)	4 (0.543795)
6	50	0	6 (1.000000)	5 (0.836458)	7 (0.793893)	8 (0.636831)	4 (0.547758)
6	90	0	6 (1.000000)	5 (0.807850)	7 (0.776373)	8 (0.598706)	4 (0.551717)
6	0	10	6 (0.914657)	7 (0.821214)	5 (0.799546)	8 (0.614092)	4 (0.551717)
6	10	10	6 (0.993790)	7 (0.821214)	5 (0.805106)	8 (0.614092)	4 (0.551717)
6	50	10	6 (1.000000)	5 (0.836458)	7 (0.793893)	8 (0.633072)	4 (0.555670)
6	90	10	6 (1.000000)	5 (0.815941)	7 (0.776373)	8 (0.594835)	4 (0.559618)
6	0	50	6 (0.999749)	7 (0.826392)	5 (0.813268)	8 (0.598706)	4 (0.598706)
6	10	50	6 (0.999998)	7 (0.826392)	5 (0.813268)	4 (0.606420)	8 (0.598706)
6	50	50	6 (1.000000)	7 (0.823815)	7 (0.802338)	8 (0.617912)	4 (0.606420)
6	90	50	6 (1.000000)	5 (0.826392)	7 (0.779351)	4 (0.590954)	8 (0.575345)
6	0	90	6 (1.000000)	7 (0.831473)	5 (0.764238)	4 (0.659097)	8 (0.587064)
6	10	90	6 (1.000000)	7 (0.831473)	5 (0.767305)	4 (0.662758)	8 (0.587064)
6	50	90	6 (1.000000)	7 (0.805106)	5 (0.770351)	4 (0.655422)	8 (0.606420)
6	90	90	6 (1.000000)	5 (0.799546)	7 (0.782305)	4 (0.629300)	8 (0.559618)

Table 5.12 Ranking of the identified damaged members by P_d^m value for different percentages of reduction of the stiffness parameter of members 4 and 6 using 1.0% noisy measurements and a_i^m's from equation (2.105).

% noise = 1.0%			Ranking of Identified Damaged Members (by P_d^m value)				
Actual Damaged Member	% Reduction of Parameter Value		1st	2nd	3rd	4th	5th
	EA	EI					
4	10	0	4 (0.993963)	1 (0.933193)	3 (0.906583)	2 (0.899728)	7 (0.888768)
4	50	0	4 (1.000000)	2 (0.992240)	3 (0.990862)	1 (0.987126)	7 (0.888768)
4	90	0	4 (1.000000)	3 (0.995975)	2 (0.991344)	1 (0.985738)	11 (0.848496)
4	0	10	4 (0.966375)	1 (0.935745)	3 (0.894351)	7 (0.853142)	2 (0.848496)
4	10	10	4 (0.999359)	2 (0.973810)	1 (0.973810)	3 (0.961637)	7 (0.904903)
4	50	10	4 (1.000000)	3 (0.996319)	2 (0.987126)	1 (0.979325)	7 (0.886861)
4	90	10	4 (1.000000)	3 (0.997445)	2 (0.991106)	1 (0.986097)	11 (0.838914)
4	0	50	4 (0.999999)	3 (0.979325)	2 (0.971284)	1 (0.930564)	7 (0.881001)
4	10	50	4 (1.000000)	3 (0.985371)	2 (0.977785)	1 (0.957284)	7 (0.901475)
4	50	50	4 (1.000000)	3 (0.998011)	2 (0.988089)	1 (0.985371)	11 (0.864335)
4	90	50	4 (1.000000)	3 (0.998462)	2 (0.988396)	1 (0.983823)	7 (0.881001)
4	0	90	4 (1.000000)	3 (0.986097)	2 (0.970621)	1 (0.959941)	7 (0.876976)
4	10	90	4 (1.000000)	3 (0.988396)	2 (0.974412)	1 (0.967116)	7 (0.888768)
4	50	90	4 (1.000000)	3 (0.997947)	2 (0.985371)	1 (0.983823)	11 (0.896166)
4	90	90	4 (1.000000)	3 (0.998693)	2 (0.985738)	1 (0.981691)	7 (0.870763)
6	10	0	6 (0.886861)	4 (0.866501)	7 (0.826392)	3 (0.788145)	5 (0.754903)
6	50	0	6 (0.999869)	4 (0.874929)	7 (0.796731)	3 (0.785237)	5 (0.770351)
6	90	0	6 (1.000000)	1 (0.919244)	4 (0.906583)	3 (0.815941)	7 (0.776373)
6	0	10	4 (0.872857)	7 (0.828945)	6 (0.799546)	3 (0.793893)	2 (0.767305)
6	10	10	6 (0.919244)	4 (0.874929)	7 (0.826392)	3 (0.793893)	2 (0.761148)
6	50	10	6 (0.999941)	4 (0.886861)	7 (0.799546)	3 (0.796731)	1 (0.776373)
6	90	10	6 (1.000000)	1 (0.926471)	4 (0.913086)	3 (0.821214)	7 (0.779351)
6	0	50	6 (0.929220)	4 (0.909878)	7 (0.831473)	3 (0.831473)	2 (0.826392)
6	10	50	6 (0.978822)	4 (0.911493)	7 (0.831473)	3 (0.831473)	2 (0.821214)
6	50	50	6 (0.999999)	4 (0.920731)	3 (0.826392)	1 (0.813268)	7 (0.807850)
6	90	50	6 (1.000000)	1 (0.952541)	4 (0.938220)	3 (0.841345)	7 (0.785237)
6	0	90	6 (0.993244)	4 (0.942947)	2 (0.888768)	3 (0.848496)	7 (0.838914)
6	10	90	6 (0.998817)	4 (0.947384)	2 (0.890652)	3 (0.850831)	7 (0.838914)
6	50	90	6 (1.000000)	4 (0.951543)	2 (0.853142)	3 (0.841345)	7 (0.815941)
6	90	90	6 (1.000000)	1 (0.968557)	4 (0.959941)	3 (0.843753)	2 (0.793893)

Figure 5.3 Variation of the P_d^m values using a_i^m's from equation (2.104) of the actual damaged member 4 with respect to different percentages of reduction of axial and bending stiffness parameters for different levels of noise in the measurements.

Figure 5.4 Variation of the P_d^m values using a_i^m's from equation (2.105) of the actual damaged member 4 with respect to different percentages of reduction of axial and bending stiffness parameters for different levels of noise in the measurements.

stiffness parameter is fixed at 0%, 10%, 50% and 90%, respectively. On the right column, figures 5.3(b), 5.3(d), 5.3(f) and 5.3(h) show the results in which the percentage of reduction of the axial stiffness parameter is fixed at 0%, 10%, 50% and 90%, respectively. Figures 5.4(a), 5.4(c), 5.4(e) and 5.4(g) on the left column and figures 5.4(b), 5.4(d), 5.4(f) and 5.4(h) on the right column also show the results in the same order.

Figures 5.5 and 5.6 show the performance of the investigated algorithm by the P_d^m value for the actual damaged member 6 using a_i^m's from equations (2.104) and (2.105), respectively. The format of the illustrations follows Figures 5.3 and 5.4 in which the left and right columns show the results for different percentages of reduction of the bending and the axial stiffness parameters, respectively.

The same sort of results is again seen. For the same level of damage the P_d^m value decreases as the level of noise in the measurements increases. Hence, it is evident that the performance of the proposed algorithm to assess damage is limited by the level of noise in the measurements. The P_d^m value approaches the unit value as the level of damage increases. Nevertheless, it is seen from Figures 5.3(a), 5.4(a), 5.5(a) and 5.6(a) that at low levels of damage the reduction of EA yields P_d^m values closer to the unit value compared with the reduction of EI. Moreover, it is also seen from Figures 5.3(b-f), 5.4(b-f), 5.5(b-f) and 5.6(b-f) that the probability of damage P_d^m is higher when EA is fixed at 10%, 50% and 90% reduction compared to when EI is fixed at 10%, 50% and 90% reduction, respectively. This suggests that the reduction of EA may affect the damage assessment results more compared with the reduction of EI, which clearly illustrates the inherent sensitivity in assessing damage from the reduction of different stiffness parameters. Further, it can be seen from Figures 5.3(a), 5.4(a), 5.5(a) and 5.6(a) that for the reduction of EA (EI fixed at 0% reduction) the P_d^m values from using the coefficients a_i^m's in equation (2.105) are higher than those from using equation (2.104) and vice versa for the reduction of EI (EA fixed at 0% reduction). In Figures 5.3(b-f), 5.4(b-f), 5.5(b-f) and 5.6(b-f), it is seen that for the reduction of EI (EA fixed at 10%, 50% and 90% reduction) the P_d^m values from using

(a) 0% *EI* Reduction

(b) 0% *EA* Reduction

(c) 10% *EI* Reduction

(d) 10% *EA* Reduction

(e) 50% *EI* Reduction

(f) 50% *EA* Reduction

(g) 90% *EI* Reduction

(h) 90% *EA* Reduction

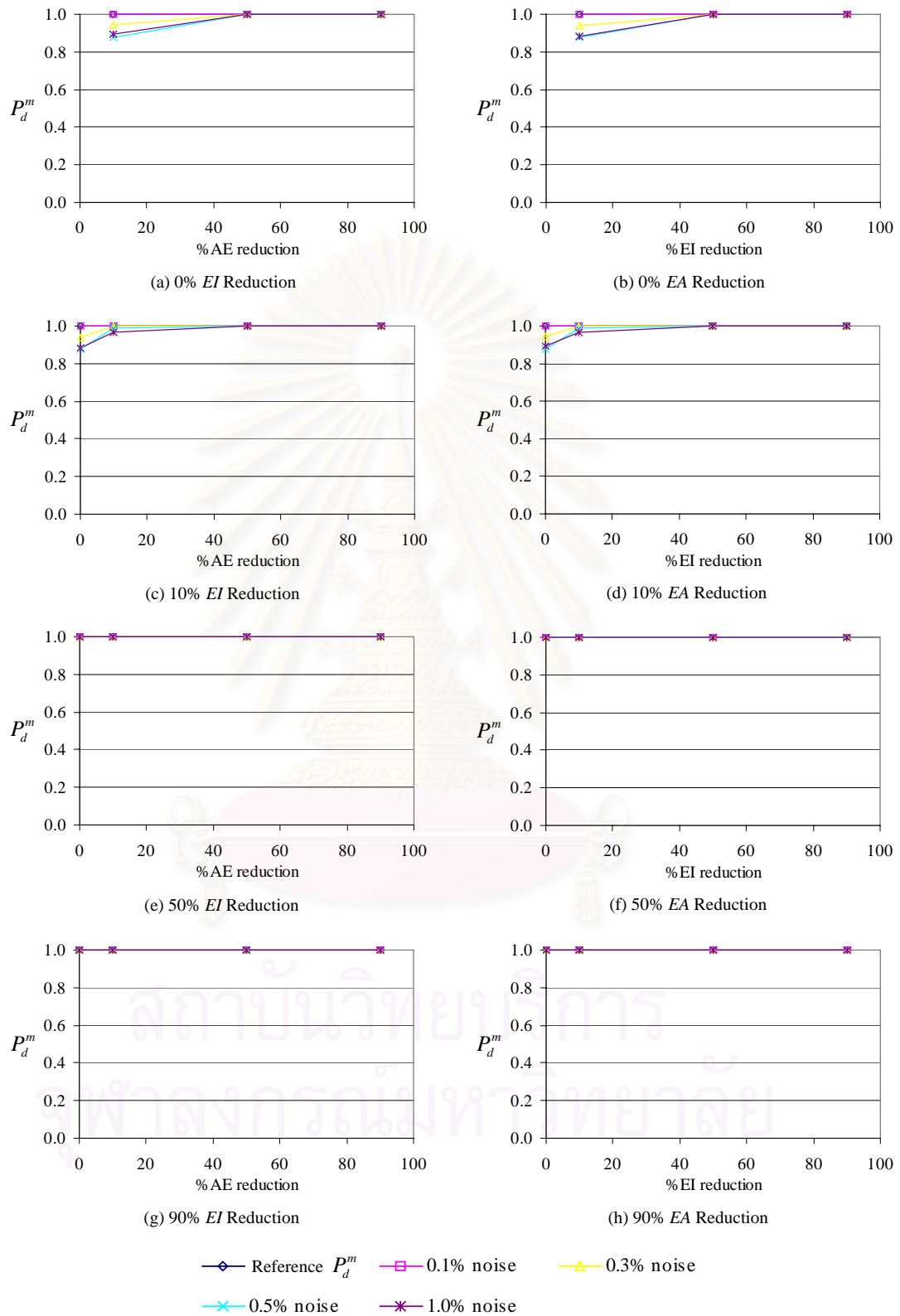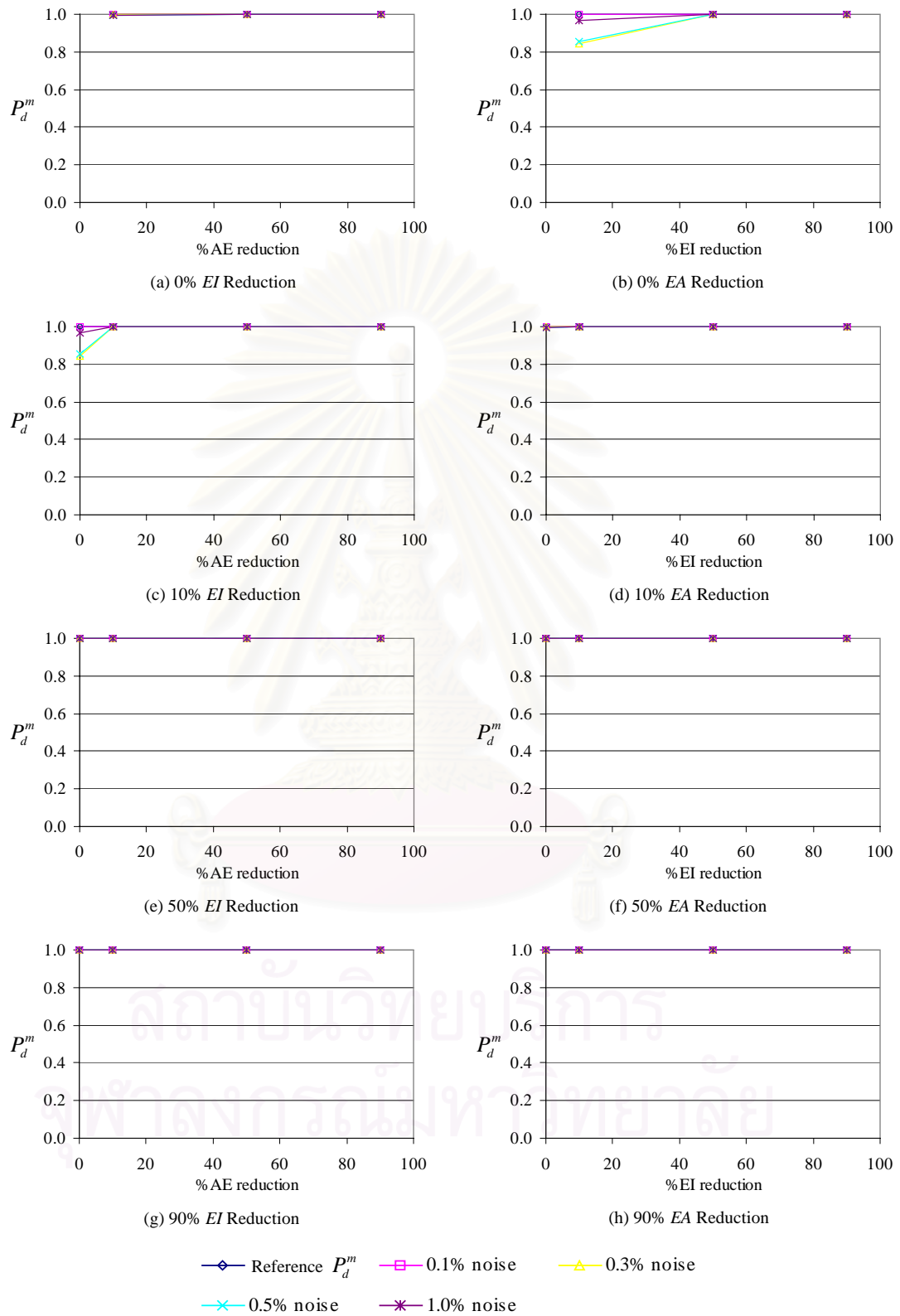Reference P_d^m 0.1% noise   0.3% noise

0.5% noise   1.0% noise

Figure 5.5 Variation of the P_d^m values using a_i^m's from equation (2.104) of the actual damaged member 6 with respect to different percentages of reduction of axial and bending stiffness parameters for different levels of noise in the measurements.
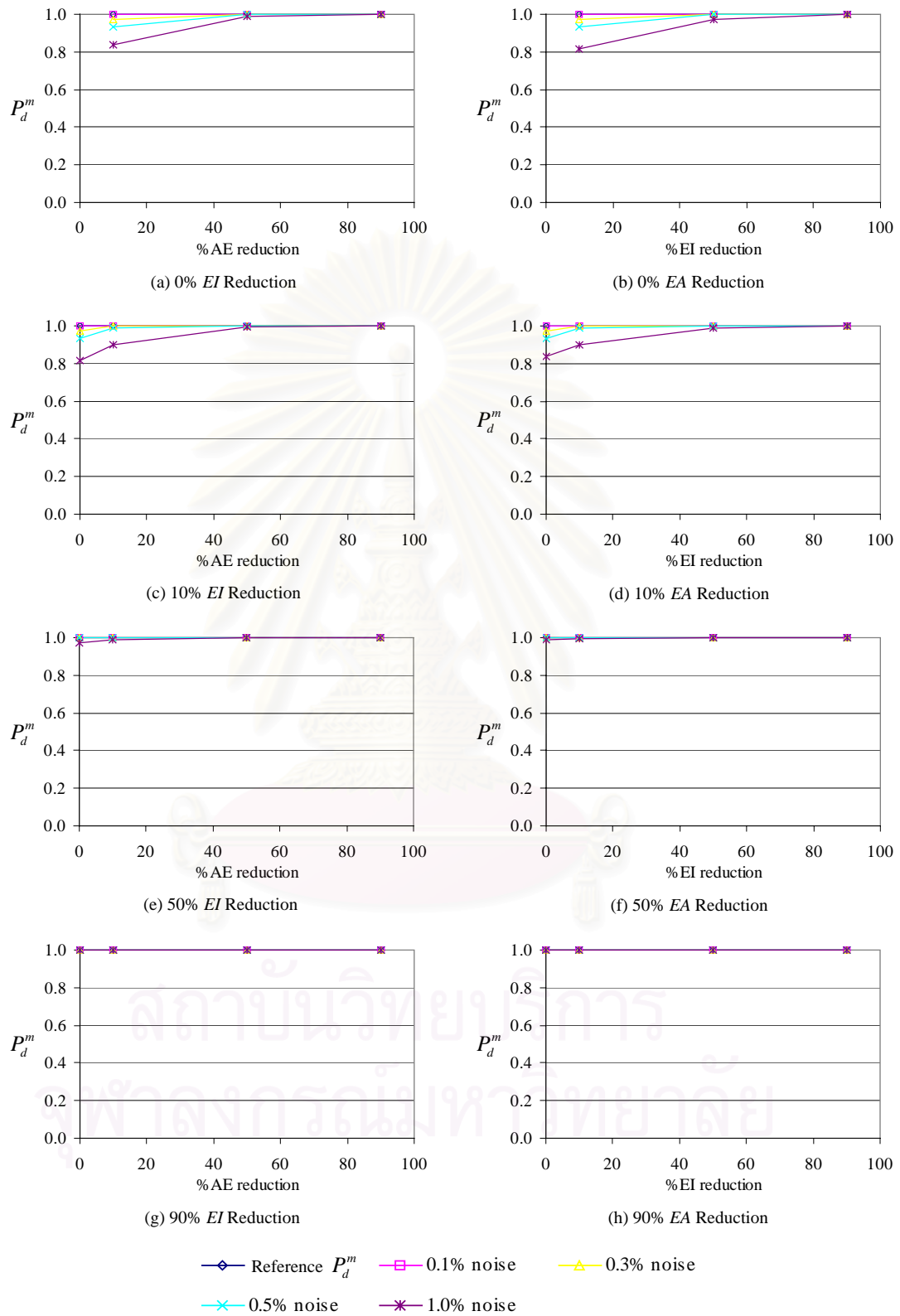
Figure 5.6 Variation of the P_d^m values using a_i^m's from equation (2.105) of the actual damaged member 6 with respect to different percentages of reduction of axial and bending stiffness parameters for different levels of noise in the measurements.
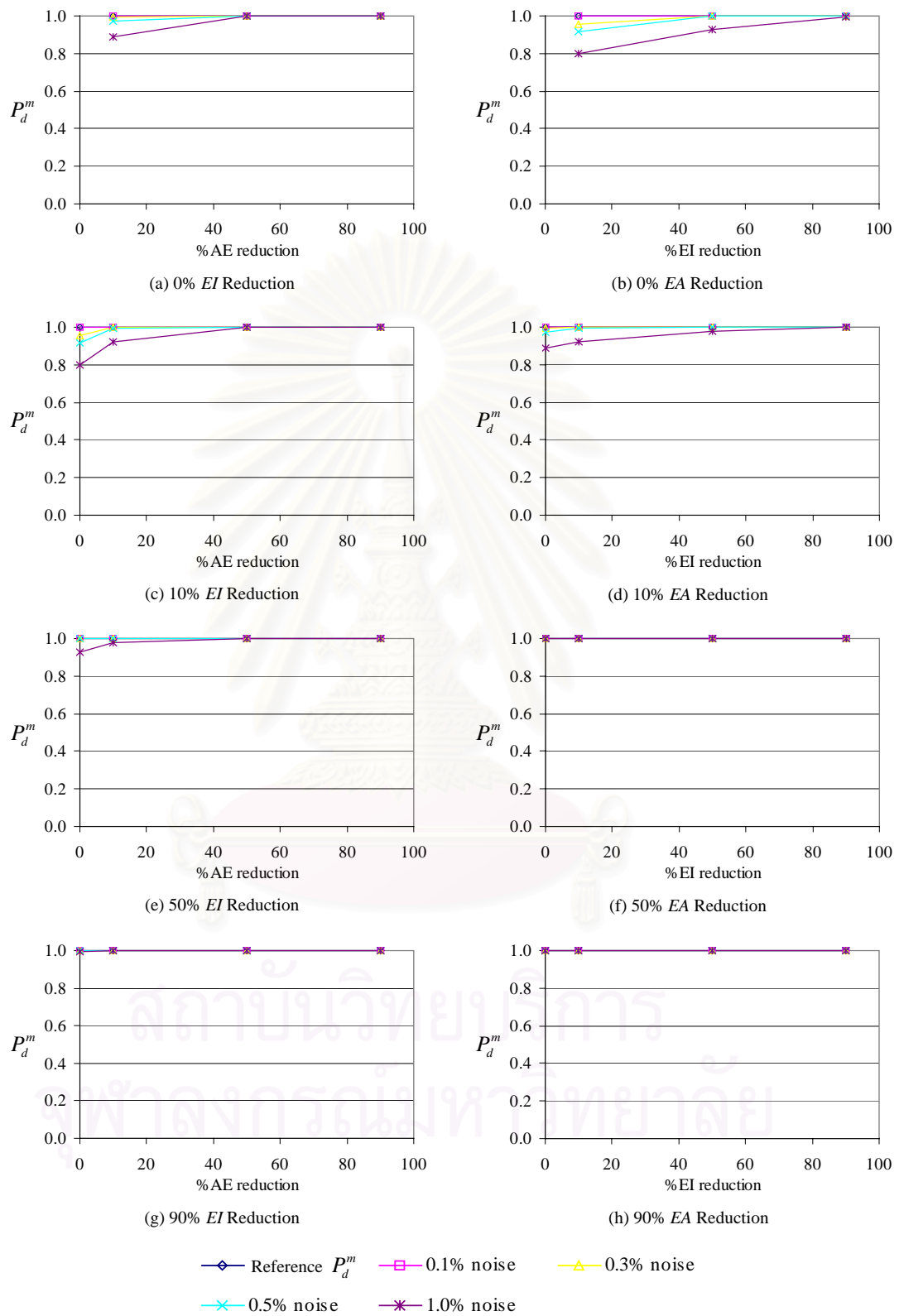
the coefficients a_i^m's in equation (2.105) are slightly higher than those from using equation (2.104) and vice versa for the reduction of *EA* (*EI* fixed at 10%, 50% and 90% reduction). In other words, the P_d^m values from using the coefficients a_i^m's in equation (2.105) are more accurate with the reduction of *EA* compared to when using the coefficients a_i^m's in equation (2.104). Thus, for the cases where damage manifests itself as the reduction of *EA*, the assessment of damage by using the coefficients a_i^m's in equation (2.105) may be more effective. Still, further investigation is needed to support this observation.

5.4 Chapter Summary

The performance of the statistical damage assessment scheme was investigated through a simulation study using a two-story braced frame with multi-parameter members as the model problem. Various damage cases with different percentages of reduction of the axial stiffness parameter *EA* were examined for the single-parameter members. For the two-parameter members, the damage was modeled with different percentages of reduction in the axial stiffness parameter *EA* and the bending stiffness parameter *EI* using different levels of noise in the measurements. The statistics of the stiffness parameters of the structure are obtained by using the optimum sensitivity-based method in conjunction with the ROEE algorithm. The baseline function $g(\mathbf{H}_m)$ proposed in Chapter 2 was used to identify whether a structural member is in the "healthy state" or the "damaged state." The performance of the damage assessment is identified by using the probability of damage P_d^m for each member that approaches the unit value when it is certain that the member is damaged. The results from the simulation study indicate that the performance of the presented statistical damage assessment method for the structure under consideration may be more sensitive with the reduction of one stiffness parameter compared with the reduction of the other stiffness parameters. It was also observed that the outcome of the damage assessment can be improved by taking into account the sensitivity of the parameter estimates when assessing damage. In addition, the maximum level of noise permitting a

structural damage assessment is 1% for the two-story braced frame compared to 20% for the simple-support truss structure in Chapter 3. This is probably due to the fact that the truss structure is more flexible and hence the free-vibration response of the truss is not affected much by its damping characteristics compared with the two-story rigid frame. However, further investigation is still needed to support this conclusion.

CHAPTER 6

CONCLUSIONS

Structural damage assessment based on the parameter estimation algorithm from the measured response is a complicated problem. Various difficulties can arise in the practical application of structural damage assessment in which field measurements of the structural responses are obtained through testing. The focus of the present study is on the presence of the measurement noise. The noise in the measurements poses a direct effect on the sensitivity of the parameter estimates. We have presented an approach to the problem of structural damage assessment based upon the measured modal information that is noise-polluted. We have assumed that a structure can be characterized with a parameterized finite element model of single or multiple stiffness parameters with known topology and geometry. These parameters may be an axial stiffness, a bending stiffness, or a shearing stiffness, which correspond to different modes of deformation considered (i.e., axial, bending, or shear). Moreover, we have assumed that all of the structural vibration modes were measured at all degrees of freedom of the structural model and all natural frequencies and mode shapes of the structure were available as our measurement information. In addition, damage was regarded as a reduction in the element stiffness parameter. Hence, the nonlinearity effect of the structural damage was not taken into account.

The key element of the present damage assessment algorithm is the estimation of the system parameters from the measured modal response. The statistical parameter estimation methods have been proved effective for the estimation of the system parameters from the measured modal response in the presence of the measurement noise. We have implemented an output error estimator as the tool for statistical parameter estimation in the face of noise-polluted data. We have used the measured data perturbation scheme to simulate the noisy measured response of the structures. The success of the output error estimator also depends on the behavior of the algorithm in the presence of the measurement errors. The regularization technique has been adopted to reduce the degree of instabilities of solutions to the statistical

parameter estimation problem by adding a regularization function algebraically to the initial objective function as a penalty term for the output error estimator (OEE). The proposed method has been referred to as the regularized output error estimator (ROEE). The statistical parameter estimation methods investigated were the Monte Carlo simulation method, the optimum sensitivity method and the sensitivity-based method.

The statistical damage assessment algorithms that compare the statistical distributions of the healthy and damaged system parameters have been proved effective for the identification of damage in the presence of the measurement noise. The statistical distribution of the parameters can be obtained from a Monte Carlo sample of the parameter estimates which is generated by repeating the parameter estimation algorithms many times using different sets of measured data. Each of the measurement data sets can be simulated by adding a random error to the noise-free measured data. Hence, the parameter estimates can be treated as random variables. Furthermore, the sensitivity-based method and the optimum sensitivity-based method have been adopted as alternatives to the Monte Carlo simulation method in the statistical parameter estimation process. In these methods, the parameter estimation problem is solved only once to find the solution from the mean of the measured response. Upon completion of the statistical parameter estimation algorithm, a numerical integration scheme is applied to the statistical distribution of the system parameters to compute the probability of damage. The computed probability indicates the likelihood that a member is damaged.

We have demonstrated the use of the statistical damage assessment algorithm on two example structures: a simple-support truss and a two-story braced frame. Numerical simulation studies were employed to examine the capabilities of the algorithm in assessing damage. The statistical damage assessment procedure has been tested with the single-damaged-member cases and the two-damaged-member cases for the simple-support truss structure. Noisy measurements were simulated by adding different amplitudes of proportional random errors to the noise-free analytical modal response of the structures. Three different methods of statistical parameter estimation have been used in conjunction with the two output error estimators to obtain the

statistical distribution of the parameter estimates that is used as an input to the statistical damage assessment algorithm. Evaluation of the statistical distribution of the parameter estimates at the potential damage locations has proved reliable as a method for assessing whether damage is detectable above the noise in the measurements. It has been shown that the proposed algorithm was able to assess damage effectively at low levels of noise in the measurements. For higher levels of noise in the measurements, there are always cases where actually damaged elements are identified as undamaged or actually undamaged elements are identified as damaged. However, the results have been shown to improve dramatically when the level of noise in the measurements decreases. In addition to the level of noise in the measurements, the severity of the damage in the structural components also limits the ability of the proposed algorithm to assess damage in a structural system.

The performance of the statistical damage assessment is identified by using a statistical identification error (SIE) index that approaches zero when the assessment is effective. The level of success of the damage detection is indicated by the probability of success in detecting damage (P_s). The performance of damage assessment with respect to the level of noise in the measurements is illustrated by the variation of the SIE values for all damage cases. The results of the simulation study showed that the performance of the proposed statistical damage assessment method can be improved by using the regularization method on the parameter estimation problem (ROEE) for all of the statistical parameter estimation schemes considered. Furthermore, the ROEE algorithm is more effective when using with the optimum sensitivity-based method compared to when using with the Monte Carlo simulation method and the sensitivity-based method.

The statistical damage assessment of a structure with members consisting of multiple stiffness parameters was investigated through a simulation study. A two-story braced frame was selected as the model problem. Various damage cases of the single-parameter bracing members were examined by reducing the members' axial stiffness parameter. For the two-parameter frame members, the damage was modeled as the reduction of the axial stiffness parameter and the bending stiffness parameter. The effect from using different levels of noise in the measurements was also

investigated. The statistics of the structural parameters are obtained by using the optimum sensitivity-based method in conjunction with the ROEE algorithm.

To assess damage for the multi-parameter structural members, a baseline function $g(\mathbf{H}_m)$ was proposed to identify whether a structural member is in the "healthy state" or the "damaged state." The boundary separating these two states is referred to as the "limit state" whose relative distance in the reduced-variate coordinate space can be used to quantify damage. The performance of the damage assessment is identified by using the probability of damage P_d^m for each member that approaches the unit value when it is certain that the member is damaged. The results from the simulation study indicate that the performance of the presented statistical damage assessment method for the structure under consideration may be more sensitive with the reduction of one stiffness parameter compared with the reduction of the other stiffness parameters. It was also observed that the outcome of the damage assessment can be improved by taking into account the sensitivity of the parameter estimates when assessing damage. In addition, the maximum level of noise permitting a structural damage assessment is 1% for the two-story braced frame compared to 20% for the simple-support truss structure in Chapter 3. This is probably due to the fact that the truss structure is more flexible and hence the free-vibration response of the truss is not affected much by its damping characteristics compared with the two-story rigid frame. However, further investigation is still needed to support this conclusion.

From the simulation studies, it has been found that the computation time in assessing damage can increase enormously as the structural model becomes more complex. In general, this computational burden depends on the number of degrees of freedom, the number of members in the finite element model of the structure and the number of parameters in each member of the structure. Possible alternatives should be investigated to improve the computation efficiency of the algorithm. One possible approach to reduce the computational burden of the current algorithm is to improve the solution algorithm for the statistical parameter estimation problem.

In the current study we have considered only the linear baseline function to assess damage in the structural members with multiple stiffness parameters. Aside from its

own usefulness, certain aspects of the linear case would be the basis for an approximation to nonlinear baseline functions. Future study needs to be carried out to investigate other nonlinear baseline functions which may be suitable for different types of structures.

REFERENCES

Ang, A. H-S., and Cornell, C. A. (1974). "Reliability bases of structural safety and design." *J. of Structural Division*, ASCE, Vol. 100, No. ST9, (September) : 1755-1769.

Ang, A. H-S., and Tang, W. H. (1990). "Probability concepts in engineering planning and design." Volume II : decision, risk, and reliability : 333-433.

Araki, Y., and Hjelmstad, K. D. (2001). "Optimum sensitivity-based statistical parameter estimation from modal response." *AIAA Journal*, Vol. 39, No. 6 : 1166-1174.

Astrom, K. J., and Eykhoff, P. (1997). "System identification--a survey." *Automatica*, 7 : 123-162.

Banan, M. R., and Hjelmstad, K. D. (1993). "Identification of structural systems from measured response." *Civ. Engrg. Studies*, SRS579, UILU-ENG-93-2002, University of Illinois at Urbana-Champaign, Ill.

Berman, A. (1995). "Multiple acceptable solutions in structural model improvement." *American Institute of Aeronautics and Astronautics Journal*, 33(5) : 924-927.

Berman, A., and Nagy, E. J. (1983). "Improvement of a large analytical model using test data." *American Institute of Aeronautics and Astronautics Journal*, 21(8) : 1168-1173.

Cornell, C. A. (1969). "Structural safety specification based on second-moment reliability." *Sym. Int. Assoc. of Bridge and Struct*, Engr., London.

Doebling, S. W., Farrar, C. R., Prime, M. B., and Shevitz, D. W. (1996). "Damage identification and health monitoring of structural and mechanical systems from changes in their vibration characteristics: a literature review." *Los Alamos National Laboratory Report*, LA-13070-MS, Los Alamos National Laboratory, N. M.

Ewins, D. J. (1984). *Modal Testing: Theory and Practice.* New York : John Wiley.

Fletcher, R. (1971). "A general quadratic programming algorithm." *J. Inst. Maths. Applics.*, 7 : 76-91.

Gersch, W. (1975). "Parameter identification: stochastic process techniques." *Shock and Vibration Digest*, 7(11) : 71-86.

Hajela, P., and Soeiro, F. J. (1990). "Recent developments in damage detection based on system identification methods." *Struct. Optimization*, 2 : 1-10.

Hajela, P., and Soeiro, F. J. (1990). "Structural damage detection based on static and modal analysis." *AIAA J.*, 28(6) : 1110-1115.

Hjelmstad, K. D. (1996). "On the uniqueness of modal parameter estimation." *J. Sound Vibration*, 192(2) : 581-598.

Hjelmstad, K. D., Banan, M. R., and Banan, M. R. (1995). "On building the finite element models of structures from modal response." *Earthquake Engrg. Struct. Dynamics*, 24(1) : 53-67.

Hjelmstad, K. D., Banan, M. R., and Banan, M. R. (1994). "Parameter estimation of structures from static response. I: computational aspects." *J. Struct. Engrg.*, ASCE, 120(11) : 3243-3258.

Hjelmstad, K. D., Banan, M. R., and Banan, M. R. (1994). "Parameter estimation of structures from static response. II: numerical simulation studies." *J. Struct. Engrg.*, ASCE, 120(11) : 3259-3283.

Hjelmstad, K. D., and Shin, S. (1996). "Crack identification in a cantilever beam from modal response." *J. Sound Vibration*, 198(5) : 527-545.

Hjelmstad, K. D., Wood, S. L., and Clark, S. J. (1992). "Mutual residual energy method for parameter estimation in structures." *J. Struct. Engrg.*, ASCE, 118(1) : 223-242.

Kozin, F., and Natke, H. G. (1986). "System identification techniques." *Structural Safety*, 3 : 269-316.

Law, S. S., Shi, Z. Y., and Zhang, L. M. (1998). "Structural damage detection from incomplete and noisy modal test data." *J. Engrg. Mech.*, ASCE, 124(11) : 1280-1288.

Mottershead, J. E., and Friswell, M. I. (1993). "Model updating in structural dynamics: a survey." *J. Sound Vibration*, 167(2) : 347-375.

Natke, H. G., editor (1982). *Identification of Vibrating Structures.* Berlin : Springer-Verlag.

Papadopoulas, L., and Garcia, E. (1998). "Structural damage identification: a probabilistic approach." *AIAA J.*, 36(11) : 2137-2145.

Pilkey, W. D., and Cohen, R., editors (1972). *System Identification of Vibrating Structures—Mathematical Models from Test Data.* New York : ASME.

Pothisiri, T. (2002). "Statistical assessment of structural integrity from modal parameter estimation." *Proc. IABSE Symposium Melbourne 2002*, IABSE/AIPC/IVBH, Melbourne.

Pothisiri, T., and Hjelmstad, K. D. (2000). "Damage detection for spatially sparse and noise-polluted modal response." *Proc., Engineering Mechanics Conference 2000*, ASCE, Austin, Texas.

Pothisiri, T., and Hjelmstad, K. D. (2001). "Identification of damage in structural systems using modal data." *Civil Engrg. Studies*, SRS632, UILU-ENG-2001-2002, University of Illinois at Urbana-Champaign, Ill.

Pothisiri, T., and Hjelmstad, K. D. (2001). "Structural damage detection and assessment from spatially sparse and noise-polluted modal response." *Civ. Engrg. Studies*, SRS632, UILU-ENG-2001-2002, University of Illinois an Urbana-Champaign, Ill.

Pothisiri, T., and Hjelmstad, K. D. (2003). "Structural damage detection and assessment from modal response." *J. Engrg. Mech.*, ASCE, 129(2) : 135-145.

Pothisiri, T., and Vatcharatanyakorn, S. (2002). "A regularization method for structural parameter estimation from measured modal response." *Proc. of the 8th National Convention on Civil Engineering*, Vol.1, Kon Kaen, Thailand : 282-287.

Pothisiri, T., and Vatcharatanyakorn, S. (2002). "The effect of measurement errors on structural parameter estimation from modal response." *Proc. of the 8th National Convention on Civil Engineering*, Vol. 1, Kon Kaen, Thailand : 221-226.

Press, W., Flannery, B., Teukolsky, S., and Vetterling, W. (1986). *Numerical recipes.* Cambridge, U.K. : Cambridge Univ. Press.

Sanayei, M., and Nelson, R. B. (1986). "Identification of structural element stiffnesses from incomplete static test data." *SAE. Tech. Papers Se. No. 861793* : 7.1237-7.1248.

Sanayei, M., and Onipede, O. (1991). "Damage assessment of structures using static test data." *AIAA J.*, 29(7) : 1174-1179.

Sanayei, M., Onipede, O., and Babu, S. R. (1992). "Selection of noisy measurement locations for error reduction in static parameter identification." *AIAA J.*, 30(9) : 2299-2309.

Sanayei, M., and Scampoli, S. F. (1991). "Structural element stiffness identification from static test data." *J. Engrg. Mech.*, ASCE., 117(5) : 1021-1036.

Sheena, Z., Unger, A., and Zalmanovich, A. (1982). "Theoretical stiffness matrix correction by using static test results." *Israel Journal of Technology*, 20 : 245-253.

Shin, S., and Hjelmstad, K. D. (1994). "Damage detection and assessment of structural systems from measured response." *Civ. Engrg. Studies*, SRS593, UILU-ENG-94-2013, University of Illinois at Urbana-Champaign, Ill.

Shin, S., and Hjelmstad, K. D. (1997). "Damage detection and assessment of structures from static response." *J. Engrg. Mech.*, ASCE, 123(6) : 568-576.

Torn, A., and Zilinskas, A. (1987). *Global Optimization.* New York : Springer-Verlag.

Udwadia, F. E., and Sharma, D. K. (1978). "Some uniqueness results related to building structural identification." *SIAM Journal of Applied Mathematics*, 34(1) : 104-118.

Vatcharatanyakorn, S., and Pothisiri, T. (2002). "A regularization scheme for structural parameter estimation from measured modal response." *Civ. Engrg. Studies,* 4997, ISBN 974-17-1027-5, College of Engineering, Chulalongkorn University.

Yeo, I., Shin, S., Lee, H. S., and Chang, S.-P. (2000). "Statistical damage assessment of framed structures from static responses." *J. Engrg. Mech.*, ASCE, 126(4) : 414-421.

VITA

Mr. Montree Jitmoud was born in Chacheangsaw 1978. He graduated from Faculty of Engineering, Chulalongkorn University in 1999. He continued his study for Master Degree in Civil Engineering at Chulalongkorn in 2000.